Department of Mechanical Engineering

Mechanical Behaviour of Tendinopathic Tendon:

An Engineering Perspective

Alex John Cullen Hayes

This thesis is presented for the Degree of

Doctor of Philosophy

of

Curtin University

December 2017

DECLARATION

To the best of my knowledge and belief this thesis contains no material previously published by any other person except where due acknowledgment has been made.

This thesis contains no material which has been accepted for the award of any other degree or diploma in any university.

The research presented and reported in this thesis was conducted in compliance with the National Health and Medical Research Council Australian code for the care and use of animals for scientific purposes 8th edition (2013). The proposed research study received animal ethics approval from the University of Western Australia Animal Ethics Committee, approval number RA/3/100/1049.

Signature:

Date: 30 December 2017

ABSTRACT

The Achilles tendon, the largest and strongest tendon in the body, is among the most frequently injured. A common trait is the presence of tendinopathy, or disease of the tendon. Tendinopathy is a debilitating disease affecting millions of people worldwide, and is characterised by pain and reduced mobility and functionality. The pathology is complex and usually includes disordered and inadequate healing of the tendon. The aetiology of this disease is not well understood, and treatment remains difficult due to a lack of evidence-based management.

This dissertation sought to quantify the mechanical behaviour of tendon in order to understand the difference between healthy and tendinopathic tendons. This was achieved through the development of a series of methodologies derived from rigorous analysis of the literature and validated through testing. The methodologies developed may be considered best-practice for measurement of cross-sectional area, uniaxial mechanical testing, and viscoelastic testing of tendon. A comprehensive protocol for evaluating the elastic and viscoelastic static and dynamic behaviours was proposed and validated against a collagenase-induced tendinopathy model.

Three methodologies were developed and utilised in five experiments using New Zealand White rabbit Achilles tendon. The following conclusions may be drawn from the results of this dissertation:

1. Structured light scanning is an effective tool for measuring the morphology of soft tissue;
2. Tendon demonstrates a measurable change in cross-sectional area with stress;
3. Engineering stress may be used as an approximation of true stress when testing is performed in or near the toe region;
4. Rabbit Achilles tendons should be tested as bone-tendon-muscle constructs to preserve the anatomy of the tendon;
5. Rabbit Achilles tendon is strain rate insensitive;
6. Strain is the limiting factor in determining failure properties;

7. The minimum duration of testing required to assess the viscoelastic properties of tendon is 100 seconds;

8. Tendinopathy does not cause significant differences from control values; and,

9. Management of the tendon should involve pain relief, coupled with tendon strengthening exercises.

This dissertation represents the first study to investigate the rate of change for creep and relaxation in a rabbit model, to report viscoelastic properties in a rabbit tendinopathy model, and to provide a detailed mechanical analysis of tendinopathic tendons.

The methodologies developed offer researchers standardised means of assessing mechanical properties of soft tissue; in particular, elucidating abnormal behaviours with a view to isolating and identifying contributory factors to the aetiology and true effect of the disease.

Using these methodologies, it was found that tendinopathy had little influence on the mechanical behaviour of the tendon within the bounds and limitations of the study. These findings offer significant insights that may contribute to the development of better clinical management of tendinopathy, suggesting that treatment should be primarily concerned with pain management and tendon strengthening.

ACKNOWLEDGEMENTS

DEDICATION

I dedicate this thesis to the following people:

To my mum, Louise, and dad, Harry, who supported me through the entire process and went above and beyond as parents, editors, and mentors.

To my sister, Genevieve, who followed in my footsteps and inspired me to reach completion by beating me to the finish line.

To my girlfriend, Alison, for understanding when my thesis took priority.

To my mentor, Robert, who inspired me so much to work in the field.

And to my supervisor, Brett, who showed faith in me many years ago and allowed me to get to where I am.

Without your help, this thesis would not be.

TABLE OF CONTENTS

TABLE OF FIGURES

TABLE OF TABLES

TABLE OF EQUATIONS

TABLE OF ACRONYMS

Acronym	Meaning
μCT	Micro computed tomography
3D	Three dimensional
ACL	Anterior cruciate ligament
ARC	Australian Research Council
AUD	Australian dollar
BMDC	Bone marrow-derived cells
CCD	Charged couple device
COX	Cyclooxygenase
CSA	CSA
CT	Computed tomography x-ray
CUT	Curtin University of Technology
CV	Correlation of variation
DIC	Digital image correlation
DNA	Deoxyribonucleic acid
ECM	Extracellular matrix
EGF	Epidermal growth factor
EMG	Electromyography
FEA	Finite element analysis
FEM	Finite element modelling
FGF	Fibroblast growth factor
GAGs	Glycosaminoglycans
GPs	Glycoproteins
HP	Hydroxylysyl pyridinium
IFT	Implantable force transducer
IGF	Insulin-like growth factor
IL	Interleukin
JNK	C-Jun N-terminal kinase
LM	Linear model
LMER	Linear mixed effects regression
LM-MLE	Linear model-Maximum likelihood estimate
LSCM	Laser scanning confocal microscopy

LTB	Leukotriene-B
MLE	Maximum likelihood estimate
MMP	Matrix metalloproteinase
MPa	Megapascal
MRI	Magnetic resonance imaging
mRNA	Messenger ribonucleic acid
MSC	Mesenchymal stem cell
MTS	Materials testing system
MVCs	Maximum voluntary contractions
NLMER	Nonlinear mixed effect regression
NLS	Nonlinear least-squares
NSAID	Non-steroidal anti-inflammatory drugs
NZW	New Zealand White
PBS	Phosphate buffered solution
PDGF	Platelet-derived growth factor
PG	Proteoglycan
PGE	Prostaglandin-E
PMMA	Poly-methyl methacrylate
QLV	Quasi-linear viscoelastic
RICE	Rest-ice-compression-elevation
SAPK	Stress activated protein kinases
SLS	Structured-light scanning
SWL	Structured white light
TEC	Thermoelectrically cooled
TEM	Transmission electron microscope
TGF	Transforming growth factor
TIMP	Tissue inhibitor of metalloproteinase
TOST	Two one-sided test
UTS	Ultimate tensile strength
UWA	University of Western Australia
VEGF	Vascular endothelial growth factor

CHAPTER 1.   PROLOGUE

1.1. Purpose

This dissertation forms part of an Australian Research Council (ARC) Linkage project, LP110100581, titled *Bioengineered Bioscaffolds for Achilles Tendinopathy Treatment*. The aim of the project is to improve the outcomes of surgical treatment of Achilles tendinopathy via research based on a New Zealand White (NZW) rabbit (*Oryctolagus cuniculus*) tendinopathy model. In order to evaluate the efficacy of the techniques developed, the validity of the tendinopathy model was rigorously tested. This dissertation aimed to evaluate the tendinopathy model from an engineering perspective.

1.2. Problem

Musculoskeletal conditions are common, with 30 million cases of injury reported annually worldwide (Walden *et al.*, 2016). Despite being the largest and strongest tendon in the body, the Achilles tendon is reported to be involved in the most sports-related tendon injuries (Freedman *et al.*, 2014a). Injury is regularly seen in ageing athletes who participate in repetitive explosive activities (Flood and Harrison, 2009; Woo *et al.*, 2000). It has been reported that ruptured tendons show significant degeneration compared with normal controls (Kannus and Józsa, 1991; Tallon *et al.*, 2001), suggesting disease may precede and possibly contribute to rupture.

1.3. Tendon

Tendons are a soft connective tissue designed to efficiently transfer loads generated by muscles to the skeletal system, facilitating joint movement (O'Brien, 2005; Thorpe and Screen, 2016). These can be found as rounded cords, strap-like bands, or flattened ribbons, depending on the function.

1.3.1. Structure

Tendons exhibit a complex hierarchical structure arranged longitudinally to resist the direction of most tension (Kastelic *et al.*, 1978). Procollagen and tropocollagen molecules form collagen fibrils, considered the smallest structural unit of tendon (Screen and Evans, 2009; Sharma and Maffulli, 2005b; Wang, 2006). Fibres, comprised of fibrils, are bound by the endotenon,

a thin reticular connective tissue, and distributes various vessels and nerves (Sharma and Maffulli, 2005b; Wang, 2006). Fascicles, or fibre bundles, are the largest of the sub-units of tendon and exhibit a crimped waveform (Kastelic *et al.*, 1978). The whole tendon is usually surrounded by the epitenon, another thin reticular connective tissue which provides the primary vascular, lymphatic and nerve supplies for the tendon (James *et al.*, 2008; O'Brien, 2005). This structure is bound by cross-links at low levels of the hierarchy and a proteoglycan (PG) matrix at higher levels (James *et al.*, 2008; Thorpe and Screen, 2016). This hierarchy behaves like a composite material with complex micromechanics that allow the muscle-tendon-bone construct to act efficiently. Due to their composition and structure, tendons demonstrate viscoelastic behaviour (Arnoczky *et al.*, 2004; Kalson *et al.*, 2010; Woo *et al.*, 2000); that is, they exhibit time and strain rate dependent properties (Abrahams, 1967; Couppe *et al.*, 2009; Woo *et al.*, 2000).

1.3.2. Constituents

Tendons primarily consist of water (65–70% of wet weight) and collagen type-I (70–80% dry weight), with different types of collagen fibres, elastin, PG, and glycolipids making up the remainder (Calve *et al.*, 2004; Goh *et al.*, 2003; Lavagnino *et al.*, 2005; Rigozzi *et al.*, 2009; Woo *et al.*, 2007; Woo *et al.*, 2000).

Collagen type-I represents approximately 95% of all collagen in the tendon, with the remaining 5% collagen type-III and type-V (James *et al.*, 2008; Paavola *et al.*, 2002; Wang, 2006; Woo *et al.*, 2011). Collagen type-III is primarily found in aged and healing tendon, and in normal tendon is mainly limited to the insertion sites of highly stressed tendons and in the endo- and epitenons (Wang, 2006; Woo *et al.*, 2011).

Glycosaminoglycans (GAGs), glycoproteins (GPs), PGs make up the non-collagenous matrix components (Calve *et al.*, 2004; Paavola *et al.*, 2002; Sharma and Maffulli, 2005b; Wang, 2006). The non-collagenous matrix plays an important role within the tendon, including contributing to the mechanical properties (Thorpe *et al.*, 2013a), particularly the viscoelastic behaviour (Elliott *et al.*, 2003; LaCroix *et al.*, 2013a). For example, tenascin-C has been shown

to contribute to the mechanical stability of the extra-cellular matrix through interactions with collagen fibrils (Wang, 2006) and is up-regulated in tendinopathy (Sharma and Maffulli, 2005b), suggesting a role in injury or healing. GAGs have also been shown to influence the structural integrity and to regulate the mechanics of tendon (Connizzo *et al.*, 2013; Rigozzi *et al.*, 2009; Rigozzi *et al.*, 2013; Screen, 2008; Screen *et al.*, 2002a; Screen *et al.*, 2005b).

The remaining tissue consists of tendon cells, in the form of tenocytes (mature cells) and tenoblasts (immature cells), which are responsible for tissue homeostasis. Tendons have a low cell density (<5%) and this is thought to contribute to their limited healing capacity (Calve *et al.*, 2004; Woo *et al.*, 2011). Cells sit between the collagen fibres in short rows and their orientation is associated with the organisation of the fibres in the hierarchical tendon structure (Calve *et al.*, 2004; Sharma and Maffulli, 2005b; Wang, 2006; Woo *et al.*, 2011). These cells are responsible for developing and maintaining the tissue, as well as altering expressions of the extracellular matrix (ECM) proteins in order to adjust to changes in tendon environment, including healing of the tendon (Calve *et al.*, 2004; Wang, 2006).

1.3.3. Properties

Tendons exhibit properties well suited to their function – transferring forces from muscle to bone – such as stiffness, resilience, and strength (Doral *et al.*, 2010). It has been observed that tendons exhibit a wide range of mechanical properties due to the breadth of functions performed (Abramowitch *et al.*, 2010; Butler *et al.*, 1984; Woo *et al.*, 2011). As a result, tendon properties have been of interest to researchers for many decades (Benedict *et al.*, 1968; Blanton and Biggs, 1970; Cronkite, 1936). Knowledge of the mechanical properties not only contributes to understanding of the tendon function, but also provides inputs for simulations of the human body (Arampatzis *et al.*, 2005).

The Achilles tendon is generally regarded as the strongest tendon in the body (Bogaerts *et al.*, 2016; Doral *et al.*, 2010; Freedman *et al.*, 2014a; Peek *et al.*, 2016). Forces of 1–4kN have regularly been measured during jumping and

cycling, and peak forces of 9kN, or 12.5 times body weight, have been measured during running at full speed (Kongsgaard *et al.*, 2005; Paavola *et al.*, 2002; Peek *et al.*, 2016; Sharma and Maffulli, 2005b; Wang, 2006). The breaking stress of tendon is estimated to be 50–100MPa (Benedict *et al.*, 1968; Butler *et al.*, 1978; Hashemi *et al.*, 2005b; Kongsgaard *et al.*, 2005; Maganaris and Narici, 2005; Shadwick, 1990; Woo *et al.*, 2011). Stresses in excess of 70MPa have been measured *in vivo* (Kongsgaard *et al.*, 2005), and are regularly reported between 30 and 60MPa (Couppe *et al.*, 2009; Geremia *et al.*, 2015; Hansen *et al.*, 2006; Stenroth *et al.*, 2016). Stress in the Achilles tendon *in vivo* has been estimated to be as high as 110MPa (Komi, 1990). Hence, peak stress *in vivo* may in some cases exceed the measured ultimate tensile strength (UTS) of the tendon (Sharma and Maffulli, 2005b), illustrating the complexity of tendon mechanics *in vivo*.

1.4. Tendinopathy

Disease of the tendon, known as tendinopathy, is characterised by pain and reduced mobility and functionality. The pathology is complex, including disordered healing causing fibre disruption and disorientation, generally with an absence of inflammatory cells. The aetiology and progression of the disease is not well known, leading experts to coin the term tendinopathy to describe the clinical presentation of the condition (Almekinders *et al.*, 2003; Maffulli, 1998).

Degenerated tendons exhibit decreased mechanical properties, such as stiffness and UTS (Hansen *et al.*, 2013; Helland *et al.*, 2013), and are generally observed to be disordered with a larger cross-sectional area (CSA), a lower stiffness, and a lower elastic modulus (Arya and Kulig, 2010; Helland *et al.*, 2013). However, tendons are known to exhibit plasticity (the adaptability of an organism to changes in its environment or differences between its various habitats) (Arampatzis *et al.*, 2010; Bohm *et al.*, 2014) via mechanobiological responses (Arnoczky *et al.*, 2007; Wang, 2006). Mechanical loading may, therefore, play an important role in the degradation, and possibly treatment, of tendinopathic tendons.

1.4.1. Prevalence and incidence

The true population prevalence and incidence rates of tendinopathy are not known. Most studies have been performed retrospectively and limited by factors such as population sample and database (Huttunen *et al.*, 2014). The prevalence of tendinopathy has been estimated at 11.83 per 1000 persons per year, with an incidence rate of 10.52 per 1000 persons per year (Albers *et al.*, 2016). Achilles tendinopathy has been reported to be as prevalent as 6–9% of some populations (de Jonge *et al.*, 2011), with 4% of sufferers going on to suffer rupture of the tendon (Yasui *et al.*, 2017).

1.4.2. Aetiology

Tendinopathy is traditionally considered an overuse injury caused by repetitive strain of the tendon (Paavola *et al.*, 2002; Rodenberg *et al.*, 2013; Sharma and Maffulli, 2005b; Woo *et al.*, 2000). However, this traditional view is unproven, and has been challenged by several authors, including Arnoczky *et al.* (2007) and Rees *et al.* (2009). Previous studies attempting to elucidate the aetiology for tendinitis found that repetitive loads caused microscopic failure of the collagen matrix, triggering an inflammatory response (Almekinders, 1998; Woo *et al.*, 2000). However, the lack of inflammatory markers in many cases means tendinitis can only be confirmed with histology, and thus tendinopathy is the preferred term (Rees *et al.*, 2009). A recent hypothesis is that microdamage may lead to isolation of segments of the tendon which in turn leads to underuse (Arnoczky *et al.*, 2007).

1.4.3. Treatment

Due to a lack of evidence-based management, treatment has traditionally been conservative, with surgery considered the last resort due to the lack of evidence for its efficacy (Maffulli *et al.*, 2015; Woo *et al.*, 2000). Conservative management techniques primarily aim to relieve the symptoms of tendinopathy(Paavola *et al.*, 2002). Counterintuitively, many conservative treatment options now involve applying load to the tendon via eccentric exercise, but this remains controversial (Peek *et al.*, 2016; Rees *et al.*, 2009; Sharma and Maffulli, 2005b).

The consequences of tendon injuries are pronounced, and the underlying causes and tissue responses must be better understood in order to develop improved treatment and prevention techniques.

1.4.4. Models

Study of tendinopathy in humans is difficult – biopsy of patients is invasive and clinical presentation is usually advanced, thereby limiting information of disease progression (Warden, 2007). Many animal models have been developed to investigate tendinopathy (Dirks and Warden, 2011; Lake *et al.*, 2008; Lui *et al.*, 2011; Warden, 2007). These offer the advantage of being controlled and reproducible, allowing for regular observation and evaluation over time (Lake *et al.*, 2008). There is no 'gold standard' model, leading researchers to utilise a variety of animals depending on the application (Warden, 2007). Understanding of the behaviour and physiology of the animal is essential for comparing with humans (Lui *et al.*, 2011). Ultimately, a valid animal model must be repeatable and be substantially similar to humans clinically, histopathologically and functionally (Lui *et al.*, 2011). Rabbits are a popular model as their cellular and tissue physiology approximates that of humans (Warden, 2007). Additionally, their larger tendons are easier to work with and provide larger samples compared to rodents (Lui *et al.*, 2011).

1.5. Structure of dissertation

The thesis of this dissertation is that tendinopathy adversely affects the mechanical behaviour of tendon, via disruption of the collagen matrix, resulting in a decrease in strength, stiffness, and resilience. This thesis will be evaluated through analysis of the literature and experimental testing.

This dissertation comprises nine (9) body chapters:

Chapter 2 summarises the literature regarding tendons and tendinopathy.

In order to accurately describe the mechanical properties of tendons, it is first necessary to accurately measure the morphology, in particular CSA which is used to calculate stress. Chapter 3 discusses the literature regarding CSA measurements, the importance of accuracy with respect to mechanical properties, and the development of improved measurement techniques.

Chapter 4 presents published work describing the use of structured light scanning (SLS) as a means of capturing the morphology of tendon. This chapter details an experiment to assess the efficacy of scanning compared to previously accepted methods for measuring CSA.

Chapter 5 investigates the measurement of tendon CSA under load using the methodology developed in Chapter 4. Since CSA is thought to decrease with increasing strain, engineering stress (force divided by initial area) may underestimate the true stress at higher strains.

Assessing the validity of the tendinopathy model from an engineering perspective requires physiologically relevant mechanical testing of the tendon. Chapter 6 provides a summary of the literature on mechanical testing of tendons, focussing primarily on the types of tests performed and experimental considerations.

Chapter 7 demonstrates the efficacy of the materials testing setup used for the remainder of the dissertation by way of load-to-failure testing of eight tendons.

Chapter 8 investigates the duration of testing required to accurately model long term viscoelastic behaviour of tendon, namely stress relation and creep behaviour. Many experiments have measured viscoelastic behaviour; however, there is little consensus on the duration required to accurately calculate the parameters. Since long intervals over multiple in vitro tests may result in degradation, it is necessary to determine an optimal testing duration in order to best predict the true parameters.

Chapter 9 defines a methodology for comprehensively describing the behaviour of tendon under physiological loads. With reference to the literature, the methodology proposes testing tendons in ramp, cyclic, stress relaxation and creep.

Using the proposed methodology, Chapter 10 compares the viscoelastic properties of healthy and degraded tendon. A collagenase model was employed to simulate tendinopathy in NZW rabbits. Viscoelastic parameters were determined by curve fitting using accepted viscoelastic models and

statistically compared to determine the effect of tendinopathy on the properties.

Chapter 11 discusses the thesis in relation to the methodologies and experimental findings and, most notably, evaluates the behaviour of normal and tendinopathic tendons from a mechanical perspective.

CHAPTER 2. LITERATURE REVIEW: TENDON

This review seeks to describe the current body of knowledge around tendon. There is a particular focus on the Achilles tendon – the specimen-of-choice in this dissertation – which is supported by reference to other tendons within the body.

2.1. Anatomy of the Achilles Tendon

The Achilles tendon is located at the posterior of the lower leg and extends from the calf muscles to the heel of the foot, or calcaneus (Doral *et al.*, 2010; Saladin, 2003). More specifically, it is the distal insertion of the triceps surae musculotendinous unit (Paavola *et al.*, 2002; Woo *et al.*, 2000). The Achilles is the largest and strongest tendon in the human body (Doral *et al.*, 2010; Freedman *et al.*, 2014a), with an average length of 15 centimetres (Doral *et al.*, 2010; Nickisch, 2009). The anatomy of the lower limb is shown in Figure 2-1.
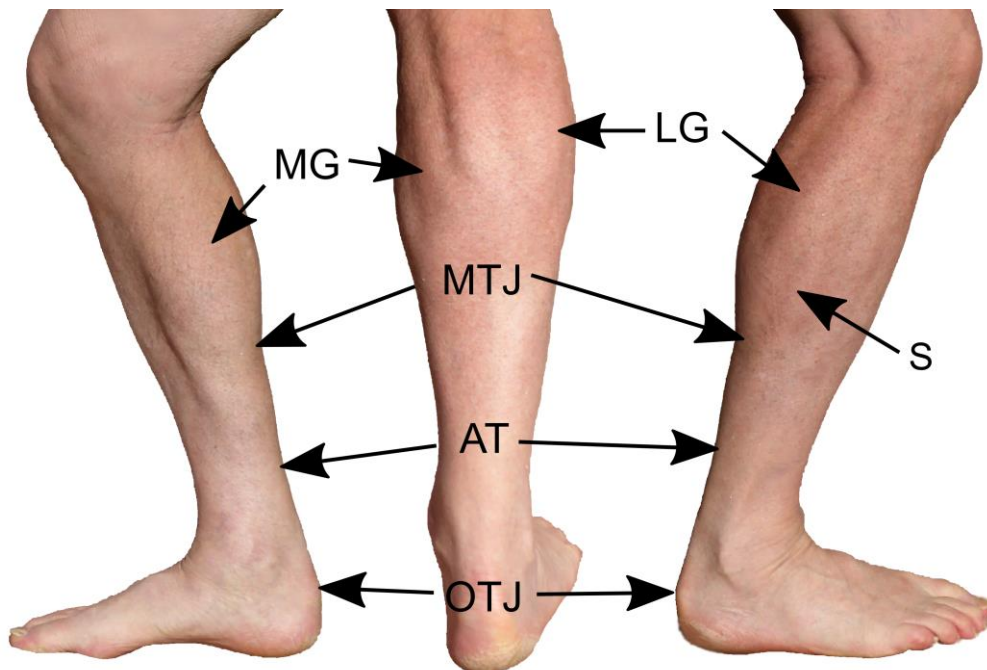
Figure 2-1: Anatomy of the lower limb as shown from the (left) medial, (middle) posterior and (right) lateral views. The medial (MG) and lateral (LG) gastrocnemius, soleus (S), myotendinous (MTJ) and osteotendinous (OTJ) junctions, and Achilles tendon (AT) are labelled.

The muscle unit, commonly referred to as the calf, is the composition of the soleus muscle and the two heads of the gastrocnemius, with the Achilles tendon being the fusion of the tendons and aponeuroses from these muscles (Paavola *et al.*, 2002; Saladin, 2003). The musculotendon unit is designed to enable plantar flexion, and limit dorsiflexion of the ankle joint (Saladin, 2003). The soleus muscle is primarily responsible for plantar flexion of the ankle, aided by the gastrocnemius, the muscle which also flexes the knee joint (Paavola *et al.*, 2002).

The soleus usually contributes more fibres (around 52%) (Nickisch, 2009) than the gastrocnemius (48%) (Doral *et al.*, 2010). Fibres of the tendon internally rotate approximately 90 degrees in a spiral manner so that the posterior fibres of the soleus terminate in the medial aspect of the calcaneus (Doral *et al.*, 2010; Nickisch, 2009). This rotation is thought to make elongation and elastic recoil possible during locomotion (Nickisch, 2009), and may result in an increase in strength (Doral *et al.*, 2010). *In vivo* measurements have also shown that the Achilles tendon can be subjected to uneven forces due to changes in the force generation of the individual muscles (Paavola *et al.*, 2002).

2.1.1. Myotendinous junction

The myotendinous, or muscle-tendon junction, allows the muscle to transfer forces to the tendon (Benjamin and Ralphs, 1996; O'Brien, 2005; Wang, 2006). Collagen fibrils from the tendon insert into deep recesses formed by myofilaments (Sullivan and Best, 2005; Thorpe and Screen, 2016). Muscle fibres produce tension via intra cellular contractile proteins (for example, actin and myosin), and this arrangement allows tension transfer to the collagen fibres (Trotter, 2002). This complex structure also reduces stress exerted on tendon during contraction, as it allows for a smooth gradient across the tendon-muscle boundary (Sullivan and Best, 2005; Thorpe and Screen, 2016). The myotendinous junction contains organs of Golgi and nerve receptors (O'Brien, 2005). This junction is considered the weakest point of the muscle-tendon unit (Sharma and Maffulli, 2005b; Wang, 2006); however, muscle-failure *in situ* has not been associated with failure of the junction, but rather of the muscle just proximal to the junction (Trotter, 2002).

2.1.2. Osteotendinous junction

The osteotendinous junction, or enthesis, connects the tendon to the bone (Almekinders *et al.*, 2003; Lu and Thomopoulos, 2013; Wang, 2006). This interface acts effectively to transfer loads from the tendon to the mechanically dissimilar bone with a minimal stress gradient (Almekinders *et al.*, 2003; Lu and Thomopoulos, 2013). The osteotendinous junction of the Achilles tendon and calcaneus creates a fulcrum, providing a mechanical advantage by increasing the lever arm (Doral *et al.*, 2010).

Two types of enthesis have been identified – fibrous, and fibrocartilaginous (Benjamin *et al.*, 2006; Lu and Thomopoulos, 2013; Wang, 2006). Fibrous entheses typically occur over a large area (Lu and Thomopoulos, 2013), and may attach indirectly to the periosteum or directly to the bone in adults (Benjamin *et al.*, 2006; Wang, 2006). Fibrocartilaginous entheses have a transitional fibrocartilage layer that helps to distribute the load and reduce the stress gradient between the two tissues (Wang, 2006). Achilles tendon insertions are an example of a fibrocartilaginous enthesis (Lu and Thomopoulos, 2013). Fibrocartilage is thought to be an adaptation to non-uniform tensile, compressive and shear forces (Almekinders *et al.*, 2003; Benjamin and Ralphs, 2004). The fibrocartilaginous enthesis can be considered four zones: tendon, fibrocartilage, mineralised fibrocartilage, and bone (Benjamin *et al.*, 2006; Lu and Thomopoulos, 2013; Nickisch, 2009).

This structure prevents the collagen fibre from bending, fraying, shearing, and failing at the enthesis (Sharma and Maffulli, 2005b). Directly anterior to the osteotendinous junction is the retrocalcaneal bursa which allows free movement between the tendon and the bone and sesamoid fibrocartilage (Benjamin *et al.*, 2006; Nickisch, 2009).

Estimates indicate the enthesis may experience four times the tensile forces of the mid-substance and may contribute to aetiology of enthesopathy – insertional tendinopathy (Wang, 2006). A review by Almekinders *et al.* (2003) on the role of compression in tendinopathy found that a non-uniform stress distribution within the tendon leads to lower stress on the joint side, coinciding

with areas with higher cartilaginous tissue. This has also been attributed with sites of pathological change in enthesopathy.

2.2. Physiology

Tendons are bands of soft connective tissue that connect muscle to bone, transmit forces, and facilitate joint movement (O'Brien, 2005; Sharma and Maffulli, 2005a; Woo *et al.*, 2000). They have been described as brilliant white with a fibroelastic texture, and can be found in the body as rounded cords, strap-like bands, or flattened ribbons depending on the requirements of the joint (Franchi *et al.*, 2007b; Sharma and Maffulli, 2005b). Tendons have high mechanical strength, good flexibility, and an 'optimal' level of elasticity (Screen and Evans, 2009; Sharma and Maffulli, 2005b) to ensure that they withstand the high loads that occur during daily activities (Screen *et al.*, 2002b).

Tendons act as shock absorbers and energy storage sites, and help to maintain stability (O'Brien, 2005). They are composed of densely packed fibres that act as a relatively inextensible link to efficiently transfer the loads generated by the muscle to the skeletal system (Benjamin *et al.*, 2008; Calve *et al.*, 2004). Tendons may be considered to be 'engineered' to their function requirements and, as such, tendons around the body exhibit different structures and compositions (Abate *et al.*, 2009; Thorpe and Screen, 2016).

Fibres are orientated parallel to the axis of loading to resist tensile forces (Almekinders *et al.*, 2003). At rest, fibres can be seen to have a wavy or crimp pattern under polarised light, which is thought to allow low-levels of tendon extension to protect the muscle and tendon from damage during high-impact loading (Franchi *et al.*, 2007a; Screen *et al.*, 2004a). The fibres of the Achilles tendon are known to spiral through 90 degrees between the myotendinous and osteotendinous junctions. This allows for the storage of energy which can be released for more efficient locomotion (Woo *et al.*, 2000).

Baratta and Solomonow (1991) demonstrated that, within the physiological range of forces developed via isometric contraction of the muscle, tendon acted as a near-rigid linkage, supporting the idea of efficient load transport

while suggesting that, at higher loads, the well-known nonlinear behaviour of the tendon may protect the muscle during loading.

2.3. Composition

Tendon is composed primarily of water (65–70% by mass) and collagen, the structural components of the extra-cellular matrix (Calve *et al.*, 2004; Sharma and Maffulli, 2005b; Wang, 2006; Woo *et al.*, 2011). Elastin is present in small quantities and has recently been shown to form complex structures with cells and collagen within the structural hierarchy of rabbit Achilles tendon (Pang *et al.*, 2016). Glycosaminoglycans (GAGs), glycoproteins (GPs), and proteoglycans (PGs) make up the most of the remaining non-collagenous matrix components (Calve *et al.*, 2004; Paavola *et al.*, 2002; Screen *et al.*, 2002a; Sharma and Maffulli, 2005b; Wang, 2006). The remaining tissue consists of tendon cells, in the form of tenocytes (mature cells) and tenoblasts (immature cells), which are responsible for tissue homeostasis.

2.3.1. Collagen

Tendon has a high collagen content (60–80% by dry weight), with 95% being collagen type-I and the remaining 5% collagen type-III and type-V (Calve *et al.*, 2004; Sharma and Maffulli, 2005b; Wang, 2006; Woo *et al.*, 2011). Collagen type-III is primarily found in aged and healing tendon, while in normal tendon it is mainly limited to the enthesis of highly stressed tendons and in the endo- and epitenons (James *et al.*, 2008; Wang, 2006; Woo *et al.*, 2011). Collagen type-III form smaller, less organised fibrils that are associated with a decrease in mechanical strength (Wang, 2006). In contrast, type-V collagen is intercalated into the core of type I collagen fibrils and regulates fibril growth and diameter (Wang, 2006; Woo *et al.*, 2011). Other collagens, including types II, VI, IX, X, and XI, are present in trace quantities in tendons (Benjamin *et al.*, 2008; Fukuta *et al.*, 1998). These collagens are mainly found at the bone insertion site of fibrocartilage (Wang, 2006).

2.3.2. Proteoglycans

PGs are the most abundant non-collagenous matrix molecules in the tendon (Screen *et al.*, 2005b). They are strongly hydrophilic and promote rapid diffusion of water-soluble molecules and the migration of cells (Kannus, 2000;

Sharma and Maffulli, 2005b). Content varies within the tendon and is dependent on the mechanical loading conditions, varying between 0.2–0.5% (dry weight) in purely tension-bearing tendon, and 3.5% (dry weight) in compression-bearing tendon (Wang, 2006). PGs are primarily responsible for the viscoelastic behaviour of tendons, but do not make any major contribution to their tensile strength (Benjamin *et al.*, 2008).

Tendons are known to contain decorin and aggrecan. Decorin, a small leucine-rich PG, is located on the surface of the middle portions of collagen fibrils (Screen *et al.*, 2002a; Wang, 2006). The interaction of decorin and collagen has been investigated in healthy tendon (Screen, 2008; Screen *et al.*, 2005b) and decorin has been found to influence the structural integrity of tendon by attracting water to the collagen fibrils to create a hydrated microenvironment (Screen *et al.*, 2002a). Decorin is also capable of controlling interfibril mechanics, in particular the facilitation of fibrillar slippage during deformation (Screen and Evans, 2009; Wang, 2006). Aggrecan holds water within fibrocartilage regions to resist compression via osmotic pressure (Wang, 2006).

2.3.3. Glycoproteins

Tendons contain the glycoproteins Tenascin-C, fibronectin, thrombospondin and elastin (Kannus, 2000). Tenascin-C is an important component of the extracellular matrix (ECM) and is abundant through the tendon body and at the junctions (Sharma and Maffulli, 2005b; Wang, 2006). Tenascin-C is elevated in response to stress and in degenerative and reparative processes (Benjamin *et al.*, 2008; Pajala *et al.*, 2009; Sharma and Maffulli, 2005b) It has been shown to contribute to the mechanical stability of the extra-cellular matrix through interactions with collagen fibrils (Wang, 2006) and may play a role in fibre alignment and orientation (Sharma and Maffulli, 2005b).

Fibronectin and thrombospondin are adhesive and participate in repair and regeneration processes (Sharma and Maffulli, 2005b). Fibronectin is located on the surface of collagens and is up-regulated to facilitate wound healing (Wang, 2006). Tendon usually contains 1–2% elastin (dry weight), which is

thought to contribute to the recovery of the tendon crimp pattern after stretching (Paavola *et al.*, 2002; Sharma and Maffulli, 2005b; Wang, 2006).

2.3.4. Tendon cells

Tendon contains fibroblasts in the form of tenoblasts and tenocytes, with reports of endothelial cells, synovial cells and chondrocytes (Paavola *et al.*, 2002; Sharma and Maffulli, 2005b; Wang, 2006). Tendons have a low cell density (<5%) and this is thought to contribute to their limited healing capacity (Calve *et al.*, 2004; Woo *et al.*, 2011). Cells sit between the collagen fibres in short rows and their orientation is associated with the organisation of the fibres in the hierarchical tendon structure (James *et al.*, 2008; Screen *et al.*, 2005b; Thorpe and Screen, 2016). These cells are responsible for developing and maintaining the tissue, as well as altering expression of the ECM proteins in order to adjust to changes in tendon environment (Calve *et al.*, 2004; Wang, 2006).

Tenoblasts are immature tendon cells with high metabolic activity (Kannus, 2000). They are spindle-shaped and have numerous cytoplasmic organelles. Tenoblasts mature into tenocytes (Kannus, 2000; Sharma and Maffulli, 2005b), elongated tendon cells with decreased metabolic activity and a low nucleus-to-cytoplasm ratio (Sharma and Maffulli, 2005b). Tenocytes are responsible for controlling matrix synthesis, metabolism, and repair in response to the activation of mechanotransduction pathways (Screen and Evans, 2009).

2.4. Structure

2.4.1. Hierarchy

Much of the heterogeneous and specialised mechanical behaviour of tendon can be attributed to its complex hierarchical structure. This structure can be seen clearly in Figure 2-2, as described by Kastelic *et al.* (1978).

Procollagen is a soluble molecule that is formed within the cells. Cross-links are then formed between the procollagen to produce tropocollagen, and then again to form insoluble collagen molecules (Kannus, 2000). These molecules are again cross-linked and aligned end-to-end in a quarter-staggered array to form collagen fibrils, which are the smallest structural unit of the tendon
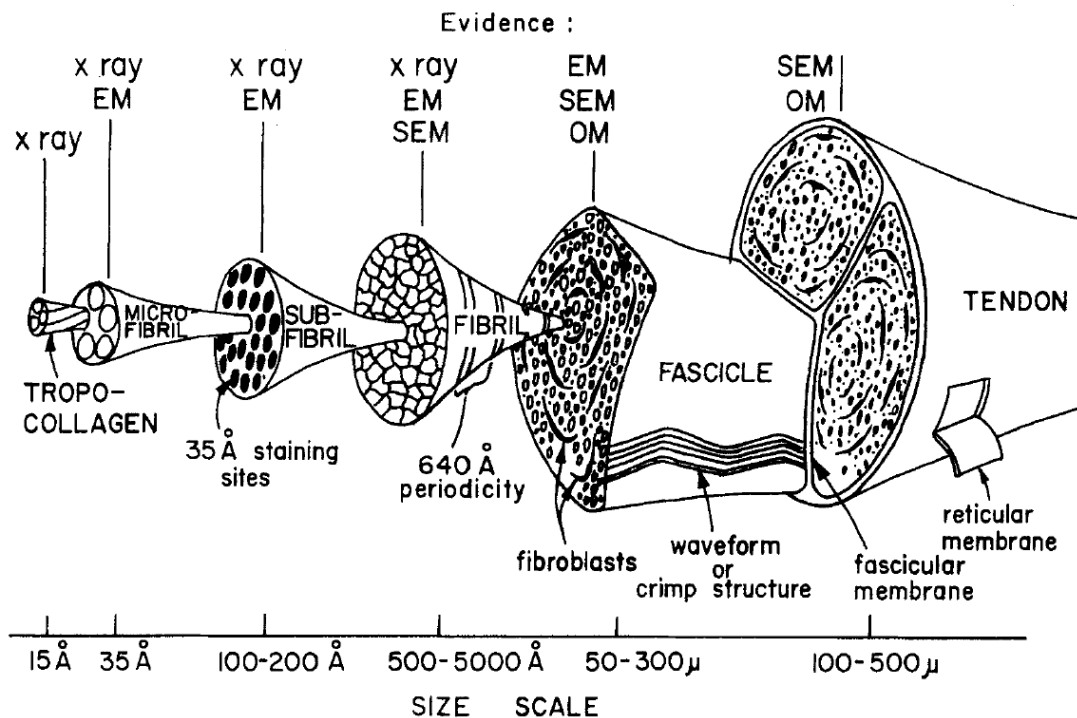
Figure 2-2: Tendon hierarchical structure described and published by Kastelic *et al.* (1978). Used with permission from Taylor & Francis Group (http://www.tandfonline.com).

(Screen, 2009; Thorpe and Screen, 2016). These fibrils have a diameter of 10–500nm depending on the species, age and sample location of the tendon (Thorpe and Screen, 2016; Wang, 2006). Fibrils mainly run longitudinally along the axis of loading; however, it has been noted that some fibrils run transversely and horizontally, forming spirals and plaits which may contribute to maintaining fibre binding (Sharma and Maffulli, 2005b). Studies have shown that younger specimens have a bimodal distribution of small and large fibrils, indicating that fibril diameter may play a role in the function of the tissue (Wang, 2006). It has been observed that extension and sliding of the collagen fibrils permits extension of the tendon (Arnoczky *et al.*, 2002a; Connizzo *et al.*, 2014; Lavagnino *et al.*, 2006; Lavagnino *et al.*, 2005; Screen, 2008; Screen *et al.*, 2004b; Thorpe *et al.*, 2013b). It has been hypothesised that these fibrils may be continuous, allowing the transmission of load directly rather than through interfibrillar couplings (Screen, 2008); however, due to limitations in medical imaging, it was previously not possible to image the entire tendon at a high enough resolution *in situ* to test this hypothesis. This remains inconclusive, as a recent study by Svensson *et al.* (2017) presented evidence to support this

hypothesis, while a second study by Wu *et al.* (2017) demonstrated discontinuity in the fibrils along the length of the tendon.

The next level of the hierarchy is composed of fibrils that are bound by the endotenon (Sharma and Maffulli, 2005b; Wang, 2006). Known as fibres, these are the smallest mechanically testable unit and are visible using light microscopy (Sharma and Maffulli, 2005b). Tendon fibres are known to exhibit a wavy configuration at rest, in what is commonly known as the crimp pattern (Kastelic *et al.*, 1978). This arrangement is best seen under a polarised microscope, but can also be seen using other techniques, such as transmission electron microscopy (TEM) and laser scanning confocal microscopy (LSCM) (Franchi *et al.*, 2007a; Harvey *et al.*, 2009; Wang, 2006). Tenocytes are located at the fibre level in rows along the line of the crimp (Screen *et al.*, 2004a).

The endotenon is a thin reticular connective tissue that envelopes the tendon fibres and also distributes many of the blood vessels, lymphatics and nerves within the tendon (O'Brien, 2005). Above the fibres are the fascicles of the tendon, or fibre bundles, which have been shown to exhibit interfascicular sliding as well as stretching, in order to more effectively and efficiently transmit load (Shepherd *et al.*, 2014).. New work has suggested that fascicles in the Achilles tendon are made directly of collagen fibrils rather than fibres (Wu *et al.*, 2017), potentially influencing understanding of tendon micromechanics.

Surrounding the fascicles is the epitenon, another thin reticular sheath of connective tissue, that binds the tendon body (James *et al.*, 2008; O'Brien, 2005; Paavola *et al.*, 2002). It sits loose on the tendon surface, and contains the primary vascular, lymphatic and nerve supplies for the tendon. It extends between the fascicles to bind with the endotenon and supply the tendon interior (Sharma and Maffulli, 2005b; Wang, 2006). In tendons without a true synovial sheath, the paratenon, or peritenon, is the outermost layer of loose areolar connective tissue (Kannus, 2000; O'Brien, 2005). This is designed to provide a sliding membrane, or elastic sleeve, that reduces friction and permits movement of the tendon within the surrounding tissue, such as between the crural fascia and the tendon (Kannus, 2000).

The mechanism of tendon elongation affects local strains, leading to the development of non-homogenous strain fields (Screen *et al.*, 2002a; Screen and Evans, 2009). The crimp pattern has developed to deal with the non-homogenous strain fields, straightening during loading and increasing the stiffness of the tendon to better match the dynamic requirements (Calve *et al.*, 2004; Screen *et al.*, 2002a; Screen *et al.*, 2002b). Due to the non-homogeneity of the tendon, it is difficult to predict the local strain based on gross loading conditions (Screen and Evans, 2009).

It has been observed that the crimp angle and length depend on tendon type and sample location and these affect the tendon's mechanical properties (Wang, 2006). Unpublished work by Screen *et al.* (2002b) suggests crimp periodicity is similar in bovine and rat tail fascicles under histological examination, and thus models would behave similarly during fibre straightening. This may indicate that cross-animal models are more reliable that cross-tendon models for studying tendon.

2.4.2. Extracellular matrix

The properties and behaviour of tendon are attributable to its ECM, which can be a product of the cellular response to the tissue loading. The primary structure is a collagen network, with a ground substance of PGs, GAGs, GPs, and several other small molecules (Benjamin *et al.*, 2008; Kannus, 2000). A non-collagenous matrix of PGs binds the structure together and maintains structural integrity throughout the tendon hierarchy (Screen *et al.*, 2004a; Screen and Evans, 2009). For example, dermatan sulphate GAG chains, found on the PG decorin, create links with collagen in tendon (Thorpe *et al.*, 2013a). It has been shown that other PGs and GPs may also bridge connections, making it difficult to determine maintenance of structural integrity (Screen, 2008). Elasticity within the tendon can be attributed to the presence of elastin fibres, as well as elastic proteins such as tenascin-C which provide additional elasticity in tendons such as the Achilles (Paavola *et al.*, 2002).

Tenocytes attach to the matrix via surface molecules called integrins, which also allow the cells to sense mechanical strains through the ECM (Screen *et al.*, 2004a). Through a process known as mechanotransduction, it is

believed that changes in the ECM are cell mediated – a biochemical response to mechanical stimulus designed to maintain long-term homeostasis in the tendon (Arnoczky *et al.*, 2004).

2.4.3. Vascularity and innervation

Tendons are relatively hypovascular, most likely due to their mode of function (Woo *et al.*, 2011). They have three primary blood supplies – two intrinsic vascular sources (myotendinous and osteotendinous junctions) and one extrinsic source (synovial/paratenon sheath) (Sharma and Maffulli, 2005b). The extrinsic system usually consists of the paratenon, or a combination of the synovial sheath and paratenon, depending on the presence of this sheath.

Tendon innervation originates from cutaneous, muscular and peritendinous nerve trunks (Sharma and Maffulli, 2005b). Nerves form a longitudinal plexus and enter the tendon via the endotenon septa (O'Brien, 2005; Sharma and Maffulli, 2005b). Branches may also pass from the paratenon via the epitenon to the surface or interior of the tendon (O'Brien, 2005). Myelinated fibres act as mechanoreceptors to detect changes in pressure or tension, while unmyelinated fibres act as nociceptors to sense and transmit pain (Sharma and Maffulli, 2005b).

The human Achilles tendon has a hypovascular region of 2–6cm proximal to the calcaneal insertion (Paavola *et al.*, 2002; Rees *et al.*, 2009). This was confirmed by angiographic injection techniques (Sharma and Maffulli, 2005b). Laser Doppler flowmetry has also indicated reduced blood flow near the insertion (Sharma and Maffulli, 2005b). Laser Doppler flowmetry of the Achilles tendon suggests a uniform blood supply along the tendon (Paavola *et al.*, 2002; Rees *et al.*, 2009; Sharma and Maffulli, 2005b).

Innervation in the Achilles tendon is primarily supplied via the attaching muscle and small fasciculi from the cutaneous nerves, in particular the sural nerve (Paavola *et al.*, 2002). The midportion of Achilles tendon is poorly innervated, with the majority of fibres terminating in the paratenon (Benjamin *et al.*, 2008). The Achilles contains numerous receptors relating to both pain and other neurotransmitter actions that connect to sensory nerve endings (Benjamin *et al.*, 2008; Paavola *et al.*, 2002).

2.5. Injury

Musculoskeletal conditions are common, with 30 million cases of injury reported annually worldwide (Walden *et al.*, 2016). Ranked as the fourth most common problem managed by General Practitioners in Australia (Australian Institute of Health and Welfare, 2010), annual expenditure of around AUD$4.0 billion make it the third costliest category in the health budget (Australian Institute of Health and Welfare, 2017). Resulting claims for compensation make up 16% of the nation's serious workers' compensation cases and result in a median loss of 8.4 working weeks and average costs of AUD$14,600 (Safe Work Australia, 2016).

Tendon injury and disease accounts for over 30% of all musculoskeletal injuries (Andarawis-Puri *et al.*, 2015) and up to 50% of all sport-related injuries (Walden *et al.*, 2016). Patient-induced and iatrogenic tendon and ligament injuries, in the form of traumatic and repetitive strain, can dramatically affect a patient's quality of life, with the number of injuries and cost expected to rise with an active ageing population (Butler *et al.*, 2008; Calve *et al.*, 2004). Tendons can be injured in a variety of ways, including trauma, repetitive strain, general degeneration, or donor-site morbidity from tissue grafts, leading to various pathologies, including tendinitis (acute condition) and tendinosis (chronic condition), up to partial or even complete rupture of the tendon (Woo *et al.*, 2011; Woo *et al.*, 2000). Injury is regularly seen in athletes who participate in repetitive explosive activities, such as running and playing basketball, and is significant in ageing athletes who are not regularly active (Flood and Harrison, 2009; Woo *et al.*, 2000).

Despite being the largest and strongest tendon in the body, the Achilles is reported to be involved in the most sports-related tendon injuries (Freedman *et al.*, 2014a). Approximately three quarters of Achilles tendon ruptures occur in middle-aged men participating in sport (Freedman *et al.*, 2014a), and the incidence is increasing significantly (Lantto *et al.*, 2015). It is thought that Achilles tendon rupture may be the result of gradual degeneration combined with a single traumatic event that results in tendon failure (Woo *et al.*, 2000). It has been reported that ruptured tendons show significant degeneration

compared with normal controls (Kannus and Józsa, 1991; Tallon *et al.*, 2001), suggesting disease may precede and possibly contribute to rupture.

There are four main pathologies of tendon – midportion tendinopathy, rupture, paratendinopathy, and insertional tendinopathy (Del Buono *et al.*, 2013) – that may be caused by one or many of the proposed aetiological factors (Sharma and Maffulli, 2005b; Woo *et al.*, 2000), including:

- Single traumatic event (such as an explosive push-off);
- External force, such as a blow, during contraction;
- Ischemia;
- Chronic degeneration (numerous causes, including age and diabetes);
- Shear stress between the gastrocnemius and soleus tendons;
- Malfunction of the normal protective pathways of the musculotendinous unit; and
- Use of pharmaceutical drugs, such as steroids.

However, despite the many suggested factors, the aetiology of tendon injury remains unclear (Sharma and Maffulli, 2005b).

The acceleration-deceleration mechanism has been reported as the cause of up to 90% of Achilles tendon ruptures, while degenerative tendinopathy is the most common histological finding associated with spontaneous ruptures (Sharma and Maffulli, 2005b). This has been reported by Arner *et al.* for 100% of cases (74 patients) and 97% of cases (891 patients) by Kannus and Jozsa, who also reported that 33% (of 445 patients) in the control group had degenerative changes (Sharma and Maffulli, 2005b). As a consequence of these studies, Sharma and Maffulli (2005b) proposed that tendon degeneration may predispose the tendon to rupture by gradually reducing the its tensile strength. It should be noted that this degeneration is more prevalent in ruptured tendon than in chronically painful overuse injuries, which are often associated with tendon degeneration (Sharma and Maffulli, 2005b).

Successful treatment of tendon injuries (that is, restoring functional outcomes) remains a clinical challenge (Butler *et al.*, 2008). Repaired tendon is often weaker than the original tendon and more susceptible to re-injury (Butler *et al.*,

2008). Rotator cuff repairs have been reported to have a failure rate of up to 40%, and can lead to alteration of normal shoulder mechanics (Butler *et al.*, 2008). As a result, there is strong debate as to whether ruptured tendons should be treated operatively or non-operatively (Woo *et al.*, 2000). It has been claimed that operative treatment may produce better results with a higher risk of complication, while non-operative treatment avoids the risk but yields lower return of function (Woo *et al.*, 2000).

Surgical management with tendon grafts is often required, but such treatment is associated with complications of reduced strength, joint stiffness, and repair-rupture, as well as donor-site morbidity (Sahoo *et al.*, 2010). Ideally repair (for partial or whole reconstruction) would utilise autologous tendon, but this option is limited due to tissue availability (Calve *et al.*, 2004). A tendon with similar mechanical and functional characteristics as the native tissue can prevent these complications (Sahoo *et al.*, 2010). However, in the case of the Achilles, no viable autologous sources are available. Synthetic materials are viable for short term solutions but lack long term suitability due to irreparable degradation. This in turn can result in additional damage to the surrounding tissue (Calve *et al.*, 2004). Thus there has been a push in recent years to find replacements with long term viability and property matching (Calve *et al.*, 2004). Tissue engineering is favoured as the most effective solution to persistent tendon injury as it is capable of addressing all the issues associated with surgical intervention (Butler *et al.*, 2008; Woo *et al.*, 2011).

2.5.1. Definition

Tendinopathy has been adopted as the general term for degenerative tendon disorders (Almekinders *et al.*, 2003) for use in clinical situations to describe conditions associated with pain and impaired performance where pathological changes are likely (Almekinders *et al.*, 2003; D'Addona *et al.*, 2017; Rees *et al.*, 2009; Sharma and Maffulli, 2005b; Wang, 2006). The terms tendinosis and tendinitis should only be used after histopathological confirmation (Rees *et al.*, 2009). There is currently no time period to define acute and chronic conditions; however, arbitrary time frames have been proposed to define acute as less than two weeks, sub-acute as two to six weeks , and chronic as more than six weeks (Paavola *et al.*, 2002). The anatomical location of the

tendinopathy within the tendon plays a role in determining the type of tendinopathy (Almekinders *et al.*, 2003).

2.5.2. Tendinopathy

The aetiology, pathogenesis, and natural course of Achilles tendinopathy, including the pathways and cellular mechanisms, are largely unknown (Paavola *et al.*, 2002). It has previously been proposed that tendinosis (chronic condition) is preceded by tendinitis (acute, inflammatory condition); however, no inflammatory cells have been found in chronic or degenerated tendons (Paavola *et al.*, 2002). No pathology has been performed on the acute disorder to confirm the progression (Paavola *et al.*, 2002). However, more recent reviews has argued for the role of inflammation in the early stages of tendinopathy (Battery and Maffulli, 2011; D'Addona *et al.*, 2017).

Tendon injuries can produce significant morbidity, with disability lasting up to several months despite appropriate management (Sharma and Maffulli, 2005b). Tendinopathy is often considered an overuse injury, as it is associated with intrinsic and extrinsic factors that can lead to chronic disorder (Sharma and Maffulli, 2005b). It has been suggested that tendinopathic degeneration is a failure of the tissue to adapt to mechanical loading, leading to an imbalance between degradation and synthesis of the matrix (Sharma and Maffulli, 2005b). Rather than degeneration, tendinopathy may be considered a failed healing response (D'Addona *et al.*, 2017).

Most of the treatment studies have been retrospective, and only a few have included objective criteria to evaluate the outcome (Paavola *et al.*, 2002; Rees *et al.*, 2009).

Tendinopathy is associated with pain, swelling, loss of mobility, and pain induced limitations (Paavola *et al.*, 2002; Rees *et al.*, 2009). Pain is a contentious symptom, as currently no scientifically-accepted hypothesis linking pain to the disease has been proposed, and evidence has shown no link between the disease state and level of pain (Sharma and Maffulli, 2005b) (Paavola *et al.*, 2002).

2.5.3. Pathology

It has been observed that ruptured tendons are often significantly more degenerated than tendinopathic tendons; however, the patterns of degeneration are similar (Arnoczky *et al.*, 2007). The pathology of tendinopathy is complex, as the causes and effects of the disease are known, but the process by which the disease develops is currently not well understood (Almekinders *et al.*, 2003). The pathological markers include (Arnoczky *et al.*, 2007; Sharma and Maffulli, 2005b):

- Disordered, haphazard healing causing fibre disruption and disorientation;
- Absence of inflammatory cells;
- Poor healing response;
- Non-inflammatory intratendinous collagen degeneration;
- Fibre disorientation and thinning;
- hypercellularity or hypocellularity;
- Scattered vascular ingrowth; and
- Increased interfibrillar GAGs.

Histologically, intratendinous changes are visible in 90% of biopsies, and include (Arnoczky *et al.*, 2007; Paavola *et al.*, 2002; Sharma and Maffulli, 2005b):

- Poorly demarcated intratendinous regions with a focal loss of structure; including a risk of discrete palpable nodules;
- Hypoxic degeneration associated with subcutaneous tendon rupture in more than 75% of ruptured tendons;
- Hyaline degeneration;
- Mucoid or myxoid degeneration;
- Fibrinoid degeneration;
- Fatty and lipoid degeneration;
- Calcification;
- Fibrocartilaginous or osseous metaplasia; and
- Greater variation in cellular density across areas of degeneration.

The enthesis is the site of pathological changes in many common athletic injuries (Rees *et al.*, 2009), while insertional tendinopathy is commonly seen in the supraspinatus (rotator cuff tendinopathy), common wrist extensor (lateral epicondylitis), patellar (Jumper's Knee) and Achilles tendons (Almekinders *et al.*, 2003)

In Achilles tendinopathy, there is often an irregular hypervascular pattern of capillaries and arterioles in the peritendinous tissue, along with development of loose granulated tissue that leads to scar formation. The prevalence and clinical relevance of these changes in Achilles tendinopathy is largely unknown (Paavola *et al.*, 2002). In chronic Achilles tendinopathy, histological examination has revealed (Paavola *et al.*, 2002; Sharma and Maffulli, 2005b):

- Peritendinous tissue appears thickened (macroscopic examination);
- Fibrinous exudate;
- Prominent and widespread proliferation of fibroblasts;
- Formation of new connective tissue; and
- Adhesions.

Imaging and surgical studies on insertional tendinopathy have demonstrated that thicker tendons with broad insertional sites are most commonly affected, and that the pathology appears predominantly on the joint side of the enthesis (Almekinders *et al.*, 2003).

Tendinopathic tendons exhibit degeneration of the tendon body, inflammation of the sheath, and sometimes degeneration of the sheath (Sharma and Maffulli, 2005b). The tendon body often shows limited or no inflammation at the time of diagnosis (Almekinders *et al.*, 2003), but can be hyper-cellular with a loss of collagen bundling, increased PG content and neovascularisation (Rees *et al.*, 2009). Animal models suggest there is no inflammatory process except in the most acute phase of the disease, and therefore it is expected that inflammation may only play a role in the initiation and not the progression of the disease (Battery and Maffulli, 2011; D'Addona *et al.*, 2017; Rees *et al.*, 2009). This is supported by Kannus and Jozsa, who found no evidence of inflammation in 398 ruptured tendons (Sharma and Maffulli, 2005b). However, other studies have found

inflammatory markers (Sharma and Maffulli, 2005b) suggesting other mechanisms may be involved.

During healing and remodelling of the Achilles tendon, myofibroblasts can be found in areas of scar formation within the peritendinous tissue, representing up to 20% of cells presented in chronic tendinopathy (Paavola *et al.*, 2002). These myofibroblasts use stress fibres to create forces for wound contraction and create an abundant amount of collagen, resulting in the formation of scar tissue and shrinkage of the peritendinous tissue (Paavola *et al.*, 2002). It appears that these cells may also play a role in the symptoms of tendinopathy, possibly causing contraction around the tendon, resulting in intratendinous tension and pressure and an increase in friction between the tendon body and surrounding tissue (Paavola *et al.*, 2002).

Apoptosis of tenocytes may also play a role in tendinopathy (Arnoczky *et al.*, 2007). Many patients exhibit an induction of apoptosis, and this is potentially linked to an up-regulation of strain-activated protein kinases (SAPK) (Arnoczky *et al.*, 2007; Sharma and Maffulli, 2005b), or the release of cellular tension (Arnoczky *et al.*, 2007). This potentially inhibits the rate of tendon repair (Arnoczky *et al.*, 2007) and could explain the gradual degeneration seen. However, it is unknown whether apoptosis is a cause or a result of tendinopathy (Arnoczky *et al.*, 2007).

Degenerative changes are seen in 30% of healthy, asymptomatic individuals 35 years or older and, therefore, the patient's history should be factored into the diagnosis of tendinopathy (Paavola *et al.*, 2002).

Similar to tendons exposed to repetitive strain, tendinopathic tendons exhibit an increase in degradative enzymes and inflammatory mediators, and understanding their induction has been the focus of many studies (Arnoczky *et al.*, 2007). For example, matrix metalloproteinase (MMP) mediated degradation of tendon ECM has been found in histological evaluation (Arnoczky *et al.*, 2007), in agreement with the observation of upregulation of the MMPs in the mechanical theory of tendinopathy.

2.5.4. Aetiology

The aetiology of tendinopathy is currently unknown. This is likely due to the interaction of intrinsic and extrinsic factors (Sharma and Maffulli, 2005b; Wang, 2006). Several theories have been proposed to describe the progression of tendinopathy (Arnoczky *et al.*, 2007; Sharma and Maffulli, 2005b); however, excessive and repetitive mechanical stimulation is considered to be the most likely trigger (Almekinders *et al.*, 2003; Wang, 2006; Woo *et al.*, 2000), causing an accumulation of micro-injuries (Shepherd *et al.*, 2014), especially in the presence of high risk intrinsic factors (Sharma and Maffulli, 2005b). This is akin to fatigue damage in engineering materials (Shepherd *et al.*, 2014). One controversial, but strongly related theory, is that it is a lack of mechanical stimulation that results in degeneration (Arnoczky *et al.*, 2007). While it is clear that degeneration is likely to be a cell-mediated event (Arnoczky *et al.*, 2002b), due to the lack of a reliable experimental model the cellular mechanism of tendinopathy remains elusive (Woo *et al.*, 2000) and the clinical and scientific basis for this hypothesis is incomplete (Almekinders *et al.*, 2003).

Many studies have investigated the aetiology of tendinopathy by studying the histology of tendinopathic samples; however, these studies are retrospective and do not identify the trigger that initiated the degenerative process (Woo *et al.*, 2000). An alternative method for studying tendinopathy has been to use a bacterial or chemical agent to degenerate the tendon. This method appears to represent the chronic condition with no evidence of the acute condition, and may offer a reliable model for studies of treatments (Woo *et al.*, 2000) .

Theories

Several theories have been proposed for the aetiology of tendinopathy, with mechanical theory, vascular theory, and neural theory the most prevalent.

Mechanical theory appears most fitting due to the association between repetitive loading and degeneration. It proposes that repetitive loading results in micro-failure of the ECM, and that sustained repetitive loading may lead to insufficient healing of the tendon, in turn leading to gradual degeneration. The initial degeneration can lead to non-physiological strains within the tendon,

which may cause additional damage and alter the cellular response, eventually resulting in tendinopathy (Arnoczky *et al.*, 2007; Paavola *et al.*, 2002; Rees *et al.*, 2009; Sharma and Maffulli, 2005b; Wang, 2006). It has been suggested, therefore, that tendinopathy is a failure of the cell matrix to adapt to excessive changes in load, and that the cycle of degeneration be known as the 'tendinosis cycle' (Paavola *et al.*, 2002). This theory has been criticised due to the positive response of other tissues, such as muscle and bone, which increase in strength when exposed to excessive loading (Rees *et al.*, 2009). The theory appears plausible, due to the lower cellularity of the tendon, but no mechanism has been implicated in altering the cell-matrix interactions (Arnoczky *et al.*, 2007). One proposed mechanism, based on cellular response *in vitro*, is that over-stimulation of the tendon cells creates a degenerative environment which, if sustained, may lead to chronic degeneration. Nevertheless, these studies have generally made use of non-physiological strain patterns or the use of external factors, thus limiting their clinical relevance (Arnoczky *et al.*, 2007).

Vascular theory suggests that overuse causes localised ischemia due to relatively poor blood supply, which in turn leads to tissue degeneration (Rees *et al.*, 2009). Ischemia has been shown to occur when a tendon is under maximal tensile load, with reperfusion releasing oxygen free radicals on relaxation, and is supported by an upregulation of the anti-oxidant enzyme Peroxiredoxin5 to protect the cells (Sharma and Maffulli, 2005b). This enzyme has been found to be upregulated in tendinopathy, indicating that oxidative stress may play a role in its progression (Sharma and Maffulli, 2005b). This theory is controversial in relation to a tendon such as the Achilles, as it suggests that the tendon is not hypovascular as is usually reported. An alternative theory is that the ischemia, or exercise-induced hyperthermia, may result in localised cell apoptosis which leads to an inhibited healing response (Rees *et al.*, 2009; Sharma and Maffulli, 2005b).

The final theory, neural theory, suggests that degenerative mediators are released by the neural system. This does not explain, however, why the pain is not present in all cases (Rees *et al.*, 2009).

Training has been identified as a likely factor in the development of tendinopathy, through repetitive overload that results in a persistent injury (Almekinders *et al.*, 2003). This has been attributed to poor technique, as well as athletic equipment, such as shoe wear in runners or choice of racquet in tennis players (Almekinders *et al.*, 2003).

It has been identified that, without a proper experimental design, any conclusions regarding the aetiology of tendinopathy are purely speculative (Almekinders *et al.*, 2003). A review by Almekinders *et al.* (2003) of various studies found that:

- There is a moderate relationship between injury rate and mileage (but did not distinguish between other potential factors);
- Rest in military recruits did not prevent injury;
- There is not a significant relationship between most intrinsic factors and patellar tendinopathy;
- Flexibility is correlated with overuse injuries (but is not limited to tendinopathic injuries);
- Shoe modification can reduce stress fracture rate, but not tendon problems; and
- Overuse injuries, including tendon problems, are more common in older athletes (compared to younger athletes) but found there is no correlation between Achilles tendon problems and the amount of training or years of involvement in a sport.

It has been argued that intrinsic factors may increase the likelihood of the development of tendinopathy (Rees *et al.*, 2009). However, there is a need to discriminate between the effect of age resulting in intratendinous changes, and predisposition to tendinopathy (Rees *et al.*, 2009). For example, tendons become stiffer and less capable of tolerating excessive load as age increases; however, moderate loading in older people should not increase prevalence of tendinopathy (Rees *et al.*, 2009). It has been found that that factors such as alignment issues and biomechanical faults, including ankle instability, flexibility and muscle imbalance, play a role in two-thirds of Achilles tendon disorders in athletes (Almekinders *et al.*, 2003; Sharma and Maffulli, 2005b) and,

therefore, patients should be examined for these factors (Paavola *et al.*, 2002). For example, hyperpronation of the foot has been linked with an increase in the prevalence of Achilles tendinopathy (Sharma and Maffulli, 2005b), and thus identification may enable correction and subsequent prevention of further injury.

Overuse

Tendons such as the Achilles are subject to strains of 8–10% during physiological loading (Rees *et al.*, 2009). The term 'overuse injury' has been used to describe a mode of injury through repetitive stretching that results in the inability of the tendon to endure further tension (Wang, 2006). This can lead to pathological changes in the tendon, known as tendinopathy (Rees *et al.*, 2009). This is known as the mechanical theory of tendinopathy.

While usually restricted by a pain-response in the tendon, continual overuse may progress from fatigue damage to complete rupture of the tendon (Sharma and Maffulli, 2005b), and may explain the high correlation of spontaneous ruptures exhibiting degenerative changes. Due to difficulties in identifying and studying the onset of tendon degeneration, few studies have been conducted in non-traumatic overuse tendon injuries (Wang, 2006).

Studies have suggested that insulin-like growth factor-1 (IGF-1) may be involved in the development of tendinitis (Woo *et al.*, 2000), as it is upregulated during overstimulation. This has also been shown to upregulate inflammatory mediators such as prostaglandin-E_2 (PGE$_2$), interleukin-1 (IL-1), and IL-6 and leukotriene B_4 (LTB$_4$) (Sharma and Maffulli, 2005b; Wang, 2006; Woo *et al.*, 2000). The presence of abundant leukotrienes in injured tissue is sufficient to induce tissue oedema, which is seen in tendons with tendinopathy (Wang, 2006). Additionally PGE$_1$ and PGE$_2$ have been shown to result in degeneration of the tendon matrix (Wang, 2006). Levels of PGE$_2$ have been shown not to be significantly different in healthy and symptomatic tendons; however, further studies may be necessary (Wang, 2006). Cells in the presence of IL-1β have been shown to increase production of messenger ribonucleic acid (mRNA) for degenerative proteins cyclooxygenase-2 (COX), MMP-1, MMP-3, and PGE$_2$,

while tendons stretched in the presence of IL-1β also increased production of MMP-3 (Sharma and Maffulli, 2005b).

Mechanical loading studies have varied with regard to the strain protocol used, and direct comparison of their results is often difficult. The amount and frequency of application of strain may determine the type and amount of cytokines released (Sharma and Maffulli, 2005b).

A downregulation of MMP-3 mRNA, as well as an upregulation of MMP-2 and vascular endothelial growth factor (VEGF) has been seen in Achilles tendinopathy, compared to control, while decreased MMP-2 and MMP-3 and increased MMP-1 activity has been seen in ruptured supraspinatus tendons (Sharma and Maffulli, 2005b). This is challenged by a rabbit model of supraspinatus tears, which showed an increase in the expression of MMP-2 and tissue inhibitor of metalloprotenaise-1 (TIMP-1) (Sharma and Maffulli, 2005b). It has been suggested that repetitive load may cause a release of cytokines, which may in turn lead to an increase in MMP production resulting in degradation of the ECM (Sharma and Maffulli, 2005b).

Studies into mechanotransduction pathways have demonstrated that cells respond to physical stress by activating SAPKs, including c-Jun N-terminal kinase (JNK). While the SAPKs are associated with a diversity of biological processes, SAPK/JNK have been implicated in the initiation of apoptosis in some cell lines when exposed to repetitive strains and, therefore, may be involved in creating localised areas of hypo-cellularity in tendinopathy tendons (Arnoczky *et al.*, 2002b).

Underuse

An alternative hypothesis in the mechanical theory of tendinopathy states that it is understimulation, not overstimulation, of the tendon that leads to tendinopathy (Rees *et al.*, 2009). It is suggested that micro-trauma may lead to localised areas of under-stimulated cells which, in turn, leads to a catabolic response and degeneration (Arnoczky *et al.*, 2007; Rees *et al.*, 2009). While contradicting the traditional assumption of overuse as the protagonist in tendinopathy, it is argued that the micro-damage of fibrils precludes transmission of strain to the tenocytes which results in under-stimulation, and

a catabolic response, further weakening the tissue (Arnoczky *et al.*, 2007). This micro-damage can be the result of a single traumatic event, such as a fall, or from repetitive or abnormal stresses within the tendon (Arnoczky *et al.*, 2007). Stress shielding, or stress deprivation, has been shown to upregulate MMP-1, while the reintroduction of mechanical load has been shown to inhibit production *in vitro* (Arnoczky *et al.*, 2004). This theory is supported by Almekinders *et al.* (2003). Stress shielding of the transversely-compressed side of the enthesis shows atrophic changes similar to those described, and has been seen to develop degenerative lesions within this region over time. A counterproposal is that weakening caused by stress shielding may enable overuse-associated microdamage (Almekinders *et al.*, 2003).

Avenues identified for future study include histopathological description of acute and subacute tendinopathy, accurate description of the mechanisms of pain, and the magnitude of tendon forces experienced during common activities (Arnoczky *et al.*, 2007; Paavola *et al.*, 2002). In addition, randomised, controlled trials should be explored for corticosteroids, strengthening modalities, growth factors, and gene therapy (Paavola *et al.*, 2002).

2.6. Management

Due to the poor correlation between pain and degeneration in tendinopathic tendons, management becomes an important factor. Management has been described as "more art than science" as it lacks evidence-based support (Kader *et al.*, 2005; Kader *et al.*, 2002). Pain is often the only obvious symptom, therefore the need to modulate pain is the limiting factor in dealing with tendinopathy (Rees *et al.*, 2009). The results of treatment in chronic tendinopathy are unpredictable, and so early treatment is advised (Kader *et al.*, 2005; Maffulli *et al.*, 2004). As prevention is better than cure, particularly in the case of repetitive loading, it is important to have appropriate coaching, technique, and equipment to minimise the risk of injury (Kader *et al.*, 2002; Rees *et al.*, 2009). Counterintuitively, many conservative treatment options involve loading the tendon in some way, though most evidence is still pre-clinical and can be contentious (Sharma and Maffulli, 2005b). It has been suggested that the success of this may lie in the belief that it is underuse through gradual degeneration that leads to disease (Arnoczky *et al.*, 2007),

and that loading may mitigate the stress deprivation. Still, the mechanisms that lead to the development of tendinopathy must be understood in order to develop effective treatment strategies (Wang, 2006). In most situations, conservative management is preferable, with surgical intervention limited to chronic conditions (Maffulli *et al.*, 2004).

2.6.1. Conservative management

Conservative management techniques primarily aim to relieve the symptoms of tendinopathy, including the control of inflammation (Paavola *et al.*, 2002). The literature describes many interventions that have not been studied in a controlled or prospective manner, and their effectiveness is not well evaluated, especially long term (Paavola *et al.*, 2002). Unfortunately, current conservative treatment options are not universally effective and 24–45.5% of patients will require surgical intervention (Kader *et al.*, 2002; Maffulli *et al.*, 2004; Woo *et al.*, 2000).

Rest and mobilisation

Rest has traditionally been the most commonly-prescribed treatment, affording the tendon time to heal (Kader *et al.*, 2002). In extreme cases, controlled immobilisation such as splinting and taping may be used (Paavola *et al.*, 2002; Wang, 2006). Early rehabilitation has been found to be one of the most effective treatment methods, as the mechanical stimulation can increase tendon regeneration and reduce scar tissue and formation of adhesions (Rees *et al.*, 2009). Conversely, prolonged immobilisation has been shown to result in adhesion formation and a decreased range of motion, as well as atrophy of the tendon (Schwartz *et al.*, 2015; Woo *et al.*, 2000). Thus, passive mobilisation is preferred to complete immobilisation (Schwartz *et al.*, 2015). This is in keeping with the hypothesis of underuse being the driver of degeneration (Arnoczky *et al.*, 2007) and current management trends which encourage mechanical stimulation of the tissue via passive and active mobilisation, such as exercise and physical therapy (Rees *et al.*, 2009; Wang, 2006).

Training, stretching, and massage

Training modification has been recommended to combat the risks of extrinsic factors, such as poor technique (Alrashidi *et al.*, 2015; Maffulli *et al.*, 2015; Magnan *et al.*, 2014; Paavola *et al.*, 2002; Roche and Calder, 2013). It has been suggested that stretching may provide assistance, as it elongates the muscle tendon unit and returns elasticity which, in turn, helps to restore joint mobility and decrease tendon strain in normal function (Kader *et al.*, 2002; Paavola *et al.*, 2002; Rees *et al.*, 2009; Wang, 2006). However, a literature search by Peters *et al.* (2016) reported that there is little evidence to support training modification or stretching in the management of tendinopathy.

Deep frictional massage has also been suggested way of providing stimulation (Kader *et al.*, 2002; Maffulli *et al.*, 2004), but has been shown to have little or no benefit (Rees *et al.*, 2009; Roche and Calder, 2013).

Exercise

Eccentric exercise is considered the greatest advance in tendinopathy management in recent times (Rees *et al.*, 2009) and is now a fundamental treatment for patellar tendinopathy (Schwartz *et al.*, 2015). Exercise has been shown to reduce pain in short-term controlled trials, and may help to normalise the structure (Kader *et al.*, 2002; Paavola *et al.*, 2002; Rees *et al.*, 2009). Eccentric bias has been shown to produce superior results to concentric bias (Kader *et al.*, 2002; Paavola *et al.*, 2002; Rees *et al.*, 2009), which may be due to the larger loads being able to more effectively stimulate the tendon. Nevertheless, prophylactic eccentric exercises may in fact increase the risk of tendinopathy in asymptomatic athletes (Peters *et al.*, 2016).

Therapies

Cryotherapy, following the Ice part of the Rest-Ice-Compression-Elevation (RICE) response to injury, seeks to reduce blood flow and swelling at the site of injury (Rodenberg *et al.*, 2013), and has been regarded as the most useful intervention in the acute phase (Maffulli *et al.*, 2004). It is primarily used as an analgesic but may also offer some therapeutic effects (Rees *et al.*, 2009; Schwartz *et al.*, 2015).

Controversial techniques include therapeutic ultrasound, electrotherapy, extracorporeal shock-wave therapy, laser phototherapy, pulsed magnetic fields, and radiofrequency coblation. Extracorporeal shock-wave therapy has shown benefits in some studies, and no benefit in others, and is recommended only after exhausting other options (Rees *et al.*, 2009; Sharma and Maffulli, 2005b). More recent reviews suggest extracorporeal shock-wave therapy is beneficial over a period of not less than three months, and in combination with eccentric exercises (Al-Abbad and Simon, 2013; Alrashidi *et al.*, 2015; Roche and Calder, 2013; Sussmilch-Leitch *et al.*, 2012).

Laser phototherapy increased collagen production in one study, and reduced post-operative oedema in another, but with no improvement in pain relief, grip strength, or functional results compared with controls (Sharma and Maffulli, 2005b). A more recent review suggests there are some benefits from laser therapy, such as a reduction in pain, but that it may be more applicable to inflammatory diseases (Rowe *et al.*, 2012). A second review supported the use of laser therapy in addition to eccentric exercise (Sussmilch-Leitch *et al.*, 2012).

Electrotherapy using electric fields, such as low-intensity galvanic current and direct current, has been successfully applied to tendon to promote healing (Ahmed *et al.*, 2012; Paavola *et al.*, 2002; Sharma and Maffulli, 2005b; Wang, 2006). Pulsed magnetic fields were shown to improve fibre alignment in one study, but found no difference in adhesion formation in another (Sharma and Maffulli, 2005b; Wang, 2006). Therapeutic ultrasound has been proposed for the acute stages and may benefit tendon healing (Kader *et al.*, 2002; Maffulli *et al.*, 2004). Again, systematic reviews of the literature have failed to reveal any benefits (Roche and Calder, 2013; Rowe *et al.*, 2012). Radiofrequency coblation stimulated an angiogenic response in normal rabbit Achilles tendon. When used in humans, rapid pain relief was seen in a preliminary study of 20 patients with tendinopathy, with magnetic resonance imaging (MRI) showing complete or near complete resolution of the tendinopathy in 10 of the 20 patients (Sharma and Maffulli, 2008; Sharma and Maffulli, 2005b).

Injections such as platelet-rich plasma and autologous blood injection have been suggested, but no conclusive evidence has been presented to support their use (Maffulli *et al.*, 2010).

Pharmaceuticals

The most controversial treatment is the use of pharmaceutical agents, in particular non-steroidal anti-inflammatory drugs (NSAIDs) (Paavola *et al.*, 2002; Wang, 2006). These have been shown to provide only symptomatic relief (Roche and Calder, 2013; Wang, 2006). A review of 32 studies into the use of NSAIDs showed only nine prospective and placebo-controlled trials, and of these five demonstrated analgesic effects, while healing was not evaluated in any of the studies (Rees *et al.*, 2009). It is thought that NSAIDs could potentially interfere with the healing process, as demonstrated in some animal studies (Rees *et al.*, 2009).

Corticosteroidal injections have also been trialled, but currently there is a lack of good evidence for their use (Kader *et al.*, 2002; Paavola *et al.*, 2002; Rees *et al.*, 2009). While no consensus has been reached on whether local injection increases the risk of tendon failure, has some short term benefits or has no adverse effects, a higher recurrence of injury has been seen in injected tendons compared to those that went untreated (Paavola *et al.*, 2002; Rees *et al.*, 2009). Peritendinous injections, such as autologous red cells and sclerosants, have been shown to be beneficial; however, a majority of studies surveyed by Paavola *et al.* (2002) and Rees *et al.* (2009) did not include controls, were underpowered or used generic assessment tools. Therefore, the effect of their use also remains unclear. Conversely, several quality studies have shown, using double-blind placebo control, that glycerol trinitrate applied topically can improve symptoms when compared to controls. This is most likely due to an increase in nitric oxide which enhances ECM and leads to improved mechanical properties in injured tendons (Rees *et al.*, 2009). However, its use as a treatment option remains contentious (Peek *et al.*, 2016).

2.6.2. Assisted healing

In the event that a patient is expected to outlive synthetic implants, it is desirable that a biological alternative be available to ensure satisfactory

durability. As a result, new biologically-based treatment methods to encourage repair and regenerate tissue are being explored (Mikos *et al.*, 2006). One particular avenue is the emerging field of tissue engineering, which may offer a more effective treatment option for tendon disorders. However, optimisation of engineered constructs is required in order to achieve desirable properties, vascularisation, and innervation (Sharma and Maffulli, 2005b).

Articles outlining functional tissue engineering, a roadmap, and parameters, intended to assist in the development of more complex and effective tissue-engineered constructs, have been published by Butler and colleagues throughout the 2000s (Butler *et al.*, 2008). This approach combines molecular biology, biochemistry and biomechanics (Woo *et al.*, 2011) but, as the treatments have developed, so too has the involvement from fields such as engineering. The primary objective is to augment the healing response by aiding the body's biological response (Butler *et al.*, 2008). The three primary areas of focus in this respect are cell-seeding, growth factors and cytokines, and the use of mechanical stimulation (Butler *et al.*, 2008). The desired outcome of these repairs is to replicate the behaviour of the tendon in terms of normal stress-strain behaviour and normal viscoelastic response, thereby returning tissue functionality (Butler *et al.*, 2008; Mikos *et al.*, 2006).

It is expected that tissue-engineered constructs will assist in areas where damage is irreparable and replacement is necessary (Sharma and Maffulli, 2005b). Many studies have met with limited success due to the complex nature of replicating *in vivo* conditions *in vitro* (Calve *et al.*, 2004). Nevertheless, as techniques are continually optimised, tissues are being produced that are replicating the original tissue (Mikos *et al.*, 2006). Calve *et al.* (2004) developed a protocol that repeatedly produced neonatal-like rat Achilles tendons, and was seen to be suitable for further research into each aspect of engineered constructs.

Scaffolds

Scaffolds are often the first area of focus in developing a tissue-engineered construct, as they provide the base from which the construct may develop, and as such should mimic the ECM of the native tissue in both structure and

function, and provide an attractive environment to promote tissue regeneration (Sahoo *et al.*, 2010; Woo *et al.*, 2011). As with current synthetic devices, a reliance on artificial scaffolds can lead to mechanical difficulties (Calve *et al.*, 2004). Therefore, it is desirable to find a biocompatible and resorbable scaffold. To this end collagen type-I has become one of the most common, although many collagen scaffolds have been found to have inferior properties and a high level of disorganisation (Calve *et al.*, 2004). Porcine small intestine submucosa, a collagen based scaffold, was found to be a viable scaffold (Woo *et al.*, 2011). Advances in scaffolds, through techniques such as cross-linking, have improved mechanical properties but have not yet reached optimal properties (Calve *et al.*, 2004). Sahoo *et al.* (2010) produced a biohybrid scaffold that demonstrated improved collagen production resulting in a stronger construct, and indicated that mechanical stimuli could be used to further enhance the quality of the constructs. It is anticipated that when used in conjunction with the other components of tissue-engineered constructs, bioscaffolds can enhance tissue regeneration (Woo *et al.*, 2011).

Cell therapy

One commonly discussed issue with tendon tissue is the low cellular density contributing to a sub-par healing response. Thus, a new avenue of treatment is the use of cell therapy, whereby additional cells are cultured and integrated into the site for regeneration. This is also a component of engineered tissue.

Fibroblasts and tenocytes are commonly used as they are the native cells of tendon; however, a recent focus has been on the use of adult stem cells, such as mesenchymal stem cells (MSCs) and bone marrow-derived cells (BMDCs) (Woo *et al.*, 2011). Use of these adult stem cells has been shown to improve healing in tendon compared to natural healing (Butler *et al.*, 2008; Rees *et al.*, 2009; Woo *et al.*, 2011).

There are several advantages to using adult stem cells over native tendon fibroblasts, including the ability to harvest from tissue not near the site of injury, an increased lifespan, faster differentiation, increased collagen production, low immunogenicity, and immunosuppressive properties allowing use as allogenic treatment. Additionally, they possess the ability to be cryo-preserved for

several years while retaining their ability to differentiate (Sahoo *et al.*, 2010). Stem cells are capable of differentiation into one of several mesenchymal tissues: careful biochemical and mechanical signalling can promote formation of specific tissues (Sahoo *et al.*, 2010).

Growth factors

Growth factors are one of the components of assistive healing, and can be boosted without requiring a full surgical intervention. Growth factors influence the process of regeneration, but finding the optimal dose and timing of the factors is necessary (Rees *et al.*, 2009; Woo *et al.*, 2011). Research has shown the potential for an increase in cell proliferation and migration, and ECM synthesis and production *in vitro*. (Woo *et al.*, 2011). The primary growth factors associated with tendon tissue healing are platelet-derived growth factor-BB (PDGF-BB), epidermal growth factor (EGF), IGF-I, and transforming growth factor-β (TGF-β) (Kofron and Laurencin, 2005). Fibroblast growth factor (FGF), EGF, PDGF-BB and TGF-β1 and TGF-β2 have been well studied *in vitro*; however, *in vivo* results have been contradictory (Sharma and Maffulli, 2005b; Woo *et al.*, 2011). While the focus is often on factors that promote synthesis of collagen, MMPs are important regulators of ECM and their expression is altered during healing (Sharma and Maffulli, 2005b). Injury and healing also results in a release of growth factors and cytokines from platelets, leukocytes, macrophages and other inflammatory cells, and these chemicals act to induce neovascularisation as well as migration and proliferation of tenocytes and collagen synthesis (Sharma and Maffulli, 2005b). The response of growth-factors and cytokines may be site-specific, further complicating the translation to clinical treatment (Sharma and Maffulli, 2005b). Nevertheless, growth factor delivery is an important area of tissue engineering. Incorporation into scaffolds, gene therapy and direct delivery are currently viable methods; however, researchers must now focus on the controlled timing of the delivery of these growth factors in order to optimise the healing process (Mikos *et al.*, 2006).

Gene therapy

Gene therapy involves the transfer of foreign nucleic acids into cells to alter protein synthesis or induce the expression of therapeutic proteins

(Sharma and Maffulli, 2005b; Woo *et al.*, 2011). This is done through mammalian viruses (adeno- and retro-viruses) and cationic liposomes as delivery vectors to deliver genes directly or indirectly (Woo *et al.*, 2011). Alternatively, antisense gene therapy can be used to block the transcription of specific genes that may be undesirable in tissue regeneration (Woo *et al.*, 2011). Using these techniques, gene expression can last for up to 10 weeks, making it suitable for clinical applications, and has been shown to be able to manipulate tissue environment in animal models (Sharma and Maffulli, 2005b). This technique has been identified as a potential solution to conventional drug delivery issues (Kofron and Laurencin, 2005). While several studies have shown improvements in healing in animal models, additional research is required to optimise and safely control the process (Sharma and Maffulli, 2005b).

Several studies have investigated the efficacy of gene therapy on ligament and tendon, as well as bone and cartilage. Concern still remains regarding the appropriate therapeutic dosage of specific cytokines. However, the first human clinical trial in the treatment of rheumatoid arthritis has shown that there is great potential in gene therapy (Kofron and Laurencin, 2005).

2.6.3. Prevention of adhesions

Adhesion formation is undesirable in tendons as it can prevent smooth load transfer during locomotion. Attempts to reduce adhesion formation include mechanical barriers, pharmaceutical agents, and hyaluronate, a component of synovial fluid, but no method is universally effective (Legrand *et al.*, 2017; Sharma and Maffulli, 2005b; Walden *et al.*, 2016). Myofibroblasts, a line of cells that resembles a fibroblast but expresses α-smooth muscle actin which permits it to behave as a muscle fibre, have been implicated in wound healing as a means of closing the wound but may also been responsible for the formation of adhesions (Sharma and Maffulli, 2005b). Further research, such as investigating engineered solutions (Baymurat *et al.*, 2015), is required to identify the mechanisms of adhesion formation in order to develop better prevention strategies (Legrand *et al.*, 2017; Sharma and Maffulli, 2005b).

2.6.4. Operative management

Surgical treatment of chronic tendinopathy is associated with poor outcomes (Kader *et al.*, 2002). Nevertheless, it has been found that between 24 and 45.5% of Achilles tendinopathy patients require surgery after exhausting conservative methods (Kader *et al.*, 2002; Paavola *et al.*, 2002; Rees *et al.*, 2009). Surgical treatment may include debridement, resection, muscle recession, or osteotomy to alter the biomechanics of the tendon (Peek *et al.*, 2016). Generally, the aim of surgery is to remove adhesions and degenerated areas and the outcomes are debatable (Kader *et al.*, 2002; Maffulli *et al.*, 2010). Complications have been reported in 10% of surgical treatments, but with 83% success (Peek *et al.*, 2016). A review of 23 studies by Rees *et al.* (2009) showed a favourable outcome was achieved in between 46% and 100% of cases, and that in three studies with more than 40 patients the figures were approximately 80–90%.

It has been noted in reviews that the scientific methodology behind published outcomes of tendinopathy after surgery is poor, and the higher rates of success are attributed with lower quality science (Paavola *et al.*, 2002; Rees *et al.*, 2009). For example, no prospective randomised studies have been used to compare surgical to conservative interventions (Paavola *et al.*, 2002).

It is not surprising, therefore, that the relationship between surgery and healing is not well understood (Paavola *et al.*, 2002). Part of the uncertainty can be attributed to the post-operative period of immobilisation, rest, and rehabilitation, which may also contribute to the rate of complication (Paavola *et al.*, 2002). Unfortunately, traditional repair techniques lack sufficient initial strength and potential for defects that prevent early active mobilisation. Therefore, new techniques, such as tissue engineering , are required to address this issue and permit a more active and controlled post-operative regimen (Woo *et al.*, 2000).

Post-operative treatment of tendon generally consists of various phases such as immobilisation, non-weight bearing mobilisation, weight bearing mobilisation, and a gradual return to exercise (Paavola *et al.*, 2002).

2.6.5. Mobilisation

Almost two decades ago, the prevailing view was that surgical repair of Achilles tendon disruption should be followed by a period of immobilisation. This is no longer supported, with many authors supporting early mobilisation and rehabilitation (Akizuki *et al.*, 2001; Calve *et al.*, 2004; Sharma and Maffulli, 2005b), because the introduction of mechanical stimulation promoting improved healing, strength and structure, while reducing stiffening, atrophy, and adhesions. After the inflammatory phase of healing, stretching may assist in fibre realignment as well as stimulate an increase in DNA content and protein synthesis through mechanical stimulation (Sharma and Maffulli, 2005b). Early mobilisation and weight bearing has seen patients return strength and power to similar levels pre-injury (Akizuki *et al.*, 2001).

2.6.6. Prognosis

The prognosis for Achilles tendinopathy is unclear since little is known about the natural course of tendinopathy (Paavola *et al.*, 2002). An eight-year follow-up study of 83 patients determined the long-term outcome for acute-to-subchronic tendinopathy is favourable (Paavola *et al.*, 2000). Twenty-four patients (29%) went on to undergo surgery; however, the vast majority of patients (84%) returned to full physical activity. A recent review by Scott *et al.* (2011) noted that this study was over 10 years old (now approaching 20 years) and "may not reflect current successes with comprehensive rehabilitation". However, no recent studies have been found.

2.7. Healing

Tendons that have been injured, such as through trauma, usually heal autonomously, while degenerative tendons do not and generally require intervention. Healing can occur intrinsically, by proliferation of epitenon and endotenon tenocytes, or extrinsically, by invasion of cells from the surrounding sheath and synovium (Sharma and Maffulli, 2005b). Intrinsic healing generally results in better biomechanics and fewer complications, such as normal gliding mechanism, while extrinsic healing can result in increased scar tissue formation, which in turn can lead to adhesions (Sharma and Maffulli, 2005b). The low metabolic rate results in slow healing of the tendon after injury (Calve *et al.*, 2004; Woo *et al.*, 2011). Healing tendons exhibit no difference with age

across a variety of metrics, such as maximum stress, strain, and modulus, suggesting the healing process is not age dependent (Voleti *et al.*, 2012).

2.7.1. Phases of healing

Tendon healing occurs in three distinct, but overlapping, phases: inflammatory, repair, and remodelling (Voleti *et al.*, 2012).

Inflammatory phase

The initial, inflammatory phase occurs immediately after injury and lasts for a few days. During this period, erythrocytes, platelets, and inflammatory cells, such as neutrophils, enter the injured site (Sharma and Maffulli, 2005b; Voleti *et al.*, 2012; Wang, 2006). Monocytes, macrophage, and neutrophils then begin phagocytosis of the necrotic and damaged tissue (Sharma and Maffulli, 2005b; Voleti *et al.*, 2012). Vasoactive and chemotactic factors are released to promote an increase in vascular permeability, initiate angiogenesis and recruit more inflammatory cells, as well as tenocytes, to assist in the stimulation of tenocyte proliferation (Sharma and Maffulli, 2005b; Wang, 2006). As tenocytes become more involved, type-III collagen synthesis begins repairing the tissue (Sharma and Maffulli, 2005b).

Repair phase

The repair phase, commonly referred to as the proliferation phase, begins towards the end of the inflammatory phase and lasts a few weeks (Voleti *et al.*, 2012). During this period tenocyte proliferation peaks, and synthesis of collagen, especially type-III and type-V, also peaks, indicating tissue healing (Sharma and Maffulli, 2005b; Woo *et al.*, 2011). Synthesis of other ECM compounds, including PGs, increases and water content and GAG concentrations remain high (Sharma and Maffulli, 2005b; Wang, 2006).

Remodelling phase

The remodelling phase is the final phase and can last anywhere from six weeks to one year. This phase sees a decrease in cellularity and a decrease in collagen and GAG synthesis (Sharma and Maffulli, 2005b; Voleti *et al.*, 2012; Wang, 2006). The remodelling phase can be considered in two stages – the consolidation stage and the maturation stage (Sharma and Maffulli, 2005b). The consolidation stage lasts for up to 10 weeks, during which the repaired

tissue changes from cellular to fibrous, tenocyte metabolism remains elevated, synthesis of collagen type-I increases (Sharma and Maffulli, 2005b; Wang, 2006), and tenocytes and collagen fibres gradually begin to realign with the direction of loading (Sharma and Maffulli, 2005b). The maturation stage sees a gradual change in the fibrous tissue to scar-like tendon tissue over the course of a year (Sharma and Maffulli, 2005b; Wang, 2006). Tenocyte metabolism and vascularity fall, while cross-linking of the collagen fibres increases, resulting in higher stiffness and tensile strength (Wang, 2006). Total collagen content and hydroxylysyl pyridinoline (HP) cross-link densities remain lower than normal healthy tissue, which is evident in the reduction of the mechanical properties of the tendon (Woo *et al.*, 2011).

2.7.2. Biochemistry

Nitric oxide

Several biochemical compounds have been shown to play a role in aspects of tendon healing. Nitric oxide has been shown to peak during the initial healing phases while nitric oxide synthase (which produces nitric oxide) inhibition results in a reduction in cross-sectional area (CSA) and failure load (Bokhari and Murrell, 2012; Murrell, 2007). Production of collagen and angiogenesis decrease with critically low oxygen levels and increase with elevated lactate (Voleti *et al.*, 2012).

Matrix metalloproteinases

MMPs have also been shown to be involved at different stages of healing. For example, MMP-9 and MMP-13 are thought to be involved in collagen degradation, whereas MMP-2, MMP-3 and MMP-14 are involved in degradation and remodelling (Voleti *et al.*, 2012; Wang, 2006). Other compounds identified include Substance P and calcitonin gene-related peptide (Sharma and Maffulli, 2005b). Imbalances between TIMPs and MMPs are associated with tendinopathy (Voleti *et al.*, 2012).

Cytokines and growth factors

Growth factors and cytokines also play important roles in the healing process. Five primary growth factors have been identified in the tissue healing process – IGF-I, PDGF, VEGF, basic FGF, and TGF-β. All of these growth factors have

been shown to upregulate and remain active during the healing process (Voleti *et al.*, 2012; Wang, 2006). IL1β, IL4, IL6, and IL10 have also been implicated in tendon healing (Voleti *et al.*, 2012).

2.7.3. Healed tendon

Complete restoration of the tendon to natural properties is never achieved, and can be seen in the reduction in the collagen type-I to type-III ratio (Rees *et al.*, 2009; Voleti *et al.*, 2012), resulting from a large increase in type-III collagen during the repair phase. This leads to less HP cross-linking and a subsequent reduction in the mechanical strength of tendon (Rees *et al.*, 2009). A study of transected sheep Achilles tendons indicated that the mechanical strength was only 56.7% of normal after one year (Sharma and Maffulli, 2005b). Another study of supraspinatus repair in rats found that stiffness and peak load were 40% and 60% lower after injury, respectively (Voleti *et al.*, 2012). Studies of tendon healing after a partial tenotomy has shown that the tendon progresses from developmental morphology to mature morphology in approximately 16 weeks (Calve *et al.*, 2004).

Healed tendons often exhibit complications such as scarring, resulting in decreased strength and increased stiffness, and adhesions, which disrupt tendon gliding (Sharma and Maffulli, 2005b; Voleti *et al.*, 2012). Healed tendon remains scar-like and never completely regains the properties pre-injury (Sharma and Maffulli, 2005b; Voleti *et al.*, 2012).

2.8. Mechanical stimulus

A fundamental feature of living tissue is a responsiveness to mechanical stimulation (Arnoczky *et al.*, 2007). Cells have the ability to sense and respond to load in order to maintain tissue homeostasis, a concept known as mechanotransduction (Ingber, 2006, 2008; Tamiwa *et al.*, 2006). This mechano-responsiveness elicits several mechanisms, including changes in metabolism, DNA synthesis, protein upregulation, ECM development, mitosis, and cell differentiation (Arnoczky *et al.*, 2002b; Butler *et al.*, 2008; Wang, 2006). Such changes can result in an improvement in tissue properties, such as an increase in CSA and tensile strength in tendon (Wang, 2006). Thus, mechanical forces are important in tissue development and repair (Shearn

et al., 2007; Wang *et al.*, 2015). They are also an essential element in successful tissue engineering of tendon constructs, repair, or regeneration (Butler *et al.*, 2008; Wang, 2006).

The importance of mechanical stimulation on tendon is well established in literature (Screen *et al.*, 2005b; Wang *et al.*, 2015), and is likely mediated through deformation of the ECM, which then deforms the cells (Arnoczky *et al.*, 2002a). It has been suggested that this is a mechano-electrochemical sensory system, whereby deformation of the cell via the membrane and cytoskeleton is sensed to elicit a response (Arnoczky *et al.*, 2007; Arnoczky *et al.*, 2002a; Arnoczky *et al.*, 2004). The concept of tensegrity was proposed by Ingber (1997) and suggests that cells are capable of maintaining constant tension between them and the ECM via a physical connection, whereby changes in the tension can be sensed by the nucleus (Arnoczky *et al.*, 2002a; Arnoczky *et al.*, 2004). It is known that integrins provide such a connection (Arnoczky *et al.*, 2007; Baria *et al.*, 2005); however, the exact attachment patterns of tenocytes within the tendon hierarchy is unknown (Arnoczky *et al.*, 2002a).

Deformation has also been shown to trigger stretch-activated ion channels, which control the influx of second-messenger molecules such as calcium. These molecules are known to trigger a myriad of cellular events (Arnoczky *et al.*, 2002a). Research by Arnoczky *et al.* (2002b) demonstrated that strain in the tendon caused nucleus deformation and noted a resulting increase in cytosolic calcium levels. Both of the signalling pathways – stretch-activated ion channels and tensegrity – rely on membrane anchored structures such as integrins to provide a direct feedback mechanism from the ECM to the cell (Arnoczky *et al.*, 2002a).

Cyclic loading has been shown to play a key role in the mechanotransduction response of tendon, regulating tendon health (Wang *et al.*, 2015) but playing a key part in the aetiology of overuse injuries (Arnoczky *et al.*, 2004; Arnoczky *et al.*, 2002b). It has been established that mechanical loading plays a role in tendon development (Gaut and Duprez, 2016); however, few studies have investigated this explicitly (Calve *et al.*, 2004). Calve *et al.* (2004) hypothesised that mechanical stimuli would induce cell-seeded tissue engineered constructs

to remodel and mature, and that studies on constructs could be used to elicit the roles of the various components of the tendon during loading. Understanding the effect of these loads on ECM interactions and adaptations would be beneficial in understanding tendon health (Arnoczky *et al.*, 2004).

Early studies investigating isolated tendon cells have identified changes in gene expression and proliferation as a result of cyclic strain regimes (Arnoczky *et al.*, 2002b; Banes *et al.*, 1999; Gilbert *et al.*, 1994; Petersen *et al.*, 2004; Screen *et al.*, 2005a; van Griensven *et al.*, 2003; Waggett *et al.*, 2006). More recent studies have investigated tendon cell response in three-dimensional (3D) models (Connelly *et al.*, 2010; Kuo and Tuan, 2010; Legerlotz *et al.*, 2013a; Maeda *et al.*, 2010; Saber *et al.*, 2010; Wang *et al.*, 2015). These studies continue to improve understanding of the role of tendon cells in homeostasis and repair, and in the aetiology of diseases such as tendinopathy (Sun *et al.*, 2015).

While the parameters for maintaining homeostasis are not known, it has been suggested that changes to the mechanobiological stimulation may play a role in the aetiology of tendinopathy (Arnoczky *et al.*, 2007). Abnormal loading can produce markers synonymous with degradation; for example, overuse and underuse can be catabolic (Rees *et al.*, 2009). Stress shielding and stress deprivation has been shown to reduce mechanical integrity and function (Arnoczky *et al.*, 2002a; Arnoczky *et al.*, 2004; Screen *et al.*, 2004a; Screen *et al.*, 2002b), including tissue catabolism through ECM degradation by MMPs (Arnoczky *et al.*, 2004). A reduction in loading with age leads to resorption of ECM, reduction in collagen fibre alignment and a decrease in mechanical integrity (Screen *et al.*, 2005b). In contrast, exercise has been shown to prevent hypertrophy and increase tensile strength (Screen *et al.*, 2002b) while the application of low-level cyclic load has been shown to prevent the degeneration of stress deprived tendon (Arnoczky *et al.*, 2004).

Tenocytes detect load and respond via mechanotransduction pathways to actively remodel ECM (Screen *et al.*, 2002b). Studies have examined different pathways in a variety of cell types to determine their contributions (Screen *et al.*, 2002b). For example, mechanical stimulation is thought to be important

in controlling fibre diameter distributions during maturation (Calve *et al.*, 2004; Screen *et al.*, 2005b), while compressive loading in tendon leads to an increase in fibrocartilage, collagen-II, and the PG aggregate (Screen *et al.*, 2005b). One sign of degradation is the change in cell morphology that has been correlated with gene expression associated with the degradation and synthesis of extracellular macromolecules (Arnoczky *et al.*, 2004). Chemically-induced changes to cell shape and the actin cytoskeleton have been shown to upregulate collagenase expression (Arnoczky *et al.*, 2004). Change of state of actin assembly in cells has been linked to collagenase expression, and was shown to nullify the load-induced inhibition of MMP-1 mRNA expression in a study by Arnoczky *et al.* (2004), further supporting this link and the efficacy of the mechanosensory tensegrity theory.

It has been hypothesised that the stimulation delivered during exercise may lead to improved tendon strength and stiffness. Arampatzis *et al.* (2007) demonstrated this may be true of sprinting; however, results for endurance runners were no different to those for non-exercisers. This may be due to the lower magnitude of stimulation.

2.8.1. Mechanotransduction

The importance of mechanical loading on tendons has been well documented; however, the effect of this load on tendon cells and mechanism of mechanotransduction is not well understood (Wang, 2006). It is known that the cellular response includes changes in gene expression, protein synthesis and cell phenotype, which can lead to changes in the overall mechanical properties (Wang, 2006). The mechanisms by which these microscale responses are triggered from the macroscale loading are not well understood.

Many cellular components are implicated in the mechanotransduction pathways, including the cytoskeleton, integrins, stretching-activated ion channels (Wang, 2006).

2.8.2. Micromechanics

The mechanisms involved in mechanotransduction are unclear (Arnoczky *et al.*, 2002a; Arnoczky *et al.*, 2004; Wang, 2006), but to understand the pathways there is a need to understand the local strain patterns (Screen *et al.*,

2002b). There is currently limited understanding of micromechanics in tendon and the role of the hierarchical structure in strain transfer from the gross tendon structure to the cells (Screen and Evans, 2009). An understanding of this strain transfer will not only provide knowledge of the function of the tendon, but may assist in the development of improved prevention and treatment options (Screen and Evans, 2009). Little information is known about the *in situ* strains at cellular level (Arnoczky *et al.*, 2002a), so it is important to investigate these strains (Screen and Evans, 2009). However, it has been previously noted that due to the heterogeneity of tissue, it is impossible to predict the exact strains likely to be experienced by individual cells (Screen *et al.*, 2002b). Therefore, it is important to understand how the magnitude of strain influences the cellular response.

With the use of surface markers, studies into tendon fascicle and gross tendon mechanics have demonstrated that strain is not homogenous along the length, illustrating the limitations of using grip-grip measurements (Screen and Evans, 2009). *In vivo*, strain has been measured within muscle-tendon units during muscle contraction using ultrasonography and MRI (Obst *et al.*, 2014a; Obst *et al.*, 2014b).

In order to measure the true micromechanical behaviour of tendon, studies will need to analyse viable, intact, and untreated tissue (Screen and Evans, 2009), preferably *in situ* or *in vivo*. Confocal microscopy is a useful technique for investigating intact tissue, allowing the ECM and cells to be visualised at resolutions of approximately 1µm. Studies using LSCM have shown a weak but positive correlation between tenocyte deformation and applied load (Screen and Evans, 2009). Several studies using LSCM to investigate tendon micromechanics (Screen and Evans, 2009; Screen *et al.*, 2005b), have shown:

- Crimp-straightening occurs at low loads, followed by fibre sliding and extension to facilitate further tissue extension, in agreement with X-ray diffraction studies;
- Collagen components are capable of independent movement within the matrix;

- Molecular and fibrillar level extension of collagen accounts for approximately 40% of the total tendon extension, suggesting that the primary extension mechanism is through sliding behaviour between fibrils and fibres within the tendon hierarchy;

- In addition to axial stresses, tensile loading may include shear and compression stresses; and,

- Local strains within the ECM are smaller than the applied strain.

Many *in vitro* studies into the effect of mechanical overstimulation on tendon cells have utilised artificial substrates to allow for greater control of the mechanical conditions (Arnoczky *et al.*, 2007; Arnoczky *et al.*, 2002a; Arnoczky *et al.*, 2004; Screen *et al.*, 2002b). These studies have demonstrated an activation of DNA synthesis, mitosis, gene expression and cell differentiation (Arnoczky *et al.*, 2002a). It has been previously discussed that these conditions do not replicate the normal *in situ* environment of tendon cells due to a lack of 3D ECM-cell interactions, while the strain magnitudes and durations used may not be physiologically relevant (Arnoczky *et al.*, 2007; Screen *et al.*, 2005b). As shown by Screen and colleagues, cell strains *in situ* have been shown to be considerably less than gross tendon strains (Arnoczky *et al.*, 2007; Arnoczky *et al.*, 2002a; Screen *et al.*, 2005b) and it is, therefore, unlikely that these conditions would be reached or maintained by cells *in vivo* (Arnoczky *et al.*, 2007). Additionally, tendons exhibit non-homogenous strain patterns that are impossible to replicate by uniform straining of a substrate (Arnoczky *et al.*, 2007). It has also been suggested that cell signalling in high density cell cultures may result in different behaviour compared to the low density of tendon cells *in vivo* (Arnoczky *et al.*, 2007). A further suggestion was that the gene response seen *in vitro* may not reflect that of *in vivo* conditions due to the lack of innervation and vascularisation, which may help to regulate the gene response of the tissue (Arnoczky *et al.*, 2004).

It has been shown, using LSCM, that chondrocytes found in articular cartilage deform in response to loading and that local strain results in measurable deformation of both the cell and nuclei (Arnoczky *et al.*, 2002a). A similar relationship was found in tendon (Arnoczky *et al.*, 2002a; Arnoczky *et al.*,

2004). The role of cellular deformation in mechanotransduction pathways has been the subject of great interest (Arnoczky *et al.*, 2002a).

A nonlinear loading behaviour has been observed in tendon, where cell movement was variable and attributed to the heterogeneity of the tendon hierarchical structure, as well as the geometric shape through the Poisson effect (Arnoczky *et al.*, 2002a).

Cell nuclei have been shown to have a stiffness comparable to the ECM, while the stiffness of the membrane is less (Arnoczky *et al.*, 2002a), suggesting that deformation of the cell may be involved in the mechanotransduction pathways. It has also been shown that local non-uniform deformation can occur in isolated fibroblasts under tensile load. The impact of the cell structure and the role of intracellular structures is not well understood (Arnoczky *et al.*, 2002a).

A study by Arnoczky *et al.* (2002a) suggested evidence for sequential straightening and loading of individual crimped collagen fibrils, which may produce a distinct pattern of signalling for various applications of strain. Abnormal loading regimes may alter this signalling pattern and lead to localised tendon pathology. Impact of total load deprivation on this process has not been examined in whole tendons *ex vivo* (Arnoczky *et al.*, 2004)

2.8.3. Exercise and mobilisation studies

Exercise has been shown to improve the mechanical properties of tendon in animal studies, compared to non-exercised controls. For example, the peroneus brevis tendon in rabbits exercised for 40 weeks demonstrated higher ultimate load and absorbed energy at failure than in non-exercised rabbits, while 12 months of exercise improved the tendon insertion site in pigs and one week of exercise improved the number and size of collagen fibrils and CSA of the digital flexor tendons (Wang, 2006).

Biochemically, training has been shown to increase the metabolism of collagen type-I in tendon and tendon-related tissue, with a tendency towards net synthesis of collagen. In addition, exercise was shown to increase the expression of IGF-I in tenocytes. IGF-I is known to stimulate collagen synthesis and cell proliferation, making a useful protein marker for remodelling activities. However, endurance training in roosters displayed a 50% reduction in

pyridinoline crosslinks, indicating a reduction in the maturation of the newly formed collagen (Wang, 2006). This knowledge could be particularly useful in the development of rehabilitation programs.

Studies have shown that controlled mobilisation of the tendon after the inflammatory phase enhances the quality of healing when compared to immobilised control samples. Outcomes included an increase in ultimate strength, elastic stiffness, CSA, and a reduction in adhesions (Sharma and Maffulli, 2005a; Sharma and Maffulli, 2005b). Additionally, mechanical loading, in particular eccentric loading, has been shown to relieve symptoms of chronic tendinopathy in some patients. It is believed that the loading stimulates cellular response that promotes healing (Wang, 2006).

Interpretation of animal studies must take into account the inability to compare trained with untrained animals and limitations in confined animals, which may experience reduction in connective tissue mass and tendon tensile strength, which may be returned to normal with physical training (Sharma and Maffulli, 2005b).

Many studies on the effects of mechanical stimuli have been undertaken *in vitro*, as it permits greater control over the experimental conditions. For example, Wang et al. (2006) used a uniaxial stretching device to study the response of human patellar tendon fibroblasts in serum-free conditions. It was found that cyclic stretching in these conditions only slightly increased proliferation. Other cyclic studies found an increase in PGE_2, LTB_4, collagen type-I, TGF-β1, fibronectin, and COX. Several of these increases were found to be magnitude and/or duration dependent. Biaxial cyclic stretching was shown to cause fibroblasts at the edges to orientate perpendicular to the direction of minimal surface deformation (Wang, 2006). Cyclic stretching of tendon cells was shown to activate the JNK (Arnoczky *et al.*, 2002b). This was shown to be time dependent, peaking at 30 minutes and returning to base-line by 120 minutes. Mild cyclic stretching (1% strain) decreased expression of MMP-1 while higher strains (3% and 6%) completely inhibited the gene expression (Wang, 2006). Compared with stretched fibroblasts, relaxed fibroblasts had lower collagen type I mRNA expression and protein levels, and

an increase in the synthesis of MMP-1. Stretched fibroblasts were shown to produce more tenascin-C and collagen XII. It was hypothesised that tension exerted on the ECM by fibroblasts may maintain tissue structure and function (Wang, 2006).

2.8.4. Immobilisation and stress deprivation

Stress deprivation, through means such as immobilisation, has been shown to cause atrophy, leading to compositional changes, including a decrease in the mass of tendon, water content, and cross-linking, and mechanical changes such as stiffness, failure strain, and tensile strength (Sharma and Maffulli, 2005b; Wang, 2006). While degeneration of tendon is slower than that of skeletal muscle, the faster recovery of muscle can subsequently leave stress deprived tendons vulnerable to injury.

In vitro, changes in cell morphology, cell number, and fibre alignment were also found, in addition to a decrease in the elastic modulus. Conversely, cyclic loading was shown to improve the elastic modulus versus stress deprived tendon, and the application of strain in rabbit patellar tendon was shown to protect against degradation by bacterial collagenase (Wang, 2006). It has been suggested that the aetiology of tendinopathy may lie in local stress deprivation caused by micro-failure of the ECM.

CHAPTER 3. LITERATURE REVIEW: MEASUREMENT OF CROSS-SECTIONAL AREA

3.1. Background

Cross-sectional area (CSA) of tissue is often used as an indication of injury and degeneration, as an enlarged area may suggest swelling, inflammation, and general disorder of the tissue. This is true of tendinopathy, where affected tendons have exhibited larger CSA compared to controls (Arya and Kulig, 2010). CSA is also an important measurement for determining the mechanical properties and behaviours of materials, particularly the stress, strength, and elastic modulus of the material. This makes CSA a significant measurement in the context of a mechanical study of degenerated tendons.

Typically, CSAs are measured at a single location prior to testing, thereby allowing for loads to be converted to engineering stresses, the force divided by original area ($\sigma_E = F/A_0$), post-testing. According to Poisson's effect, the transverse strain changes with axial strain, resulting in changes to CSA. In many situations the engineering stress gives a reasonable approximation; however, even at low loads a difference can be detected (Pokhai *et al.*, 2009). It is therefore desirable to measure the true stress, the force divided by the actual area ($\sigma_E = F/A_i$), to better estimate the stress experienced by soft tissue. This requires measurement of both instantaneous and local CSA along a sample, which can be used to better define the relationship between stress and strain (Pokhai *et al.*, 2009), as well as to develop more accurate geometric models for finite element analysis (FEA) (Langelier *et al.*, 2004).

Many historic methods are not compatible with a materials testing system (MTS), which often means the condition of the sample changes between CSA measurement and mechanical testing, especially when cryo-grips are employed (Pokhai *et al.*, 2009). Additionally, the time taken to measure CSA is critical to minimise the influence of the viscoelastic response of a tendon to a load or gravity on CSA measurement (Pokhai *et al.*, 2009; Vergari *et al.*, 2010). It is, therefore, necessary to employ a technique capable of instantaneous and temporal measurement that is compatible with existing MTSs.

Many methods have been employed over the years to measure CSA of soft tissue, since inaccuracies can result in large errors when calculating the stress (Seitz *et al.,* 2012). These methods can be categorised as destructive, by approximation, contact, and non-contact (Vergari *et al.*, 2010).

3.2. Destructive

Historically, specimens were sectioned, traced and the areas measured using a planimeter (Cronkite, 1936); however, this is inherently destructive and prevents further testing of the sample. Chatzistergos *et al.* (2010) measured tendon CSA by taking sections of the tissue post-rupture. This assumes no plastic deformation has occurred during testing, as this may influence the final shape of the tissue. Recently, Iriuchishima *et al.* (2014) evaluated CSA of anterior cruciate ligaments (ACL) versus the grafts used to replace them. The authors revisited Cronkite's technique and sectioned ACL at the bone attachments and through the midsection. With the use of modern technologies, namely digital photography and image processing, they were able to measure CSA with a higher degree of accuracy and reproducibility. The authors did not discuss a method for measuring CSA of the grafts in a non-destructive fashion, limiting the clinical value of the study. It was, however, noted that a three-dimensional (3D) measurement system would provide a higher degree of anatomical accuracy due to the natural path of the ligament.

3.3. By estimation

'By estimation' techniques have ranged from estimating the shape of the specimens and measuring the height and width of the sample to 'fit' the shape, to the gravimetric method of calculating the area based on the length and volume, and even ocular micrometry (Ellis, 1969). These techniques often assume uniformity within the tissue and, while simple, can introduce errors such as those discussed by Seitz *et al.* (2012).

3.4. Contact

Area micrometry allows for irregularity in the shape of soft tissue by using adjustable blocks to compress the tissue into a channel with known size, from which the volume can be calculated (Allard *et al.*, 1979; Butler *et al.*, 1986;

Ellis, 1969); however, these measurements generally underestimate CSA (Pokhai *et al.*, 2009).

Race and Amis (1996) approached the measurement of CSA differently, taking a silicone rubber cast and creating poly-methyl methacrylate (PMMA) replicas of the tissue for analysis. This technique was developed further by Goodship and Birch (2005) and Schmidt and Ledoux (2010) using new materials and improved techniques. Images were taken of the replicas and then analysed *in silico* to measure the area. These newer techniques were shown to improve measurement accuracy compared to existing methods. The casting method offers the advantage of being able to revisit measurements as the cast can be preserved even after destructive testing of the tendon. This technique has many advantages but is time-intensive, making it incompatible with dynamic mechanical testing.

3.5. Non-contact

Shadow amplitude

Shadow amplitude was developed in the 1960s to measure whole tissues. Of the aforementioned techniques, it was identified as the only non-destructive method able to be adapted to measure local CSAs (Ellis, 1969). It was also noted that there was an inherent need for refinement in the measuring of CSAs, due to the poor repeatability of the technique and inability to identify concavities.

Advances

Technological changes have led to improved non-contact devices, such as laser micrometres, developed by Lee and Woo (Lee and Woo, 1988; Woo *et al.*, 2000), video dimension analysers (Smutz *et al.*, 1996), and charged couple device (CCD) laser sensors (Moon *et al.*, 2006a), as well as advances in medical imaging, including computed tomography x-ray (CT) (Durrington *et al.*, 1982; Faraj *et al.*, 2009; Januário *et al.*, 2008), magnetic resonance imaging (MRI) (Doherty *et al.*, 2006; Kainberger *et al.*, 1997), and ultrasonography (Noguchi *et al.*, 2002).

Laser micrometry

When evaluating their new technique, Race and Amis (1996) pointed out that laser micrometry is potentially the most precise method of measuring the tendon; however, laser micrometry is affected by specimen geometry and concavities which also make it potentially the least accurate when dealing with complex shapes, leading researchers to develop new ways to measure CSA as technology improved.

Langelier *et al.* (2004) developed a new computer-controlled laser micrometre based on the work of Lee and Woo (1988). The system utilised a 10µm laser and was found to be accurate and highly repeatable, but unable to identify concavities in the tissue. Liu *et al.* (2008) proposed the use of a coordinate measurement machine, utilising laser micrometry of 1µm to scan the tendon. This method was shown to be more accurate than that developed by Langelier *et al.* (2004) when scanning a standard block (0.4%, with 1.6% repeatability), however, the tendon measurements were only compared to the less accurate shape fitting technique.

Translucency of tendon is a known issue in microscopic investigation of tissue and may inhibit laser-based measurement systems due to refraction of light at the surface. Langelier *et al.* (2004) discussed this issue briefly in relation to problems they identified in certain samples. This was later attributed to the density of the sample being insufficient to interrupt the laser beam (Langelier *et al.*, 2004); however, this does not exclude the issue of refraction playing a part. Neither Langelier *et al.* (2004) or Liu *et al.* (2008) evaluated their techniques against reliable existing methods for tissue, thus the accuracy and repeatability of their experiments may be lower than reported when applied to hydrated soft tissue.

Moon *et al.* (2006a) trialled CCD laser sensors to address some of these issues, finding that the new system was able to measure concavities in an accurate and repeatable fashion. Measurement time was less than 80 seconds per cross-section. It was, however, susceptible to underestimation of CSA due to laser penetration of the semi-transparent surface of the tissue. Therefore, the tendon was stained with Indian ink. The system was also limited to objects

with CSA larger than 20mm^2. It was noted that the improvements over other measurement techniques were negligible for rabbit ligaments and tendon (Moon *et al.*, 2006a).

Salisbury *et al.* (2008) sought to develop a new method for characterising CSA, using a laser-slice method. The technique was effective at measuring the concavities in CSA profile, and did not require any surface modification. Measurement time was approximately four minutes per cross-section. The tendon was required to be rotated almost perfectly vertical in order to accurately measure CSA, which limits the potential use on tissues which have a 3D anatomical path. The accuracy was comparable to other methods, but was deemed cheaper and more reliable when dealing with cavities than other methods.

The importance of understanding the local variations in shape and area in soft tissues has previously been identified in relation to the development of CSA measurement systems (Langelier *et al.*, 2004; Woo *et al.*, 1990). These papers discussed calculating local stresses and strains based on the local shape data. This information improves understanding of how the tissue changes with load and may be used to create more accurate FEA models. To date, almost all methods have required researchers to measure CSA outside of the MTS. This can often mean the condition of the sample can change between measurement of CSA and the final testing procedure (Pokhai *et al.*, 2009). It is not necessarily practical to measure the tendon immediately prior to testing, such as when using cryo-grips (Pokhai *et al.*, 2009). Therefore, a measurement system capable of integration with an MTS is desirable. The importance of measuring the instantaneous CSA so that true stress can be calculated has previously been discussed (Pokhai *et al.*, 2009); however, this requires a system capable of measuring the local CSA much faster than previous techniques.

Pokhai *et al.* (2009) developed a laser reflectance system for an MTS capable of capturing one scan every 20 seconds; however, it is sensitive to opacity, reflectivity, and orientation, as well as small specimen size and small concavities. These are all important considerations in the rabbit Achilles

tendon. It was also noted that the 20-second acquisition may be a limitation in studies requiring a higher strain rate. Slow strain rates can be affected by a viscoelastic response in the tissue, as well as creep, and depending on the orientation, possibly sag (Pokhai *et al.*, 2009; Vergari *et al.*, 2010).

Vergari *et al.* (2010) developed a linear scanner to measure CSA of the tendon. While this new method was much faster (under 2 seconds per measurement) than existing techniques, and also highly accurate (less than 2% error), it is limited in the shapes that are measurable, due to the linearity of the measurements. As with previous techniques, it is only able to measure one region at a time, meaning that whole tendon shape data are not available during mechanical testing.

Heuer *et al.* (2008) developed a 2D laser scanner to measure the deformation of an intervertebral disc in three dimensions in only four seconds. This scanner cannot distinguish tissue morphological complexities such as the concavities and has a relatively limited viewing window.

Computed tomography and magnetic resonance imaging
Measurements of soft tissue have been performed using CT (Durrington *et al.*, 1982; Faraj *et al.*, 2009; Januário *et al.*, 2008) and MRI (Doherty *et al.*, 2006; Kainberger *et al.*, 1997). While regularly used for medical imaging and diagnostics, these modalities require expensive equipment and trained operators, making them impractical for researchers.

Ultrasonography
Ultrasonography provides a method of measuring CSA of tissue both *in vitro* and *in vivo.* It was shown to be as effective as 'by approximation' methods, while preserving the shape information of the tissue (Noguchi *et al.*, 2002). It does, however, risk overestimation of CSA *in vitro* due to fluid absorption, as the tissue must be imaged in a bath of saline. A scan time of one minute was seen as acceptable by the researchers. Three-dimensional freehand ultrasound also offers a way to measure tissue to study the morphological response of a tendon to a tensile force, such as the Achilles tendon *in vivo* (Fan, 2010; Obst *et al.*, 2014a; Obst *et al.*, 2014b), but requires a well-trained operator and is not readily available in a research environment. To date, laser

and ultrasound techniques have shown the most potential for 3D measurement of tissue in a dynamic setting.

Structured light scanning

Recent developments in 3D laser and structured light scanning (SLS), as well as advanced digital image correlation (DIC), have made these techniques affordable and suitable options for research. Although affordable, commercial laser-based systems suffer from relatively slow scan times (2 minutes per scan), making them no more attractive than the laser-based techniques previously discussed. Commercial DIC and SLS, on the other hand, offer faster scan times (greater than one fps) to record the 3D shape of objects.

Hashemi *et al.* (2005a) utilised a commercially available 3D photographic scanner to scan the ACL. The scanning process was approximately 30 minutes, from which a 3D model was generated. The accuracy was similar to that seen with early laser micrometres; however, it also lacked the ability to detect concavities. The advantage of this technique over the lase-based systems is that CSA can be calculated at any point along the length of the tissue.

Three-dimensional structured white light (SWL) scanners have been used by Nebel (2001) to create photo-realistic 3D models of human bodies with an accuracy of one millimetre. These models were then converted to FEA compatible models. More recently, Ahn *et al.* (2014) used a 3D SWL scanner to evaluate the changes in the dentoalveolar protrusion in patients before and after orthodontic work. This involved scanning the face from three angles simultaneously and reconstructing the model to ensure that any change between angles was not a product of patient movement or positioning. Scans were taken in under one second and, though the accuracy for this was not definitively measured (the scanner specifications were quoted), changes in protrusion were discussed in the magnitude of one millimetre.

Digital image correlation

DIC has been used to investigate the deformation of biological materials under load (Gao and Desai, 2010; Genovese *et al.*, 2011; Genovese *et al.*, 2013; Lionello *et al.*, 2014; Pyne *et al.*, 2014; Spera *et al.*, 2011; Tung *et al.*, 2010).

The principle of DIC is to detect gradient differences in a greyscale image to find patterns which can be subsequently tracked between images. Often this requires application of an irregular pattern of similar sized dots to the material. This has led to DIC sometimes being referred to as 'speckle imaging'. There are currently methods of calculation able to determine sub-pixel resolution of the strain-fields (Chen *et al.*, 2005). Commercial packages are available that utilise stereophotogrammetry to map the strain field in 3D. The limitation of this system is usually in applying the speckle pattern, which must be fine and irregular, but with good contrast in order to visualise the gradient. The technique allows for use of high resolution or high-speed cameras to maximise the quality of data captured. However, a big advantage of DIC over other modalities is the ability to record local strain in addition to calculating the shape data. Evans *et al.* (2007) have previously discussed the advantages of using DIC in mechanical testing, as it provides more information, such as differences between regions of the test sample, which would otherwise be unmeasurable.

CHAPTER 4. STRUCTURED WHITE LIGHT SCANNING OF RABBIT ACHILLES TENDON

This chapter was published in the *Journal of Biomechanics*. It is presented here with the content unchanged, but reformatted to the dissertation. Figure and Table numbers have been updated accordingly.

4.1. *Abstract*

4.1.1. Background

The cross-sectional area (CSA) of a material is used to calculate stress under load. The mechanical behaviour of soft tissue is of clinical interest in the management of injury; however, measuring CSA of soft tissue is challenging as samples are geometrically irregular and may deform during measurement. This study presents a simple method, using structured light scanning (SLS), to acquire a 3D model of rabbit Achilles tendon *in vitro* for measuring CSA of a tendon.

4.1.2. Method

The Artec Spider™ 3D scanner uses structured light and stereophotogrammetry technologies to acquire shape data and reconstruct a 3D model of an object. In this study, the 3D scanner was integrated with a custom mechanical rig, permitting 360-degree acquisition of the morphology of six New Zealand White rabbit Achilles tendon. The reconstructed 3D model was then used to measure CSA of the tendon. SLS, together with callipers and micro-CT, was used to measure CSA of objects with a regular or complex shape, such as a drill flute and human cervical vertebra, for validating the accuracy and repeatability of the technique.

4.1.3. Results

CSA of six tendons was measured with a coefficient of variation of less than 2%. The mean CSA was $9.9 \pm 1.0\text{mm}^2$, comparable with those reported by other researchers. Scanning of phantoms demonstrated comparable results to μCT.

4.1.4. Conclusion

The technique developed in this study offers a simple and accurate method for effectively measuring CSA of soft tissue such as tendons. This allows for localised calculation of stress along the length, assisting in the understanding of the function, injury mechanisms and rehabilitation of tissue.

4.2. Introduction

CSA (CSA) is an important parameter in studying the mechanical properties of a material. Inaccurate measurement of CSA can result in large errors when calculating the stress on an object (Seitz *et al.*, 2012). As soft biological tissue samples have irregular shapes and are load-, time- and hydration-sensitive, careful selection of measurement technique is required to achieve a desirable result.

Destructive methods have successfully been used to measure CSA of soft tissue (Chatzistergos *et al.*, 2010; Cronkite, 1936; Iriuchishima *et al.*, 2014), while non-destructive methods such as shape approximation and gravimetric or ocular approximations (Ellis, 1969) are susceptible to introducing errors (Seitz *et al.*, 2012). Another non-destructive method, area micrometry, involves compressing the specimen into a channel of rectangular cross-section (Allard *et al.*, 1979; Butler *et al.*, 1986; Ellis, 1969), but is pressure sensitive and underestimates CSA. Casting methods (Goodship and Birch, 2005; Race and Amis, 1996; Schmidt and Ledoux, 2010) allow the measurements to be revisited; however, these are indirect and unable to be used in a dynamic setting. Advanced measurement techniques include optical tracers (Iaconis *et al.*, 1987), video dimension analysis (Smutz *et al.*, 1996), ultrasonography (Du *et al.*, 2013; Noguchi *et al.*, 2002), coordinate measurement machines (Liu *et al.*, 2008), and laser based systems (Heuer

et al., 2008; Langelier *et al.*, 2004; Lee and Woo, 1988; Moon *et al.*, 2006a; Salisbury *et al.*, 2008; Woo *et al.*, 1990; Woo *et al.*, 2000).

Many techniques are not compatible with materials testing systems (MTS) so the condition of the sample may change between measurement and testing (Pokhai *et al.*, 2009; Vergari *et al.*, 2010). A laser reflectance system compatible with MTS captures a scan in under 20 seconds but can be sensitive to opacity, reflectivity, orientation, size, and morphology of a sample (Pokhai *et al.*, 2009). A linear scanner recorded CSA of tendon with less than 2% error in under two seconds per measurement (Vergari *et al.*, 2010). While a 2D laser scanner can measure the deformation of an intervertebral disc in 3D in four seconds (Heuer *et al.*, 2008), it cannot distinguish tissue morphological complexities such as concavities.

The capability of a measurement system to characterise the detailed morphology of soft tissue is important to the accuracy of CSA measurements (Langelier *et al.*, 2004; Woo *et al.*, 1990). An example is 3D freehand ultrasound (Fan, 2010; Obst *et al.*, 2014a; Obst *et al.*, 2014b). To date, laser and ultrasound techniques have shown the most potential for 3D measurement of soft tissue in a dynamic setting.

Structured light scanning (SLS) uses a variation on stereophotogrammetry to reconstruct 3D digital models. Previously, multiple cameras or angles were used in order to create the stereo-image pairs necessary for 3D spatial recognition; however, commercially available units are now designed for handheld scanning.

This study developed a simple technique using SLS technologies for measuring CSA of a tendon along the length. The accuracy and repeatability of the technique was evaluated using micro-CT (µCT), elliptical approximation (EA), and area micrometry (AM).

4.3. Method

4.3.1. Samples
Six Achilles tendons from six New Zealand White rabbits were harvested and the calcaneal tuberosity potted in dental cement (Vertex Self Curing, Vertex-

Dental B.V., The Netherlands). The rabbit was obtained from an unrelated study with approval from animal ethics committees at The University of Western Australia and Curtin University of Technology.

The dimensions of the midsection of the tendon were measured using digital callipers with 0.01mm accuracy. This region was measured using a custom-built AM with rectangular section 3mm by 4mm at a pressure of 0.1MPa. Three measurements were taken using each method. Tendons were recovered in saline for five minutes between measurements.

4.3.2. SLS scanning of Achilles tendon

Each tendon was scanned with a light coating of corn flour to prevent excessive reflection, as suggested by the manufacturer. The tendons were tested again without coating, after rinsing and bathing in saline. The samples were suspended from a custom test rig for scanning (Figure 4-1). A commercially available structured light scanner, the Artec Spider™ (Artec Group, Luxembourg), was used in this study. The Spider™ has an accuracy of 50 microns, resolution of 100 microns, and maximum capture rate of eight frames per second. The scans were processed in Artec Studio (Artec Group,
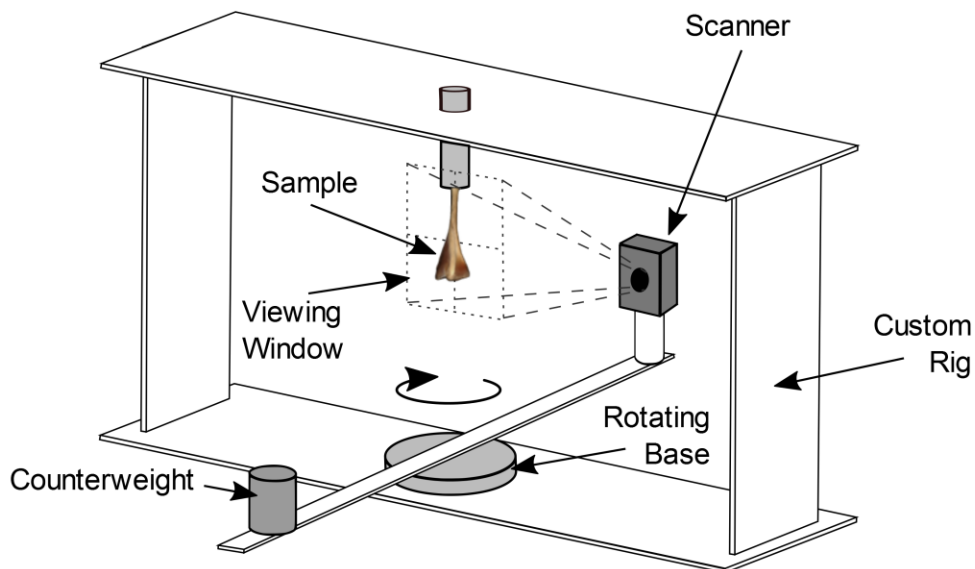
Figure 4-1: A custom rig was used to acquire 3D models of rabbit Achilles tendon using an Artec Spider scanner. The hand held scanner was placed on a rotating base to allow faster scanning. Tendons were gripped by the calcaneus in a custom grip and suspended above the axis of the rotating base.

Luxembourg) to produce a 3D model (Figure 4-2C). Using the section measurement tool, CSA was measured along the longitudinal axis at intervals of 0.1mm (Figure 4-2A).

Six different scan speeds were trialled to determine a maximum scanning speed. Each tendon was scanned three times with and without coating. Ten scans were acquired for one tendon to evaluate the repeatability of the technique at this speed with and without corn flour. The tendon was rinsed and returned to the saline bath for five minutes between scans. Corn flour was reapplied to the coated samples before each scan.
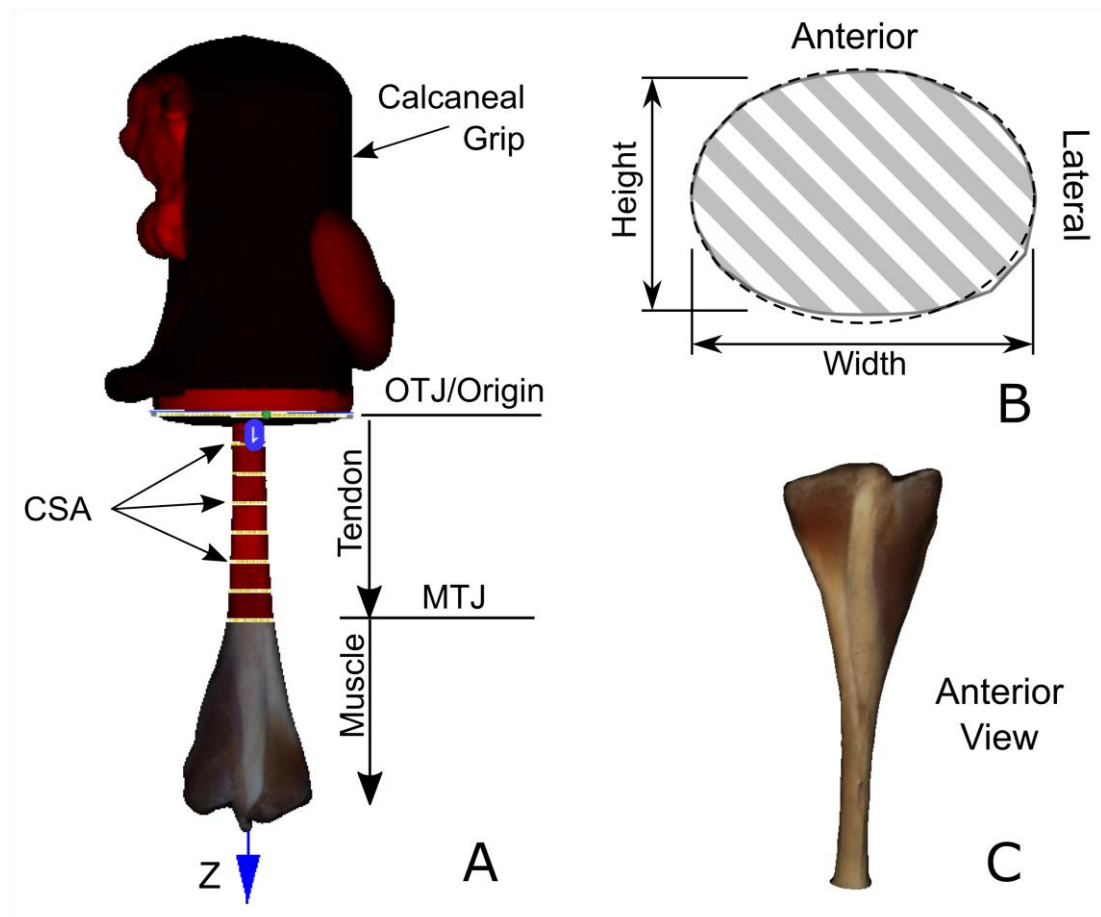
Figure 4-2: (A) A 3D model of the rabbit Achilles tendon muscle unit gripped in the calcaneal grip. The tendon portion is highlighted as red. CSAs (yellow lines) were measured at regular intervals along the tendon between the osteotendinous junction (OTJ) and myotendinous junction (MTJ) using the Section tool in the Artec Studio package. (B) Cross-section of the tendon at 5 mm compared to an ellipse. (C) Anterior view of the tendon muscle.
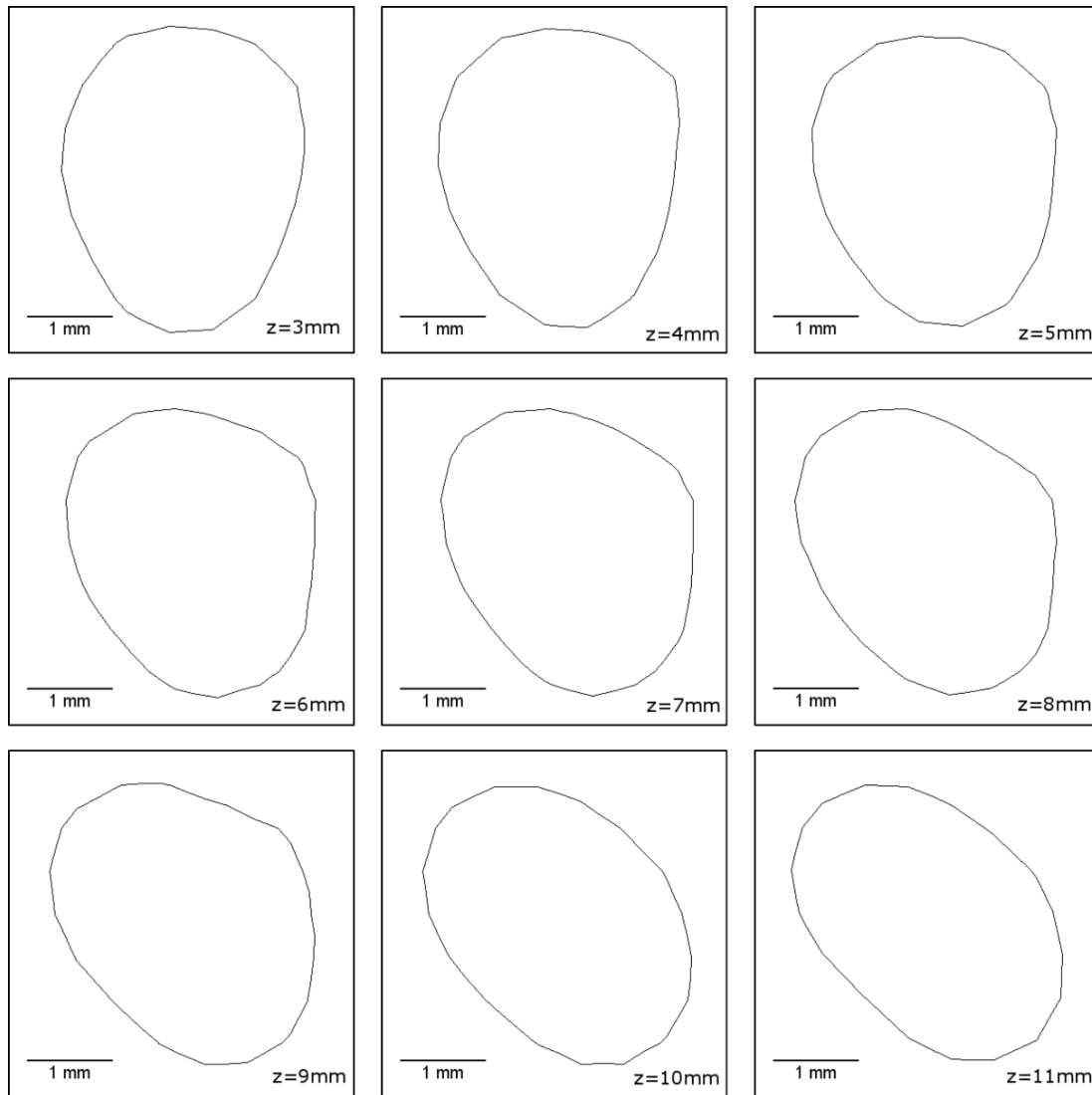
Figure 4-3: Cross-sections of the tendon at 1mm intervals along the tendon length, from 3mm above the origin (top left) through to 11mm (bottom right).

4.3.3. Evaluation of the technique

An ordinary two-flute drill bit (Ø3.9mm, Figure 4-4A) was selected as a standardised object. The cylindrical shank and complex geometry of the flute provided excellent shapes for evaluating the accuracy and sensitivity of SLS to morphological features. Nominal measurements were made using digital callipers. Six 3D models of the drill bit, obtained using SLS, were used to measure the diameter, perimeter, CSA, and circularity of the cross-section of the shank (Figure 4-4B), and dimensions of the minor axis, major axis, perimeter, and CSA of the flute (Figure 4-4C/D). The circularity (c_f) of the drill shank was defined as a ratio of CSA and circumference of the shank cross-
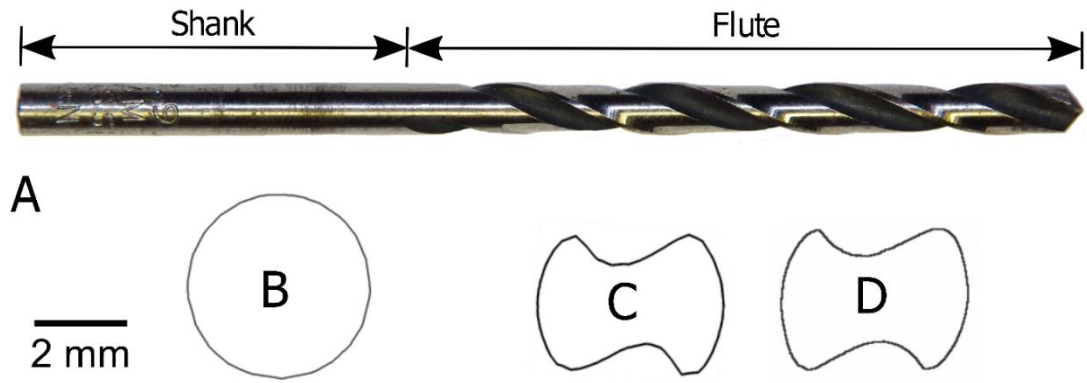
Figure 4-4: (A) standard 3.9mm drill bit. (B). the cross-section of the drill shank obtained from the SLS technique. (C) & (D). The cross-section of the drill flute obtained using SLS technique and micro-CT respectively. Cross-sections B, C and D have been scaled.

section: ($c_f = (4\pi \times CSA)/circ^2$), where a c_f value of 1.0 indicates a perfect circle.

Computed Tomography (CT) is a non-destructive tool for assessing cross-sections of objects in industrial and medical applications (Carmignato, 2012; De Chiffre *et al.*, 2014; Kruth *et al.*, 2011). The full body of the drill bit was scanned using micro-CT (SkyScan1176) at a resolution of 18 microns and a rotation step of 0.1 degrees using a 0.1mm copper filter and source voltage of 90kV at an exposure time of 300ms. The µCT scans were processed using ImageJ (version 1.49e)(Schneider *et al.*, 2012) as shown in Figure 4-4D.

One human cervical vertebra, approved by the Curtin University Human Research Ethics Office, was used as a µCT biological test phantom and subsequently scanned using SLS. The CT images were processed in Mimics Innovation Suite (Materialise NV, Belgium).

4.3.4. Statistics

Statistical analysis was completed using MS Excel (2013), and the R statistical environment (R Core Team, 2014; RStudio, 2013).

4.4. Results

4.4.1. Tendon measurement

The irregular 3D shape of tendon (Figure 4-2A/C) results in variation of CSA along the axis (Figure 4-3 and Figure 4-5). The tendon CSA noticeably increases toward the junctions. The fastest scan time achievable by the

operator using the current rig was 6 seconds and results did not differ from scans of up to 90 seconds (unpublished results). An average minimum tendon area of 9.9 ± 1.0mm^2 without coating, and 10.2 ± 0.9mm^2 with coating was measured from the six samples, with intra-tendon standard deviations of less than 0.2mm^2 (<2% coefficient of variation, or CV) (Table 4-1 and Figure 4-6).

4.4.2. Accuracy and repeatability of SLS technique
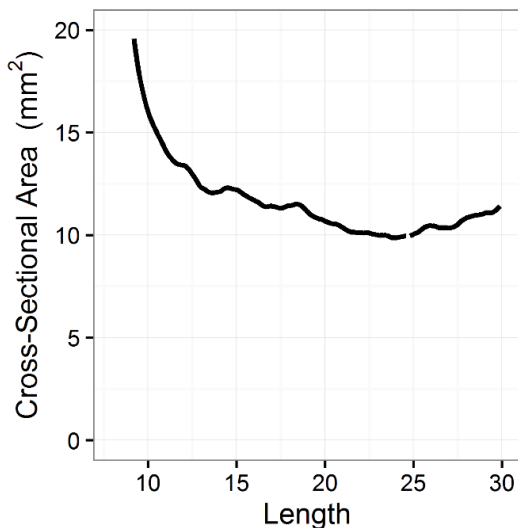
Figure 4-5: CSAs of a rabbit Achilles tendon is irregular and increases as it transitions into the junctions.

The mean CSA of the tendon using EA and AM was 9.5 ± 0.86mm^2 and 8.0 ± 0.7mm^2 respectively by EA and AM (Table 4-1). SLS measurements were 6.3% different with the addition of corn flour, 11.8% different than EA and 19.3% larger than AM. The coefficient of variation of SLS was marginally improved with the addition of a coating (1.3% vs. 1.5%), but still outperformed EA and AM (5.7% and 2.6% respectively).

SLS measurements of the diameter, perimeter, circularity, and CSA of the drill shank (Figure 4-4B), averaged across six measurements, differed by 1.3%, 1.0%, 0.0% and 0.8% from the nominal values obtained with digital callipers (Table 4-1 and Table 4-2). The SLS technique demonstrated a similar error compared with the µCT measurements.

The shape acquired using both µCT and SLS methods clearly outlines the geometry of the drill flute (Figure 4-4C/D). SLS measurements of the minor axis, major axis, perimeter, and CSA of the flute (Figure 4-4C) were 2.6 ± 0.1mm, 3.9 ± 0.0mm, 12.4 ± 0.2mm and 7.9 ± 0.2mm^2 (Table 4-2). These values are 11.6%, 5.1%, 4.9% and 16.0% larger than those measured using µCT (Figure 4-4D).
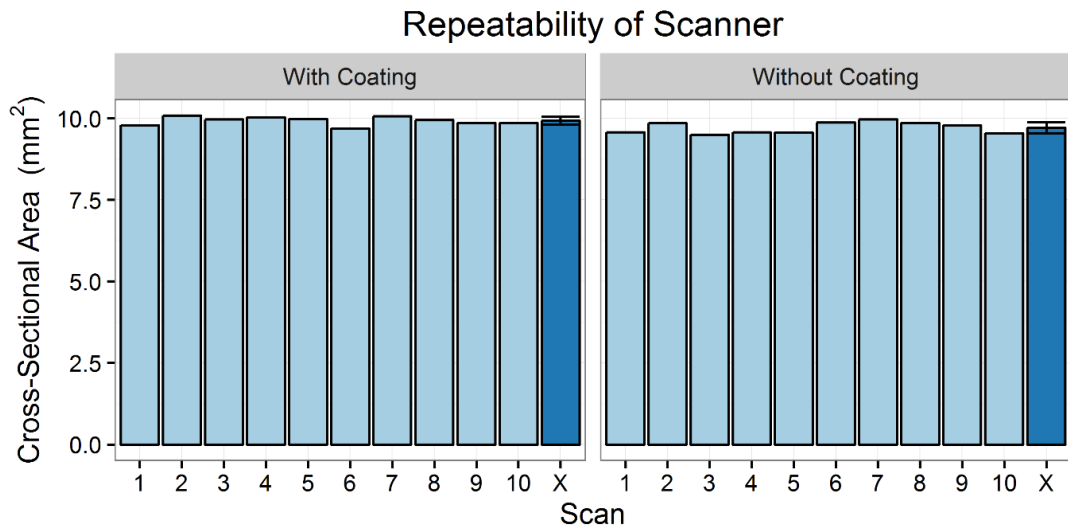
Figure 4-6: CSAs of the rabbit Achilles tendon were calculated 5 mm from the origin, in the region of constant CSA. The mean CSA (mean ± SD) of all scans is shown in the last column, labelled as X.

Table 4-1: Comparison of the SLS (n=3), AM (n=3), and EA (n=3) area measurements (mean ± SD mm2) on tendon. Tendon 4 (n=10) was used for the repeatability assessment.

Tendon	SLS Coated	SLS Uncoated	EA	AM
1	11.1 ± 0.3	10.7 ± 0.1	9.7 ± 0.8	8.4 ± 0.4
2	10.7 ± 0.2	11.4 ± 0.1	9.9 ± 0.3	8.7 ± 0.3
3	9.3 ± 0.1	8.8 ± 0.1	8.3 ± 0.1	6.8 ± 0.1
4*	9.7 ± 0.2	9.9 ± 0.1	11.1 ± 1.0	7.6 ± 0.1
5	8.2 ± 0.1	9.3 ± 0.1	9.5 ± 0.5	7.7 ± 0.2
6	10.4 ± 0.1	11.1 ± .3	9.4 ± 0.6	8.5 ± 0.2

The µCT and SLS models of the vertebra were compared via the surface measurement tool in Artec Studio, showing minimal distance between model surfaces (Figure 4-7A). The contour of SLS model accurately describes the bone shape on the µCT slice (Figure 4-7B).

Variation in CSA of tendon using SLS was less than 0.2mm^2 (1.3% CV) with corn flour and 0.2mm^2 (1.5% CV) without corn flour, with a mean of 9.7mm^2 and 9.9mm^2 respectively.

Table 4-2: Measurements of the drill shank. Digital callipers were used to provide a nominal measurement.

Measure	Callipers	µCT	Error (%)	SLS	Error (%)
Diameter (mm)	3.85	3.84 ± 0.01	0.26	3.9 ± 0.0	1.3
Perimeter (mm)	12.08	12.72 ± 0.02	5.30	12.2 ± 0.1	1.0
CSA (mm^2)	11.61	11.53 ± 0.01	0.69	11.7 ± 0.1	0.8
Circularity	1.00	0.90 ± 0.00	10.0	1.0 ± 0.00	0.0

Table 4-3: Measurements of the drill flute

Measure	µCT	SLS	Diff. (%)
Minor Axis (mm)	2.33 ± 0.00	2.6 ± 0.1	11.6
Major Axis (mm)	3.71 ± 0.00	3.9 ± 0.0	5.1
Perimeter (mm)	11.82 ± 0.04	12.4 ± 0.2	4.9
CSA (mm^2)	6.81 ± 0.01	7.9 ± 0.2	16.0

4.5. Discussion

This study demonstrates the use of structured light scanning for reconstructing 3D models of soft tissue samples and measurement of CSA. SLS was evaluated against commonly accepted tools for measuring CSA, including AM, shape approximation, and µCT. The results indicate that SLS possesses the required accuracy and repeatability for use in metrology. The scanner measured the dimensions of the test object with errors of less than 2%, similar to casting (Goodship and Birch, 2005; Race and Amis, 1996; Schmidt and Ledoux, 2010) and recent evolutions of laser measurement systems (Langelier *et al.*, 2004; Liu *et al.*, 2008; Moon *et al.*, 2006a; Pokhai *et al.*, 2009; Salisbury *et al.*, 2008; Vergari *et al.*, 2010).

Tendon CSA was found to be 9.9 ± 1.0mm^2 without corn flour, similar to that reported previously (Ikoma *et al.*, 2013; Imai *et al.*; Nagasawa *et al.*, 2008; Zhou *et al.*, 2007). The area was relatively constant along the mid-portion (3–8mm proximal to the origin), suggesting that the location of measurement in this region may not be sensitive in rabbit Achilles tendon. SLS measurements were shown to vary by less than 0.2mm^2 with (n=10) and without (n=10) coating of the tendon, equating to a CV of less than 2% (Figure 4-6 and
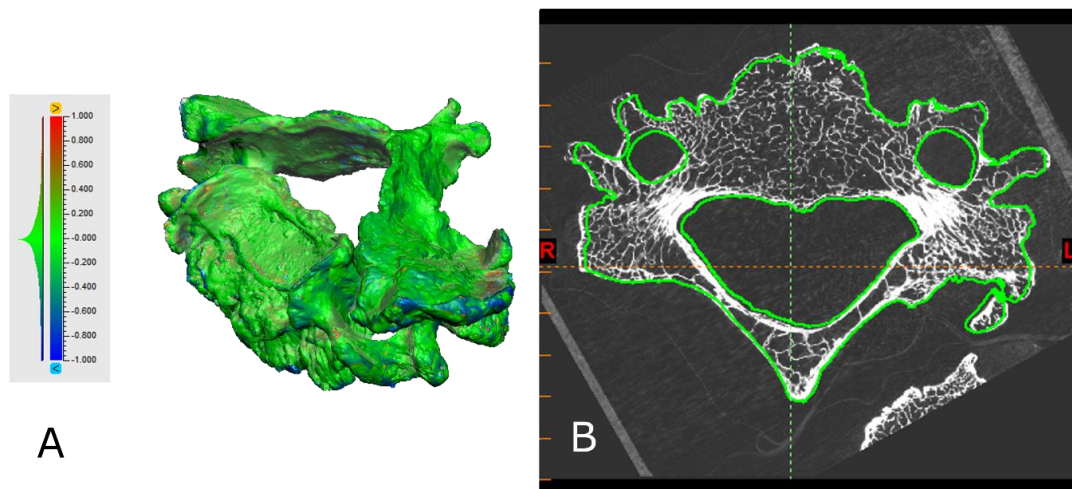
Figure 4-7: (A) Surface difference map between SLS and µCT models of a human cervical vertebra, measured in millimetres. (B) The contour of the SLS model overlayed on an axial µCT

Table 4-1). It can be seen that coating the tissue creates a difference from the uncoated CSA, and should be discouraged as the benefits may not outweigh the potential risk of use.

While many imaging techniques, such as MRI, CT, and ultrasound require an experienced operator to achieve accurate and repeatable results, the technique presented is operator-independent. 3D models are stored digitally, allowing for further analysis. Alignment can be performed in post-processing, thereby eliminating the need for physical alignment prior to scanning.

CT scanning has previously been described for non-destructive assessment (Carmignato, 2012; De Chiffre *et al.*, 2014; Kruth *et al.*, 2011). As shown in Figure 4-4C/D and Figure 4-7, both SLS and µCT were able to acquire shape of a standard two-flute drill bit and a human cervical vertebra, despite the presence of deep concavity features. The close resemblance of the cross-sections of both objects indicate SLS is comparable to µCT. A distance map of the vertebra (Figure 4-7A) shows a minimal distance between the two surfaces, with the histogram weighted heavily near 0mm of difference. This is confirmed by the fit of the SLS model contour to the µCT images (Figure 4-7B). CSA of the drill flute measured using SLS differed by 16% to µCT (Table 4-3 and Table 4-2); however, CSA of the drill shank measured using SLS only varied by 0.8%. The larger variation in acquiring complex cross-sections is

likely caused by the difference in image acquisition of the two techniques, namely that the depth of cavities prohibits capture of the structured light pattern. As shown in Figure 4-4B, SLS is capable of accurately reconstructing the shape of the drill shank with a circularity ratio of approximately 1.0 (Table 4-2). This is more accurate than the ratio of 0.9 measured using µCT, indicating that reconstruction of regular 3D shapes is reliable.

Errors as low as 2% have been documented in calliper measurements (Woo *et al.*, 1990). The repeatability of estimation techniques and AMs has previously been shown to be low, with errors of 15–40% being presented (Schmidt and Ledoux, 2010). AMs have consistently underestimated CSA by up to 20% due to the need to apply a minimum pressure to improve the reliability of the technique (Allard *et al.*, 1979; Ellis, 1969; Race and Amis, 1996; Woo *et al.*, 1990). While a pressure of 0.2MPa or greater would result in a more consistent area measurement (Allard *et al.*, 1979), a pressure of 0.1MPa was used in this study as the associated deformation was minimal and easily recoverable, while providing adequate repeatability. AM underestimated CSA by almost 20%, while EA differed from the uncoated SLS tendon area by approximately 12% when compared with SLS (Table 4-1) in agreement with previous studies.

The scanning speed was slower than latest-generation laser measurement devices, which has improved to fractions of seconds (Langelier *et al.*, 2004; Liu *et al.*, 2008; Moon *et al.*, 2006a; Pokhai *et al.*, 2009; Salisbury *et al.*, 2008; Vergari *et al.*, 2010). Evaluation of various scan times found the maximum speed achievable, via manual operation, was a scan time of 6 seconds. Modification of the current rig, such as automation, may improve scan times using the single scanner setup; however, dynamic MTS testing would require multiple scanners in order to achieve the speeds by Vergari *et al.* (2010).

It is evident from the repeatability testing that the scanner can reliably capture tendon measurements without the need to coat the tendon; however, long term reliability has been identified as a potential weakness of the Spider™ and warrants further investigation. Scanning in an environment other than air is of interest, but the authors have found the current technique results in poor

quality scans of tendon in a saline bath. A further limitation of the technique is the cost of the device.

4.6. Conclusion

SLS is an effective technique for measuring CSA of biological tissue. It offers fast, simple and accurate measurements of samples, with minimal preparation. The technique reported demonstrates a high degree of repeatability due to its non-contact nature, and the ability to revisit measurements post-testing is highly desirable. Of particular interest is the ability to measure the entire shape, thereby permitting calculation of the actual stresses across the sample. Currently, SLS is not suitable for use in dynamic testing; however, with ongoing developments this is a promising technique for the future.

4.7. Conflict of interest statement

Neither the authors nor members of their immediate families have a current financial arrangement or affiliation with the commercial companies whose products are mentioned in this manuscript.

4.8. Acknowledgements

CHAPTER 5.   EFFECT OF STRESS ON CROSS-SECTIONAL AREA OF ACHILLES TENDON

5.1. Introduction

One assumption commonly made when performing mechanical testing is that the cross-sectional area (CSA) remains constant and is uniform along the length of the specimen. As a result, most stresses reported are in the form of engineering, rather than true, stress. The limitation is due, in part, to the lack of simple three-dimensional (3D) measurement techniques capable of measuring CSA along the length of the specimen. Four studies have measured CSA in a quasi-dynamic test, finding that instantaneous CSA is proportional to strain (or load) in tendon (Du *et al.*, 2013; Pokhai *et al.*, 2009; Vergari *et al.*, 2011; Vergari *et al.*, 2010). It was found that the engineering stress underestimated the true stress of tendon by 7.1–13.6% at failure, due to changes in CSA of approximately the same magnitude (Vergari *et al.*, 2011). Only one technique, a 2D laser scanner, has been shown to measure CSA along the length of a sample during mechanical testing, although no stress analysis was reported (Heuer *et al.*, 2008).

The technique described in Chapter 4, utilising structured light scanning (SLS), was able to measure CSA along the entire length of a tendon from a single revolution and within seconds. This chapter investigates the effectiveness of the SLS technique in measuring the change in CSA along the length of the tendon at various static loads and dynamic loads. It was hypothesised that tendons exhibit measurable transverse deformation proportional to the tensile load applied.

5.2. Method

5.2.1. Samples

Eight Achilles tendons from eight New Zealand White (NZW) rabbits were used for this experiment. The rabbits were obtained from an unrelated study under University of Western Australia (UWA) Animal Ethics Committee approval RA/3/100/1049. The tendon was immediately frozen at -20°C post-excision and defrosted at room temperature prior to use. The calcaneal bone

was potted in poly-methyl methacrylate (PMMA) (Vertex Self Curing, Vertex-Dental B.V., The Netherlands) and the excess muscle, sheath and superficial digital flexor were removed.

The muscle was secured between custom aluminium blocks with a wire-cut sinusoidal tooth pattern. Sandpaper was used to provide extra friction at the surface to prevent slippage. A line of India ink was drawn on the surface of the tendon at the grip edge, and served as a marker to evaluate movement at the interface.

Tendons were mounted axially on an Instron 5848 MicroTester™ (Instron, MA, USA) and preconditioned for 120 seconds at 1Hz to 4% strain, then recovered in a bath of Ringer's solution (Baxter Healthcare, NSW, Australia) for approximately 1200 seconds.

5.2.2. Scanning

A commercially available SLS scanner, the Artec Spider™ 3D scanner (Artec Group, Luxembourg), was used in this study, with an accuracy of 50 microns, a resolution of 100 microns, and a maximum capture rate of eight frames per second (fps).

5.2.3. Testing

The tendon was suspended from the potted bone in a custom test rig for scanning using the Artec Spider™ (Figure 5-1). This design made use of the portable nature of the scanner to permit 360° rotation. Tendons were suspended in the custom rig and sequentially loaded with a 30g (weight of grip unloaded), 500g, 1kg, 2kg or 5kg calibration weight. One scan was performed at each load in a sequential fashion, with the sequence repeated three times. The tendon was wrapped in saline-soaked gauze for five minutes between sequences.

Quasi-static ramp testing was performed on the Instron 5848 under load control. Using the same sequence of loads extended to 10kg, 15kg and 20kg, the Instron cross-head was paused at each load for 60 seconds to allow scanning. Scanning was performed by hand as the configuration of the Instron 5848 did not allow for a suitable rig to be fixed.

5.2.4. Post-processing

Scans were processed in the Artec Studio software package (Artec Group, Luxembourg) to reconstruct a 3D model of the tendon for each load in each trial. Each model was then fitted to an elliptical prism, via the in-built registration algorithms, to define the longitudinal axis. CSA of the tendon was then calculated at intervals of 0.1mm along this axis using the software's sectioning tool.

5.2.5. Statistics

Statistical analysis was completed using MS Excel 2013, and the R statistical environment (Lianoglou and Antonyan, 2014; R Core Team, 2015; RStudio, 2016; Wickham, 2009, 2011, 2015). A linear regression was fitted to the data to determine slope. One-way ANOVAs and Tukey's honest significant difference *post hoc* test were used to determine statistical significance of the means. All tests were performed assuming an alpha level of 0.05.

5.3. Results

A total of 120 usable static scans were obtained – eight tendons tested three times at five loads. No usable scans were obtained for dynamic testing during pilot tests and so further testing was abandoned.
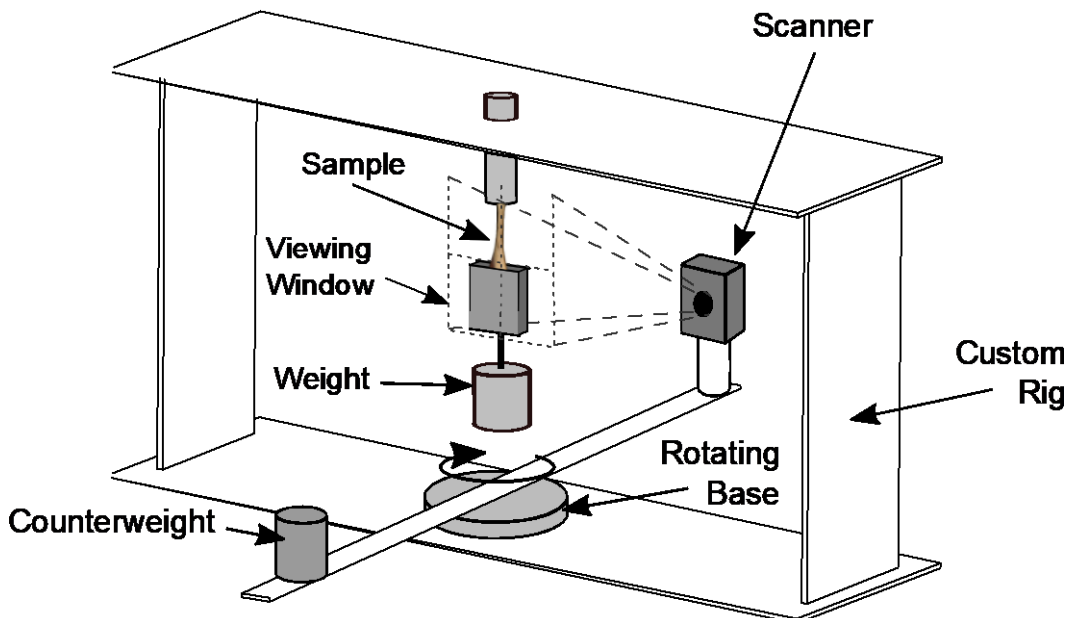
Figure 5-1: A custom rig designed for use with the Artec Spider, adapted from Chapter 4 (Figure 4-1). Calibration weights were attached to a the rabbit Achilles tendon via a soft tissue grip.

Table 5-1: Mean area (± SD) of the rabbit Achilles tendon at each load. The slope of the linear regression is presented. * indicates statistically significant values.

ID	0N	5N	10N	20N	50N	Slope (mm²/MPa)	Slope (%/MPa)
1	8.6 ± 0.1	8.6 ± 0.1	8.6+0.2	8.6+0.1	8.5 ± 0.2	-0.02	-0.18
2	6.8 ± 0.0	6.6 ± 0.2	6.5+0.3	6.5+0.0	6.4 ± 0.2	-0.04	-0.63
3	7.3 ± 0.2	7.3 ± 0.1	7.3+0.1	7.0+0.1	6.9 ± 0.2*	-0.06*	-0.81*
4	9.9 ± 0.5	9.7 ± 0.7	9.7+0.7	9.6+0.5	9.2 ± 0.8	-0.11*	-1.11*
5	8.4 ± 0.4	8.4 ± 0.2	8.4+0.2	8.5+0.1	8.2 ± 0.3	-0.04	-0.46
6	8.7 ± 0.5	8.6 ± 0.2	8.6+0.3	8.6+0.2	8.6 ± 0.1	-0.01	-0.04
7	6.9 ± 0.3	6.4 ± 0.1	6.7+0.1	6.4+0.1*	6.4 ± 0.1*	-0.07	-0.99
8	7.9 ± 0.3	7.7 ± 0.2	7.8+0.3	7.7+0.2	7.9 ± 0.3	0.0	0.03

The minimum CSA was extracted for each scan and averaged at each load (Table 5-1). There was an average standard deviation of less than 0.3mm² (range 0.0–0.8mm²) at each load, indicating repeatable measurements. The repeatability at each load was similar to that reported in Chapter 4. Minimum areas were plotted against the respective stresses, and a linear regression fitted to determine the slope of changes in area (Figure 5-2).

The average unloaded tendon CSA was 8.1 ± 1.0mm², smaller than the 9.9 ± 1.0mm² reported in Chapter 4. Only two tendons exhibited a statistically
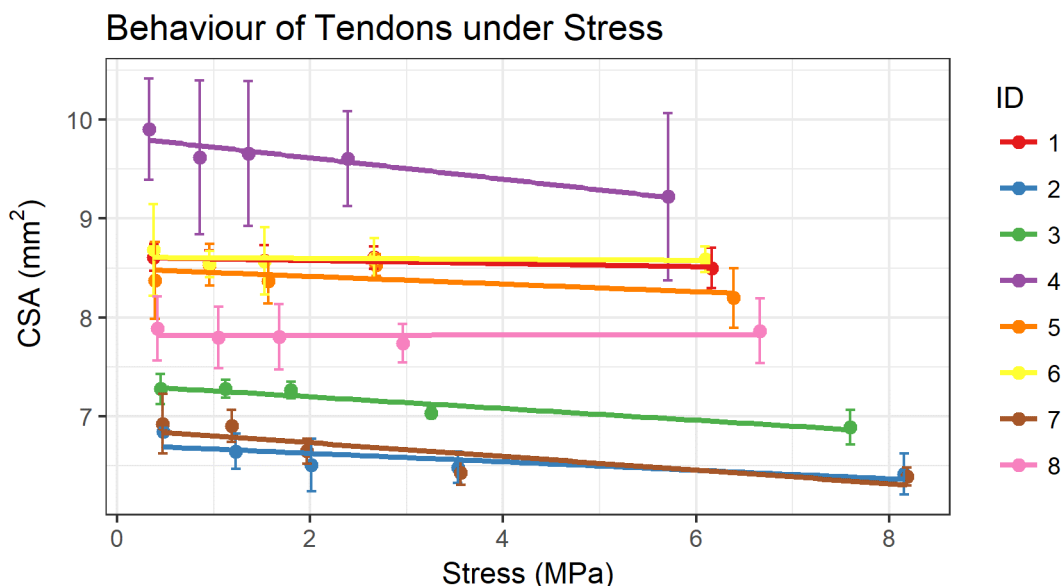
Figure 5-2: Behaviour of rabbit Achilles tendon under stress, as measured by change in CSA (mm²) with increasing stress (MPa). Coloured lines indicate individual tendon behaviour with mean and standard deviations of the repeated measurements shown.
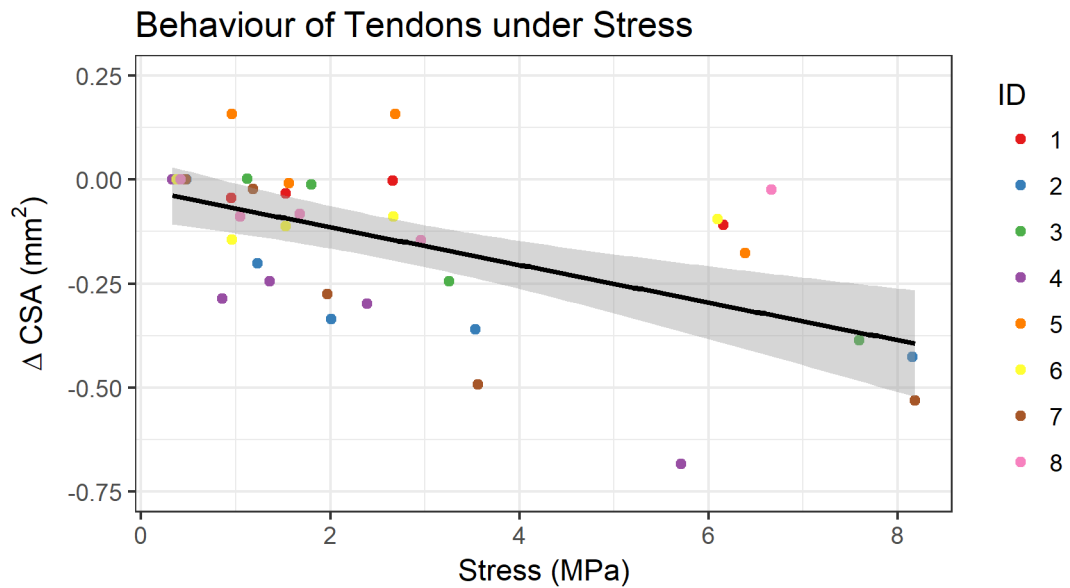
Figure 5-3: Behaviour of rabbit Achilles tendon under stress, as measured by change in CSA (mm²) with increasing stress (MPa). Coloured points indicate mean individual tendon behaviour with a line-of-best-fit ($y = -0.02 - 0.05x$, p<0.001, R² = 0.33).
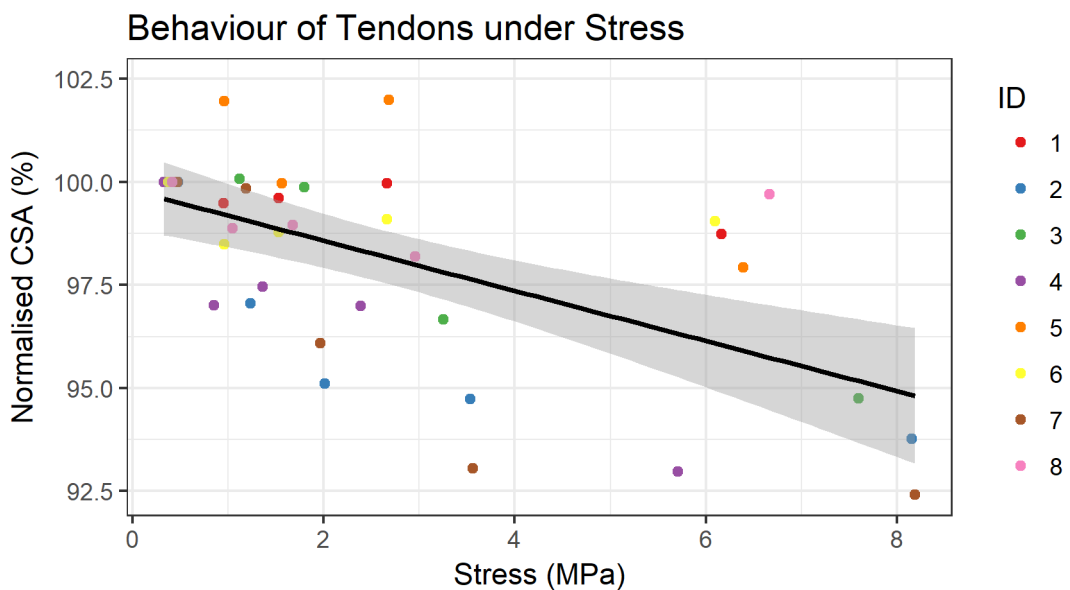
Figure 5-4: Behaviour of rabbit Achilles tendon under stress, as measured by normalised CSA (%) with increasing stress (MPa). Coloured points indicate mean individual tendon behaviour with a line-of-best-fit ($y = 99.79 - 0.61x$, p<0.001, R² = 0.33).

significant slope – tendon 3 and tendon 4 (mm²/MPa, p=0.015 and p=0.018, or %/MPa, p=0.015 and p=0.019, respectively). Three areas were found to be significantly different from the initial area – tendon 3 at 50N (p=0.018), and tendon 7 at 20N (p=0.042) and 50N (p=0.028). An average decrease of 0.05mm²/MPa, or -0.52%/MPa was calculated using the linear regression. The

change in CSA was plotted for each tendon (Figure 5-3). This showed a weak but significant relationship for all tendons (R^2 = 0.18, p<0.01),

The change in area relative to the unloaded area is shown in Figure 5-3 as mm^2 and in Figure 5-4 as a percentage. A clear decrease in CSA with stress is reported in both figures. Engineering stress was shown to be nearly equal to true stress in Figure 5-5.

5.4. Discussion

This experiment shows a small but significant change in CSA with increasing stress, of approximately -0.05mm^2/MPa, or -0.61%/MPa, similar to results found previously (Table 5-2). Using samples from larger animals, namely porcine (Du *et al.*, 2013), bovine (Pokhai *et al.*, 2009), and equine tendons (Vergari *et al.*, 2010), previous studies have also demonstrated a decrease in area with increasing stress or strain. Pokhai *et al.* (2009) reported a large change in area, with an estimated change of 13.5% at a strain of 2.5% (Vergari *et al.*, 2011), equivalent to a rate of approximately 5.4%/%. However, from the
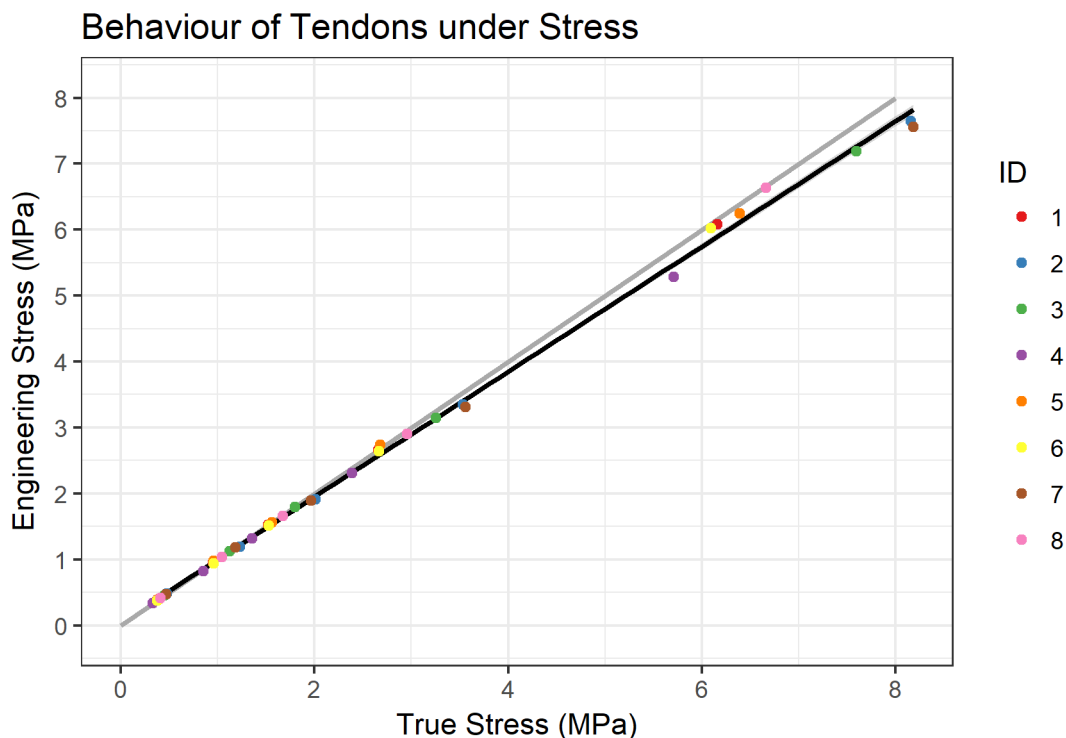
Figure 5-5: Behaviour of rabbit Achilles tendon as described by engineering stress (MPa) versus true stress. (MPa) Coloured points indicate mean individual tendon behaviour with a one-to-one ratio (grey) and line-of-best-fit (black, *y = 0.05 + 0.95x,* p<0.001, R^2 > 0.99).

values reported by Du *et al.* (2013), it is estimated that a change in area of only -0.51%/MPa, or -0.19mm^2/MPa, was present in their study. Vergari *et al.* (2010) demonstrated slopes of approximately -0.08%/MPa, equating to a change of approximately -0.09mm^2/MPa, determined over a range of greater than 100MPa. A follow up study by Vergari *et al.* (2011) reported a change of -0.96%/%, or approximately -1.08mm^2/%.

Reports of the effect of strain and load on CSA vary greatly in the literature. This is, in part, due to the variation in units reported, with no fewer than four units of measure used to describe the changes in CSA (Table 5-2). Tendon properties are known to be related to the specific function (Evans and Barbenel, 1975; Shepherd *et al.*, 2014; Thorpe *et al.*, 2012b). Additionally, reports in the literature have been from different animal species. Nevertheless, the values reported in this study are similar to those reported previously.

Table 5-2: Previously reported relationships between CSA (mm^2 and %) and stress (MPa) and strain (%).

Study	mm^2/MPa	%/MPa	%/%	mm^2/%
Pokhai *et al.* (2009)			-5.4	
Du *et al.* (2013)	-0.19	-0.51		
Vergari *et al.* (2010)	-0.09	-0.08		
Vergari *et al.* (2011)			0.96	1.08
This Study	-0.05	-0.61		

In the current study, the measured change in area within the tendon showed only a weak relationship with stress (Figure 5-3). The loads used in this study will have generated strains within the toe region of the stress-strain behaviour of rabbit Achilles tendon (West *et al.*, 2004). These results indicate that the tendon exhibits some transverse strain in the toe region, with the relationship showing a change in CSA of approximately 5%. It is known that the uncrimping of the fibrils allows the tendon to extend easily under load, as seen by the low stiffness in the toe region. It is possible that this same mechanism results in only small changes in the tendon CSA as the tendon undergoes axial strain with little transverse strain. Larger changes in CSA may be evident once the

tendon enters the linear region, as the fibrils exhibit sliding and extension, leading to 'thinning' of the tendon body.

These findings may have important implications for interpreting the results of mechanical tests. If testing of tendons remains within or near the toe region, engineering stress may be a sufficiently accurate approximation of true stress. Figure 5-5 shows a relationship where engineering stress is approximately 95% of true stress up to a stress of 8MPa. This relationship between engineering stress and true stress is similar to that reported by Vergari *et al.* (2011). In Figure 5-5., comparing engineering stress to true stress, engineering stress was approximately 90% of true stress at failure but showed no practical difference at strains below 4%. While engineering stress still underestimates the true stress, a common issue highlighted in Chapter 3, the ability to approximate true stress would greatly simplify testing protocols as CSAs would not need to be recorded during testing. However, further investigation, using a suitable MTS, is necessary to confirm this finding.

There are several limitations in this study. A major limitation of the commercial system is that the focal length and cables of the scanner require a reasonably large space for the scanner to pass in order to achieve maximum, and accurate, coverage. This inhibited the ability of the commercial scanner to be used with the Instron 5848 MicroTester™, thus loading was only able to be applied using calibration weights. Since the frame of this testing system is common to many MTSs, a custom implementation of the SLS technique may be necessary to be more readily interfaced with existing systems. The inability to scan during dynamic loading limited testing to quasi-static and static protocols and potentially introduced transient viscoelastic behaviours. The commercial system is only able to capture objects in air, preventing longer temporal studies and risking dehydration. Finally, the high cost of some commercial systems may prevent easy implementation of this technology. Nevertheless, the advantages of SLS were demonstrated through the ability to scan and measure tendon shape with ease and accuracy. As well as demonstrating a significant improvement in the measurement of engineering stress, the application of SLS during mechanical testing would permit the

calculation of true stress in a dynamic system and provide shape information for use in computer modelling.

5.5. Conclusion

The SLS technique for measuring CSA has been applied to rabbit Achilles tendon under a static loading environment. This study demonstrates that there is indeed a decrease in CSA proportional to the applied load up to 50N, equivalent to 8MPa. A subtle but significant decrease in CSA was seen with increasing stress. This is the first reported relationship between CSA and stress in rabbit tendon. The magnitude of this relationship suggests that, within the toe region, engineering stress may provide a sufficiently accurate estimation of the true stress of tendon.

CHAPTER 6.   LITERATURE   REVIEW: MECHANICAL PROPERTIES OF TENDON

6.1. Introduction

The structure and function of tendons has been of interest to researchers for many decades (Benedict *et al.*, 1968; Blanton and Biggs, 1970; Cronkite, 1936; Maganaris and Narici, 2005; Rigby *et al.*, 1959). Tendons exhibit properties – stiffness, resilience, and strength – well suited to transferring force from muscle to bone (Doral *et al.*, 2010), and are highly sensitive to their mechanical environment (Arampatzis *et al.*, 2010). It has been observed that tendons exhibit a wide range of structures and mechanical properties due to the breadth of functions they perform (Abramowitch *et al.*, 2010; Benjamin *et al.*, 2008; Birch *et al.*, 2013; Butler *et al.*, 1984; Evans and Barbenel, 1975; Jung *et al.*, 2009; Kjær *et al.*, 2009; Screen *et al.*, 2013; Shadwick, 1990; Shepherd *et al.*, 2014; Thorpe *et al.*, 2012b; Woo *et al.*, 2011)., as well as other factors such as age (Birch *et al.*, 1999; Connizzo *et al.*, 2013; Dressler *et al.*, 2006; Galeski *et al.*, 1977; LaCroix *et al.*, 2013a; Liu *et al.*, 2009; Nakagawa *et al.*, 1996; Shadwick, 1990; Thorpe *et al.*, 2012a; Thorpe *et al.*, 2013b; Wren *et al.*, 2001a).

The mechanical properties of tissue develop to resist the loads encountered *in vivo*. Several factors affect the mechanical properties of tendon (Wang, 2006), including:

- Magnitude of loading experience during physiological activity;
- Level of muscle contraction;
- Tendon size;
- Variety of loading patterns experienced;
- Rate and frequency of mechanical loading; and
- Relative operating distance

Each of these contributes to the overall properties of the tendon. For example, the Achilles tendon is subject to the highest forces has developed to be the largest tendon in the body in terms of cross-section. Flexor tendons of the other hand are subject to smaller forces and have a smaller cross-section.

Tendons have also displayed location-specific properties, showing heterogeneity of the tissue that provides a gradual transition between the properties of the muscle and bone (Abramowitch *et al.*, 2010; Butler *et al.*, 1992; Butler *et al.*, 1986; Pearson and Hussain, 2014). Stress in the Achilles tendon may be non-uniform due to differences in the forces generated by the different muscles of the triceps surae (Arndt *et al.*, 1998). The strain within the tendon may also differ, as seen in the difference in strain between the tendon and aponeurosis as a result of the non-uniform loading by the triceps surae (Benjamin *et al.*, 2008).

Healthy tendons may be considered overdesigned compared to the attached muscle and bone (Almekinders *et al.*, 2003), tissues which have a greater capacity for spontaneous healing. Despite being the largest tendon in the body, the Achilles tendon is also one of the most frequently injured (Wren *et al.*, 2001b). It has been suggested that the high incidence of injury is related to the loading during physical activity (Wren *et al.*, 2001b). It has been noted that the Achilles tendon may operate repetitively at or near failure (Freedman *et al.*, 2014b; Maganaris and Paul, 2002; Wren *et al.*, 2001b).

Tendon strain has been described as the best predictor for tendon damage accumulation (Wren *et al.*, 2003), while elastic modulus has been strongly correlated with ultimate stress (LaCroix *et al.*, 2013b). Since elastic modulus represents the ability of a material to resist load (with changing displacement), it can be inferred that increasing the modulus would increase the factor of safety under physiological loads (Arampatzis *et al.*, 2007), as the ultimate strain of the tendons does not change significantly (Abrahams, 1967; Nakagawa *et al.*, 1996).

Understanding the interplay of the structure, function and mechanical properties may help to identify factors contributing to injury and disease, potentially resulting in improved treatment and repair techniques. Despite the behaviour of the tendon being well-studied, the basic science behind treatment remains weak or inconclusive (Freedman *et al.*, 2014b). Both time-independent and time-dependent properties are necessary to better understand the natural behaviour of the tendon and underlying factors that

may lead to injury. However, methodologies in the literature are inconsistent, leading to varying results, and few studies have performed multiple testing modes, despite studies demonstrating that they must be assessed together to properly characterise tendon (Foure *et al.*, 2012). Providing more complete data sets will not only contribute to our understanding of the tendon function, but also provides inputs for simulations of the functions of the human body (Arampatzis *et al.*, 2005).

While much of the focus of this chapter will be on the Achilles tendon, other tendons have been included for comparison.

6.2. *In vivo* properties

Mechanical behaviour, including stresses and strains, may be estimated from joint mechanics using measures such as maximum voluntary contractions (MVCs) or electromyography (EMG) signals, or measured by fibre optics, ultrasound, or implantable force transducers (IFT).

The human Achilles tendon, the largest tendon in the body, experiences forces of 550N during walking, 1000–4000N during jumping and cycling, and peak forces of 9000N, equivalent to stresses of 110MPa, have been measured during sprinting (Akizuki *et al.*, 2001; Komi, 1990; Komi *et al.*, 1992; Paavola *et al.*, 2002; Sharma and Maffulli, 2005b; Wang, 2006). Oliveira *et al.* (2016) underlined that true stress is underestimated by engineering stress (as discussed in Chapter 3), suggesting *in vivo* stresses may in fact be higher. It has been said that most tendons experience peak stresses below 30MPa during physiological activities, while the human Achilles tendon is estimated to experience stresses closer to 70MPa (Wren *et al.*, 2001b), or nearly 70% of its ultimate force during explosive activities (Freedman *et al.*, 2016).

It is thought that tendon usually elongates 3–4% during physiological loading (Benjamin *et al.*, 2008), below the onset of micro-failure. However, tendon strains of 4.9–8.3% (Arampatzis *et al.*, 2007; Arampatzis *et al.*, 2010; Farris *et al.*, 2013; Kongsgaard *et al.*, 2011; Lichtwark and Wilson, 2005; Maganaris and Paul, 2002; Obst *et al.*, 2014b) and up to 21% (Oliveira *et al.*, 2016) have been reported using the techniques described above, corresponding to forces of 875–4420N and stresses of up to 72MPa

(Arampatzis *et al.*, 2007; Arampatzis *et al.*, 2010; Kongsgaard *et al.*, 2005; Maganaris and Paul, 2002; Oliveira *et al.*, 2016). Strain has been shown to be heterogenous, due to differences in the structure and muscle contributions (Arndt *et al.*, 1998; Farris *et al.*, 2013).

Using fibre optic techniques, peak loads were measured at 1320N (19MPa) during walking, increasing to 1490N (22MPa) for fast walking, with an absolute peak of 2400N in one subject (Finni *et al.*, 1998). Arndt *et al.* (1998) measured peak forces in the Achilles tendon of up to approximately 3000N for maximum isometric plantar-flexion contractions. However, forces measured using the fibre optic techniques have been shown to be affected by skin movement and may be overestimated (Erdemir *et al.*, 2003).

Several studies have looked at the *in vivo* forces in tendons using IFTs, including the flexor tendons, patellar tendon and Achilles tendon (Butler *et al.*, 2008; Meyer *et al.*, 2004; Wang, 2006; West *et al.*, 2004). IFTs can give us insight into the patterns and magnitudes of *in vivo* loading conditions, including their contributions to biomechanical function (Glos *et al.*, 1993). EMG and other methods of muscle activation have limitations, since they are statistically indeterminate problems, and thus a direct measurement, such as IFT, is preferable (Glos *et al.*, 1993). However, IFTs have higher risks and longer experiment times compared to indirect measurements (Erdemir *et al.*, 2003). Komi *et al.* (1992) reported peak stresses in human Achilles tendon of 59MPa and 111MPa for walking and running (Wren *et al.*, 2001b). Using IFT in rabbits, forces on the Achilles tendons were measured as approximately 1.4MPa during rest, increasing to approximately 4.9MPa and 6.7MPa during level and inclined hopping, respectively (Juncosa *et al.*, 2003; West *et al.*, 2004). Strains in this study were approximately 4% at peak load, and the peak stress and strain were 20% and 25% of ultimate values measured at the conclusion of the experiment, in agreement with much of the literature (West *et al.*, 2004).

Analysis of the literature revealed that tendons are responsive to loading (Bohm *et al.*, 2015; Obst *et al.*, 2013). This is supported by studies that demonstrated a correlation between activity demands and maximum forces generated *in vivo* (Arampatzis *et al.*, 2007; Kongsgaard *et al.*, 2005), while

high strain exercises were shown to increase the stiffness of tendon (Arampatzis *et al.*, 2010). Similarly, tendon properties were correlated to muscle strength in cyclists (Morrison *et al.*, 2015). Several other factors may influence *in vivo* measurements. Loading rate has been found to influence measured properties such as peak force and stiffness, particularly as it is difficult to control (Pearson *et al.*, 2007). Cross-linking of the collagen has also been seen to influence the properties, and has been suggested as a mechanism for age-related differences (Couppe *et al.*, 2009), while the fibrillar properties likely govern sub-failure responses (Svensson *et al.*, 2012), It has been noted that removal of the tendon from the body likely has an adverse effect on testing outcomes (Svensson *et al.*, 2012).

6.3. Types of mechanical testing

Typically, testing of materials consists of one of four methods: tensile, cyclic, relaxation, and creep. Tensile testing, also known as ramp or traction testing, is the most common method and involves applying a constant strain rate or stress rate, often until rupture. Tensile testing is used to describe the time-independent isochronal behaviour of the sample. Cyclic testing is the repetitive loading and unloading, usually as a sine or triangle waveform. Relaxation, or stress relaxation, applies a constant strain to the sample and the change in stress is recorded over time. Conversely, creep applies a constant stress and measures the change in length over time. Relaxation and creep may indicate the static time-dependent properties of the sample, while cyclic testing may indicate the dynamic time-dependent properties.

It is, therefore, of value to define the behaviour of the tendon across a variety of conditions to elucidate the effect of diseases such as tendinopathy and, specifically, the mechanism by which it affects the tendon. Experiments should seek to extract the most information from each specimen, and help to discriminate between constitutive models (Duenwald *et al.*, 2009b). For example, a tensile test and relaxation test are able to demonstrate tissue nonlinearity and viscoelasticity, but may result in a false linear elastic model (Duenwald *et al.*, 2009b). Models have shown the dependence of soft tissues on strain and stress levels (Duenwald *et al.*, 2009b; Provenzano *et al.*, 2001; Sverdlik and Lanir, 2002), but creep predictions from relaxation are poor

(Lakes and Vanderby, 1999). Therefore, it is necessary to strategically test in multiple modes (Duenwald *et al.*, 2009b).

6.3.1. Tensile

Tensile, or ramp, testing is the application of a constantly stress or strain rate over time, thereby creating a 'ramp' profile with a constant gradient equivalent to the rate of stress or strain. Mechanical properties that are measured during tensile testing of a sample can either be extrinsic (structural) or intrinsic (material) (Woo *et al.*, 2000), and are usually a function of load, displacement, and/or time.

The results of tensile testing are typically presented in the form of the isochronal stress-strain plot, which can be used to determine the mechanical properties of a material independent of time. There are three identifiable regions of interest within the isochronal stress-strain profile – the toe, linear and plastic region – culminating in complete failure. In biological tissues, the plastic region is often split into the microscopic failure and macroscopic failure zones (Screen *et al.*, 2004a).

The toe region has been identified in studies of the mechanical properties of tendon and has been estimated to extend up to 4–5%, corresponding to complete straightening of the crimp, and alignment and recruitment of all the fibre bundles in the direction of loading (Arnoczky *et al.*, 2002a; Arnoczky *et al.*, 2004; Connizzo *et al.*, 2013; Lake *et al.*, 2009, 2010; Miller *et al.*, 2012a; Miller *et al.*, 2012c; Screen, 2008; Screen *et al.*, 2004a; Screen *et al.*, 2002b; Sharma and Maffulli, 2005b; Wang, 2006). It has been suggested the toe region may consist of two micromechanical phenomena – crimp straightening and fibre elongation (Arnoczky *et al.*, 2004; Screen *et al.*, 2002a). It is generally agreed that the low apparent stiffness in this region allows the tendon to absorb energy (Paavola *et al.*, 2002; Screen *et al.*, 2002a). It has been suggested that this region remains nonlinear over larger strains due to the presence of a range of crimp angles, which affects the rate of crimp straightening and fibre recruitment (Screen *et al.*, 2002b). This may be an advantageous in dealing with the wide range of loading conditions encountered (Screen *et al.*, 2004a). For example, rat-tail tendon has been

shown to have a toe region of 1–2%, while human Achilles tendon has a region of 4–5% (Screen *et al.*, 2004a). The most likely reason for this difference is in the physiological loading behaviours of both tendons. The Achilles tendon is subject to high impact loads and benefits from the shock absorbing nature of the toe region, while rat-tail tendon does not encounter such extreme loading. It is believed that the majority of physiological strain levels are within the toe region, allowing the tendon to return seamlessly to initial length when unloaded (Screen *et al.*, 2002b; Sharma and Maffulli, 2005b). It has been shown that, as tendons dry out, the stiffness increases and the toe region becomes shorter (Calve *et al.*, 2004). It has also been noted that removing decorin, or increasing tissue hydration, results in greater fibril slippage and thus a lower stiffness (Screen, 2008; Screen *et al.*, 2002a). It is thought the properties of the toe region may be as important as those of the linear and failure regions (Chandrashekar *et al.*, 2012).

The linear region of the tendon is thought to be a result of the extension and sliding of collagen components at the fibre and fibril level (Screen, 2008; Screen *et al.*, 2004a; Screen *et al.*, 2002a; Sharma and Maffulli, 2005b). The slope of the linear region is often associated with the elastic modulus of the tendon (Wang, 2006).

The plastic region begins as microscopic failure at the fibril and fibre structural levels (Arnoczky *et al.*, 2002a; Wang, 2006). It has been estimated to occur anywhere between 2–5% strain (Almekinders *et al.*, 2003; Provenzano *et al.*, 2002b). Failure has been described as fibre pull-out (Screen, 2008).

Values in the literature show a great deal of variation in human tendon properties. Maximum stresses of 52–100MPa and strains of 5–20% have been reported (Benedict *et al.*, 1968; Benjamin *et al.*, 2008; Butler *et al.*, 1978; Butler *et al.*, 1984; Butler *et al.*, 1986; Devkota and Weinhold, 2003; Screen, 2008; Wang, 2006; Woo *et al.*, 2011; Wren *et al.*, 2001b). Failure forces of up to 7300N have been documented (Wren *et al.*, 2001a). It should be noted that the peak stresses reported *in vivo* often appear to exceed the tensile strength of the tendon (Sharma and Maffulli, 2005b), illustrating the complexity of measuring tendon properties. Few studies have utilised identical testing

setups, which suggests that testing methodology may have a profound influence on the measured properties. It has been suggested that tendinopathy may result in failure of the tendon at as low as one-quarter of ultimate tensile load (Korvick *et al.*, 1996; Malaviya *et al.*, 1998), in agreement with clinical observations of tendinopathy in ruptured tendons (Kannus and Józsa, 1991; Tallon *et al.*, 2001).

6.3.2. Cyclic/dynamic

Cyclic testing is used to measure the dynamic properties applicable to daily activities such as walking and is, therefore, important for assessing tendon mechanics (Nagasawa *et al.*, 2008). Komi *et al.* (1992) demonstrated that, due to muscle tone, physiological loading patterns are best-approximated by a tension-tension square wave (Schechtman and Bader, 1997). However, physiological loading is typically approximated by a series of sinusoidal or triangular waveforms.

Biological materials, such as tendon, possess time-dependent properties which are clearly exhibited in the formation of a hysteresis loop during cyclic testing, representative of the energy lost (Woo *et al.*, 2000). Hysteresis is measured as the energy absorbed during loading minus the energy released during unloading, or $\Delta h = E_{in} - E_{out}$. An efficient material will return close to 100% of energy absorbed. The ability for tissues to 'lose' energy during loading is believed to be one of the many self-defence mechanisms employed to protect the tissue from damage caused by overloading.

Mechanical hysteresis in tendons has historically been measured *in vitro* (Ciarletta *et al.*, 2008). Hysteresis in tendon has been found to be in the range of 5–10%, most of which is dissipated as heat (Screen, 2008). Advances in measurement techniques are now permitting measurements *in vivo*. Hysteresis measurements of 18–26% have been measured using ultrasound techniques (Lichtwark and Wilson, 2005; Maganaris and Paul, 2002). Peltonen *et al.* (2013) demonstrated hysteresis values of less than 10% and suggested that higher values may be an artefact of the methodologies used to estimate the stress-strain profile of tendon *in vivo,* with *in vitro* properties closer to the physiological values.

The loss tangent, tan δ, represents how efficiently the material loses energy to molecular rearrangements and internal friction (Nagasawa *et al.*, 2008) and is a function of dynamic modulus and the storage modulus. The dynamic modulus in tendon has been shown to be largely composed of the storage modulus, with a relatively small loss modulus (Schechtman and Bader, 1997, 2002). This suggests low energy loss during physiological loading (Schechtman and Bader, 2002). In Achilles tendon, the dynamic modulus appears to reflect binding between collagen molecules and the dynamic properties of tendon recover more quickly than static properties following injury (Nagasawa *et al.*, 2008). Frequency has been shown not to affect the dynamic parameters in tendon (Nagasawa *et al.*, 2008; Schechtman and Bader, 1994; Schechtman and Bader, 2002).

6.3.3. Viscoelastic

One of the most interesting properties of tendon is its viscoelasticity, as the importance of this property is not as well understood in tendon as for other tissue, such as articular cartilage. Viscoelasticity contributes to the unique mechanical behaviour of tendon (Wang, 2006), allowing tendons to act as mechanical buffers to protect muscle fibres while maintaining energy transfer efficiency (Ciarletta *et al.*, 2008). Viscoelasticity is evident in physiological activities: stretching induces relaxation, isometric contractions induce creep, and cyclic loading, for example running, produces hysteresis (Oza *et al.*, 2006b).

Many different materials, including plastics, rubbers, and biological tissues, are characterised as viscoelastic, the result of microstructural rearrangement processes under load (Carniel *et al.*, 2013). In tendon, this process is thought to be a complex interaction between ECM and ground substance (Woo *et al.*, 2000). Altering proteoglycan (PG) content, such as removing decorin, and hydration of the tissue have been shown to influence viscoelasticity via the internal friction (Screen, 2008). The nonlinearity of tendon behaviour has been attributed to the wavy collagen fibres that are progressively loaded at low load until all fibres are engaged (Sverdlik and Lanir, 2002). Reduction in cross-link density has been shown to cause biomechanical weakening of soft tissue (Couppe *et al.*, 2009; Nagasawa *et al.*, 2008) and is associated with age-

related changes such as stiffening and a reduced plasticity (Ciarletta *et al.*, 2008).

Viscoelasticity is defined by stress relaxation, creep, hysteresis, and strain rate sensitivity (Sharma and Maffulli, 2005b; Wang, 2006; Woo *et al.*, 2000). Strain rate sensitivity means that tendons become stiffer at higher strain rates, most likely due to higher friction forces and resistive pressure caused by the faster deformation, enabling them to more efficiently transfer large loads (Wang, 2006). Conversely, at lower strain rates, tendons are more deformable but also less efficient (Wang, 2006).

Stress relaxation testing involves keeping the sample at a constant length and measuring the change in stress over time, while creep testing involves applying a constant stress and measuring the change in length over time (Woo *et al.*, 2000). Stress relaxation is attributed to the rearrangement of the microstructure allowing for a redistribution of stress, while creep is attributed to crimp straightening and fibre recruitment (Schechtman and Bader, 2002; Shepherd *et al.*, 2014). The shape of these responses over time has been described by a power law (Duenwald *et al.*, 2009b; Provenzano *et al.*, 2001). It has been previously shown that creep and relaxation are dependent on the strain rate and strain magnitude (Carniel *et al.*, 2013).

The initial ramp used to apply the stress or strain for testing should be as close to a step as possible (Sverdlik and Lanir, 2002). This is impossible to achieve in experimental testing so corrections are necessary (Sorvari *et al.*, 2006). Use of slower ramp times have been proposed to avoid overshoot and vibration (Abramowitch and Woo, 2004; Gimbel *et al.*, 2005), but risks inducing relaxation or creep during loading. Historically, this issue has been corrected by removing a portion of data at the start of the test that is affected by the overshoot (Duenwald *et al.*, 2009b). Newer techniques include mathematical adjustments for curve fitting of the data (Abramowitch and Woo, 2004; Gimbel *et al.*, 2005).

An example of the importance of defining the viscoelastic behaviour of soft tissue lies in surgical interventions for orthopaedics. Tendon and ligaments are often considered interchangeable from a surgical standpoint; however, they

have been shown to have different viscoelastic behaviours (Duenwald *et al.*, 2010). For example, relaxation of ligament has been shown to decrease with increasing strain, while the opposite is true of tendon (Duenwald *et al.*, 2010; Hingorani *et al.*; Provenzano *et al.*). Preconditioning and pre-tensioning of graft tissue for ligament reconstructions have been investigated to reduce the risk of laxity due to relaxation (Ejerhed *et al.*, 2001; Lockwood *et al.*, 2016). Understanding the distinction between tissues, and within tissues, may lead to improved clinical outcomes for patients by helping to restore physiological functionality.

6.3.4. Fatigue

Fatigue properties offer an indication of the potential for overuse damage, as proposed in the aetiology of tendinopathy. Testing of human Achilles tendon specimens demonstrated faster times to failure when cycled, suggesting that repetitive loading may indeed contribute to tendon injuries (Wren *et al.*, 2003). Studies have demonstrated that this micro-damage caused by normal daily locomotion may be overcome by a healing rate of as little as 1% over 20 hours (Schechtman and Bader, 1997). High-stress tendons, such as Achilles tendon, have been shown to exhibit a lower safety factor but higher fatigue resistance when compared to positional tendons (Shepherd *et al.*, 2014). It has been hypothesised that, following the recruitment of fibres, failure of the fibres occurs at a strain limit and that a failure of the majority of these fibres leads to gross tendon failure (Schechtman and Bader, 2002).

6.4. Conclusion

Tendons exhibit complex mechanical behaviours well suited to their functional role in the body. However, this behaviour is not well understood in either healthy or diseased tendon. This has contributed to difficulty in understanding the aetiology of disease and in developing effective clinical management. Knowledge of tendon mechanical properties improves our understanding of injury and how it may be prevented (Hansen *et al.*, 2017). By understanding the normal behaviours of tendon, irregularities may become evident and be correlated to one of the many factors that contribute to mechanical damage, potentially leading to improved treatment and repair techniques.

The *in vivo* and *in vitro* tendon behaviour reported in literature is varied. One of the of the reasons for this variation is a lack of consensus of standardised testing protocols. Furthermore, few studies have provided complete data sets by testing in multiple modes. It is, therefore, difficult to compare within and between studies to elucidate differences in behaviour. Standardised protocols and complete data sets are necessary to ensure that tendon behaviour is adequately described and comparable. These will be explored in detail in later chapters.

CHAPTER 7.   TENSILE TESTING OF ACHILLES TENDON

7.1. Introduction

The properties of tendon are known to be difficult to measure accurately for several reasons, which include their high water content (70% of which can be expelled during deformation), the need to maintain hydration, temperature sensitivity, and their low transverse stiffness (Screen *et al.*, 2004a). This combination makes for a tissue that is difficult to grip and measure during testing. While the properties are well documented (Arnoczky *et al.*, 2002a; Screen *et al.*, 2004a), each application is different and there is little standardisation of testing procedures.

When measuring mechanical properties, several test variables require consideration as they may affect the behaviour of the tissue. These include:

- Storage;
- Hydration;
- Temperature;
- Geometry and orientation;
- Gripping;
- Strain and strain rate;
- Preconditioning;
- Time; and
- Recovery.

The subjects of geometry (Chapters 3–5), and time dependence (Chapter 8) are explored elsewhere.

This chapter describes and validates a testing protocol, derived from the literature, that represents a best practice approach to uniaxial tensile testing in tendon. It is intended that this will standardise testing in future studies to allow more reliable comparisons of results between studies, as well as achieving consistent testing between laboratories.

7.2. Analysis of literature

7.2.1. Storage and treatment

The effects of storage and treatment on the mechanical properties of soft tissue have been studied for many decades. While there have been

investigations into the effects of freezing, storage time, and freeze-thaw cycles, the results remain inconclusive. Early studies recommended testing within 30 minutes of death for the results to be considered valid (Matthews and Ellis, 1968; Woo *et al.*, 1986). However, storage of tissue is necessary as it is not always practical to test specimens immediately, such as with human cadavers (Matthews and Ellis, 1968; Woo *et al.*, 1986), or during complex and time-consuming testing (Moon *et al.*, 2006b).

A study by Cronkite (1936) found no difference between embalmed and untreated samples (24–48 hours after death). Matthews and Ellis (1968) found a decrease in apparent elastic modulus associated with freezing, but no other notable findings. Woo *et al.* (1986) found that with proper and careful storage the cyclic and tensile properties of New Zealand White (NZW) rabbit medial collateral ligaments were not affected after being frozen for three months. A follow-up study by Moon et al (2006b), investigating the effects of multiple freeze-thaw cycles and with a more robust viscoelastic analysis, found no significant difference in ultimate stress, strain, modulus, or quasi-linear viscoelastic (QLV) parameters after refreezing. They suggested that fresh samples should still be considered for sensitive viscoelastic tests. Clavert *et al.* (2001) found no difference in relaxation behaviour of biceps brachii tendon after freezing, but did note a decrease in tensile strength and elastic modulus. Giannini *et al.* (2008) found that deep-freezing (to -80 C) patellar tendon samples resulted in a decrease in ultimate load and strain.

Recent testing has focused on the effect of repetitive freeze-thaw cycles on the biomechanical properties of soft tissue. Chen *et al.* (2011b) reported significant changes in the ultimate load of rabbit Achilles tendon after three and ten deep-freeze-thaw cycles. Jung *et al.* (2011) found no significant difference in creep, stiffness, and ultimate tensile load in bone-patellar tendon-bone (BPTB) samples following one, four, and eight freeze-thaw cycles. Huang *et al.* (2011) found that five or more deep-freeze-thaw cycles negatively affected the ultimate load and stiffness of flexor tendons, while three cycles or less showed no difference to fresh samples. Ren *et al.* (2012), noted a similar result, with a significant decrease in ultimate load and stiffness following four deep-freeze-thaw cycles of flexor tendons.

Current practice is to discard grafts, as a precaution, after undergoing freeze-thaw cycles (Huang *et al.*, 2011), so understanding the effect on properties may aid in better management of grafts. The use of gamma irradiation on soft tissue was found to be detrimental to the stiffness and ultimate load and elongation of flexor tendons, and it was recommended that irradiation not be performed on allograft samples (Ren *et al.*, 2012).

It can be seen from the reports above that deep-freeze-thaw cycles negatively affect the biomechanical properties of soft tissue, while standard domestic freezers (-20 C) appear to have no effect. Thus, careful attention should be given to the freezing procedures (Chen *et al.*, 2011b; Clavert *et al.*, 2001; Duenwald *et al.*, 2009a; Giannini *et al.*, 2008; Jung *et al.*, 2011; Kamiński *et al.*, 2009; Matthews and Ellis, 1968; Moon *et al.*, 2006b; Smith *et al.*, 1996; Woo *et al.*, 1986). Altering the procedures for storage of grafts in order to preserve the mechanical properties through the various freeze-thaw cycles should be considered.

7.2.2. Hydration and temperature

The high water content of tendon means hydration is an important factor during testing, especially during viscoelastic testing. Tissue hydration has been reported to affect the flexibility (Elden, 1964) and strain rate sensitivity (Ciarletta *et al.*, 2008; Haut and Haut, 1997) of tendon. Similarly, temperature has been shown to affect the behaviour of soft tissue (Cohen *et al.*, 1976; Hooley and Cohen, 1979; Hooley *et al.*, 1980; Huang *et al.*, 2009; Woo *et al.*, 1987), with a noticeable change in behaviour near body temperature (Cohen *et al.*, 1976). Interestingly, Rigby *et al.* (1959) reported that variations in the temperature between 0 C and 37 C had no effect on the mechanical properties of rat tail tendon, but above 37 C there were changes that may be of importance. Still, many mechanical studies of soft tissue have been performed at room temperature (Benedict *et al.*, 1968; Bonner *et al.*, 2015; Chen *et al.*, 2011a; Dressler *et al.*, 2006; Duenwald *et al.*, 2009a; Duenwald *et al.*, 2010; Fink *et al.*, 1999; Haraldsson *et al.*, 2005; Jimenez *et al.*, 1989; LaCroix *et al.*, 2013a; Liu *et al.*, 2009; Nakagawa *et al.*, 1996; Sverdlik and Lanir, 2002; Szczesny *et al.*, 2012; Tohyama *et al.*, 1992; Wren *et al.*, 2001b).

Masouros *et al.* (2009) reviewed testing conditions for joints and suggested that the ideal testing environment would be a bath of interstitial fluid at 37 C. A similar recommendation had previously been made by Funk *et al.* (1999). Several studies have attempted to match this environment by heating physiological solutions to body temperature (Abramowitch and Woo, 2004; Awad *et al.*, 1999; Butler *et al.*, 1986; Fujie *et al.*, 2000; Johnson *et al.*, 1994; Majima *et al.*, 1996; Nekouzadeh *et al.*, 2007; Ohno *et al.*, 1993; Shepherd *et al.*, 2014; Takai *et al.*, 1991; Thornton *et al.*, 2001; Tohyama *et al.*, 1992; Woo *et al.*, 1986; Yamamoto *et al.*, 1999, 2000). Alternative methods include a bath of solution, such as phosphate buffered (PBS) and Ringer's solutions (Abramowitch *et al.*, 2010; Hingorani *et al.*, 2004; Screen *et al.*, 2004b), and humidity chambers (Chaudhury *et al.*, 2012; Gautieri *et al.*, 2013; Helmer *et al.*, 2004; Myers *et al.*, 1991; Pioletti and Rakotomanana, 2000a, 2000b; Pioletti *et al.*, 1998; Race and Amis, 1996; Thornton *et al.*, 2007). However, a great many experiments have maintained tissue hydration by a regular spray or mist of solution (Abdel-Wahab *et al.*, 2011; Bonner *et al.*, 2015; Cheng and Gan, 2008; Cheung and Zhang, 2006; Ciarletta *et al.*, 2008; Ciarletta *et al.*, 2006; Hashemi *et al.*, 2005b; Ikoma *et al.*, 2013; Legerlotz *et al.*, 2010; Lockwood *et al.*, 2016; Machiraju *et al.*, 2006; Miller *et al.*, 2012a; Miller *et al.*, 2012b; Moon *et al.*, 2006a; Rigozzi *et al.*, 2009; Schmidt and Ledoux, 2010; Screen, 2008; Screen *et al.*, 2006; Screen *et al.*, 2005c; Screen *et al.*, 2013; Su *et al.*, 2008; Thorpe *et al.*, 2013b; Troyer and Puttlitz, 2012).

7.2.3. Orientation

Specimen orientation of samples with heterogenous microstructures, such as composite materials, is known to influence the results in a typical tensile test. Several studies have shown the transverse properties of tendon to be inferior to the longitudinal properties (Lake *et al.*, 2010; Lynch *et al.*, 2003; Yamamoto *et al.*, 2000). Therefore, in *ex vivo*/*in vitro* testing the longitudinal axis of tendon should be aligned with the anatomical direction of load. In a typical tensile ramp test, or a traction test, one or two universal joints may be used to allow the sample to align as load is applied. While it is preferable to clamp the sample

rigidly along the direction of load, this method allows for small deviations to be corrected.

Shim *et al.* (2015), presenting to the Orthopaedic Research Society, indicated that the twist in the Achilles tendon may improve efficiency and strength. The twist was likened to that of reinforcing bars in composite materials. Therefore, it is important not only to align samples with the direction of load, but also to consider the original anatomical positioning to improve the accuracy of the biomechanical measurements during testing. Similar results have previously been presented by Kim *et al.* (2014), who found that the strength of the medial patellofemoral ligament was highest when oriented in an anatomical position.

Therefore, efforts should be made to accurately replicate *in vivo* orientations and loading conditions.

7.2.4. Length

The exchange by Anssari-Benam and colleagues with Horgan (Anssari-Benam *et al.*, 2012b, 2013; Horgan, 2013) highlights one of the lesser-considered difficulties with the gripping and testing of soft tissue. It was shown that specimen length affects the mechanical behaviour of tissues with short gauge lengths, as the act of gripping creates an irregular strain field around the gripped area. This follows the Saint-Venant's principle, which states that this strain field decays away from the point of gripping. Anssari-Benam *et al.* (2012b) described that, past the characteristic decay length, tissues behave consistently and, therefore, if the specimens of choice do not meet the minimum length, the data should be 'calibrated' against an appropriate constitutive model. In response to Horgan (2013), Anssari-Benam *et al.* (2013) stated: "one of the primary aims of our letter was to improve awareness of end-effects within the biomechanical community, as end-effects in many biological tissues can be substantial, but are often poorly understood or, at worst, ignored."

Studies on Achilles tendon grafts, leather, and carbon fibres, noted that ultimate load decreased with increasing gauge length (DeFrate *et al.*, 2004; Naito *et al.*, 2011; Thanikaivelan *et al.*, 2006). No comment was made on the effect of gripping, but this could be due to a 'positive' influence of Saint-

Venant's principle at shorter gauge lengths. An investigation by Jimenez *et al.* (1989) demonstrated the influence of Saint-Venant's principle by showing that grip proximity significantly affected the local strains in tendons. Nirmalanandhan *et al.* (2007) subsequently found that increasing the length of tissue engineered constructs to minimise the Saint-Venant's effect also increased the material properties, such as stiffness and fibre alignment. Legerlotz *et al.* (2010) found, similarly, that grip-to-grip length played a significant role in measured properties of rat and bovine tendon fascicles and attributed these to the end-effects.

In many cases, the choice of tissue is dictated by factors such as location, size, or pathology. It is for the following reasons that the NZW rabbit Achilles tendon was selected as the tissue of choice for the ARC Linkage Project:

- It is easily accessible for both treatment and excision
- It is a large in a small animal, making it easier to work with
- Achilles tendon pathologies are common and relevant

The length of tendon, therefore, is not considered as a factor, except in the context of gauge length for calculating strain. Legerlotz *et al.* (2010) noted that it is not always possible to control sample lengths, but they should be considered when comparing samples due to the influence of end-effects. With this in mind, Lynch *et al.* (2003) discussed the importance of grip selection to minimise these end-effects when testing soft tissue. Gripping, therefore, may be one of the most important factors to consider when designing experiments.

7.2.5. Gripping

Gripping of soft tissue has been historically difficult, due to the slippery and delicate but strong structures. Inadequate gripping will likely result in slippage, leading to measurement errors (Masouros *et al.*, 2009). Typically, soft tissue is clamped, or compressed, between rigid grips to create high friction forces, but this can lead to end-effects (Shi *et al.*, 2012; Wieloch *et al.*, 2004), as discussed in subsection 7.2.4. As a result, some of the following attempts have been made to find suitable means of holding tissue. Flat surfaced grips with serrated or sinusoidal faces have been common (Cheung and Zhang, 2006; Rincón *et al.*, 2001). Self-tightening wedge action grips have been used to

maintain compression (Butler *et al.*, 1984; Kahn *et al.*, 2010). Sandpaper, and other additives, have been a common addition to grips to improve the friction on the sample, thereby reducing the necessary clamping force (Kahn *et al.*, 2010; Masouros *et al.*, 2009; Pardes *et al.*, 2016; Schechtman and Bader, 1997; Sverdlik and Lanir, 2002). A significant drawback is the risk of plastic deformation of the samples, meaning repeat tests may not be possible (Cheung and Zhang, 2006).

The use of bony attachments has been identified as a solution since bone is easier to fix (Riemersa and Schamhardt, 1982). Potting, using a resin or poly-methyl methacrylate (PMMA), has been used extensively to secure the bony portion of structures, such as bone-ligament-bone and bone-tendon complexes (Amis and Scammell, 1993; Butler *et al.*, 1984; Butler *et al.*, 1986; Duenwald *et al.*, 2009a; Duenwald *et al.*, 2010; Fryhofer *et al.*, 2016; Kahn *et al.*, 2010; Nagasawa *et al.*, 2008; Pardes *et al.*, 2016; Wren *et al.*, 2001b). Of most importance, and often overlooked, is the anatomy of the rabbit Achilles tendon. The fusion of the gastrocnemius and soleus tendon bodies occurs much closer to the calcaneus than in humans. A study by Doherty *et al.* (2006) comparing human and rabbit Achilles tendon noted that the human Achilles fused 200mm proximal to the calcaneus out of 260mm full length of the triceps surae, while the rabbit tendon fused at only 5.2mm above the calcaneus out of 70mm of triceps surae. By removing the tendon from the calcaneus, test results will not truly represent the properties of the Achilles tendon.

Cryo-grips, or freezing grips, are increasingly being used to grip soft tissue for testing, as they eliminate the need to compress the tissue, potentially minimising the Saint-Venant's effect. Riemersa and Schamhardt (1982) developed what is considered the original cryo-grip, and many variations have been developed since (Chatzistergos *et al.*, 2010; Duenwald *et al.*, 2009a; Duenwald *et al.*, 2010; Lepetit *et al.*, 2004; Morelli *et al.*, 2002; Riemersa and Schamhardt, 1982; Rincón *et al.*, 2001; Sharkey *et al.*, 1995; Shi *et al.*, 2012; Wieloch *et al.*, 2004), including thermoelectrically cooled (TEC) grips (Kiss *et al.*, 2009; Warden, 2007). These grips have been shown to resist large loads without slippage and are now considered the gold standard for mechanical testing of tendons (Shi *et al.*, 2012).

7.2.6. Strain and strain rate

Grip-to-grip strain has been shown to overestimate strain compared to local measurements (Butler *et al.*, 1984; Sverdlik and Lanir, 2002). Chapters 3–5 sought to describe the importance of understanding these local strains. One of the reasons for utilising grip-to-grip is the simplicity of the measurement. While it may not be the most accurate method, as it assumes no slippage and uniform strain, but it is easily implemented. Extensive work by Screen *et al.* (Anssari-Benam *et al.*, 2012a; Cheng and Screen, 2007; Gupta *et al.*, 2010; Screen, 2008; Screen *et al.*, 2004a; Screen and Evans, 2009; Screen *et al.*, 2002b; Screen *et al.*, 2013; Thorpe *et al.*, 2012a), Arnoczky *et al.* (Arnoczky *et al.*, 2002a; Arnoczky *et al.*, 2004; Arnoczky *et al.*, 2002b; Lavagnino and Arnoczky, 2005; Lavagnino *et al.*, 2006; Lavagnino *et al.*, 2005; Lavagnino *et al.*, 2008; Lavagnino *et al.*, 2014) and others (Bogaerts *et al.*, 2016; Duenwald *et al.*, 2011; Han *et al.*, 2013; Jimenez *et al.*, 1989; Khodabakhshi, 2011; Khodabakhshi *et al.*, 2013; Kuo *et al.*, 1999; Lersch *et al.*, 2012; Miller *et al.*, 2012a; Miller *et al.*, 2012b; Miller *et al.*, 2012c; Obst *et al.*, 2014b; Okotie *et al.*, 2012; Rigozzi *et al.*, 2009), has sought to measure local strains within the tendon. These are primarily strains of the microstructure, but significant strides have been made in relating the macro- and micro-strains (Fang and Lake, 2015, 2016; Gupta *et al.*, 2010; Han *et al.*, 2013; Kahn *et al.*, 2013; Stella *et al.*, 2008; Upton *et al.*, 2008). A significant advantage of capturing local strain data is the ability to inform finite element models (FEM) (Ahmadzadeh *et al.*, 2015; Fornells *et al.*, 2007; Guilak and Mow, 2000; Handsfield *et al.*, 2017; Hansen *et al.*, 2017; Lavagnino *et al.*, 2008; Peña *et al.*, 2007; Screen and Evans, 2009; Shim *et al.*, 2015; Shim *et al.*, 2014; Wilkes *et al.*, 2009). As a result, technologies such as video strain transducers (Lam *et al.*, 1992; van Bavel *et al.*, 1996; Woo *et al.*, 1992) and digital image correlation (DIC) (Chen *et al.*, 2005; Evans *et al.*, 2007; Gao and Desai, 2010; Genovese *et al.*, 2011; Genovese *et al.*, 2013; Okotie *et al.*, 2012; Spera *et al.*, 2011) have been employed to more accurately measure the surface strain of the tendon. These techniques have limitations in that they assume the surface of the tendon is representative of the internal structures, which may not be the case in hierarchically-structured

tissue such as tendon. However, they provide a platform for linking the microstrain and local strains.

Mechanical behaviour of soft tissue is viscoelastic and is, therefore, dependent on strain rate (Pioletti *et al.*, 1998). It has been suggested that strain rate dependence may only exist in the toe region (Masouros *et al.*, 2009; Pioletti *et al.*, 1999). Strain rates of 0.1–14,000%.s^{-1} have been reported in many tissues, with a common finding of increased stiffness and modulus, but not necessarily an increase in failure properties (Bonner *et al.*, 2015; Clemmer *et al.*, 2010; Crisco *et al.*, 2002; Lewis and Shaw, 1997; Lynch *et al.*, 2003; Mattucci *et al.*, 2013; Pioletti *et al.*, 1999; Robinson *et al.*, 2004; Theis *et al.*, 2012; Thornton *et al.*, 2007; Wren *et al.*, 2001a). Studies into the effects of collagenase demonstrated no change in failure load using high strain rates but a reduced failure load when testing at low strain rates (Chen *et al.*, 2004; Hsu *et al.*, 2004a; Hsu *et al.*, 2004b; Lake *et al.*, 2008; Stone *et al.*, 1999). It has been suggested that the influence of strain rate has been overstated (Masouros *et al.*, 2009). In many cases though, strain rate selection can be narrowed down to machine capabilities and data acquisition rate (Duenwald *et al.*, 2009b).

7.2.7. Preconditioning

The importance of preconditioning was discussed by Fung as far back as 1981 (Shoemaker *et al.*, 1986), and has since been identified as an essential part of testing protocols for soft tissue (Lanir, 2010). Preconditioning is the cycling of a sample multiple times until a steady-state is reached, at which point the tissue will behave in a repeatable fashion when tested. Preconditioning is only partially reversible and requires time for recovery (Abrahams, 1967; Duenwald *et al.*, 2010; Lanir, 2010; Rigby *et al.*, 1959; Sverdlik and Lanir, 2002). It was highlighted as a component of the time-dependent characteristic of tissue, as its role is to develop a long term, or even irreversible, recovery component when compared to the elastic response (Sverdlik and Lanir, 2002). Preconditioning effectively shifts the stress-strain curve to the right due to an increase in the 'stress free' tendon length (Sverdlik and Lanir, 2002) and has been shown to realign the collagen fibres along the direction of loading via progressive fibre recruitment (Miller *et al.*, 2012c; Quinn and Winkelstein,

2011; Teramoto and Luo, 2008). This may in part be due to the uncrimping and alignment of the collagen matrix without recovery. Ciarletta *et al.* (2008) and Ratchada (2013) have suggested preconditioning represents the stabilisation of links between the collagen and proteoglycan (PG) matrices.

Despite its importance, relatively few studies in literature have explicitly investigated preconditioning, with many investigating this phenomena to achieve better tissue graft fixation (Bergomi *et al.*, 2009; Cheng *et al.*, 2009; Ejerhed *et al.*, 2001; Jaglowski *et al.*, 2016; Jisa *et al.*, 2016; Liu and Yeung, 2006; Liu and Yeung, 2008; Lockwood *et al.*, 2016; Miller *et al.*, 2012c; Quinn and Winkelstein, 2011; Schatzmann *et al.*, 1998; Sverdlik and Lanir, 2002; Teramoto and Luo, 2008).

Pradas and Calleja (1990) discussed the importance of preconditioning on the nonlinear behaviour of hand flexor tendons during creep experiments. They found that preconditioning removed the irrecoverable portion of the tendon extension, thus permitting full recovery between creep tests on the same tendon. Most studies assume a steady response after 10–20 cycles; however, it has been reported that effects can continue after 1000 cycles (Rigby *et al.*, 1959; Sverdlik and Lanir, 2002), and up to 2000 (Bergomi *et al.*, 2009). One thousand cycles was recommended for longer testing durations (Bergomi *et al.*, 2009). Cheng *et al.* (2009) recommended that preconditioning strain should be the highest strain used in the study, and that it should be reported for comparison purposes. Similar recommendations were made by Jaglowski *et al.* (2016) and Lockwood *et al.* (2016), who found that high-load preconditioning reduced subsequent extensions. Nevertheless, some studies have reported no effect of preconditioning (Ejerhed *et al.*, 2001; Jisa *et al.*, 2016).

Preconditioning is not always appropriate. To avoid interference with measurements, Kahn *et al.* (2010) preferred to simply preload the rabbit Achilles tendon so as not to influence the loading history.

7.2.8. Time dependence

Of great interest is the duration of testing required to accurately describe the behaviour of soft tissue over a long period. Many different time periods have

been used to test tendon behaviour in both static and dynamic creep and relaxation tests. However, many of these appear to have been selected arbitrarily. Ideally, tissue would be measured for several hours in order to determine whether an equilibrium is achieved. However, this is impractical in most applications, and a compromise must be achieved. To the author's knowledge, only one previous study, by Manley Jr *et al.* (2003), has investigated time explicitly. The effect of time on mechanical testing will be investigated in Chapter 8.

7.2.9. Recovery

Viscoelastic tissues require a period of recovery between testing to prevent influence of previous loading histories on subsequent tests. Failure to allow for adequate recovery may result in measurement errors when compared to untested or fully-recovered samples (Duenwald *et al.*, 2009a). Few studies have investigated recovery, but it has been shown that recovery requires more time than the duration of loading (Legerlotz *et al.*, 2013b), with recommendations of at least one order of magnitude longer than the test length; that is, 1000s for a 100s test (Duenwald *et al.*, 2009a). It was noted that recovery was incomplete after seven hours following a 50-minute cyclic test of cat spine, but fully recovered in wrist ligaments and intervertebral discs after 24 hours following creep tests (Duenwald *et al.*, 2009a; O'Connell *et al.*, 2011). While this likely has little influence on tensile tests, it may significantly influence the behaviour of viscoelastic testing.

7.3.   Methodology

7.3.1. Samples

Sixteen NZW rabbit Achilles tendon were obtained from an unrelated study under University of Western Australia (UWA) Animal Ethics Committee approval RA/3/100/1049. The triceps surae, tendon and calcaneus were excised as a single unit, and the aponeurosis removed from around the tendon. Tendons were wrapped in saline-soaked gauze and stored at -20°C in accordance with the recommendations in subsection 7.2.1. On the day of testing, tendons were thawed at room temperature in a bath of Ringer's solution to maintain hydration. The calcaneal tuberosity was potted in poly-

methyl methacrylate (PMMA) (Vertex Self Curing, Vertex-Dental B.V., The Netherlands) inside of a 25mm section of OD20mm PVC pipe. Cross-sectional area (CSA) was measured using an Artec Spider™ structured light scanner (Artec Group, Luxembourg) as described in Chapter 4.

7.3.2. Test setup

Mechanical testing was performed on an Instron 5566 uniaxial materials testing system (Instron, MA, USA). The myotendinous junction was secured within TEC grips (Bose Enduratec, MN, USA) by freezing between the gripping faces using the Peltier thermoelectric effect. The calcaneus was secured perpendicular to the tendon axis, in an anatomical position. The setup (Figure 7-1) was similar to that described by Warden (2007). A line of India ink was applied at the interface of the TEC grip to assess slippage. Once the musculotendon junction was secured, a preload of 1N was applied and the grip-to-grip length measured using digital callipers (accuracy 0.01mm). Tendons were kept moist by spraying with saline.

7.3.3. Mechanical testing

Tendons were preconditioned for 20 cycles, from 0% to 4% strain at $1\%.s^{-1}$. Eight tendons were stretched to failure at $10\%.min^{-1}$ and the remaining eight
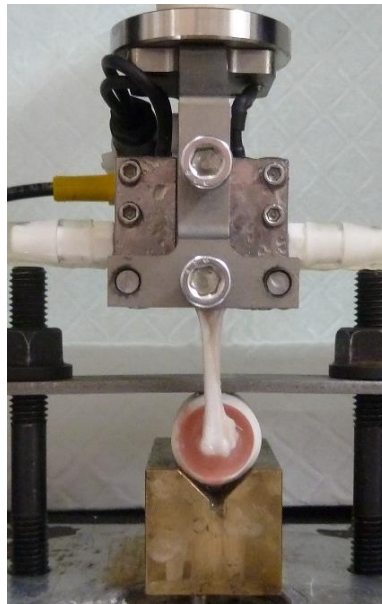
Figure 7-1: The rabbit Achilles tendon tensile test setup on the Instron 5566. The calcaneus was potted in poly-methyl methacrylate (PMMA) and secured perpendicular to the tendon axis in an anatomical position. The myotendinous junction was frozen within the thermoelectrically cooled (TEC) grips.

tendons stretched at 1000%.min^{-1}. Tendons that failed by avulsion were retested at the same strain rate, without the calcanues, and secured with a second grip.

7.3.4. Measurements

Load and displacement were recorded at 60Hz. Stress and strain were calculated from CSA and gauge length. Maximum values of load, stress, displacement, and strain were calculated. Stiffness, and elastic modulus, were calculated using a custom implementation of the Instron BlueHill 2 automatic slope algorithm. This algorithm, described in detail in the Instron BlueHill Calculation Reference manual (version 1.1), divides the data into six equal regions between zero and the maximum load, calculates the slope of each region using least-squares linear fit, and finally returns the highest slope value from the pair of regions with the 'highest slope sum'.

7.3.5. Statistics

Data were analysed using Microsoft Excel (2016) and in the R Statistical Environment (Lianoglou and Antonyan, 2014; R Core Team, 2015; RStudio, 2016; Wickham, 2009, 2011, 2015). Results are presented as mean and standard deviation.

7.4.   Results and discussion

7.4.1. Samples

In all, 16 tendons were tested at both 10%.min^{-1} (~2.2mm.min^{-1}), herein referred to as Slow, and 1000%.min^{-1} (~220mm.min^{-1}), herein referred to as Fast. The mean gauge length of the tendons was 21.87 ± 3.54mm (mean ± SD). The mean minimum CSA was 8.25 ± 1.08mm^2. CSA measurement was smaller than that measured in Chapter 4 (9.9 ± 1.0mm^2) but similar to others reported in literature (Ikoma *et al.*, 2013). CSA is likely lower due to the young age of the rabbits.

7.4.2. Failure properties

All samples in the 10%.min^{-1} group failed by avulsion and were subsequently retested as tendon-only samples for comparison. These are herein referred to as Slow-T. Five out of eight, or 62.5%, of the Fast tendons failed in the tendon midsubstance. Subsequently, no Fast tendons were repeated as there would

be insufficient statistical power in the Fast-T group. Raw data is presented in Figure 7-2.

It was noted by Noyes *et al.* (1974) that bone-ligament-bone constructs tested at slow strain rates tend to fail by avulsion more than in the midsubstance, while high strain rates fail in the midsubstance more than by avulsion. Lewis and Shaw (1997) showed similar behaviour in human Achilles tendon constructs, with avulsions only occurring in the slow strain group. The results of this study confirm these findings in bone-tendon constructs, with slow strain rates failing by avulsion in 100% of cases, compared with 37.5% of samples at the faster strain rate. The proportion of avulsion fractures in the Slow group was higher than some previous studies that reported avulsion fractures (Kiss *et al.*, 2009; Rincón *et al.*, 2001; Wren *et al.*, 2001a), while similar to others (Lewis and Shaw, 1997; Wieloch *et al.*, 2004). Avulsion rates in the Fast group were similar to the aforementioned studies. This suggests that tendons should be tested at faster strain rates to ensure that results reflect the failure mechanics of the tendon, as opposed to the failure mechanics of the construct.

This study utilised a simple means of assessing slippage at the musculotendon junction, as previous used by Butler *et al.* (1984). Slippage was not evident via observation of the India ink mark and load-displacement curve.

Avulsion fractures in this study represented a clean break of the calcaneus near the boundary of the tuberosity. This occurred within the PMMA in most cases, suggesting that the failure was related to the tensile strength of the

Table 7-1: Mean (± SD) tensile test results for rabbit Achilles tendon for the Fast, Slow, and Slow Tendon-only (Slow-T) groups. Displacement (mm) and strain (%) values correspond to the maximum force (N) and maximum stress (MPa) values, respectively. [+] denotes significantly different from Slow. [#] denotes significantly different from Slow-T.

Tensile Test	Slow	Slow-T*	Fast
Max. Force (N)	306.7 ± 69.6	249.0 ± 53.1	378.9 ± 105.4[#]
Max. Stress (MPa)	38.9 ± 11.8	31.0 ± 5.9	44.5 ± 9.3[#]
Displacement (mm)	6.5 ± 1.9	4.2 ± 1.1[+]	6.1 ± 1.3[#]
Strain (%)	28.1 ± 7.7	28.4 ± 6.1	28.8 ± 7.0
Stiffness (N/mm)	64.3 ± 9.8	99.4 ± 30.7[+]	97.4 ± 14.3[+]
Elastic Modulus (MPa)	203.0 ± 54.0	194.2 ± 53.3	249.6 ± 50.9

bone and was not caused by bending at the junction of the PMMA and bone. Midsubstance failures appeared to have been caused by fibres within the tendon body failing at their weakest point and as they reached their limits, resulting in a slower failure of the tendon and fraying of the tendon ends. Most failures occurred at or near the point of fusion. Tendon-only testing saw the tendon fail at the lower grip, near the point of minimal CSA, which is most likely due to the effect of clamping the tendon.

Testing has generally shown that the muscle-tendon-bone unit fails at the junctions (Benedict *et al.*, 1968). It has been noted that, with adequate gripping, soft tissue samples that fail at or near the grips have similar results
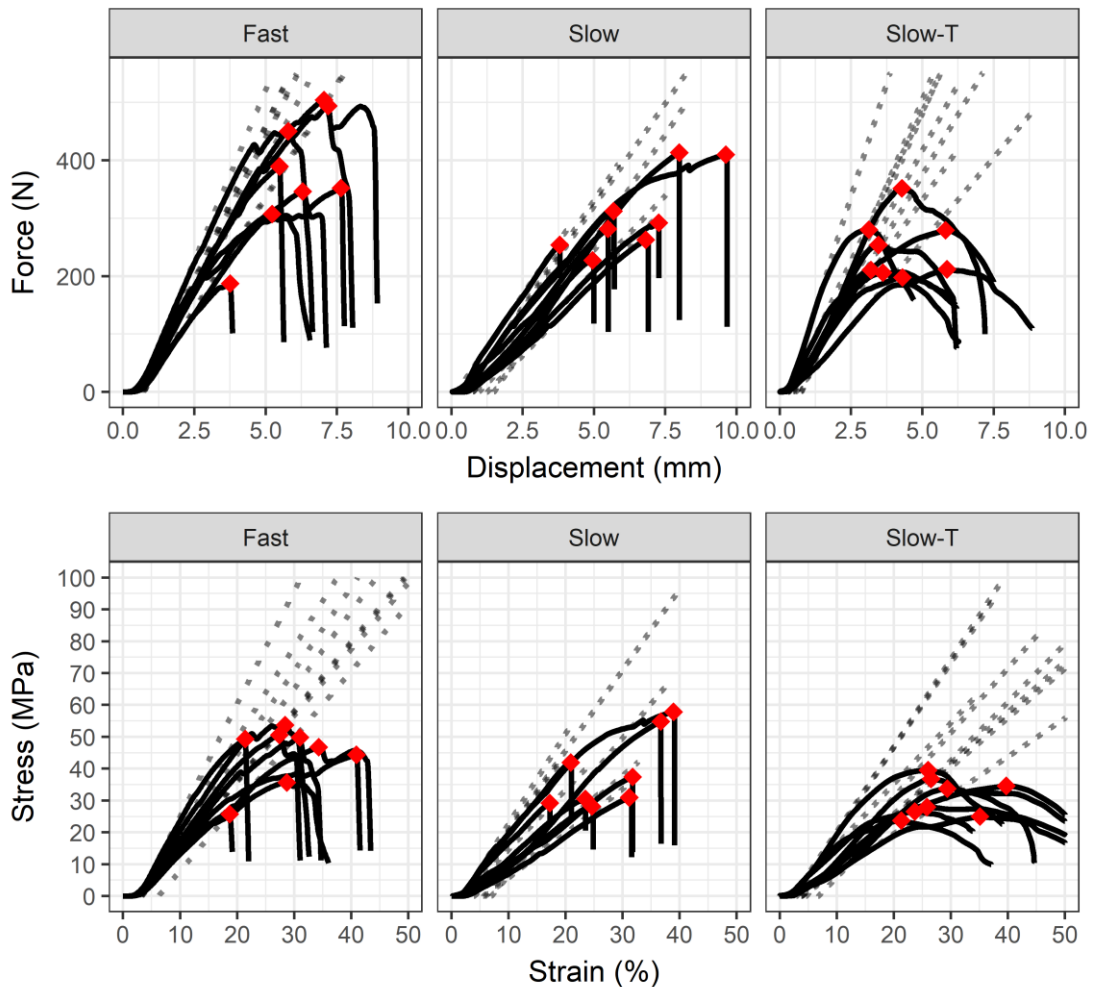
Figure 7-2: Tensile test results for rabbit Achilles tendon for the Fast, Slow, and Slow Tendon-only (Slow-T) groups. (top) Force (N) versus Displacement (mm), and (bottom) Stress (MPa) versus Strain (%). Raw values (solid), slopes (dotted) and peak values (red) are indicated.

to those that fail midportion (Masouros *et al.*, 2009). Avulsion fractures are known to be the most common mode of failure in young adults (Wren *et al.*, 2001a). While the exact ages of the rabbits used in this study were not known, the estimated age at sacrifice was 18–20 weeks. This is younger than reported skeletal maturity of six months (26 weeks) (Cacchioli *et al.*, 2012; Canavese *et al.*, 2010; Francesca *et al.*, 2015) and may explain the higher incidence of avulsion fractures at low strain rates compared with other studies. The absence of failures at the musculotendon junction can be viewed as a success, since this has previously been identified as the weak link of the muscle-tendon-bone unit (Sharma and Maffulli, 2005b; Wang, 2006), and the most difficult to grip (Masouros *et al.*, 2009). However, testing of tendon-only specimens highlighted the issues with gripping of soft tissue, as the tendon failed at the grip in a way that suggested influence by the grip.

Mean results for the tensile testing are presented in Table 7-1 and Figure 7-3. Slow-T demonstrated significantly lower values of force and stress at failure compared with Fast, but no difference with Slow. Slow-T also demonstrated significantly lower displacement at failure compared with both Slow and Fast. Stiffness was significantly higher in both Slow-T and Fast compared with Slow, but not different between Slow-T and Fast. No difference was detected between groups in strain or modulus measurements.

Reports of the mechanical properties of NZW rabbit Achilles tendon in the literature are varied. The values reported in 19 studies have been summarised in Table 7-1, along with the results of this study. The full reported values are tabulated in Table 7-3. All values reported in this study are within the ranges seen in the literature, and at or near the mean and median values, suggesting the testing protocols are representative of best practice.

Strain rate was shown to affect the mode of failure and the stiffness of the construct, but did not significantly affect any other measure of testing. Removing the bone was shown to affect the failure force and stress, compared with the Fast group, but did not appear to alter the behaviour of the tendon relative to the Slow group. When the anatomy of the tendon is considered, namely the distance of fusion proximal to the calcaneus, it may be preferable to test with the bone intact. A significant limitation of this study was that
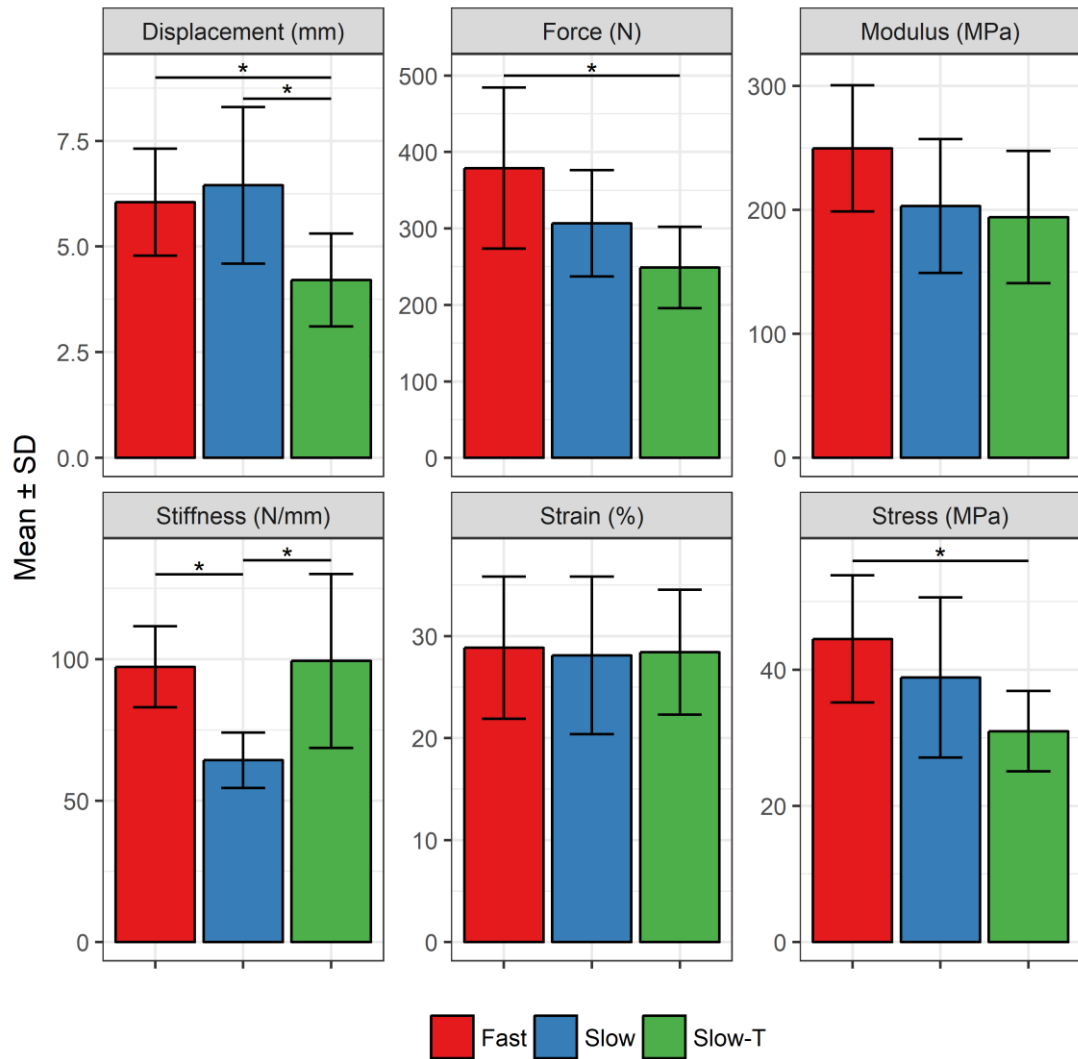
Figure 7-3: Mean (± SD) tensile test results for rabbit Achilles tendon for the Fast, Slow, and Slow Tendon-only (Slow-T) groups. Displacement (mm) and strain (%) values correspond to the maximum force (N) and maximum stress (MPa) values, respectively. Significance (p<0.05) is between groups is indicated.

tendons were reused for the Slow-T group and may have been damaged during previous testing.

The young age of the rabbits may explain the average properties in this study. Nakagawa *et al.* (1996) demonstrated an increase in tendon properties with age, with young adults considered 8–10 months compared with less than six months in this study. Force, strength, and modulus increased, but little difference was seen in maximum strain. Failure strain was seen to be consistent between strain rates and gripping techniques, lending support to the idea that strain is the limiting factor in failure of the tendon. However, strain

was higher in this study compared to the literature. Since younger bone is more elastic, it is possible that this contributed to the relatively high displacement and strain seen in this study. Hugate *et al.* (2004) reported a grip-to-grip strain of 50% but noted that the midsubstance strain was much lower at only 19%, lending plausibility to the idea that the bone contributed to the overall strain. This will have influenced the values of stiffness and modulus.

There are several possible reasons for the difference in failure load. As discussed in subsection 7.2.4, end- effects will lead to higher loads at shorter grip-to-grip lengths. To the best of the author's knowledge, the gauge length of rabbit Achilles tendon has not been reported sufficiently in the literature to compare. Of the 19 reports of rabbit tendon properties (Table 7-3), there were only three reports of failure loads greater than the mean value – Nakagawa *et al.* (1996), with both young and old rabbits, and Wang *et al.* (2015). Nakagawa *et al.* (1996) noted that the length of tendon was 50mm upon excision, and clamped both ends of the tendon within wedge-action grips, likely minimising end-effects. Although the tendon CSA was larger than in this study ($13.2/15.3mm^2$ vs. $8.1mm^2$), the maximum stresses of ~67MPa was still much greater than the 39MPa in this study. It is entirely possible that similar stresses may have been achieved in this study if the samples had not failed by avulsion. Wang *et al.* (2015) made use of liquid nitrogen to freeze the tissue within the grips. Additionally, the entire bone-tendon junction was frozen within the grip.

Table 7-2: Summary of 18 papers with 19 relevant reports of tensile test results of healthy rabbit Achilles tendon. Results from this study are presented for comparison.

N = 19	Reports	Mean	Median	Range (Min – Max)	Slow	Slow-T*	Fast
Strain rate (mm/min)	19	216.6	60.0	1.0 – 600.0	~2.2	~2.2	~220
CSA (mm^2)	9	11.7	13.2	4.3 – 16.8	8.1 ± 0.8	8.1 ± 0.8	8.5 ± 1.3
Force (N)	18	415.8	342.8	189.0 – 1010.4	306.7 ± 69.6	249.0 ± 53.1	378.9 ± 105.4
Stress (MPa)	15	37.5	33.4	8.4 – 85.3	38.9 ± 11.8	31.0 ± 5.9	44.5 ± 9.3
Displacement (mm)	3	5.5	5.5	5.0 – 6.0	6.5 ± 1.9	4.2 ± 1.1	6.1 ± 1.3
Strain (%)	10	22.4	16.2	10.7 – 50.0	28.1 ± 7.7	28.4 ± 6.1	28.8 ± 7.0
Stiffness (N/mm)	10	117.4	97.0	36.5 – 224.7	64.3 ± 9.8	99.4 ± 30.7	97.4 ± 14.3
Modulus (MPa)	15	180.2	68.3	1.62 – 618.0	203.0 ± 54.0	194.2 ± 53.3	249.6 ± 50.9

Since the liquid nitrogen technique did not permit exact freezing – the grips required submersion in the liquid nitrogen which may cool the tendon midsubstance – it is possible the tendon was tested below room temperature and behaved as a stiffer construct. The maximum stresses in this study match well with those previously reported, being almost equal to the mean (37.5MPa vs. 38.9MPa in this study). This highlights the importance of presenting material properties (stress, strain, and modulus), rather than construct properties (load, displacement, and stiffness) which are difficult to compare.

7.4.3. Hydration and temperature

The method of hydration in many cases is influenced by measurement and testing requirements. In the case of optical measurement systems, environmental chambers and baths may not be possible, due to the need for clear line-of-sight. Additionally, grip selection may influence the choice of hydration method. In this case, the choice of TEC grips prohibited the use of a bath, since grips would cool the bath. This, in turn, would negative influence the temperature of the testing environment. Additionally, the bath would likely reduce the effectiveness of the grips by inhibiting freezing and increasing slipperiness at the interface. Similarly, the use of TEC grips discouraged the use of an environmental chamber, since the constant warming of the chamber would also reduce the effectiveness of the grips. As a result, it was deemed more practical to perform testing at room temperature and to maintain hydration via regular pipetting of Ringer's solution onto the tendon, below the TEC grip. The means of hydration likely had limited impact on the results of this experiment since the testing time was negligible. Despite evidence of temperature not significantly affecting behaviour up to 37 C (Rigby *et al.*, 1959), testing at room temperature may be considered a limitation of this study.

7.4.4. Length, grip selection, and orientation

During pilot testing, many grips were developed, based on those described in the literature (subsection 7.2.5), and trialled. Specifically, wedge action, flat plates with sinusoidal teeth, sandpaper, cyanoacrylate, and various liquid nitrogen cooled fixations were trialled. The most successful for tensile tests to failure were the liquid nitrogen based devices; however, these were impractical as they required time in a liquid nitrogen bath to freeze and were, therefore,

unsuitable for extended testing. In line with recommendations from the literature (Kiss *et al.*, 2009), TEC grips were identified as the most suitable means of fixing the musculotendinous junction for an extensive period of time.

Pilot testing of tendon with and without bone found more reliable and repeatable results during testing with the bone. Since the length of tendon with bony attachment was only 20–30mm, gripping both ends of the rabbit Achilles tendon using clamps resulted in a very short grip-to-grip length and an increased influence of Saint-Venant's end-effects. Additionally, the proximity of the freezing grips resulted in a lower temperature of the midsubstance. It was found that the tendon still failed at the grips, usually by shredding and fraying of the tendon fibres at the point of first 'impingement' of the clamps.

Methods of bony fixation were trialled, including keyhole slots with and without cementation. PMMA cement was found to be necessary to prevent the bone pulling through at high loads and to avoid impinging on the tendon, since the insertion extended across much of the calcaneal tuberosity surface.

The bone-tendon-muscle complex was secured as close to anatomical position as possible. The orientation of muscles to the bone was noted and replicated. By fixing in bone cement, the calcaneus was able to be oriented 90 degrees to the tendon, thereby maintaining anatomical orientation as recommended in subsection 7.2.3. Coincidentally, the mechanical setup was found to be almost identical to one reported by Warden (2007).

7.4.5. Preconditioning, strain rate, and strain measurements

Tendons in this study were cycled for 20 cycles between 0% and 4% strain in line with other studies. A lower strain magnitude was required for preconditioning, contrary to recommendations by Cheng *et al.* (2009), since these tendons were to be tested to failure. Four percent was selected as it is regarded as the end of the linear region in the typical stress-strain profile. In this case, the number of cycles was selected for convenience and based on similar studies. For example, Nakagawa *et al.* (1996) used 10 preconditioning cycles while Wang *et al.* (2015) reported only five cycles. Based on the extension/strain observed, it is possible that 20 cycles were insufficient to

achieve adequate preconditioning and, therefore, the number of cycles should be considered carefully before viscoelastic testing.

Subsection 7.2.6 highlighted the effect of strain rate on stiffness and modulus, with an increase in both properties with increasing strain rate. Based on findings by Noyes *et al.* (1974) in bone-ligament-bone constructs, Yasuda *et al.* (2000) identified that use of higher strain rates in bone-tendon constructs results in less avulsion fractures. Conversely, it has been said that influence on strain rate is overstated and may not affect failure properties. The strain rate in this study can be viewed as a limitation but highlights the importance of strain rate and the need to report values in the methodology to allow for comparison between studies.

Despite the importance of measuring local strains (subsection 7.2.6), no reliable method for optical strain measurement was developed. The higher strains recorded during this study are likely explained by the use of grip-to-grip measurements in place of optical measurements. Attempts were made to utilise DIC, via the Correlated Solutions VIC-3D measurement system, using speckling techniques previously described in literature (Evans *et al.*, 2007; Genovese *et al.*, 2011; Genovese *et al.*, 2013; Lionello *et al.*, 2014; Pyne *et al.*, 2014; Spera *et al.*, 2011). This system had successfully been implemented in synthetic bone models within the Royal Perth Hospital laboratory (Giesinger *et al.*, 2014; Walcher *et al.*, 2016). Despite best efforts, a quality and reproducible speckle pattern, as described by Crammond *et al.* (2013), was not achieved in pilot testing and the technique was subsequently abandoned. One significant problem that was unresolved was the running of dyes and marks due to the water content and hydration techniques. Use of this as a technique is desirable and worthy of future investigation.

7.5. Conclusion

The literature and results of this study support the use of the methodology as an example of best practice. Achilles tendons should be tested as a bone-tendon-muscle construct so as to test the Achilles tendon body, rather than the three tendons of the gastrocnemius and soleus, as well as to provide a more suitable means of securing the tendon. Strain rates should be high enough to

ensure failure of the tendon body, rather than the bone. Faster strain rates also reduce the fluctuations in the hydration of the tendon during testing. This study did not adequately deal with the effect of temperature on uniaxial properties; however, methods of maintaining tendon temperature are fundamentally at odds with grips that employ freezing, and thus room temperature was used as a compromise. Tendon properties showed little difference between strain rates, with the exception of failure mechanism and stiffness, indicating that the strain rate may not be as important a factor in tendon mechanics as once thought. Finally, strain appears to be the limiting factor for failure of the tendon, with tendons failing at almost the same strain, regardless of technique.

This chapter reports the methodology and tensile test results of young NZW rabbit Achilles tendon. More importantly, this chapter examines the many factors affecting the testing of tendon in detail and discusses the current best practice according to literature. The results presented are in agreement with similar studies on rabbit Achilles tendon. This chapter, therefore, presents a best practice methodology for tensile testing of tendon and other soft tissue.

Table 7-3: Summary of papers reporting tensile testing of rabbit Achilles tendon.

Paper	Strain rate (mm/min)	CSA (mm²)	Force (N)	Stiffness (N/mm)	Stress (MPa)	Strain (%)	Modulus (MPa)
AHMED, A. F., et al. 2012	50		301.2	125			54.8
BUSCHMANN, J., et al. 2011	1		292		34		8.7
CHEN, J., et al. 2011	60		352.2	50.1			
CHEN, L., et al. 2011	20	6.9	208.6	58.1	30.8	37.6	145.6
HUGATE, R., et al. 2004	60	16.8	407		85.3	50	474
JUNCOSA-MELVIN, N., et al. 2006	30%/s		390	93	33	16	180
MEIER BURGISSER, G., et al. 2016	1	15	340		23		80
MEIMANDI-PARIZI, A., et al. 2013	600		227.04	62.21	22.48	11.28	1.62
MEIMANDI-PARIZI, A., et al. 2013	600	10.31	359.12	215.2	34.8	10.66	3.28
NAGASAWA, K., et al. 2008	20	~8			~35		~100
NAKAGAWA, Y., et al. 1996*	20	13.2	919.6		67.3	16.3	618
NAKAGAWA, Y., et al. 1996	20	15.3	1010.4		66.7	16.3	530.5
ORYAN, A., et al. 2015	600		345.54	208.27	33.53	10.69	3.13
REDDY, G. K., et al. 1999	250	~22	222.4		10.1	38.8	56.6
REDDY, G. K., et al. 2002*	250		306		8.4		29.6
WANG, T., et al. 2015	120		896.1	224.7			
WEST, J. R., et al. 2004	510		402.6		33.3	16	
YASUDA, T., et al. 2000	500		316	101			
YOUNG, R. G., et al. 1998*	20%/s	4.3	189	36.5	41.6		337.5

CHAPTER 8. DURATION OF VISCOELASTIC TESTING

8.1. Introduction

To understand the time-dependent viscoelastic behaviours of tissues it is necessary to observe the tissue under stress or strain for a duration of time, since it is known that tissues exhibit fast and slow transient behaviours. While many experiments have been performed to examine these behaviours in various tissues, the duration of testing required to accurately model the time-dependant behaviour of tissues is unclear (Manley Jr *et al.*, 2003). Ideally, tissues would be observed for several hours in order to determine whether an equilibrium is achieved, or whether fatigue occurs. However, this is impractical in most applications since the tissues are no longer *in vivo* and risk dehydration and damage and, therefore, a compromise must be reached.

This chapter seeks to establish a recommended time for future viscoelastic testing by surveying the literature, investigating the effect of loading step, and establishing an appropriate curve fitting technique for defining the viscoelastic response.

8.1.1. Analysis of literature

A literature survey was performed to identify current best practice and inform subsequent relaxation and creep testing. Search terms including 'stress
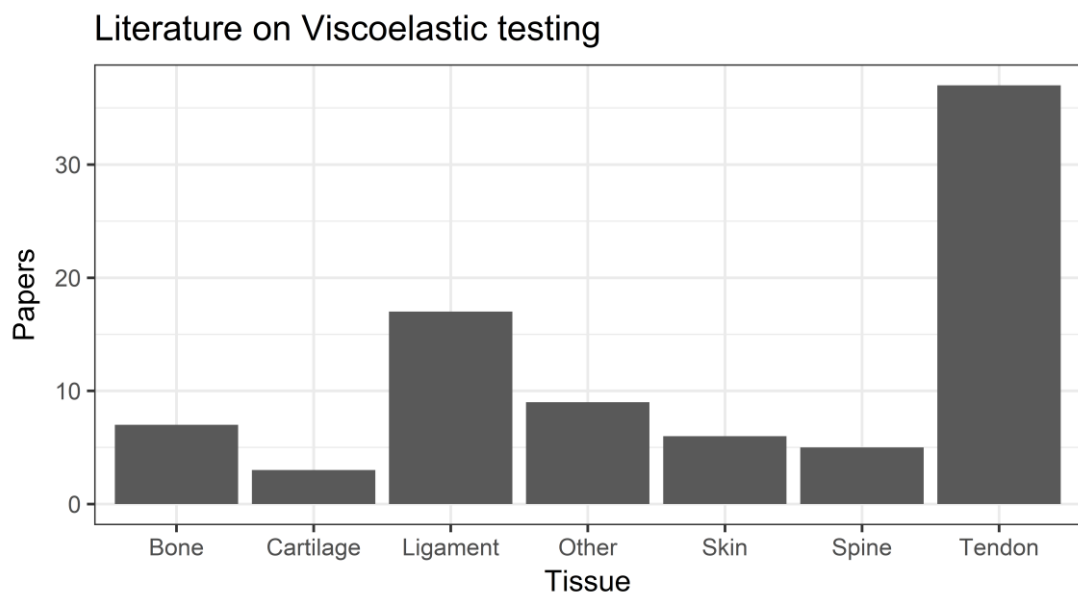
Figure 8-1: Summary of the tissue types undergoing time-dependent viscoelastic testing (n=81).

relaxation', 'creep', and 'viscoelastic testing', along with various commonly tested tissue types, were entered in the Curtin University of Technology (CUT) Library's OneSearch tool. Eighty-one (81) papers were found to be suitable and further analysed for details regarding testing duration. The complete list of papers can be found in Appendix A – Analysis of literature.

While it is known that many more papers exist, this survey sought only to establish what is considered best practice in the duration of testing. Tissues tested included bone (Abdel-Wahab *et al.*, 2011; Iyo *et al.*, 2004; Quaglini *et al.*, 2009), tendon (Abramowitch *et al.*, 2010; Duenwald *et al.*, 2009a; Duenwald *et al.*, 2010; Manley Jr *et al.*, 2003; Sverdlik and Lanir, 2002), ligament (Abramowitch and Woo, 2004; Hingorani *et al.*, 2004; Pioletti and Rakotomanana, 2000b; Thornton *et al.*, 1997), and various other soft tissues, such as skin (Lanir, 1976; Liu and Yeung, 2008; O'Connell *et al.*, 2011; Pierlot *et al.*, 2015; Reihsner and Menzel, 1998; van der Veen *et al.*, 2013; Yang *et al.*, 2006). A breakdown of the tissue types can be seen in Figure 8-1; of the 81 papers, 37 used tendon samples, with a further 17 testing ligament.

Almost all (78) of the 81 papers contained relevant information on testing duration. Many different time periods have been used to test tendon behaviour in both creep and relaxation tests, as well as cyclically, and have ranged from
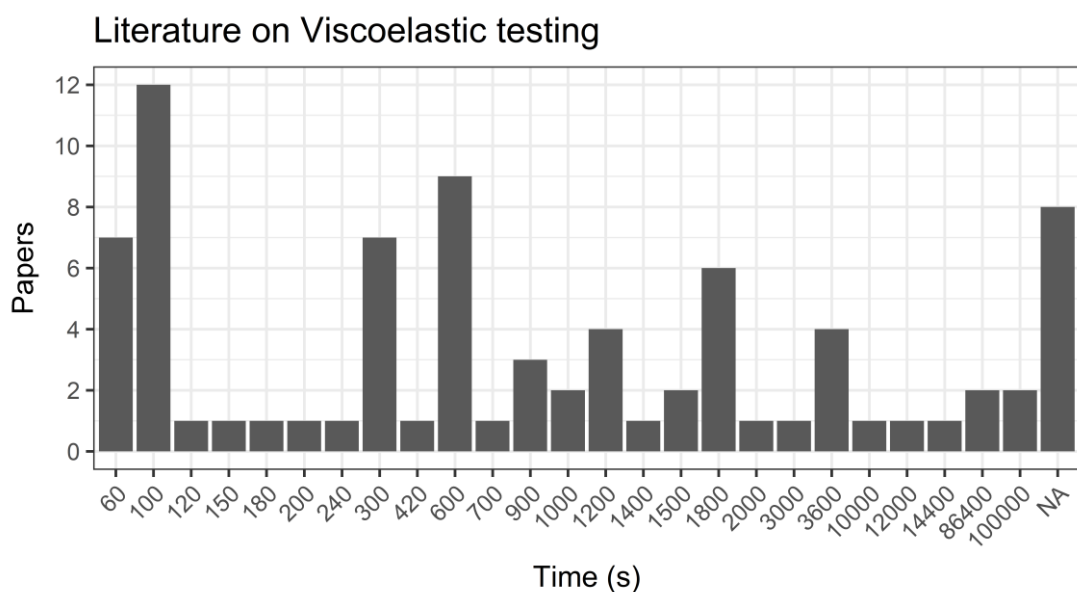
Figure 8-2: Summary of the frequency of viscoelastic testing durations (s) reported in literature (n=81).

minutes (Deligianni *et al.*, 1994; Duenwald *et al.*, 2008; Duenwald *et al.*, 2010; Hingorani *et al.*, 2004; Jensen *et al.*, 2004), to hours (Abdel-Wahab *et al.*, 2011; Abramowitch and Woo, 2004; Abramowitch *et al.*, 2010; Iyo *et al.*, 2004; O'Connell *et al.*, 2011; Sasaki and Enyo, 1995; van der Veen *et al.*, 2013). A frequency analysis of the papers identified two durations that occur more commonly – 100 seconds and 600 seconds (Figure 8-2).

Analysis of the literature demonstrated little validation for the times provided. In many cases, times appear to have been arbitrarily selected and justified post-testing. A *post hoc* analysis by Abramowitch *et al.* (2010) found that 90% of all relaxation occurred in the first 10 minutes, thereby justifying testing durations of 600 seconds. Reese and Weiss (2013) found the force at 300 seconds was within 95% of the equilibrium force, justifying their choice of duration. While this explains the high frequency at this time point, van der Veen *et al.* (2013) recommend a duration five times that required to reach equilibrium. Manley Jr *et al.* (2003) investigated testing duration in depth by testing ligaments in both creep and relaxation for 1000 seconds, and then tested the predictive power for additional relaxation tests of 10,000 seconds. Using a power law of At^B, and a Random Coefficient statistical method to assess the accuracy of curve fitting each logarithmic decade of time, it was found that 100 seconds was enough to predict the tendon behaviour with only 1% less accuracy than 1000 seconds, and that the overall error was less than the inter-specimen error. Manley Jr *et al.* (2003) suggested that it is more efficient to test a greater number of samples for shorter durations. This may explain the higher frequency of short duration testing reported in literature.

8.1.2. Instantaneous step function

Viscoelastic models often assume an instantaneous step function as the input for stress or strain since it greatly simplifies the formulation of constitutive models. Experimentally, an instantaneous step is impossible to achieve and so the model will not accurately predict the initial portion of the test. While fast strain rates reduce the error in assuming an instantaneous step, they may lead to additional sources of error such as overshoot. Slower strain rates avoid overshoot but are affected by short-term viscoelastic responses (Yang *et al.*, 2006). Therefore, it is important to consider the treatment of the initial ramp

portion of the viscoelastic test. The conservative method is to measure relaxation from 10 times the ramp time, given as $t = 10t_r$; however, this has the potential to disregard a large portion of short tests, thereby affecting any curve fitting (Duenwald *et al.*, 2009b). Duenwald *et al.* (2009b) demonstrated that starting the data from $t = 2.5t_r$ resulted in errors similar to $t = 10t_r$. This approach was used in subsequent experiments (Duenwald *et al.*, 2010). Other approaches include introducing corrections in the modelling that account for viscoelastic behaviours during the ramp phase (Abramowitch and Woo, 2004; Sorvari *et al.*, 2006).

8.1.3. Use of power law

Manley Jr *et al.* (2003) made use of a power law, via log-log transformations, to 'define' the creep and relaxation behaviour with an accurate representation. A seminal paper by Clauset *et al.* (2009) describes the appropriate use of power laws in statistics. While testing the use of power laws to describe the data was outside the scope of this experiment, several important points were identified:

- Log-log plots are crude methods for fitting power laws;
- Least-squares is not an appropriate method of fitting a power law. Maximum likelihood estimation (MLE) is preferable; and,
- Coefficient of determination (R^2) should not be used as the measure of goodness-of-fit when using a log-log plot.

The curve fitting techniques used by Manley Jr *et al.* (2003) were expanded to include MLE and nonlinear fitting equivalents of the three linear techniques.

8.2.   Methods

8.2.1. Samples

Six Achilles tendons from six New Zealand White (NZW) rabbit were harvested and the calcaneal tuberosity potted in poly-methyl methacrylate (PMMA) (Vertex Self Curing, Vertex-Dental B.V., The Netherlands). The rabbits were obtained from an unrelated study with approval from animal ethics committees at the University of Western Australia (UWA) and Curtin University of Technology (CUT). Tendons were stored in a domestic freezer at -20 degrees Celsius, as recommended in subsection 7.2.1, until the day of

testing when the tendons were defrosted in a bath of Ringer's solution (Baxter Healthcare, NSW, Australia) and allowed to reach equilibrium at room temperature.

8.2.2. Measurements

Cross-sectional area (CSA) of each tendon was measured using the technique described in Chapter 4. This technique utilises three-dimensional (3D) optical scanning to create a digital reconstruction of the tendon, from which CSA can be calculated.

8.2.3. Test setup

An Instron 5566 uniaxial materials testing system (Instron, MA, USA) with 100N load cell was used in this experiment. Tendons were loaded axially, with the bone end secured in a custom grip and the muscle end held in a thermoelectrically cooled (TEC) soft-tissue grip (Bose Enduratec, MN, USA). This grip freezes the tissue between the clamping faces, thereby reducing the chance of slippage. All samples were preloaded to 1N before testing, and the gauge length measured as the grip-to-grip length using digital callipers with an accuracy of 0.01 mm. The target levels were set to 4% and 6MPa for relaxation and creep, respectively, at a rate of 8% s^{-1}. The target levels were selected based on the results published by West *et al.* (2004).

Tendons were preconditioned for 120 cycles between 0 and 4% strain at a rate of 1Hz. As discussed in subsection 7.2.9, recovery is an important consideration when testing the viscoelastic behaviour of tissue, especially performing multiple tests on a single sample. A recovery period, one order of magnitude longer than the test length, is recommended (Duenwald *et al.*, 2009b). Tendons were, therefore, recovered for 1200 seconds (20 minutes) in a bath of Ringer's solution at room temperature.

All six tendons were tested in creep and stress relaxation for a duration of one hour (3600s), with the order alternated between tendons. Temperature was maintained at room temperature (23°C) and hydrated by spraying Ringer's solution at intervals of approximately two minutes. Measurements of time, displacement, and load were recorded at approximately 60Hz. Between tests,

tendons were wrapped in saline-soaked gauze and left to recover overnight in a sealed container.

8.2.4. Curve fitting

Results were analysed using linear methods as described in Manley Jr *et al.* (2003). Previous studies determined that results can be adequately fitted with a power law (Lakes and Vanderby, 1999; Provenzano *et al.*, 2002c)*.*

$$y \ = \ A \, t^B$$

Equation 8-1: Power Law

The power law was further simplified to a linear relationship of:

$$log \, y = A + B \ t$$

Equation 8-2: Linearised Power Law

RStudio (2016) and R statistical environment (R Core Team, 2015) were used for curve fitting and statistical analysis. Results are presented as mean and standard deviation (mean ± SD).

Results were initially fitted with a linear model (LM) using the default least-squares method, *lm*, in the R Statistical Environment. Data were centred by subtracting the mean of *log t* and *log y*. This model was fitted to subsets of the data between 10 seconds and 3600 seconds. As suggested in Duenwald *et al.* (2009b), a multiple of the rise time was subtracted from the beginning of the data to remove any effects of overshoot. To confirm the findings of Duenwald *et al.* (2009b), multipliers of 1, 2.5, and 10 were compared. Coefficient of determination (R^2) was used to assess the goodness of the fit. The response for each sample was predicted from the fit for each subset of time, excluding the initial rise time, and the R^2 values recalculated against the whole data set. The parameters were pooled and the mean and standard deviation were calculated as a representative fit for each subset of time.

As suggested by Manley Jr *et al.* (2003), a linear mixed effects regression (LMER) – may produce a better representative model since it considers all the samples simultaneously when calculating the fitting parameters. The function *lmer,* of the LME4 package (Bates *et al.*, 2015), in the R statistical environment

(R Core Team, 2015) was used. Since the intercept was set to zero by centring the data, only the slope was considered to have an associated random effect. The code for fitting the log-linear mixed linear is described in Equation 8-3. The *bobyqa* optimisation algorithm was used.

$$fit \leftarrow lmer(\log y \sim t + (t-1)/id)$$

Equation 8-3: R-code for *lmer* fitting. Note that *t-1/id* specifies that there is a random effect on the slope caused by group id, but there is no random effect for the intercept.

It has been suggested that linear regressions are inappropriate for fitting log-log plots and power laws in general (Clauset *et al.*, 2009). Therefore, an MLE function, *mle2* in R-package *bbmle* (Bolker and R Development Core Team, 2017), was used to estimate parameters. Since it was stated that that log-log plots are a crude method for fitting power laws (Clauset *et al.*, 2009), direct fitting of Equation 8-1 was performed on the untransformed data using nonlinear least-squares (NLS) regression *nls* in R-package *minpack.lm* (Elzhov *et al.*, 2016), *mle2*, and nonlinear mixed effect regression (NLMER) using the *nlmer* function (Equation 8-4) of the LME4 package (Bates *et al.*, 2015).

$$fit \leftarrow nlmer(y \sim power.f(t, A, B) \sim B/id)$$

Equation 8-4: A simplified excerpt of R-code for nlmer fitting. power.f is the input form of the power law, Equation 8-1. Note that B/id specifies that there is a random effect on parameter B caused by group id.

8.2.5. Statistical analysis

The estimated rate of change (rate of creep/relaxation) was compared across all time periods and multipliers. Manley Jr *et al.* (2003) compared the correlation-of-variation (CV) as a measure of accuracy of fit, and this comparison was replicated. CV was compared across time and multiples of t_r.

The mean rate of change at each duration was also compared to the rate of change at 3600s. Difference between the groups was evaluated using a Welch's t-test, while equivalence was assessed using a two one-sided test (TOST). Cohen's d was estimated from the standard deviations of the two groups. Statistical significance was assessed as $p < 0.05$.

Means were also compared against the 95% confidence interval (CI) calculated at 3600s. Means were considered acceptable when they existed between the upper and lower bounds.

8.3. Results

8.3.1. Raw data
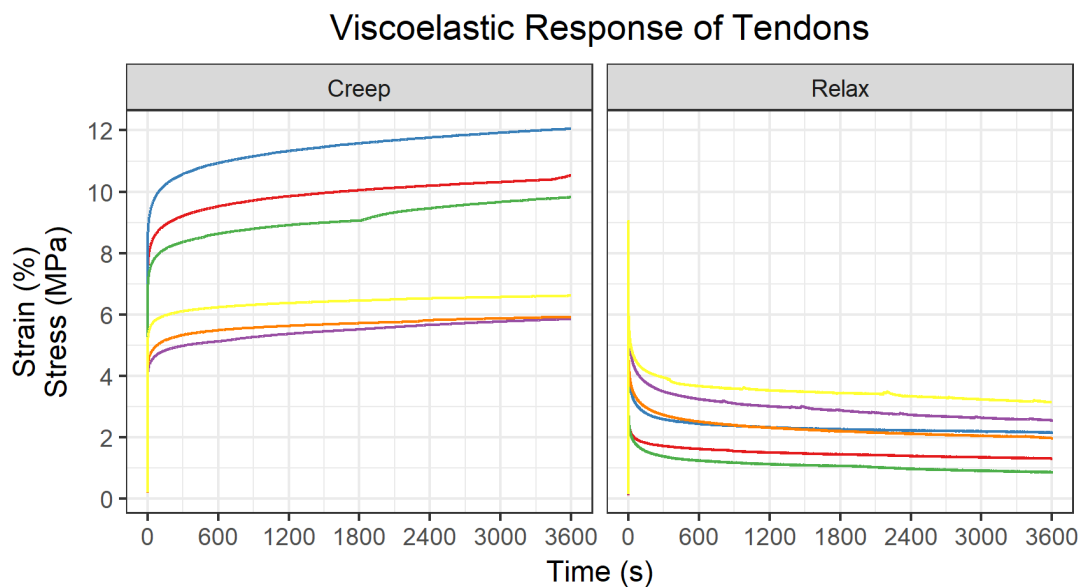
Figure 8-3: Creep (%) and Relaxation (MPa) responses of each rabbit Achilles tendon (n=6) at 4% strain and 6MPa stress.

Samples were held at values of 4% strain and 6MPa for stress relaxation and creep respectively. Figure 8-3 demonstrates the time-dependent viscoelastic response of the tendons in creep and relaxation. The rise time for all stress relaxation tests was 0.4 seconds, and ranged from 0.37–0.74 seconds (0.53 ± 0.14) for the creep tests. Overshoot was evident in all tests as expected (Figure 8-4).

Evidence of Overshoot
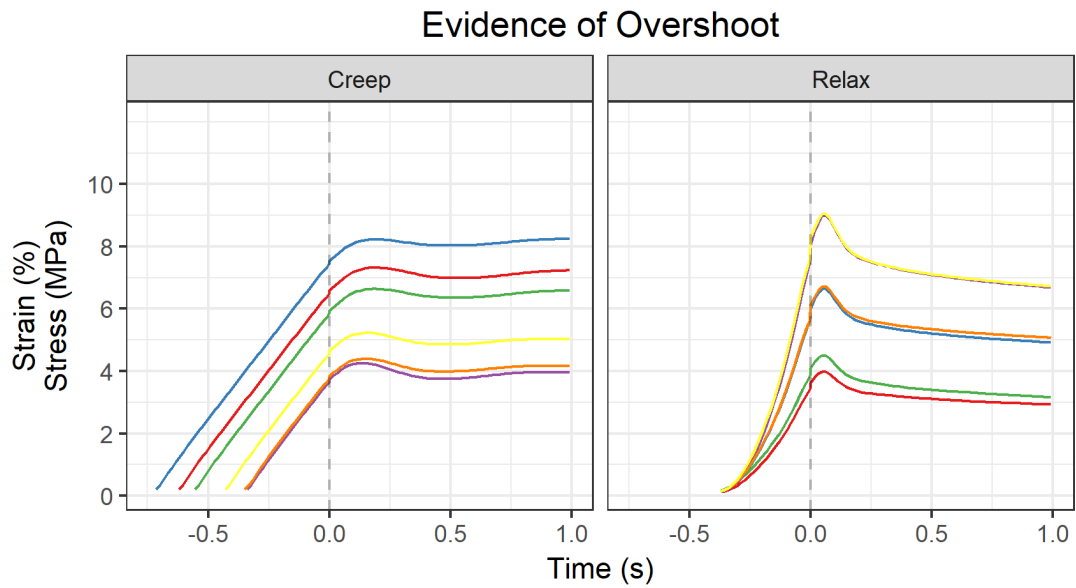
Figure 8-4: Creep (%) and relaxation (MPa) over time (s) showing overshoot following the initial ramp (negative time). The start of the hold period is indicated by a vertical dashed line (grey).

Log-log transformation of the data
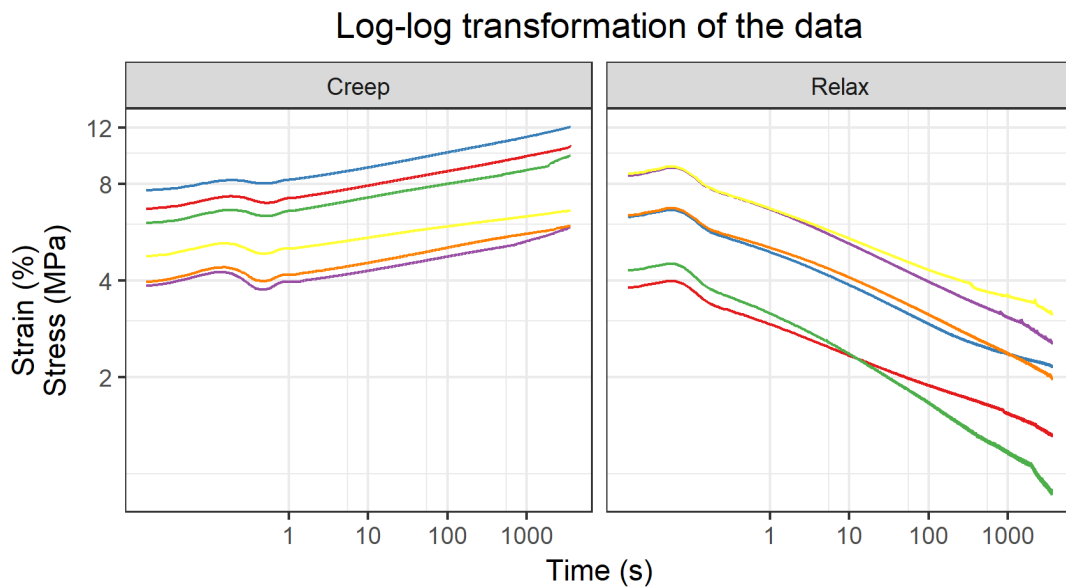
Figure 8-5: Viscoelastic response of rabbit Achilles tendon shown as a log-log relationship of creep (%) and relaxation (MPa) over time (s).

Data were well fitted by a power law ($y = At^{\beta}$). Data also underwent log-log transformation in order to fit the power law via linear fitting techniques (Figure 8-5). The coefficients of determination (R^2) for the standard regression models in both creep and relaxation demonstrate strong linear relationships when transformed, with a mean R^2 for all iterations of 0.996 ± 0.008 (range 0.939–1.000).
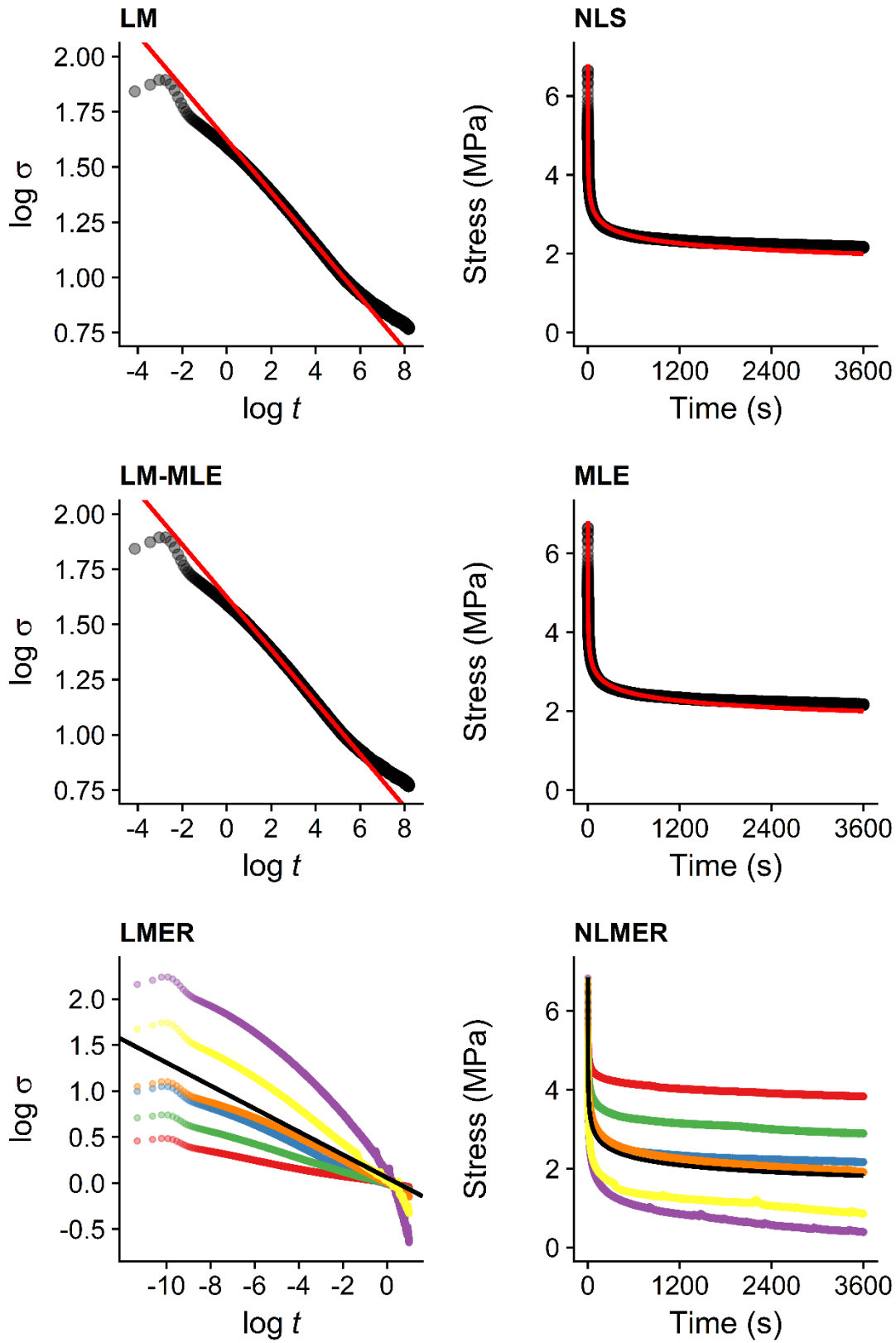
Figure 8-6: Examples of the predicted behaviour resulting from curve fitting of 100 seconds with a multiplier of 2.5t_r. Note that the data for the LMER and NLMER fits have been centred.

8.3.2. Effect of fitting technique

The mean and standard deviation for rate of change (β) was calculated for creep and relaxation via one of the six fitting methods. The rate of change for each fit over the full test duration is presented in Appendix B – Rates of change (β). Examples of each technique are presented in Figure 8-6.

Rate of change values were generally similar for LM, LM-MLE, LMER, NLS, and MLE curve fits at each duration and multiplier (Figure 8-7). Rate of change values for NLMER were similar in creep but noticeably lower in relaxation (Figure 8-7). This is an artefact of the technique used to centralise the nonlinear curves for NLMER fitting.

The standard deviations of the standard regressions and MLEs differ slightly in calculation compared with the mixed regression models, as they include within-specimen sampling errors resulting from fitting the curves individually. By calculating the rate of change for the group in one operation, mixed regression models ignore this additional variation and so the standard deviation reflects only the variation in the estimate of the true rate of change. In this experiment, no difference was observed, suggesting the within-specimen sampling error was much lower than the between-specimen
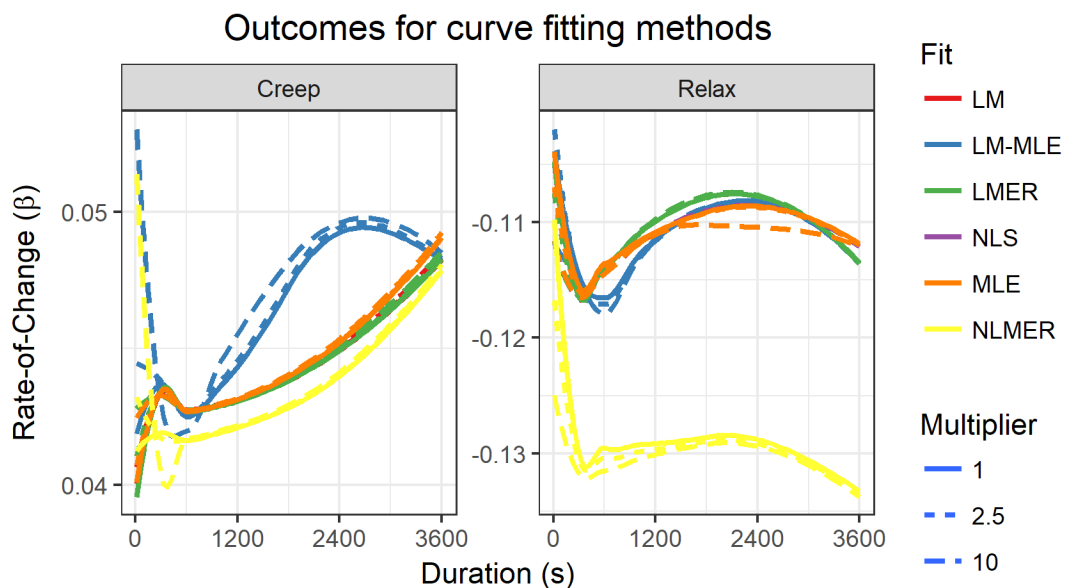
Figure 8-7: Rate of change (β) values of the power law for each curve fitting technique at various durations and multipliers.

variation. The standard deviation of the NLMER fit was higher than other techniques indicating greater variation in the estimated rate of change.

Interestingly, some linear fittings with a high coefficient of determination (R^2) gave a visually poor fit. This was due to the density of points from the long tail of the curves that became condensed when log-transformed as shown in Appendix C – Example of coefficient of determination. It is evident from the consistency in the estimated rate of change that this did not influence the predictive ability of the curve fitting techniques.

8.3.3. Effect of multipliers

The effect of multipliers on the parameters estimated by each fitting technique is presented in Appendix B – Rates of change (β). The multiplier showed a negligible effect on the quality of the curve fit, likely due to the filtering technique used to remove extraneous data prior to analysis.

8.3.4. Correlation-of-variation

CV was calculated as $CV = 100 \times {sd}/{\mu}$, where μ is the mean, and *sd* is the standard deviation. This was used as a proxy for goodness-of-fit of the parameters and is considered a measure of the relative precision. A decrease in CV represents an increase in accuracy of the estimated parameters (Manley Jr *et al.*, 2003).

CV was shown to increase with time for most fitting techniques (Figure 8-8). NLMER was the only technique to show an improvement in CV with increasing duration. However, NLMER demonstrated a high CV (30–74%), indicating a poor estimate of the rate of change. LM, NLS, and MLE, produced similar CV values, with LMER and LM-MLE producing slightly higher values. These values, approximately 8–32%, are similar to those reported by Manley Jr *et al.* (2003). Increases in CV with increasing duration were also observed in that study. CV demonstrated little change between multipliers (Figure 8-8).

Precision of curve fitting techniques
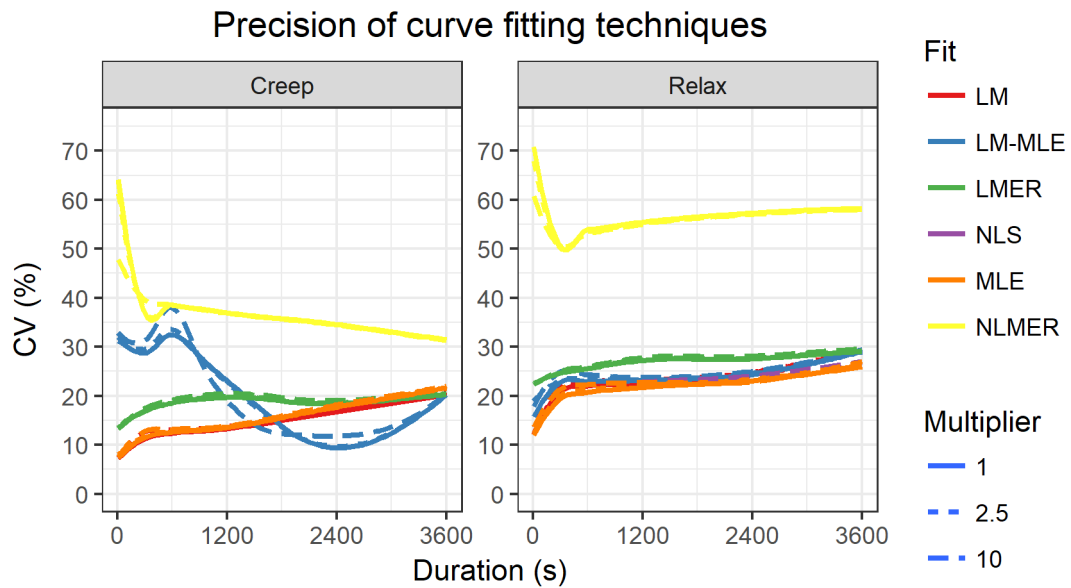
Figure 8-8: Correlation-of-variation (CV, %) of the curve fitting techniques for creep and relaxation for various durations (s) and multipliers.

8.3.5. Statistical analysis

Data were assessed using a Welch's t-test for difference and TOST for equivalence. Results from Welch's t-test demonstrated that the null hypothesis, that is that there is no difference, could not be discarded. Results from the TOST demonstrated no significance, indicating that it could not be concluded that the rates of change were equivalent. *Post hoc* assessment determined this was due to low sample numbers.

Means at all durations fell within the upper and lower bounds of the confidence interval (Appendix D – Interval test).

8.3.6. Effect of testing order

Testing order was found to significantly affect the rate of change in both creep and relaxation (Figure 8-9). Differences were detected at 3600s in creep, and in durations up to 600s in relaxation.

8.4. Discussion

The first goal of this chapter was to investigate the time required for testing tendon. Many studies have investigated the viscoelastic behaviour of soft and hard tissues; however, only one study was found that investigated the necessary time required to adequately estimate the parameters of a viscoelastic test in tendon or ligament (Manley Jr *et al.*, 2003). It was found

that tests of only 100s were enough to comfortably predict the behaviour of longer tests up to 10,000s in rat medial collateral ligament. Several factors indicated that a similar study was needed in tendon. For example, rate of relaxation has been shown to be faster than creep in ligament (Thornton *et al.*, 1997), while the rate of relaxation has been shown to increase with increasing strain in tendon, but to decrease with increasing strain in ligament (Duenwald *et al.*, 2010). Therefore, results determined for ligament may not be transferable to tendon in some situations.

The second goal was to assess the effect of the initial portion, defined as a multiple of rise time, on the estimated parameters. In an ideal time-dependent behaviour test the stress or strain would be applied instantaneously. Physical limitations, such as machine travel speed, prevent a true step-load from being achieved. A crude technique is to simply ignore a portion of the initial data so as to avoid any transient effects caused by overshoot or short-term viscoelastic behaviour (Duenwald *et al.*, 2009b). More advanced techniques have been developed to account for these in curve fitting (Abramowitch and Woo, 2004; Duenwald *et al.*, 2009b; Sorvari *et al.*, 2006; Yang *et al.*, 2006).

The third goal of the study was to investigate the use of three curve fitting techniques – least-squares, MLE, and mixed effects modelling – on the linear log-log transformed data and directly to the nonlinear data. It has been recommended that when fitting a power law, either directly to the data or via log-log transformation, a MLE should be used rather than least-squares (Clauset *et al.*, 2009). Additionally, log-log plots can be considered a crude method for fitting, since many similar relationships will present as a near linear line when transformed (Clauset *et al.*, 2009). Manley Jr *et al.* (2003) stated: "…there appears to be no statistical advantage to test fewer specimens for longer periods of time when the goal is to describe the behaviour of a group of specimens". This is particularly pertinent when the end goal is to assess the behavioural changes in tendinopathic tendons that may not be able to be tested with the rigour of a healthy tendon.
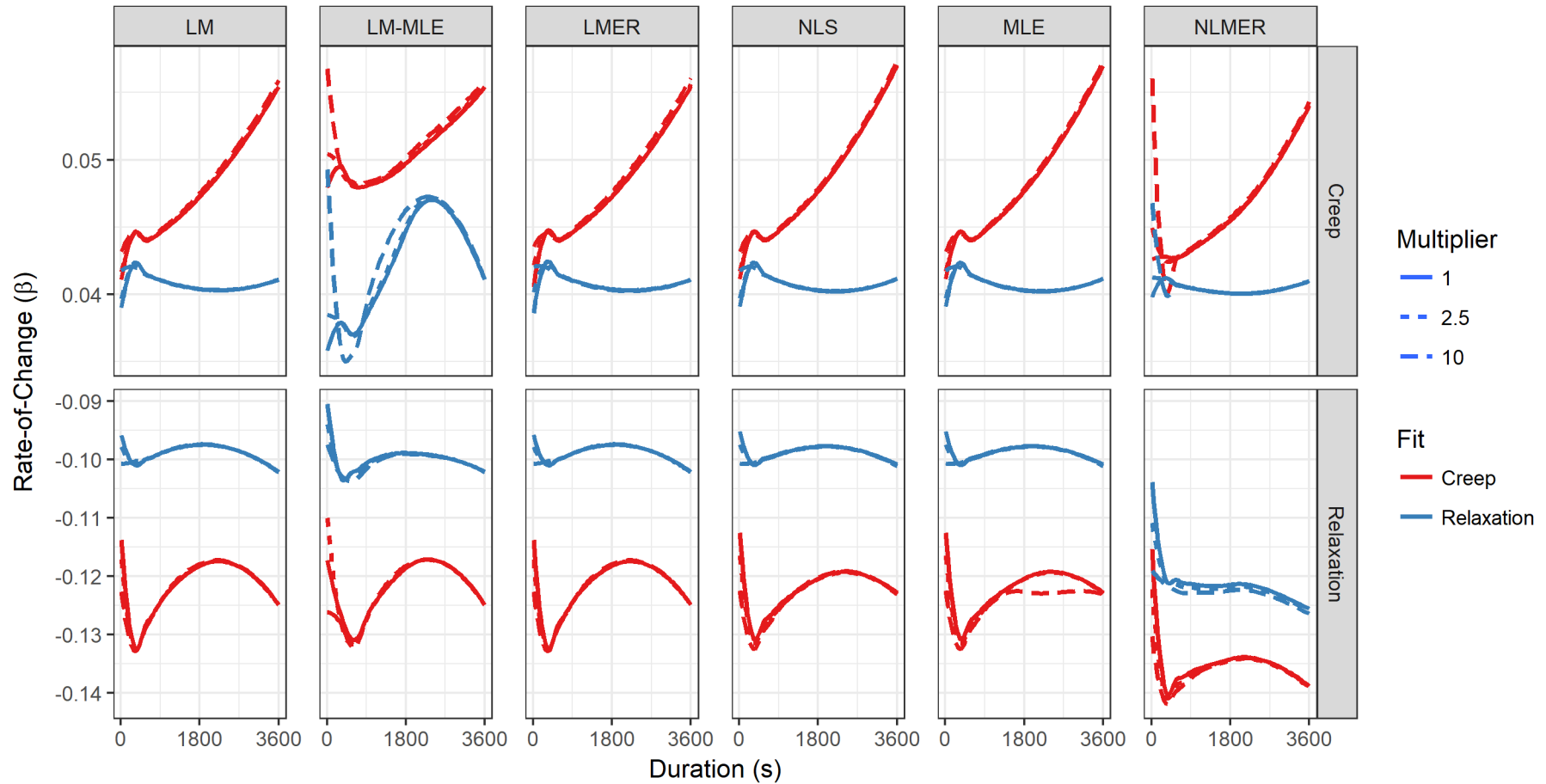
Figure 8-9: Effect of viscoelastic testing order on rate of change (β) for the curve fitting techniques with various durations (s) and multipliers.

8.4.1. Duration

Small variations in the data (Figure 8-3) were observed, particularly late in the test, possibly due to slippage, irregular hydration, or fatigue failure. Previous experiments have demonstrated that prolonged strains (even within the reproducible region) are deleterious to the tendon if the time exceeds 60 minutes; that is, the time at which the second decay begins in the relaxation phenomenon (Rigby *et al.*, 1959). This highlights the importance of duration in viscoelastic testing, as many of these effects can be mitigated by minimising testing time.

Equivalence testing and interval testing were used to evaluate the rate of change between time points. Equivalence testing, with Welch's t-test to check for differences, was inconclusive with respect to determining where the curve fitting predicts the results of the full test. In this study, this is likely because of the low samples numbers, since more samples were not available. *Post hoc* analysis indicated that a minimum of 1000 samples was necessary to determine equivalent, due to the small effect size estimated by Cohen's d (approximately 0.1). Using an interval test, several creep fitting techniques at 10 seconds estimated rates of change outside of the 95% CI, indicating that 10 seconds was insufficient to produce a reliable estimate of the mean. All durations above 10s produced rates of change deemed acceptable estimates of the mean at 3600s. It can also be observed in the nonlinear curve fitting that the data for 3600s were well fitted in all instances for durations above 10 seconds. Therefore, the 95% CI provides a reasonable test for the accuracy of the estimated rate of change even at low sample numbers.

8.4.2. Multipliers

All tests demonstrated a degree of overshoot in the data caused by a fast strain rate during the ramp phase. Many methods have been proposed to address this: the simplest is to ignore a portion of the initial data so as to begin 'data collection' once the test is stable. Duenwald *et al.* (2009b) calculated that only the first 2.5 t_r seconds need be ignored, where t_r is the rise time, rather than the conventional 10 t_r. Despite these recommendations, removal of the initial portion of the data was not found to be necessary to achieve a quality fit. That is, the multiple of t_r did not influence the outcomes of curve fitting above

10 seconds. This is likely due to the process of filtering the data performed prior to the analysis. This filtering technique involved removing data points based on the difference between the input step and the actual value as measured on the MTS. This technique appeared to remove the majority of noise caused by overshoot and may be more effective than simply removing the initial portion of the data, as it maximises the data available and may account for differing lengths of overshoot.

8.4.3. Fitting technique

The results suggest that nonlinear fitting of the data offers no significant advantage when estimating the parameters of the viscoelastic tests and may, in fact, be disadvantageous. Anecdotally, the processing time required for each technique was negligible (less than four seconds), again with the exception of NLMER (less than 10 minutes). With the exception of NLMER, each of the fitting techniques produced substantially similar results at each duration (Appendix B – Rates of change (β)).

Visually, the linear fitting techniques produce interesting results due to the log-log transformation of the data. Since the tail of the viscoelastic tests becomes condensed when transformed, the fit is disproportionately weighted toward a small segment of the x-axis. The fit appears poor, for example in the graph at the top of Appendix C – Example of coefficient of determination; however, the fit has an R^2 value of 0.974. Comparatively, the equivalent nonlinear fit, shown at the bottom of Appendix C – Example of coefficient of determination, appears to be visually suitable with an estimated R^2 of 0.968. The rate of change values are similar, suggesting the linear fits are suitable for estimating the parameters.

Both LMER and NLMER required the data for each test to be centred for fitting. Not centring the data resulted in a failure of the algorithm to converge. This centring appeared to introduce a new source of error in the fitting of relaxation curves. Although LMER also required centring, this was easily achieved by adjusting the x- and y-intercept of the log-log transforms to pass through zero and did not introduce any new sources of error.

For the mixed effects models, as well as producing reliable mean parameter estimates compared with individual fittings (Appendix B – Rates of

change (β)), LMER offers a significant speed and implementation advantage over NLMER. Of more significant interest is the high CV in the parameters estimated via NLMER (Figure 8-8) compared with other techniques. Manley Jr *et al.* (2003) reported a tendency for the CV to decrease with increasing test duration, although there were some increases noted. The LMER results above do not support this finding, instead showing an increase in variation with time (Figure 8-8). Evaluated against the CV values for all fitting techniques, the implementation of NLMER in this study appears to be unreliable for parameter estimation of the data. This may be resolved through an appropriate method of centring the data.

The choice of fitting technique does not appear to influence the estimated parameters, with the notable exception of NLMER (Appendix B – Rates of change (β)). Indeed, the standard deviation differs negligibly. Of interest is the general agreement between the rate of change values calculated from linearised data, and those calculated from directly fitting the data. This supports the use of power law to describe the viscoelastic behaviour of the tendon, as suggested by Provenzano *et al.* (2001). This is counter to the concerns raised by Clauset *et al.* (2009) regarding the use of power laws. Since the implementation of linear fitting is less complex than nonlinear equivalents, especially with respect to the mixed effects models, this finding is encouraging. Nevertheless, despite the agreement in the results above, care should be taken when fitting long-tail data for the reasons outlined by Clauset *et al.* (2009).

The tendency for the CV to increase with duration was not surprising, as the variation in the measured rate of change for each sample may indeed increase, leading to an increase in the standard deviation measured within the set of samples. While the measure of CV may be appropriate as a measure of precision at a particular time point, it does not provide a true indication of the precision of the estimated rate of change between time points as it does not compare against the 'true' population value, in this case measured at 3600s. In this respect, interval and equivalence testing may be more meaningful in evaluating the estimate of the parameters between tests.

8.4.4. Testing order

Testing order was found to affect the rate of change in both creep and relaxation. In particular, creep-first samples exhibited a higher rate of change in both modes relative to the relaxation-first samples. Creep was expected to have deleterious effect on the rate of relaxation, which was assumed by the author to be a decrease in the rate. However, the results indicate that this is not the case. This may be a product of the structural mechanisms involved in the creep and relaxation phenomena, due to the low sample numbers in each group (n=3), possible mechanical damage caused by the creep testing, or insufficient recovery between tests. While the exact mechanism for this difference is unclear and warrants further investigation, it does highlight the importance of considering the order of testing, and subsequent recovery time, on the outcomes of the study.

8.5. Conclusion

The three goals of this study were to evaluate the time required to test tendon in order to estimate long term viscoelastic behaviour; to, evaluate different fitting techniques on log-log transformed and raw data; and, to determine if removing the portion of the data immediately post-loading affects parameter estimation. With the exception of NLMER modelling, curve fitting and the initial portion of data did not influence the results. It was demonstrated that a minimum test duration of 100 seconds is recommended to achieve an acceptable estimate of the rate of change in viscoelastic testing. This is in agreement with the literature (Manley Jr *et al.*, 2003). It was also demonstrated that order of testing significantly affected the rate of change measurements and should be considered in future protocols.

8.6. Appendix A – Analysis of literature

Table 8-1: Summary of literature (n=81) involving viscoelastic testing of biological tissues. * indicates cyclic testing. Cyc is an abbreviation of cycles.

Journal Article	Animal	Tissue	Type	Time
Abdel-Wahab et al. (2011)	Cow	Bone	Creep Relaxation	3600s
Abramowitch and Woo (2004)	Goat	Ligament	Relaxation	60 mins
Abramowitch et al. (2004)	Goat	Ligament	Relaxation Creep*	60 mins 10 cyc
Abramowitch et al. (2010)	Human	Tendon	Relaxation	60s 30s*
Anssari-Benam et al. (2011)	Pig	Aortic Valve	Creep Relaxation	300s
Atkinson et al. (1999)	Human	Tendon	Relaxation	180s
Bowman et al. (1994)	Cow	Bone	Creep	Failure
Cheng et al. (2009)	Rat	Spinal cord	Relaxation	15 min
Ciarletta et al. (2006)	Pig	Tendon	Creep Relaxation	300s
Cohen et al. (1976)	Human	Tendon	Creep	60s
Davis and De Vita (2012)	Rat	Tendon fascicles	Relaxation	10 mins
Deligianni et al. (1994)	Human	Bone	Relaxation	100s
Duenwald et al. (2008)	Pig	Tendon	Relaxation	100s
Duenwald et al. (2009a)	Pig	Tendon	Relaxation	100s
Duenwald et al. (2010)	Pig	Tendon Ligament	Relaxation	100s
Duenwald-Kuehl et al. (2012a)	Pig	Tendon	Relaxation	100s 10 cyc
Funk et al. (1999)	Human	Ligament	Relaxation	1000s
Galeski et al. (1977)	Rats	Tendons	Relaxation	12,000s
Gautieri et al. (2013)	NA	Collagen Fibril	Creep Relaxation	120s
Giles et al. (2007)	Pigs	Myocardium Skin	Creep*	50 cyc
Gimbel et al. (2005)	Rat	Tendon	Relaxation	10 mins
Guilak et al. (1994)		Cartilage	Creep Relaxation	1000s 1200s
Gupta et al. (2010)	Rats	Tendon fascicles	Relaxation	60s 300s
Hawkins et al. (2009)	Human	Tendon	Creep*	7 mins

Henninger et al. (2010)	Pig Cow	Ligament Cartilage	Relaxation	1400s
Hingorani et al. (2004)	Rabbit	Ligament	Creep Relaxation	100s
Hooley and Cohen (1979)	Human	Tendon	Creep	60s
Hooley et al. (1980)	Human	Tendon	Creep	60s
Huang et al. (2009)	Human	Tendon	Relaxation	30 mins
Iyo et al. (2004)	Cow	Bone	Relaxation	100,000s
Jensen et al. (2004)	Rat	Ligament	Creep	100s
Johnson et al. (1996)	Human Dogs	Tendon Ligament	Relaxation	10–15 cyc
Johnson et al. (1994)	Human	Tendon	Relaxation	15 mins
Kahn et al. (2010)	Rabbit	Tendon	Relaxation	1 hr
Lanir (1976)	Rabbit	Skin	Relaxation	10 min
Legerlotz et al. (2013b)	Cow	Tendon fascicles	Relaxation	30 min
Liu and Yeung (2006)	Pig	Skin	Relaxation	1200s
Liu and Yeung (2008)	Pig	Skin	Relaxation	1200s
Machiraju et al. (2006)	Human	Tendon	Relaxation	700s
Mäkelä and Korhonen (2016)	Rabbit	Cartilage	Relaxation	15 mins
Manley Jr et al. (2003)	Rat	Ligament	Creep Relaxation	1000s 10,000s
Michel et al. (1994)	Cow	Bone	Creep	Failure
Moon et al. (2006b)	Rabbit	Ligament	Relaxation	25 min
Myers et al. (1991)	Human	Cervical Spines	Relaxation	150s
Komatsu et al. (2007)	Rabbit	Ligament	Relaxation	300s
Nekouzadeh et al. (2007)	N/A	Reconstituted Collagen	Relaxation	2000s
O'Connell et al. (2011)	Human	Intervertebral Disc	Creep	4 hours
Pailler-Mattei et al. (2014)	Human	Reconstructed Skin	Relaxation	200s
Pavan et al. (2014)	Human	Aponeurosis	Relaxation	240s
Pierlot et al. (2015)	Cow	Valves	Creep	30 min
Pioletti and Rakotomanana (2000b)	Human	Ligament	Relaxation	1800s
Pradas and Calleja (1990)	Human	Tendon	Creep	1000s
Provenzano et al. (2001)	Rat	Ligament	Creep Relaxation	100s 1200s
Quaglini et al. (2009)	Cow	Bone	Relaxation	600s

Reese and Weiss (2013)	Rat	Tendon fascicles	Relaxation	300s
Reihsner and Menzel (1998)	Human	Skin	Relaxation	100–300 mins
Rigby et al. (1959)	Rat	Tendon	Relaxation	24hrs
Sarver et al. (2003)	Sheep	Tendon	Relaxation	600s
Sasaki and Enyo (1995)	Cow	Bone	Relaxation	100,000s
Schatzmann et al. (1998)	Human	Tendon*	Creep*	200 cyc
Screen (2008)	Rat	Tendon fascicle	Relaxation	60s
Screen et al. (2011)	Rat	Tendon fascicles	Relaxation	60s
Screen et al. (2013)	Pig	Tendon fascicles	Relaxation	10 min
Shen et al. (2011)	Sea Cucumber	Collagen Fibril	Creep Relaxation	300s
Shepherd et al. (2014)	Cow	Tendon Fascicle	Creep* Relaxation*	5 min 15 min 30 min
Shetye et al. (2014)	Pig	Spinal cord	Relaxation	100s
Smutz et al. (1995)	Human	Tendon	Creep	30 min
Svensson et al. (2010)	Human	Tendon Fascicle	Relaxation	5 min
Sverdlik and Lanir (2002)	Sheep	Tendon	Relaxation	10 mins
Thornton et al. (1997)	Rabbit	Ligament	Creep Relaxation	20 min
Toms et al. (2002)	Human	Ligament	Relaxation	50 min
Troyer et al. (2012a)	Human	Ligament	Relaxation	100s
Troyer and Puttlitz (2012)	Human	Ligament	Relaxation	600s
Troyer et al. (2012b)	Sheep	Tendon	Relaxation	100s
van der Veen et al. (2013)	Human	Intervertebral Disc	Creep	24 hours
Woo et al. (1986)	Rabbit	Tendon	Relaxation*	10 cyc
Wren et al. (2003)	Human	Tendon	Creep	Failure
Yamamoto et al. (1999)	Rabbit	Tendon fascicle	Relaxation	600s
Yang et al. (2012)	Bovine	Collagen Fibril	Relaxation	5–10min
Yang et al. (2006)	Pig	Oesophagus	Relaxation	300s
Yoo et al. (2009)	Cow	Muscle	Relaxation	1500s

8.7.   Appendix B – Rates of change (β)

Table 8-2: Rate of creep (β) for LM fitting technique

		Multiplier		
Mode	Duration	1x	2.5x	10x
Creep	10	0.039 ± 0.003	0.040 ± 0.003	0.042 ± 0.003
Creep	100	0.043 ± 0.004	0.043 ± 0.004	0.043 ± 0.004
Creep	300	0.043 ± 0.005	0.043 ± 0.005	0.043 ± 0.005
Creep	600	0.043 ± 0.005	0.043 ± 0.005	0.043 ± 0.006
Creep	1000	0.043 ± 0.006	0.043 ± 0.006	0.043 ± 0.006
Creep	1800	0.044 ± 0.007	0.044 ± 0.007	0.044 ± 0.007
Creep	3600	0.048 ± 0.010	0.048 ± 0.010	0.049 ± 0.010
Relaxation	10	-0.103 ± 0.012	-0.106 ± 0.013	-0.111 ± 0.015
Relaxation	100	-0.114 ± 0.018	-0.115 ± 0.019	-0.116 ± 0.020
Relaxation	300	-0.115 ± 0.024	-0.115 ± 0.024	-0.116 ± 0.025
Relaxation	600	-0.114 ± 0.025	-0.114 ± 0.025	-0.114 ± 0.026
Relaxation	1000	-0.111 ± 0.025	-0.111 ± 0.025	-0.111 ± 0.025
Relaxation	1800	-0.108 ± 0.025	-0.108 ± 0.025	-0.108 ± 0.025
Relaxation	3600	-0.113 ± 0.033	-0.114 ± 0.033	-0.114 ± 0.034

Table 8-3: Rate of creep (β) for LM-MLE fitting technique

		Multiplier		
Mode	Duration	1x	2.5x	10x
Creep	10	0.042 ± 0.013	0.045 ± 0.014	0.054 ± 0.018
Creep	100	0.043 ± 0.014	0.044 ± 0.014	0.047 ± 0.014
Creep	300	0.044 ± 0.012	0.044 ± 0.013	0.044 ± 0.014
Creep	600	0.042 ± 0.014	0.042 ± 0.015	0.042 ± 0.016
Creep	1000	0.044 ± 0.011	0.044 ± 0.011	0.045 ± 0.010
Creep	1800	0.047 ± 0.007	0.047 ± 0.007	0.048 ± 0.006
Creep	3600	0.048 ± 0.010	0.048 ± 0.010	0.049 ± 0.010
Relaxation	10	-0.102 ± 0.016	-0.100 ± 0.019	-0.112 ± 0.019
Relaxation	100	-0.111 ± 0.021	-0.110 ± 0.023	-0.113 ± 0.025
Relaxation	300	-0.113 ± 0.026	-0.114 ± 0.026	-0.115 ± 0.028
Relaxation	600	-0.117 ± 0.027	-0.117 ± 0.027	-0.118 ± 0.028
Relaxation	1000	-0.112 ± 0.026	-0.112 ± 0.026	-0.113 ± 0.027
Relaxation	1800	-0.109 ± 0.026	-0.109 ± 0.026	-0.109 ± 0.026
Relaxation	3600	-0.113 ± 0.033	-0.114 ± 0.033	-0.114 ± 0.034

Table 8-4: Rate of creep (β) for LMER fitting technique

Mode	Duration	Multiplier		
		1x	2.5x	10x
Creep	10	0.039±0.005	0.041±0.005	0.043±0.006
Creep	100	0.043±0.006	0.043±0.006	0.044±0.007
Creep	300	0.043±0.007	0.043±0.007	0.043±0.007
Creep	600	0.043±0.008	0.043±0.008	0.043±0.008
Creep	1000	0.043±0.008	0.043±0.008	0.043±0.009
Creep	1800	0.044±0.008	0.044±0.008	0.044±0.009
Creep	3600	0.048±0.010	0.048±0.010	0.049±0.010
Relaxation	10	-0.103±0.023	-0.106±0.023	-0.111±0.024
Relaxation	100	-0.114±0.027	-0.115±0.027	-0.116±0.027
Relaxation	300	-0.115±0.028	-0.115±0.028	-0.116±0.029
Relaxation	600	-0.114±0.029	-0.114±0.029	-0.114±0.030
Relaxation	1000	-0.111±0.030	-0.111±0.030	-0.111±0.030
Relaxation	1800	-0.108±0.030	-0.108±0.030	-0.108±0.030
Relaxation	3600	-0.113±0.033	-0.114±0.033	-0.114±0.034

Table 8-5: Rate of creep (β) for NLS fitting technique

Mode	Duration	Multiplier		
		1x	2.5x	10x
Creep	10	0.039 ± 0.003	0.040 ± 0.003	0.042 ± 0.003
Creep	100	0.043 ± 0.004	0.043 ± 0.004	0.043 ± 0.004
Creep	300	0.043 ± 0.005	0.043 ± 0.005	0.043 ± 0.005
Creep	600	0.043 ± 0.005	0.043 ± 0.005	0.043 ± 0.006
Creep	1000	0.043 ± 0.006	0.043 ± 0.006	0.043 ± 0.006
Creep	1800	0.044 ± 0.007	0.044 ± 0.007	0.044 ± 0.007
Creep	3600	0.049 ± 0.011	0.049 ± 0.011	0.049 ± 0.011
Relaxation	10	-0.102 ± 0.012	-0.105 ± 0.013	-0.110 ± 0.015
Relaxation	100	-0.113 ± 0.017	-0.114 ± 0.018	-0.116 ± 0.020
Relaxation	300	-0.114 ± 0.022	-0.115 ± 0.023	-0.116 ± 0.024
Relaxation	600	-0.114 ± 0.023	-0.114 ± 0.024	-0.114 ± 0.025
Relaxation	1000	-0.111 ± 0.024	-0.112 ± 0.024	-0.112 ± 0.025
Relaxation	1800	-0.109 ± 0.024	-0.109 ± 0.025	-0.109 ± 0.025
Relaxation	3600	-0.112 ± 0.029	-0.112 ± 0.029	-0.112 ± 0.030

Table 8-6: Rate of creep (β) for MLE fitting technique

Mode	Duration	Multiplier		
		1x	2.5x	10x
Creep	10	0.039±0.003	0.040±0.003	0.042±0.003
Creep	100	0.043±0.004	0.043±0.004	0.043±0.004
Creep	300	0.043±0.005	0.043±0.005	0.043±0.005
Creep	600	0.043±0.005	0.043±0.005	0.043±0.006
Creep	1000	0.043±0.006	0.043±0.006	0.043±0.006
Creep	1800	0.044±0.007	0.044±0.007	0.044±0.007
Creep	3600	0.049±0.011	0.049±0.011	0.049±0.011
Relaxation	10	-0.102±0.012	-0.105±0.013	-0.110±0.015
Relaxation	100	-0.113±0.017	-0.114±0.018	-0.116±0.020
Relaxation	300	-0.114±0.022	-0.115±0.023	-0.116±0.024
Relaxation	600	-0.114±0.023	-0.114±0.024	-0.114±0.025
Relaxation	1000	-0.111±0.024	-0.112±0.024	-0.112±0.025
Relaxation	1800	-0.109±0.024	-0.109±0.025	-0.110±0.025
Relaxation	3600	-0.112±0.029	-0.112±0.029	-0.112±0.030

Table 8-7: Rate of creep (β) for NLMER fitting technique

Mode	Duration	Multiplier		
		1x	2.5x	10x
Creep	10	0.041±0.028	0.043±0.028	0.053±0.026
Creep	100	0.042±0.019	0.042±0.019	0.043±0.019
Creep	300	0.042±0.017	0.042±0.017	0.042±0.017
Creep	600	0.042±0.016	0.042±0.016	0.042±0.016
Creep	1000	0.042±0.016	0.042±0.016	0.042±0.016
Creep	1800	0.043±0.015	0.043±0.015	0.043±0.015
Creep	3600	0.048±0.015	0.048±0.015	0.048±0.015
Relaxation	10	-0.107±0.080	-0.115±0.082	-0.124±0.078
Relaxation	100	-0.123±0.068	-0.126±0.068	-0.130±0.068
Relaxation	300	-0.128±0.068	-0.129±0.068	-0.131±0.068
Relaxation	600	-0.129±0.070	-0.130±0.070	-0.131±0.070
Relaxation	1000	-0.129±0.071	-0.130±0.071	-0.130±0.071
Relaxation	1800	-0.129±0.073	-0.129±0.073	-0.129±0.073
Relaxation	3600	-0.133±0.078	-0.133±0.078	-0.134±0.077

8.8. Appendix C – Example of coefficient of determination

Example of linear and nonlinear fitting

LM Fitting

NLS Fitting
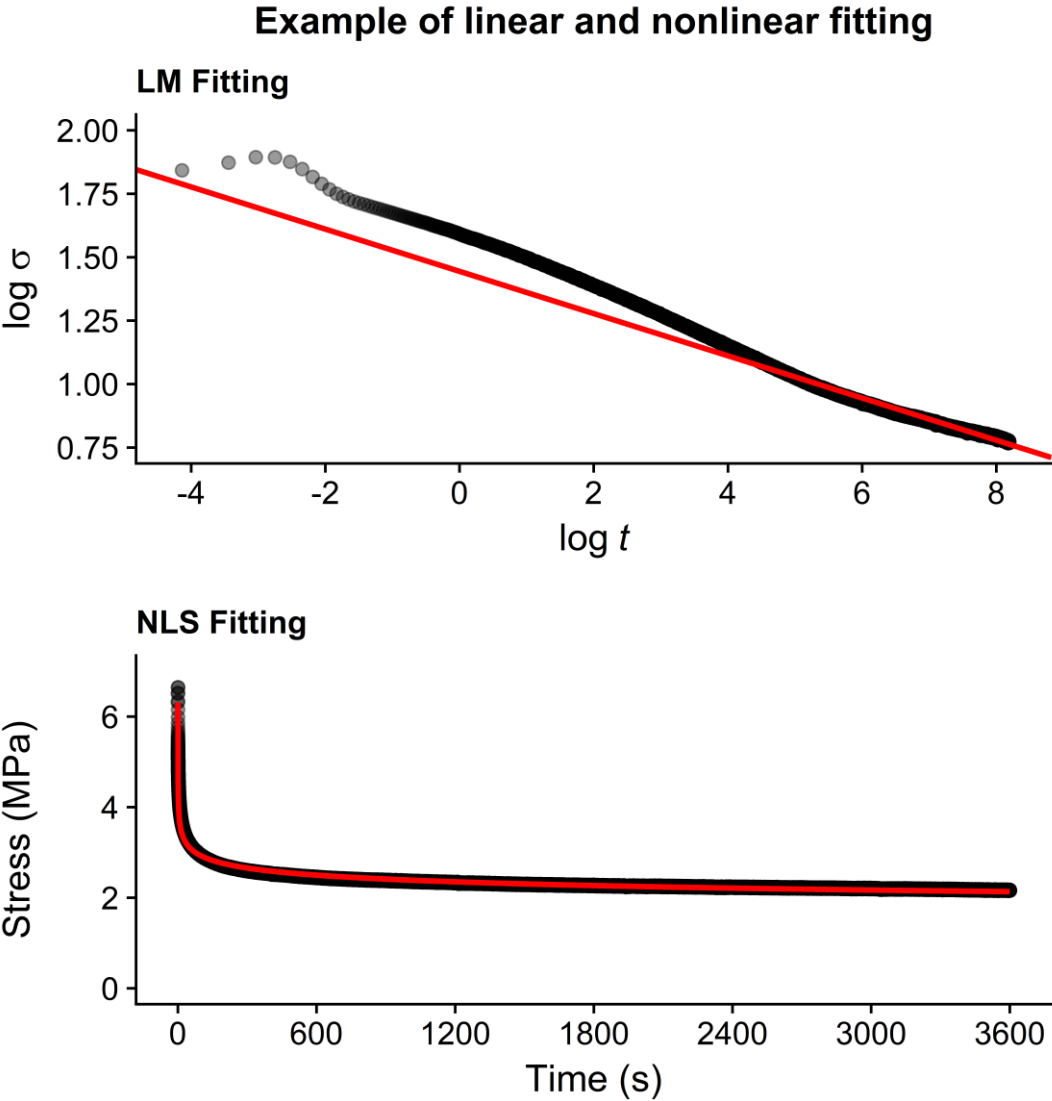
Figure 8-10: Example of a 'poor' curve fit with high R^2 using linear least-squares R^2 = 0.974 (top) and equivalent fit using nonlinear least-squares with an estimate R^2 = 0.968 (bottom). Both fits were performed on the full data set using $2.5t_r$

8.9.   Appendix D – Interval test

95%Confidence Interval for Creep

95% Confidence Interval for Relaxation
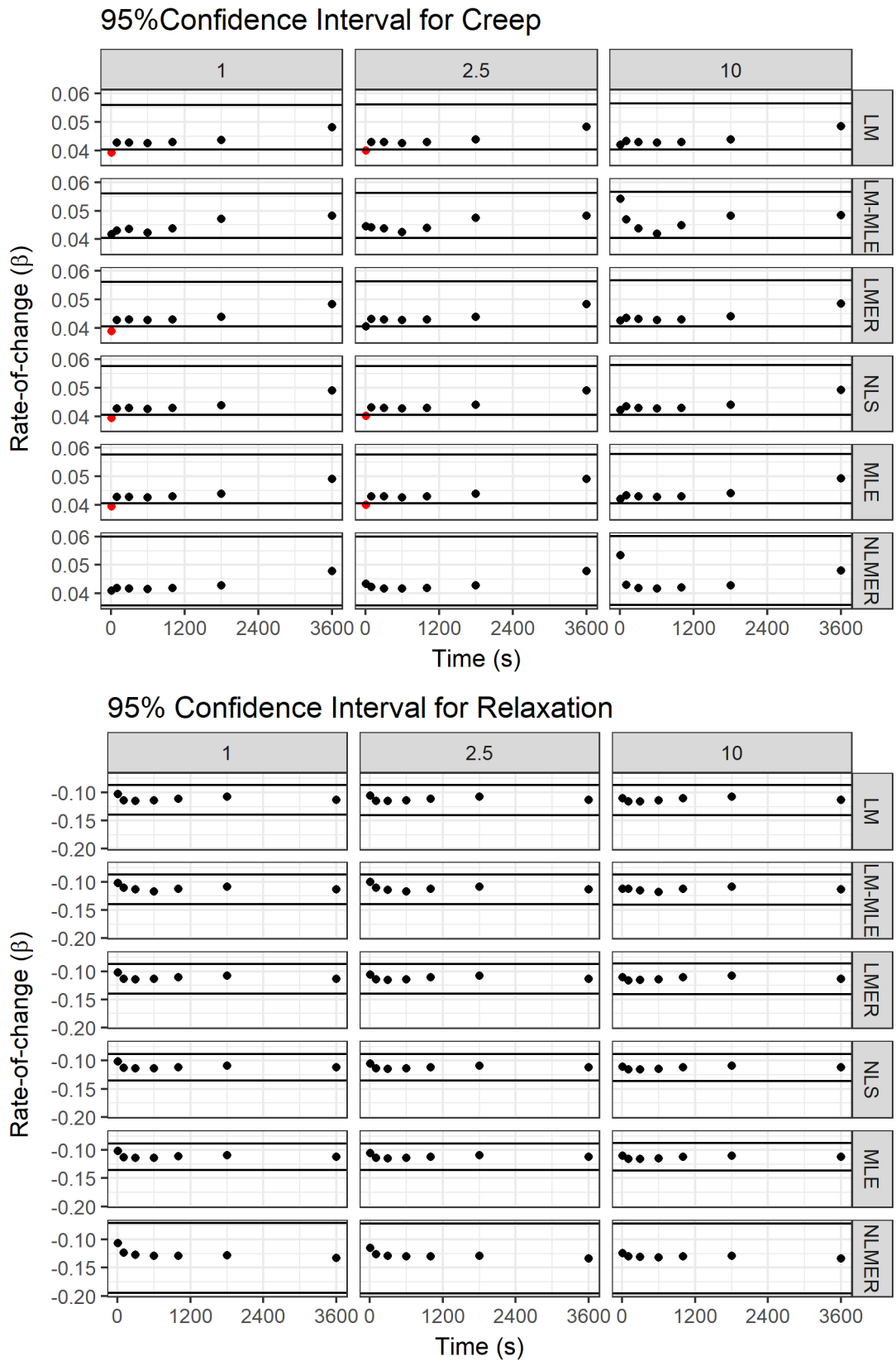
Figure 8-11: Interval test of duration (s) and fitting technique using a 95% confidence interval (CI). Values outside of the CI are coloured red.

CHAPTER 9. METHODOLOGY FOR DEFINING VISCOELASTIC BEHAVIOUR OF TENDINOPATHY

9.1. Introduction

From an engineering perspective, the mechanical behaviour of tendinopathy may offer suggestions as to the aetiology of underlying disease, particularly with respect to biomechanics and function. The mechanical behaviour also allows animal models to be validated against clinical behaviour. Furthermore, the outcomes provide inputs that can be used in computational modelling to provide more realistic descriptions of biomechanical behaviour.

This chapter seeks to develop a robust methodology for describing the viscoelastic behaviour of soft tissue that may be used to inform computational models, as well as to determine differences between tendon models.

9.1.1. Tendinopathy

Tendinopathy has historically been considered an overuse injury (Paavola *et al.*, 2002; Sharma and Maffulli, 2005b) but may be an underuse injury related to the injury mechanism (Arnoczky *et al.*, 2007; Rees *et al.*, 2009). As discussed earlier, tendinopathy may be caused by trauma or repetitive strain of the tendon (Woo *et al.*, 2000). Accounting for 48% of reported occupational illness and 30–50% of all sporting injuries (Renstrom, 1991), tendon injuries result in significant economic and social cost. It is, therefore, imperative to understand the underlying causes and tissue responses to inform development of better treatment and prevention techniques.

Tendinopathy can be regarded as degeneration with insufficient healing, with little to no inflammation (Lui *et al.*, 2011; Warden, 2007). Tendons may exhibit signs of disorganisation and microtears, as well as increases in a variety of biochemical markers (Lake *et al.*, 2008). The overall result is a reduction in strength and elasticity of the tendon (Lake *et al.*, 2008; Warden, 2007), which is rarely recovered (Marcos *et al.*, 2014). Arya and Kulig (2010) hypothesised that spontaneous rupture is the result of chronic degeneration of the tendon caused by disruption of the collagen structure, accompanied by an increase in collagen-III that may alter the mechanical and material properties of tendon.

Tendinopathy may cause failure at loads much lower than ultimate tensile load (Korvick *et al.*, 1996; Malaviya *et al.*, 1998).

Tendinopathy has been comprehensively studied and several detailed reviews, which explore the clinical approaches as well as latest research, provide greater discussion, including Sharma and Maffulli (2008), Longo *et al.* (2009), Patterson-Kane *et al.* (2012), and Sayegh *et al.* (2015).

9.1.2. Animal models

Study of tendinopathy in humans is difficult – biopsy of patients is invasive and clinical presentations of tendinopathy are usually advanced, thereby limiting information of disease progression (Warden, 2007). Animal models allow for investigation of initial disease progression in a controlled manner (Archambault *et al.*, 2007) and many have been developed to investigate tendinopathy (Dirks and Warden, 2011; Lake *et al.*, 2008; Lui *et al.*, 2011; Warden, 2007). Animal models offer the advantage of being controlled and reproducible, allowing for regular observation and evaluation over time (Lake *et al.*, 2008). There is no 'gold standard' model, leading researchers to utilise a variety of models, depending on the application (Warden, 2007). To be considered a valid animal model it must be repeatable and be substantially similar to humans clinically, histopathologically and functionally (Lui *et al.*, 2011).

While racing animals such as horses and dogs develop tendinopathy, it may be more reliably induced in rabbits and rodents (Lui *et al.*, 2011). While rats and mice offer several advantages, including genetic homology and genetically engineered models (Warden, 2007), the similarity in cells and tissue physiology between rabbits and humans make rabbits a popular choice (Warden, 2007). Additionally, the rabbit's larger tendons are easier to work with and provide larger samples compared to rodents (Lui *et al.*, 2011). However, it is important to understand the model in the context of behaviour and physiology so it can be related to humans (Lui *et al.*, 2011).

9.1.3. Methods of induction

Methods of inducing tendinopathy have ranged from mechanical overloading to chemical injection (Lake *et al.*, 2008; Lui *et al.*, 2011; Warden, 2007) with advantages and disadvantages for each method having been identified

(Dirks and Warden, 2011). For example, mechanical overloading has been shown to successfully induce tendinopathy in the rat supraspinatus tendon, demonstrated by inferior mechanical properties, including maximum stress and elastic modulus (Soslowsky *et al.*, 2002; Soslowsky *et al.*, 2000). Similar overuse studies in other tendons, such as the Achilles (Glazebrook *et al.*, 2008; Huang *et al.*, 2004), have demonstrated variable success (Warden, 2007). Backman *et al.* (1990) used repetitive loading of the rabbit Achilles tendon to induce tendinopathic changes, but this was not able to be replicated in a later study by Archambault *et al.* (2001). Alternative methods, such as artificial stimulation, have failed to induce tendinopathy in the Achilles tendon (Lui *et al.*, 2011).

Chemical induction offers an attractive alternative as it may be more consistent (Dirks and Warden, 2011; Lui *et al.*, 2011); however, individual chemical compounds do not appear to sufficiently develop the same pathology seen clinically (Warden, 2007), and may produce a state akin to acute injury (Lui *et al.*, 2011). Inspired by chemical markers found in mechanical overuse studies, repeated exposure to prostaglandins has shown degenerative changes similar to tendinopathy (Khan *et al.*, 2005; Sullo *et al.*, 2001). Collagenase has been used to replicate the clinically observed disruption of collagen fibres (Dirks and Warden, 2011). It has been used widely across many animal models (Lui *et al.*, 2011) and appears to exhibit dose-dependent responses (Lake *et al.*, 2008). Models include rats, rabbits, and horses (Chen *et al.*, 2011a; Chen *et al.*, 2004; Dowling *et al.*, 2002a; Hsu *et al.*, 2004a; Hsu *et al.*, 2004b; Kamineni *et al.*, 2015; Lui *et al.*, 2009; Marcos *et al.*, 2014; Marcos *et al.*, 2012; Nabeshima *et al.*, 1996; Perucca Orfei *et al.*, 2016; Stone *et al.*, 1999; Yoo *et al.*, 2012).

9.1.4. Responses to collagenase

In response to collagenase, rabbit patellar tendon was seen to increase in stiffness and did not regain ultimate tensile strength (UTS) compared with controls (Hsu *et al.*, 2004b; Stone *et al.*, 1999). Similar results were seen in rat Achilles tendinopathy (Chen *et al.*, 2004). Interestingly, studies in rabbit patellar tendon and rat Achilles tendon injected with collagenase exhibited no change in failure testing using high strain rates but demonstrated a reduced

failure load when tested at a low strain rate (Chen *et al.*, 2004; Hsu *et al.*, 2004a; Hsu *et al.*, 2004b; Lake *et al.*, 2008; Stone *et al.*, 1999), perhaps indicating a viscoelastic interaction between the disrupted fibre matrix and ground substance. Studies in horses showed an increase in cross-sectional area (CSA) resulting in a lower failure stress, coupled with a higher failure strain, leading to a low stiffness (Dowling *et al.*, 2002a, 2002b; Lake *et al.*, 2008).

The healing response in collagenase models is contentious, since it is argued the repair is not consistent with the defective healing response seen in degenerative tendinopathy (Lui *et al.*, 2011). Yoo *et al.* (2012) used a collagenase-induced tendinopathy model to assess extracorporeal shockwave therapy (EWST) on rat Achilles tendons using histology and atomic force microscopy. The model was said to resemble Achilles tendinitis. Lui *et al.* (2009) histologically examined rat patellar tendinopathy for 32 weeks post-induction, describing the model as viable for calcific tendinopathy and noting that healing did not begin until week 32. It was found that, after eight weeks of healing, collagenase-induced tendinopathy demonstrated a defective healing response, suggesting that the acute injury phase had increased the susceptibility for damage which had led to degeneration. Chen *et al.* (2011a) also described tendinopathic changes at eight weeks post-induction using histological scores. With the exception of these studies, most studies have not investigated degeneration past eight weeks (Lui *et al.*, 2011). Stone *et al.* (1999) found no change in CSA at 16 weeks, but a significant decrease in ultimate load, when using a cytokine and cell-activating factor injection. This injection was questionable compared with use of collagenase (Lui *et al.*, 2011). Collagenase models, when continued to eight weeks, appear to demonstrate a progressive deterioration comparable to tendinopathy (Chen *et al.*, 2011a; Stone *et al.*, 1999).

Critics have argued that collagenase develops an inflammatory reaction more similar to tendinitis than tendinopathy (Lake *et al.*, 2008; Lui *et al.*, 2011; Warden, 2007). This implies an acute pathology rather than the typical degenerative changes seen which, in turn, may affect the applicability of the results derived from the model. However, as described above, there is

evidence to suggest that, given sufficient time, collagenase-induced tendinopathy may progress to a degenerative condition (Chen *et al.*, 2011a; Lui *et al.*, 2009; Stone *et al.*, 1999). Thus, collagenase may still be a useful model since it is controllable and produces many of the clinical traits.

9.1.5. Choosing the model

Many studies have investigated the pathological changes derived from these models, including histological observations, imaging and microscopy techniques, biochemical markers, and mechanical properties (Warden, 2007). Study of the behavioural changes caused by the tendinopathy model are also important in validating the animal model (Lui *et al.*, 2011). However, given there is no perfect animal model the choice of model should be based on its appropriateness for the experiment (Lui *et al.*, 2011).

Care should be taken when using the contralateral side as a control, since it is usually compromised in patients with unilateral Achilles tendinopathy and through intervention (Andersson *et al.*, 2011; Docking *et al.*, 2015).

Fu *et al.* (2010) presented a pathway for tendon degeneration, but cited a piecewise approach to tendinopathy research that made it difficult to elucidate the underlying pathogenesis. Andarawis-Puri *et al.* (2015), reporting on the outcomes of a recent conference, identified the need for basic science to help develop a more complete model. One area of limitation is the understanding of the mechanical characteristics of tendinopathic tendons (Marcos *et al.*, 2014). Of particular interest are viscoelastic behaviours and stress-strain behaviours (Warden, 2007), since they aid in implicating different components of the structure for different mechanical purposes. Dynamic, as well as static, properties are important because of the requirements of daily movement (Imai *et al.*, 2015). Despite this, Imai *et al.* (2015) identified no previous studies of dynamic viscoelastic testing of tendinopathy, citing only static creep and stress relaxation testing.

As discussed in Chapter 2, Literature review, tendon mechanics are known to be complex. Since fibrils are discontinuous and overall tissue strain is larger than the fibril strain, it is implied that the non-collagenous matrix must permit transfer of forces, and thus is an important factor in mechanical behaviour

(Rigozzi *et al.*, 2009). Conversely, changes to the mechanical behaviour of tendons may imply a disruption to the underlying structure and this can be used to inform treatment. For example, decorin is involved in the transfer of force between collagen fibrils (Rigozzi *et al.*, 2009). The capacity for sliding between tendon fascicles was seen to decrease with ageing in injury-prone equine tendons, possibly leading to age-related tendinopathy (Thorpe *et al.*, 2013b). The increase in stiffness associated with tendinopathy, which can have a significant influence on force transmission, muscle power, and energy absorption and release during locomotion (Arya and Kulig, 2010), may be related to scarring caused by ineffective healing processes. Overuse has been shown to increase glycosaminoglycans (GAGs) in the tendon mid-portion (Bell *et al.*, 2013). A change in proteoglycan (PG) levels has been shown to affect relaxation rate, hysteresis, and strain rate sensitivity, an effect also seen with fluctuations in water content (LaCroix *et al.*, 2013a).

9.1.6. Models in literature

There have been many examples of induced tendinopathy in literature, particularly for assessing the efficacy of treatments. These include platelet-rich plasma treatment (Yan *et al.*, 2017), extracorporeal shockwave therapy (Hsu *et al.*, 2004a; Yoo *et al.*, 2012), hyperbaric oxygen therapy (Hsu *et al.*, 2004b), autologous tenocyte therapy (Chen *et al.*, 2011a), low-level laser therapy (Marcos *et al.*, 2014; Marcos *et al.*, 2012), augmented soft tissue mobilisation (Imai *et al.*, 2015), and exercise (Bell *et al.*, 2013).

Despite the opportunity to describe many aspects of mechanical behaviour of tendon, especially tendinopathic tendon, to elucidate the mechanisms for injury and degeneration, most studies involving tendinopathy models only tested the tendons in traction to failure.

Nabeshima *et al.* (1996) found that the application of strain during collagenase diffusion protected the tendon from degeneration, with stiffness and maximum force measurements similar to the control values. No strain, and delayed application of strain, resulted in significantly inferior properties. This was supported by later studies on collagen fibrils, which found strain preferentially

protected the fibrils in the presence of collagenase (Bhole *et al.*, 2009; Flynn *et al.*, 2010).

An overuse-induced rat supraspinatus tendinopathy model showed an increase in CSA and reduction in maximum stress and modulus compared to controls (Soslowsky *et al.*, 2000). The addition of extrinsic factors produced a more intense result than that of overuse alone (Carpenter *et al.*, 1998; Soslowsky *et al.*, 2002). CSA was also seen to increase in a collagenase-induced rabbit patellar tendinopathy model, while there were negligible changes in the maximum load or stiffness (Stone *et al.*, 1999).

Recombinant growth hormone was found to have no effect on mechanical properties of healthy equine superficial digital flexor tendon (Dowling *et al.*, 2002b). However, when used to treat collagenase-induced tendinopathy, recombinant growth hormone was shown to result in inferior mechanical properties (lower load and stiffness, and higher CSA) compared with sham-treatment (Dowling *et al.*, 2002a). This was also seen when comparing the untreated and healthy superficial digital flexor tendon.

Hsu *et al.* treated collagenase-induced rabbit patellar tendinopathy shockwave therapy (2004a) and hyperbaric oxygen therapy (2004b). Using shockwave therapy, ultimate tensile load was seen to increase in tendons over 16 weeks of treatment compared with sham-treatment. Using hyperbaric oxygen therapy, UTS returned to 93% of control, while the sham-treatment only recovered to 70% (raw numbers were not presented). Structural changes in the tendon were correlated with the ultimate tensile load (Hsu *et al.*, 2004a). Extracorporeal shockwave therapy was also assessed on rats with collagenase-induced Achilles tendinopathy, with failure load and stiffness seen to decrease following collagenase injection (Chen *et al.*, 2004).

Chen *et al.* (2011a) used a collagenase-induced rabbit Achilles tendinopathy model to test the efficacy of autologous tenocyte therapy. Treated tendons exhibited improvement in the ultimate tensile force compared with untreated tendons, and exceeded that of normal tendons by eight weeks.

Dry-needling-induced rat Achilles tendinopathy showed significantly larger CSA, and a significantly reduced UTS and modulus, with and without

additional overuse-activity (Kim *et al.*, 2015). An overuse-induced rat Achilles tendinopathy model showed a reduction in maximum force and 'rigidity' ($R = F/\varepsilon$, where *F* is force and ε is strain) (Jafari *et al.*, 2015).

Marcos *et al.* (2014; 2012), investigating low-level laser therapy to treat collagenase-induced rat Achilles tendinopathy, proposed a more complex loading-pattern, rather than monotonic loading, to better represent the dynamic responses seen *in vivo*. A series of load-unload cycles with increasing strain was performed. The tangential, secant, and unloading stiffness were recorded, as well as maximum force and elongation before and after induction, and with and without treatment (Marcos *et al.*, 2014; Marcos *et al.*, 2012). Collagenase was found to reduce the elongation, force and stiffness of the tendons, while treatment returned them to approximately normal values, but this was only investigated seven days post-induction (Marcos *et al.*, 2014).

In vivo investigations on human subjects showed a weakening of the mechanical characteristics in Achilles tendinopathy patients, including peak force and stiffness (Arya and Kulig, 2010). CSA was larger in the tendinopathy group ($56mm^2$ vs. $93mm^2$) which resulted in a notable decrease in the modulus compared with the stiffness. This was highlighted as a risk of using the elastic modulus when comparing controls with tendinopathic tendons, since a larger CSA may result in lower intrinsic properties even if the extrinsic properties are higher than those of the controls.

9.1.7. Models including viscoelastic testing

Chapter 6 described the need to extract the most data from each specimen, including the use of ramp, stress relaxation, and creep testing to inform constitutive models (Duenwald *et al.*, 2009b). Despite authors highlighting this and the limited understanding of tendon mechanics, few studies have performed other than tensile testing.

Matthews and Ellis (1968) performed a series of cyclic tests on cat tendon to establish the effects of freezing, finding that freezing did not negatively influence the results but should be considered as a variable. Galeski *et al.* (1977) compared the mechanical changes associated with alloxan diabetes and ageing, finding a decrease in the relaxation rate amongst other changes.

Huang *et al.* (2004) utilised an overuse-induction of rat Achilles tendinopathy to measure mechanical properties such as maximum load, elastic modulus, and percentage relaxation after 300s. Individual results were not discussed; however, the authors concluded that the changes previously observed in supraspinatus tendons (Soslowsky *et al.*, 2000) were not replicated in the Achilles tendon, as the biomechanical assay and morphological assessment did not detect any difference between groups. Imai *et al.* (2015) investigated the use of augmented soft tissue mobilisation in the Achilles tendon of New Zealand White (NZW) rabbits using collagenase injections to induce tendinopathy. Both tendons were induced, with one being treated by augmented soft tissue mobilisation and the other acting as a control. The tendons were cycled to a strain of 1% and frequencies ranging from 0.1–10 Hz. It was concluded that treatment resulted in a more favourable dynamic biomechanical behaviour; however, as there was no uninduced tendon for comparison, it is difficult to determine the true efficacy of the treatment, or the appropriateness of the collagenase model. Tucker *et al.* (2016) investigated a surgical repair model using an established supraspinatus tendinopathy model in rats (Soslowsky *et al.*, 1996; Soslowsky *et al.*, 2000). In this model, it was seen that acute changes overshadow chronic injury, with no significant differences in CSA, modulus, maximum stress, stiffness, or maximum load, and only a small increase in percentage relaxation in the overuse group.

Outside of tendinopathy research, studies investigating the deleterious effects of stress shielding in the rabbit patellar tendon have shown increases in CSA with corresponding decreases in tensile strength and elastic modulus in a rabbit patellar tendon model (Fujie *et al.*, 2000; Majima *et al.*, 1996; Ohno *et al.*, 1993; Tohyama *et al.*, 1992). Investigations of the transverse properties showed a reduction in the strength and modulus (Yamamoto *et al.*, 2000). A simple stress relaxation test (1200s at 14% strain) found a decrease in percentage relaxation due to stress shielding. It was suggested that changes to the ground substance and the mechanical interactions with the extracellular matrix (ECM) may be responsible for the change in relaxation behaviour following degenerative changes. After induced tearing of the supraspinatus tendon in a rat model, intact, uninjured rotator cuff tendons were found to have

reduced modulus, while percentage relaxation was relatively stable (Perry *et al.*, 2009). Liu *et al.* (2009), using mouse tail tendon, noted differences in strain rate and stress relaxation response with ageing.

Neviaser *et al.* (2012), highlighting the need to identify some of the mechanisms of overuse-induced degeneration, performed cyclic fatigue loading *in vivo* to investigate the damage mechanisms. An increase in stiffness at low- to medium-level fatigue loads, and a decrease in stiffness at high-level fatigue loading, were seen. Conversely, hysteresis decreased with low- to medium-level loading, and increased with high-level loading.

Soft tissues have shown a dependence on strain and stress levels during stress relaxation and creep testing (Duenwald *et al.*, 2009b; Provenzano *et al.*, 2001; Sverdlik and Lanir, 2002). Results suggest mechanical testing should explore the nonlinearity of the tissue responses to elucidate differences between healthy and unhealthy tendon that may indicate underlying changes caused by the degenerative mechanisms.

LaCroix *et al.* (2013a) utilised different magnitudes of stress relaxation, coupled with load-to-failure, to assess the effect of exercise on aged rat tail tendons. The study demonstrated a significant increase in ultimate stress and modulus, and significant decreases in relaxation rate and percent relaxation with maturity, as well as decreases in viscoelastic parameters with ageing.

Freedman *et al.* (2016) utilised a complex methodology of stress relaxation, low frequency sweeps, and load controlled fatigue testing to test the Achilles tendon following surgical treatment of rupture. This protocol was subsequently used in several studies investigating the effects of ageing, hormones, and sex (Fryhofer *et al.*, 2016; Pardes *et al.*, 2017; Pardes *et al.*, 2016). This protocol provided results with respect to percentage relaxation, dynamic modulus, and fatigue life.

As far as could be ascertained, these are the only studies which used more rigorous testing protocols to investigate changes in the viscoelastic behaviour of tendon. No studies have evaluated the viscoelastic behaviour of tendinopathic tendons in this way.

Studies on soft and hard tissues have utilised increasingly complex viscoelastic testing to attempt to extract maximum information from each sample. Rigby *et al.* (1959) made use of tensile testing, stress relaxation, and temperature creep to describe the mechanical behaviour of rat tail tendon. Dynamic viscoelasticity, or frequency response to cyclic loading, has been performed in human digital flexor tendons (Schwerdt *et al.*, 1980), sheep plantaris tendon (Ker, 1981), and rabbit Achilles tendon (Nagasawa *et al.*, 2008). To fully describe a constitutive model of the tendons, Pradas and Calleja (1990) tested human hand flexor tendons using multiple creep tests, including multistep creep testing. Strain rate sensitivity was tested by performing multiple tensile tests on anterior cruciate ligament (ACL) (Pioletti *et al.*, 1999). Pioletti and Rakotomanana (2000b) went on to test stress relaxation behaviour of human cruciate ligaments and patellar tendons at multiple strain levels to validate the assumption of variable separation in integral models of soft tissue. Sverdlik and Lanir (2002) performed a complex series of preconditioning, recovery, and stress relaxation tests to evaluate the time-dependent properties of sheep digital extensor tendons. The protocol involved five sets of tests at multiple strain levels over approximately 16,000 seconds (4 hours). Yang *et al.* (2006) made use of a multi-step stress relaxation test to evaluate the nonlinearity of the viscoelastic response of oesophageal tissue, while Nekouzadeh *et al.* (2007) developed an adaptive quasilinear viscoelastic (QLV) model for predicting viscoelastic behaviour.

The usefulness of traditional models such as Fung's QLV has been limited by tendons having demonstrated magnitude (strain and stress) and rate dependent viscoelasticity. More complex models have been developed that overcome the shortfalls, but in turn require diverse data to inform the model. For example, Schapery's nonlinear viscoelastic model, which can account for magnitude dependency, requires at least two relaxation or creep steps.

The considerable work in this area undertaken by the Department of Biomedical Engineering at the University of Wisconsin has directly influenced this dissertation. Lakes and Vanderby (1999), inspired by Thornton *et al.* (1997) demonstrating that relaxation occurs more rapidly than creep in ligament samples, proposed a mathematical framework to interrelate creep

and relaxation in soft tissue, which was further developed by Oza *et al.* (2006a; 2003; 2006b). Evidence for nonlinearity of ligament was provided by Provenzano *et al.* (2001) and Hingorani *et al.* (2004), who described stress and strain level dependence on rate of creep and stress relaxation. Rate of recovery was also shown to be faster than rate of creep in ligaments (Jensen *et al.*, 2004) and slower than relaxation in tendon (Duenwald *et al.*, 2008). A nonlinear viscoelastic model was developed to describe this behaviour (Provenzano *et al.*, 2002c). Damage and healing mechanics were also evaluated to varying degrees (Duenwald-Kuehl *et al.*, 2012b; Provenzano *et al.*, 2005; Provenzano *et al.*, 2002a; Provenzano *et al.*, 2002b). Provenzano and Vanderby (2006) demonstrated that collagen fibres are continuous or functionally continuous, disagreeing with work by Screen and colleagues who had found evidence of sliding as a component of stretching (Cheng and Screen, 2007; Gupta *et al.*, 2010; Screen, 2008, 2009; Screen *et al.*, 2006; Screen *et al.*, 2011).Testing time for viscoelastic testing was determined by Manley Jr *et al.* (2003). Behaviour was further investigated in tendon and ligament, with rate of relaxation increasing with strain in tendons and decreasing with strain in ligaments (Duenwald *et al.*, 2009a; Duenwald *et al.*, 2009b, 2010). Many recommendations for testing suggested within these studies have formed the basis of aspects of this dissertation. LaCroix *et al.* (2013a) presented one of the few studies investigating changes in the viscoelastic behaviour of soft tissue as a result of factors such as age or damage. This formed the basis of the protocol used in this study to evaluate the behaviour of tendinopathy using viscoelastic testing.

In defining the nonlinear viscoelastic behaviours of soft tissue, the group at the University of Wisconsin utilised many methodologies to explore different responses. Many studies used one or more single-step relaxation or creep tests, separated by recovery (Hingorani *et al.*, 2004; LaCroix *et al.*, 2013a; Provenzano *et al.*, 2001). Duenwald *et al.* (2009a; 2010) tested tendon and ligament using relaxation and recovery sequences at multiple relaxation and recovery strain levels, and investigated the ability to predict the curves using traditional models such as QLV, Schapery's nonlinear viscoelastic, and nonlinear superposition models. While performing only single magnitude

stress relaxation and creep tests, Manley Jr *et al.* (2003) found that testing duration could be sufficiently short so as to permit multiple tests without deleterious effects on soft tissue. This was echoed in the results of Chapter 8 in this dissertation.

Most notably, Duenwald *et al.* (2009b) identified that more comprehensive testing protocols are required to determine the best model, and that a two-step relaxation method was one example of "determining more robust viscoelastic behaviour".

9.2. Method

As discussed in Chapter 6, there are four tests regularly performed on materials to characterise their behaviour – ramp, stress relaxation, creep, cyclic/dynamic. It is clear from the literature that multiple-step viscoelastic assessment is required to identify nonlinear behaviours. When characterising soft tissue, preconditioning and strain rate sensitivity are also considerations (Chapter 7). Dynamic behaviour is representative of daily activities, such as walking, which often involve repetitive behaviour. To the author's knowledge, there is currently no published protocol that has tested the same soft tissue samples in each of these modes to provide a comprehensive picture of tissue behaviour. Therefore, a testing protocol was proposed that assesses the isochronal, static, and dynamic behaviours of tendons.

The methodology was performed in three stages – preconditioning, stress relaxation, and creep – with time for recovery between each test. Based on the results of West *et al.* (2004), peak strain was set at 4%. Strains greater than 5% have been demonstrated to cause damage to tendons (Provenzano *et al.*, 2002b), which is undesirable in a test with multiple stages. A peak stress of 4MPa was used, rather than 6.7MPa reported by West *et al.* (2004), to reduce the risk of tendon damage via fatigue. The methodology also considered the requirement for future use of the tendons within the Australian Research Council (ARC) Linkage Project and so micro- or macro-failure levels were avoided.

9.2.1. Preconditioning stage

Samples were preloaded to 5N and the strain zeroed. Tendons were preconditioned for 100 cycles from 0% to 4% strain at 1Hz. This is in accordance with the recommendation by Cheng *et al.* (2009) that preconditioning strain should be the highest strain used in the study. While recommendations of 1000 cycles have been made for longer tests (Bergomi *et al.*, 2009), a duration of 100 cycles was chosen so as to not adversely influence the loading history (Kahn *et al.*, 2010).

Samples were removed and rewrapped in saline-soaked gauze, and allowed to recover in an air-tight container for at least one order of magnitude longer than testing (Duenwald *et al.*, 2009a), in this case 1000 seconds.

9.2.2. Stress relaxation stage

Stress relaxation testing comprised a dynamic component, followed by two strain rate sensitivity components, and four relaxation steps. The dynamic component involved 100 cycles at 1Hz from 0–2% strain. The magnitude was selected as a compromise – a magnitude low enough so as not to continue preconditioning and to minimise any effects on the ramp phases, but large enough to record data. Preliminary testing showed a peak stress of approximately 4MPa during cycling. Typically, dynamic modulus is measured using small excursions around a non-zero starting magnitude; however, to maximise the available measurements, such as hysteresis, the protocol returns to zero to complete the cycle.

The last cycle of the dynamic component was used as the first of three load-unload curves to establish strain rate sensitivity in an isochronal stress-strain response. The three load-unload cycles, from 0–2%, were performed at 4% s^{1}, 0.1% s^{1}, and 1% s^{1}. This magnitude should remain within the toe and linear regions without influencing later phases of the testing (Arnoczky *et al.*, 2002a; Screen, 2008; Screen *et al.*, 2004a; Screen *et al.*, 2002b; Sharma and Maffulli, 2005b; Wang *et al.*, 2006)

Samples were then ramped at 10% s^{-1} to 1% and held for 100 seconds. The time selected was based on the results of Chapter 8. This was repeated to strain magnitudes of 4% in 1% increments. Strain was increased at each step

to continually test the effects of relaxation rather than recovery (Duenwald *et al.*, 2009a; Duenwald *et al.*, 2010). The sample was unloaded at 1%.s^{-1}.

Total testing time for the set was 554 seconds and is summarised in Figure 9-1.

Proposed Methodology
Relaxation and Creep Stages
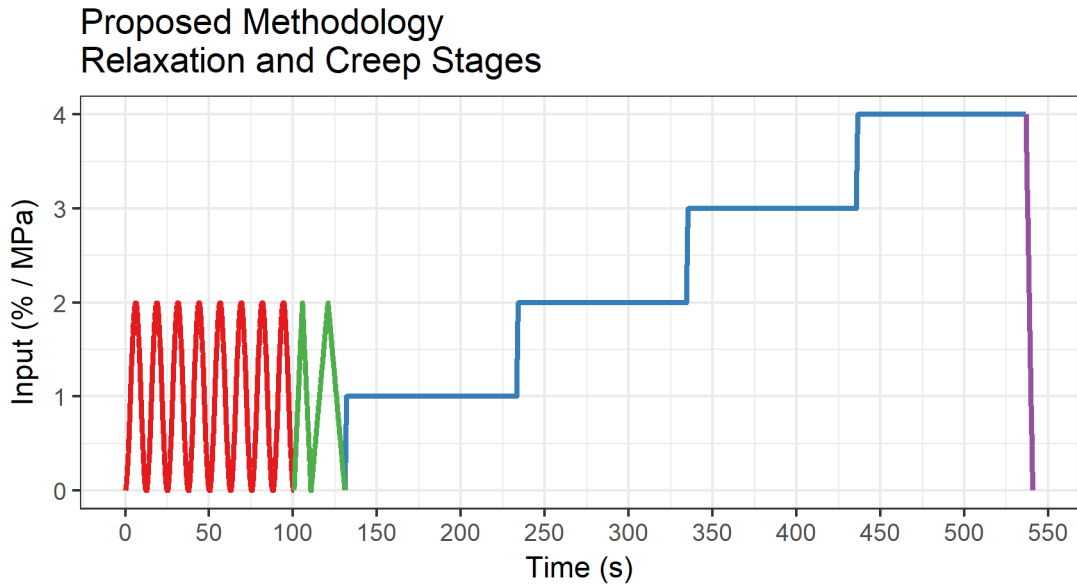
Figure 9-1: Example of loading protocol (not to scale). The protocol starts with a dynamic component (red), followed by two load-unload curves (green), four incremental steps of stress relaxation or creep (blue) and completed with an unload curve (purple).

Samples were removed and rewrapped in saline-soaked gauze, and allowed to recover for 100 minutes in an air-tight container.

9.2.3. Creep stage

Creep testing followed the same rationale as stress relaxation, with minor variations. The dynamic component involved 100 cycles at 1Hz from 0–2MPa stress.

The last cycle of the dynamic component was used as the first of three load-unload curves for the isochronal stress-strain response. The three load-unload cycles were performed at 4% s^{-1}, 0.1% s^{-1}, and 1% s^{-1}. The first of the load-unload cycles were from 0–2MPa while the two dedicated load-unload cycles were to 2% strain. Data were limited to the range 0–2% to allow direct comparison of the isochronal responses between stages.

Samples were then ramped at 10%.s^{-1} to 1MPa and held for 100 seconds. This was repeated to stress magnitudes of 4MPa in 1MPa increments. As with relaxation, stress was incrementally increased to continually measure creep, rather than any recovery or similar phenomena. The sample was unloaded at 1%.s^{-1}. A summary of the protocol is presented in Figure 9-1.

Total testing time varied as a result of the mix of displacement control and load targets.

9.2.4. Load-to-failure

It is proposed that, if tendons are no longer required, a load-to-failure test should be performed following the creep stage at 1000%.min^{-1} to define the entire isochronal stress-strain curve of the tendon for reference.

9.3.   Outcomes

9.3.1. Stress-strain response

Stress-strain responses were calculated from the three load and unload cycles, being the last cycle of the dynamic segment and the two strain rate sensitivity cycles. If the load-to-failure data are available, the results may also be determined for the entire stress-strain curve.

Maximum values of load, stress, displacement, and strain were calculated for the load and unload portion of each cycle. Stiffness and elastic modulus were calculated using a custom implementation of the Instron BlueHill 2 (Instron, MA, USA) automatic slope algorithm. This algorithm, described in detail in the Instron BlueHill Calculation Reference manual (version 1.1), divides the data into six equal regions between zero and the maximum load, calculates the slope of each region using least-squares linear fit, and finally returns the highest slope value from the pair of regions with the 'highest slope sum'.

9.3.2. Dynamic response

Storage modulus, loss modulus and loss tangent were calculated from the last five cycles of the dynamic segment of each stage. The change in stiffness and hysteresis were calculated across all cycles. Rate of relaxation and creep, and percentage change, were calculated from the peak values in each dynamic set for comparison with the static response.

9.3.3. Static response

Rate of change and percentage change were calculated for the multi-step stress relaxation and creep component. Rate of change (β) was calculated from the power law, $y = At^\beta + c$, using the nonlinear maximum likelihood estimate (MLE) method described in Chapter 8.

9.4. Conclusion

The proposed methodology offers a comprehensive approach to soft tissue testing in a single sample. To the author's knowledge, this is the first methodology to utilise a combination of dynamic, ramp, and static testing in both creep and relaxation for any soft tissue, and the first methodology to perform a multiple step viscoelastic evaluation of tendinopathic tendons. Consideration was given to protecting the integrity of the tissue during testing to ensure reliability of the results throughout the duration of the test.

Performing such a suite of testing on a single sample may help to identify subtle differences in behaviour corresponding to structural or constitutive differences in the material that may elucidate degenerative, disease, or even treatment pathways. Parameters within the methodology may be modified to examine the response at difference frequencies, at different magnitudes, or using different waveforms to elicit different responses in the tissue.

Validation of the methodology is required; however, this study represents an attempt at defining a standardised protocol for comprehensively defining the mechanical behaviour of samples within a soft tissue model. A standardised protocol would permit easier comparison between studies and potentially improve understanding of the mechanics of soft tissues by removing inter- and intra-laboratory variation.

CHAPTER 10.   VISCOELASTIC   TESTING   OF TENDINOPATHY IN THE ACHILLES TENDON

10.1. Introduction

A collagenase-induced tendinopathy model was selected as the animal model for the Australian Research Council (ARC) Linkage Project, LP110100581, of which this dissertation is part. As highlighted in Chapter 9, the mechanical behaviour of tendinopathy has not been widely studied: most studies have focussed on the failure properties (ultimate tensile stress and strain) and not the viscoelastic response. Only three studies were identified that contained a form of viscoelastic testing in a tendinopathy model – two rat studies (Huang *et al.*, 2004; Tucker *et al.*, 2016) and one rabbit study (Imai *et al.*, 2015). The author found no studies examining the viscoelastic response of tendinopathic tendons at multiple stress or strains, and no study of both stress relaxation and creep testing. Consequently, there is little knowledge of the effect of tendinopathy on the mechanics of tendon, and no knowledge of the effect of tendinopathy across a range of physiological stresses and strains.

A methodology for comprehensively testing the viscoelastic behaviour of soft tissue was proposed in Chapter 9 and subsequently used to define the behaviour of tendon from the animal model. Three approaches were taken with respect to assessing the tendons. Firstly, the results of the collagenase-induction model were evaluated. Secondly, the conventional approach of comparing groups was used to evaluate the tendinopathic group in relation to the control groups. Lastly, individual tendon results were compared to the pooled results of the control rabbits, considered to represent the behaviour of a normal tendon population, to evaluate whether tendinopathy can be identified from the mechanical behaviour of a tendon – that is, to determine whether tendinopathy has a unique mechanical fingerprint.

Based on previous collagenase-induced tendinopathy models, tendinopathy tendons will exhibit a change in stiffness (Chen *et al.*, 2004; Hsu *et al.*, 2004b; Marcos *et al.*, 2014; Stone *et al.*, 1999), although the literature is conflicted as to whether this change will be an increase or decrease. While tendinopathy has also been shown to increase percentage relaxation by a small amount

(5%) (Tucker *et al.*, 2016), collagenase-induction increases cross-sectional area (CSA) significantly (Dowling *et al.*, 2002a, 2002b; Lake *et al.*, 2008; Stone *et al.*, 1999).

It was hypothesised that:

- Collagenase-induced tendinopathy is an appropriate model when observed over a sufficient period of time (8 weeks or more);
- CSA will be increased in tendinopathic tendons;
- Stiffness and modulus will exhibit changes due to tendinopathy. Modulus and stiffness will tend toward the same direction, but at different magnitudes due to the changes in CSA;
- Tendinopathy leads to an increase in percentage creep and relaxation, as well as rate of change;
- No changes will be observed in tangent modulus, but storage and loss modulus are expected to increase due to tendinopathy;
- Tendinopathic tendons will exhibit viscoelastic behaviours that are unique to degenerative conditions; and,
- Bilateral tendinopathy is not induced in a collagenase-induced model.

10.2. Method

10.2.1.　　Samples

A total of sixty-seven (n=67) New Zealand White (NZW) rabbits were included in ARC Linkage project, LP110100581, of which this dissertation is a component. Of these, three served as pilot samples, 31 controls, 30 tendinopathy, and three were excluded due to data capture issues.

Testing, including induction of tendinopathy, was performed in accordance with the institutional requirements of the University of Western Australia (UWA) and under Animal Ethics Committee approval RA/3/100/1049.

Before and after induction, rabbits were allowed free movement within a cage, regular 'play periods' and other enrichment. Water and feed was provided *ad libitum*. Gait analysis was performed multiple times, before and after induction, as part of the ARC Linkage Project, and included load platforms and

three-dimensional (3D) motion capture. Through surgery, electromyography (EMG) and force buckle transducers were implanted in some rabbits.

Under general anaesthetic and using a 29-gauge needle, type-I collagenase of 0.025mL (30 µL/rabbit, 10,0000 UI/mL, Sigma Chemicals) was injected into the left Achilles tendon of thirty rabbits using a technique similar to that described in Chen *et al.* (2011a). The key difference was that ultrasound guidance was not available for this study. Post-surgical pain management included subcutaneous injections of buprenorphine (0.01mg/kg) and meloxicam (0.5mg/kg) for 2–3 days and 4–5 days, respectively.

Animals were sacrificed at week 4, week 8, and week 12. Tendons were excised and wrapped in saline-soaked gauze, and stored at -20°C in accordance with the recommendations in subsection 7.2.1. Samples from each group were sent for histology, architecture, and mechanical evaluation. In total, 54 tendons, 25 from control rabbits and 29 from tendinopathy rabbits, were available for the mechanical assessment that forms this chapter. Tendons were macroscopically assessed using a modified version of the scoring system presented by Stoll *et al.* (2011).

Tendons were split into subgroups by week and limb (Table 10-1). The contralateral tendon in the tendinopathy group was considered separate to the controls since contralateral tendons often exhibit tendinopathy (Andersson *et al.*, 2011; Docking *et al.*, 2015).

For clarity, tendon groups are referred to using the initials for group and limb, and the week number. For example, Tendinopathy-Left, Week 4 is referred to as TL4, and Control-Right, Week 0 as CR0.

Table 10-1: Summary of the tendons used for mechanical evaluation. A total of 54 tendons were divided into 13 groups.

		Weeks			
Group	**Limb**	**0**	**4**	**8**	**12**
Control	Left		2	5	3
	Right	3	2	7	3
Tendinopathy	Left		4	5	5
	Right		4	4	5

Despite specifying a minimum of six samples in each group, according to the initial scope of the ARC Linkage project, only one group (CR8) reached this target. A further three samples from the Tendinopathy group (TL4 and TR4, and TR8) were not tested as the tendons were received without the calcaneus.

10.2.2. Sample preparation

On the day of testing, tendons were thawed at room temperature in a bath of Ringer's solution (Baxter Healthcare, NSW, Australia) to maintain hydration. The calcaneal tuberosity was potted in poly-methyl methacrylate (PMMA) (Vertex Self Curing, Vertex-Dental B.V., The Netherlands) inside of a 25mm section of OD20mm PVC pipe. CSA was measured using an Artec Spider™ (Artec Group, Luxembourg) structured light scanner as described in Chapter 4.

10.2.3. Test setup

Mechanical testing was performed on an Instron 5566 uniaxial materials testing system with 100N load cell, and controlled via Instron BlueHill software (Instron, MA, USA). The myotendinous junction was secured within thermoelectrically cooled (TEC) grips (Bose Enduratec, MN, USA). The calcaneus was secured perpendicular to the tendon axis, in an anatomical
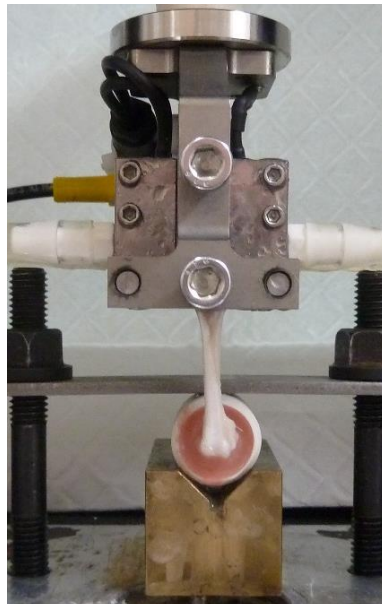
Figure 10-1: The rabbit Achilles tendon tensile test setup on the Instron 5566. The calcaneus was potted in poly-methyl methacrylate (PMMA) and secured perpendicular to the tendon axis in an anatomical position. The myotendinous junction was frozen within the thermoelectrically cooled (TEC) grips.

position. The setup (Figure 10-1) was similar to that described by Warden (2007). Once the musculotendon junction was secured, a preload of 1N was applied and the grip-to-grip length measured using digital callipers (accuracy 0.01mm). Tendons were sprayed with saline during testing to keep them moist.

CSA and gauge length were inputs to the BlueHill method allowing for strain and stress control of the machine. Load, displacement, strain, and stress were recorded at 100Hz during testing.

This testing followed the methodology outlined in Chapter 9; that is, a preconditioning stage followed by the stress relaxation and creep stages. A triangle waveform was used in the cyclic portions of the testing due to limitations in the testing software.

10.2.4.   Statistics

Data were analysed using Microsoft Excel (2016) and in the R Statistical Environment (Lianoglou and Antonyan, 2014; R Core Team, 2015; RStudio, 2016; Wickham, 2009, 2011, 2015). Results are presented as mean and standard deviation. One-way ANOVAs and Tukey's honest significant difference (HSD) *post hoc* test were used to determine statistical significance of the means. All tests were performed assuming an alpha level of 0.05.

Table 10-2: Summary of the rabbit (New Zealand White) demographics used in mechanical testing.

Week	Control				Tendinopathy			All
	0	**4**	**8**	**12**	**4**	**8**	**12**	
Male	2	1	3	1	3	2	2	14
Female	1	1	4	2	2	3	3	16
M:F	2:1	1:1	3:4	1:2	3:2	2:3	2:3	14:16
Start Age (week)	22.0 ± 0.0	30.3 ± 0.2	24.6 ± 2.0	30.2 ± 0.2	28.2 ± 0.1	22.5 ± 0.1	28.3 ± 0.1	26.1 ± 3.1
Final Age (week)	27.6 ± 0.0	32.3 ± 0.2	35.4 ± 1.6	40.4 ± 0.2	32.3 ± 0.1	34.6 ± 0.8	40.4 ± 0.1	35.1 ± 4.0
Average diff.	5.6 ± 0.0	2.0 ± 0.0	10.8 ± 0.7	10.1 ± 0.0	4.1 ± 0.0	12.1 ± 0.8	12.0 ± 0.0	
Start Mass (kg)	2.6 ± 0.2	4.0 ± 0.7	2.9 ± 0.3	3.5 ± 0.5	3.2 ± 0.5	3.1 ± 0.2	3.3 ± 0.4	3.2 ± 0.5
Final Mass (kg)	2.8 ± 0.2	4.2 ± 0.8	3.2 ± 0.3	3.7 ± 0.4	3.2 ± 0.3	3.6 ± 0.3	3.7 ± 0.4	3.4 ± 0.5
Average diff.	0.2 ± 0.1	0.2 ± 0.1	0.3 ± 0.2	0.1 ± 0.1	0.0 ± 0.2	0.5 ± 0.2	0.4 ± 0.1	0.3 ± 0.2

10.3. Results – Tendinopathy model

10.3.1.   Samples

A total of 30 rabbits – 14 males and 16 females – were used for this portion of the study. The average age of the cohort at the beginning of experiments was 26 ± 3 weeks at a starting mass of 3.2 ± 0.5kg. The average final mass was 3.4 ± 0.5kg. Gender was evenly distributed between groups. Demographics are summarised in Table 10-2.

Differences between starting age and finishing age did not match the allocated groups in all cases due to requirements for the gait analysis, which focussed on the zero and eight-week time points. As a result, starting ages for the four and twelve-week groups were later than the zero and eight-week groups as they did not require any additional assessment. Starting ages were chosen so that the youngest rabbits were of skeletal maturity (26 weeks) at sacrifice. Final ages, therefore, more closely matched the desired spacing between time points.

Average mass was consistent between the groups, with the exception of the Control group at week four which was significantly larger than the zero and eight-week Control groups (Figure 10-2). This was due to low sample numbers (n=2) and above average masses for both rabbits, including the largest rabbit in the study (4.51kg starting mass). There was no significant difference between the starting and final mass for any group. This indicates a stable
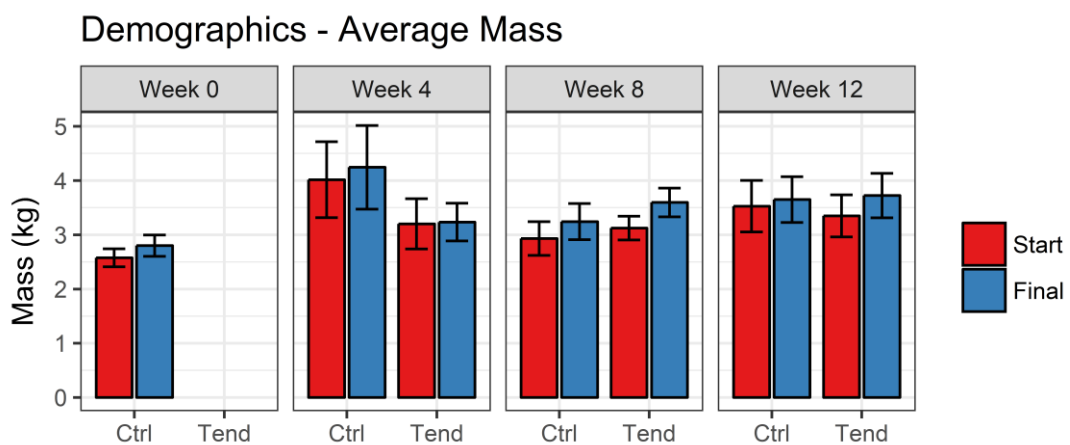
Figure 10-2: Mean (± SD) mass (kg) of rabbits used in testing. Initial masses (red) and final masses (blue) at each week are indicated.
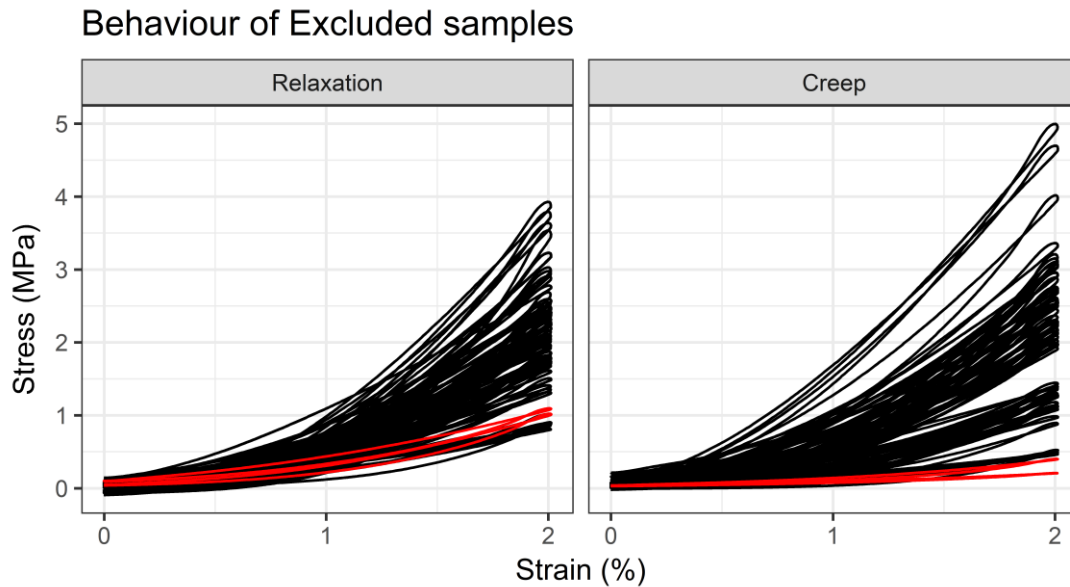
Figure 10-3: The isochronal stress-strain response at 1%.s⁻¹, showing the excluded samples (red). The excluded samples demonstrated noticeably low stiffness, supporting the observation of movement at the bony interface.

population with no influence on mass caused by exercise or induction of tendinopathy.

No slippage was observed at the myotendinous junction during testing. Two CL8 tendons failed during testing as the calcaneus was not secured adequately in the PMMA and came loose during creep analysis. These tendons were excluded from the data analysis as, upon closer inspection, it appeared that there was movement within the PMMA during preconditioning and relaxation. This was likely due to an error at time of explantation which left the calcaneus not fully intact. It was determined that movement within the PMMA likely occurred during relaxation testing and so the tendon was excluded completely to avoid issue with subsequent analysis. Revised sample

Table 10-3: Updated summary of the rabbit Achilles tendon used for mechanical evaluation. A total of 54 tendons were provided for mechanical evaluation, with 52 tested successfully.

		Weeks			
Group	Limb	0	4	8	12
Control	Left		2	3	3
	Right	3	2	7	3
Tendinopathy	Left		5	5	5
	Right		5	4	5

numbers for each group are presented in Table 10-3. Tendon appearance and morphology was still considered as evidence for tendinopathy progression. The behaviour of the excluded tendons can be seen in Figure 10-3.

10.3.2.   Histology

Given no histology results have been published for the ARC Linkage Project to date, histology cannot be assessed directly for this set of tendons. A similar study by Chen *et al.* (2011a) reported histology scores of 11.0 ± 3.5 and 11.7 ± 1.2 at 8 and 12 weeks post-induction, with no reports made for normal tendon.

10.3.3.   Tendon appearance

Stoll *et al.* (2011) proposed a macroscopic scoring system for tendon healing, where a score of 17 is considered a normal, healthy tendon. Several of these aspects were not appropriate for assessing degradation alone, as they pertained to defects and surgical intervention; however, of note are the following scores:

- Connection tendon to skin (1 point);
- Connection tendon to fascia and paratenon (1 point);
- Tendon rupture (1 point);
- Inflammation (1 point);
- Tendon surface (1 point);
- Neighbouring tendon (1 point);
- Swelling/redness of tendon (2 points);
- Shape of tendon (3 points); and,
- Colour of tendon (1 point).

Adjusting for the selection of scores, a score of 12 would be considered normal and healthy, where zero is completely degenerated and ruptured.

Representative samples of the tendons are presented in Figure 10-4, Figure 10-5, and Figure 10-6. Of the tendons tested, only six did not score 12, being four tendinopathy tendons (one TL4, two TL8, one TL12) and two CL8 tendons.
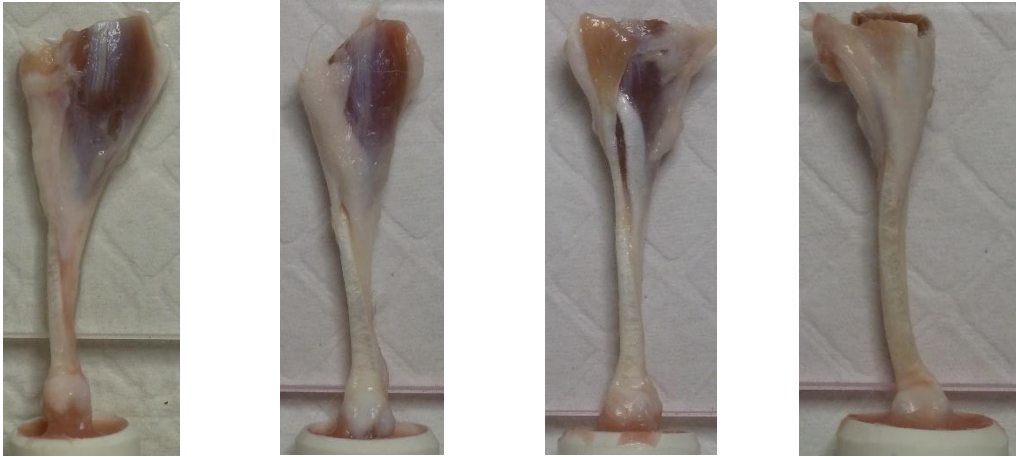
Figure 10-4: Examples of control rabbit Achilles tendon showing no signs of tendinopathy. From L to R: one tendon each from week 0, week 4, week 8, and week 12.

Figure 10-5: Examples of tendinopathic rabbit Achilles tendon showing signs of tendinopathy. From L to R: three tendons from week 8, and one tendon from the week 12.
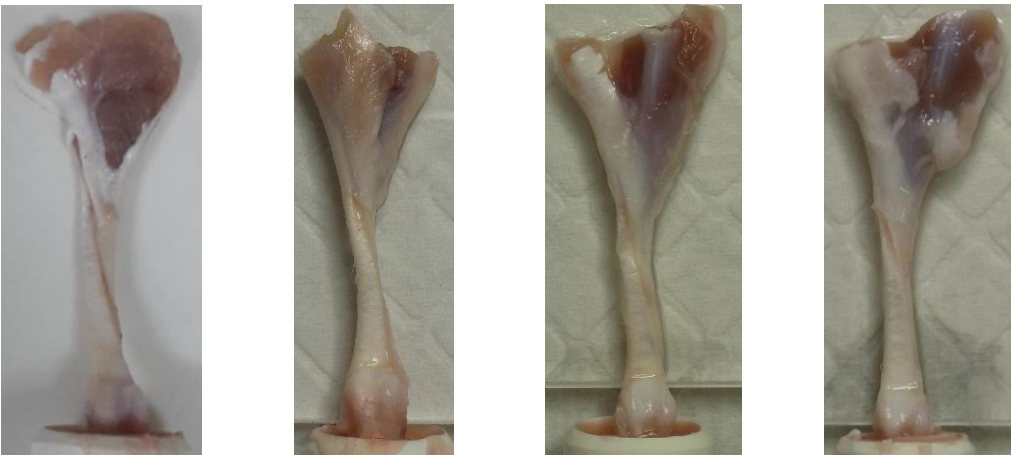
Figure 10-6: Examples of tendinopathic rabbit Achilles tendon showing no signs of tendinopathy. From L to R: one tendon from week 4, and three tendons from week 12.

Two tendons showed signs of tendinopathy, being a loss of the bright and shiny white appearance and disorganised fibre bundles representative of 'crabmeat' (Maffulli *et al.*, 2015; Schwartz *et al.*, 2015). These tendons (both TL8) scored only three, with one point each for not-conjoined, not-adnated, and no rupture. The remaining two tendinopathy tendons (TL4 and TL12) scored eight as there was also no swelling of the tendon (+2) and the tendon exhibited a normal shape (+3). The two control tendons scored 11 due to some thickening and redness of the tendon sheath likely caused by use of a force buckle during *in vivo* experimentation prior to this study, as noted above. No signs of adhesion were noted in any samples.

10.4. Results – Grouped

10.4.1.   Tendon morphology

Cross-sectional area

CSA was measured prior to each test to monitor the tendons for changes in the morphology and input to Instron BlueHill to calculate the stress during testing. For statistical calculations, only CSA prior to preconditioning was considered. The average CSA for control tendons was $8.85 \pm 1.55mm^2$ and for tendinopathy tendons was $9.30 \pm 2.20mm^2$.

CSA was significantly different between the Tendinopathy-Left group at week 8 and Control-Left, Control Right and Tendinopathy-Right. There was no significant difference within groups with time, or between groups at any other time point.

Of note was the variation in CSA at Week 8. The three tendons exhibiting signs of tendinopathy were the largest tendons at $14.0mm^2$, $14.4mm^2$ and $15.4mm^2$ (Figure 10-7) which is 50, 55, and 65% larger than average, respectively. One tendinopathy sample in week 12 also exhibited enlarged CSA ($12.2mm^2$), but was similar to other seemingly natural variations in CSA.

The larger CSA in the Tendinopathy-Left group at Week 8 is consistent with reports of continued degradation in the tendons up to eight weeks following

Table 10-4: Summary (mean ± SD) of the rabbit Achilles tendon gauge lengths (mm) for control and tendinopathy groups.

		Weeks			
Group	Limb	0	4	8	12
Control	Left		30.02 ± 1.14	25.02 ± 3.32	27.93 ± 2.24
	Right	24.87 ± 1.23	25.76 ± 5.13	24.57 ± 3.46	27.75 ± 2.01
Tendinopathy	Left		27.46 ± 1.93	25.83 ± 3.36	26.20 ± 2.70
	Right		27.97 ± 2.16	24.04 ± 3.28	26.17 ± 3.11
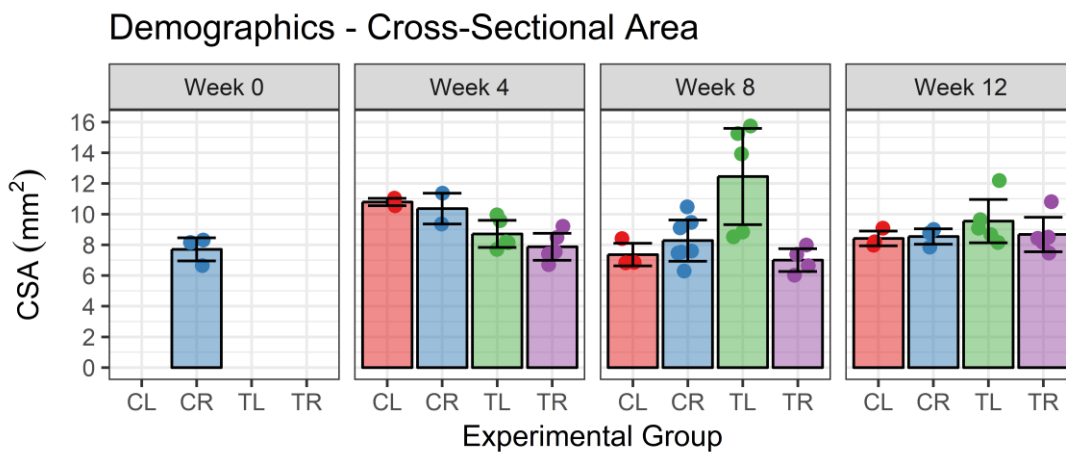
Figure 10-7: Summary (mean ± SD) of the rabbit Achilles tendon CSA measurements (mm^2) for control and tendinopathy groups. Individual measurements are shown as dots.

collagenase injection. However, CSA showed no enlargement or swelling at Week 4 or Week 12. This is consistent with the macroscopic observations and counter to expectations based on the histology reports of a similar collagenase-induced tendinopathy model (Chen *et al.*, 2011a).

Tendon length

Tendon length was unremarkable. The gauge lengths for each test are presented in Figure 10-8 and summarised in Table 10-4. All groups had gauge lengths of approximately 25mm and greater. It can be assumed that the variation is as much related to the clamping as it is to the true length of the tendon, since it is difficult to clamp the tendon at an exact location.

Significant differences were seen between the Control-Left samples at Week 4 and Control-Left at Week 8, and Tendinopathy-Right at Week 4 and Week 8. Significant differences were also seen between Control-Left at Week 4 and
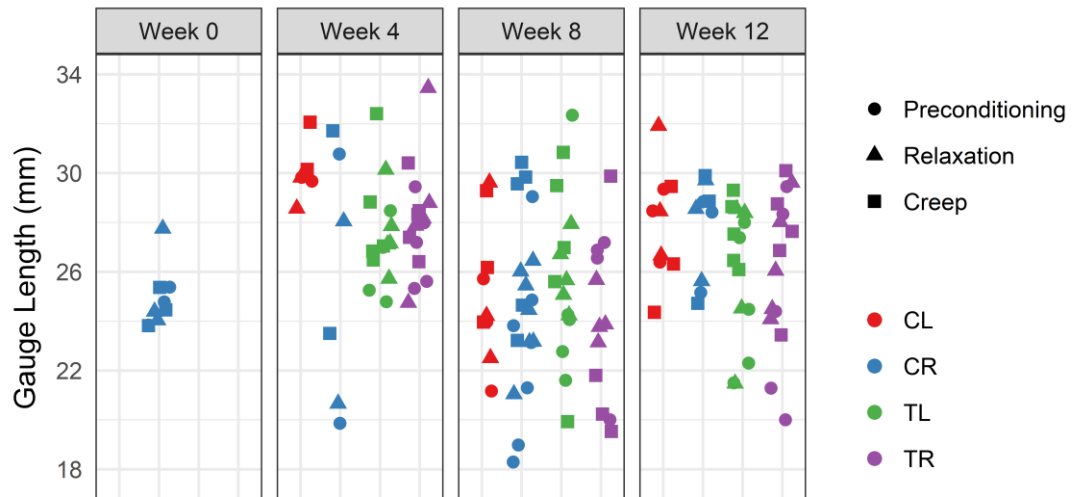
Figure 10-8: Scatter plot of the gauge lengths (mm) for the rabbit Achilles tendon during each stage (preconditioning, relaxation, and creep). Colour indicates group.

Tendinopathy-Right at Week 8 and Control-Left at Week 4 and Control-Right at Week 8.

Despite significant differences between some groups, Figure 10-8 suggests there is no difference of practical relevance in lengths between the groups.

10.4.2.　　　Isochronal response

Stress-strain response

The stress-strain response in the three load-unload cycles (Figure 10-9) showed that the tendons operated within the toe and lower portions of the linear region. This is in agreement with the literature that reports the toe region is around 0–2% with reports up to 5% (Arnoczky *et al.*, 2002a; Screen, 2008; Screen *et al.*, 2004a; Screen *et al.*, 2002b; Sharma and Maffulli, 2005b; Wang *et al.*, 2006).

Modulus was measured using the automatic slope algorithm from the stress-strain data between 0% and 2% strain to ensure consistency when including the last cycle from the dynamic segment of the creep stage (Figure 10-10).
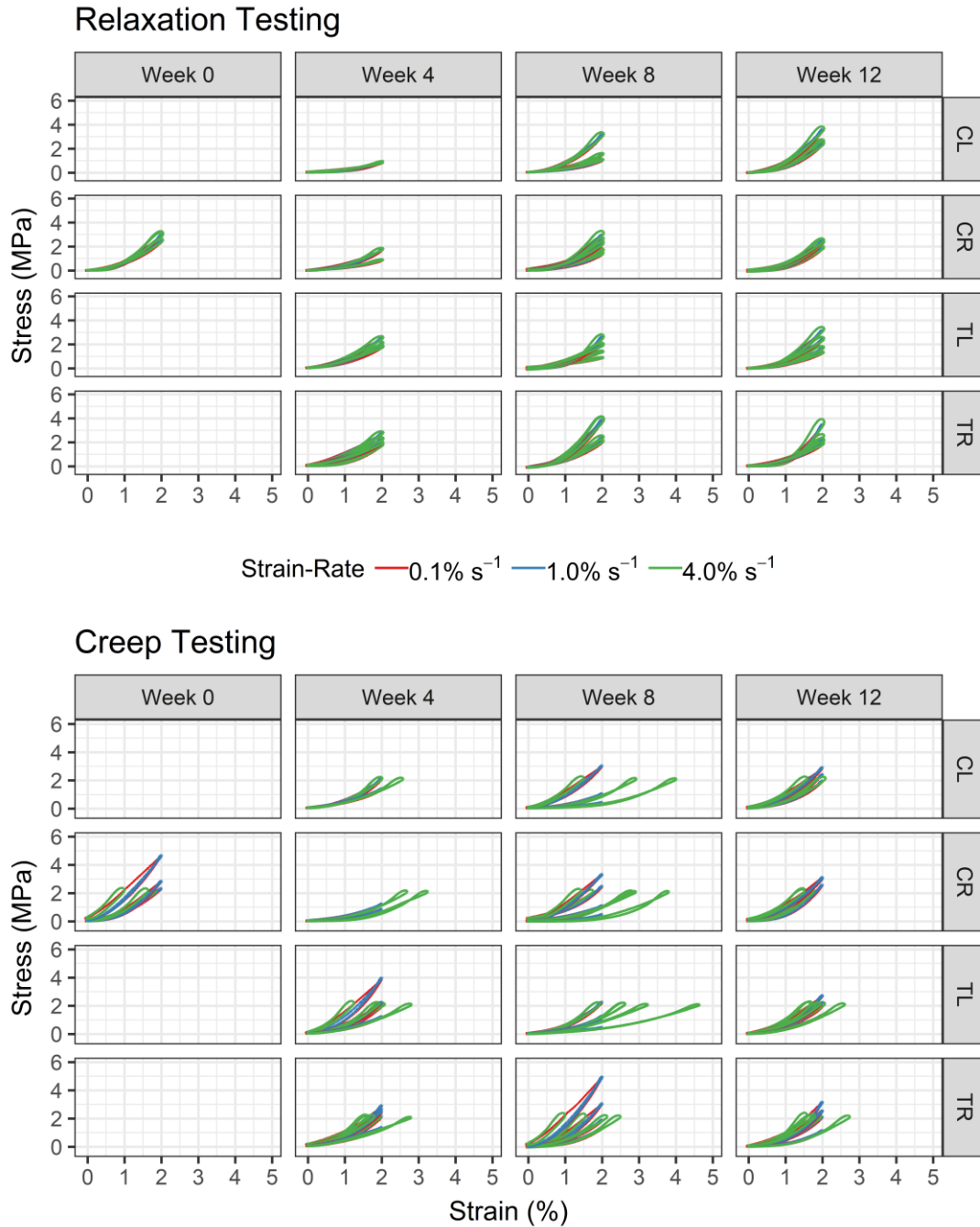
Figure 10-9: Stress-strain response of the rabbit Achilles tendon in relaxation (top) and creep (bottom) at different strain rates.

The stress-strain behaviour of the excluded samples was compared to those that were included (Figure 10-3). As expected, the excluded tendons demonstrated abnormally low modulus and abnormal excursion compared to other tendons. Three tendons exhibited similarly large displacements (greater than 3.5% strain) during this stage of the testing, as seen in Figure 10-3. One

sample was identified earlier as showing signs of tendinopathy. The remaining tendons were control tendons (one right and one left) with no signs of degeneration or damage. These samples displayed behaviour similar to the excluded samples, suggesting movement at the bony interface most likely within the PMMA as with the excluded samples.
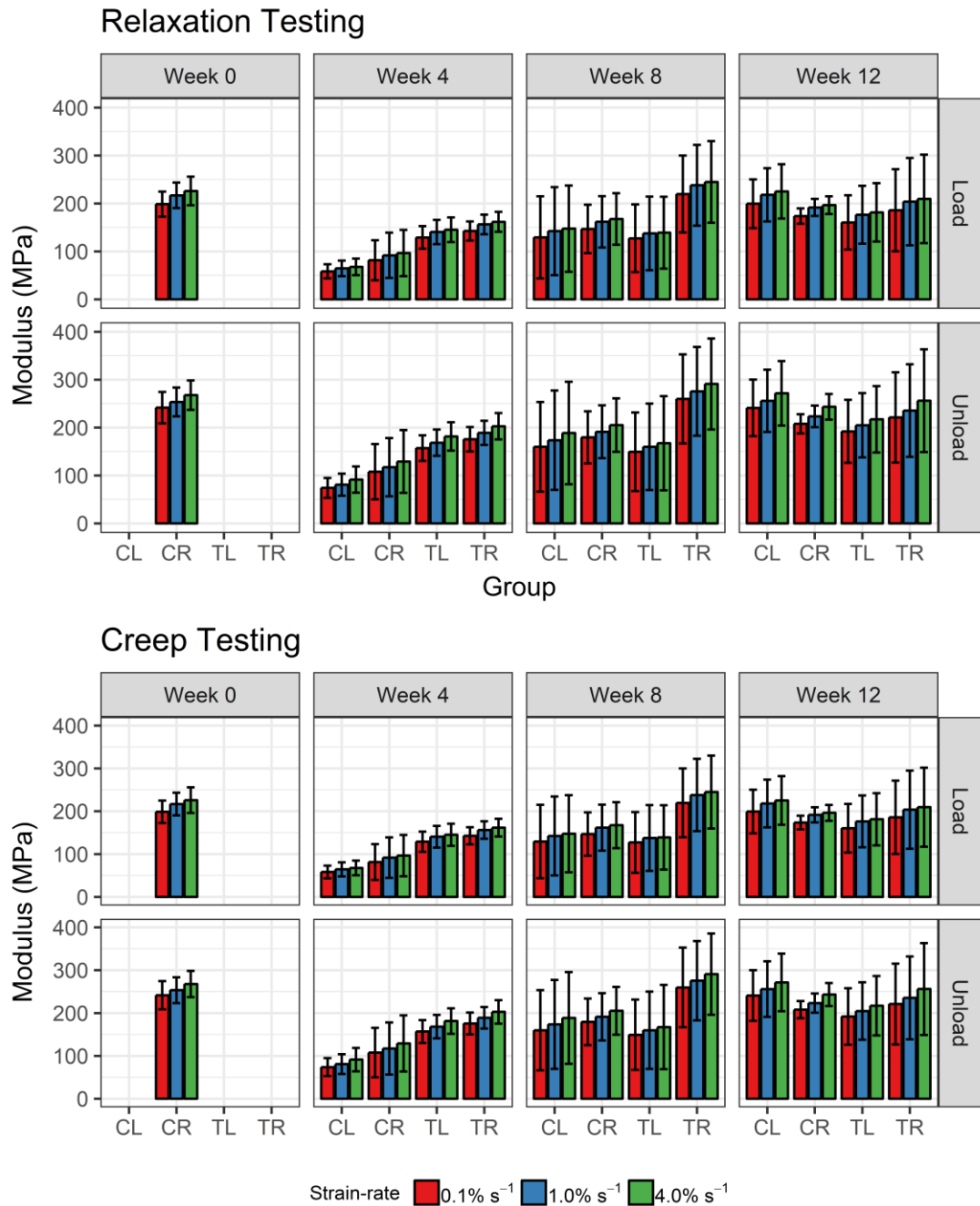
Figure 10-10: Summary (mean ± SD) of the elastic modulus (0-2% strain) for the rabbit Achilles tendon in relaxation (top) and creep (bottom) at different strain rates.
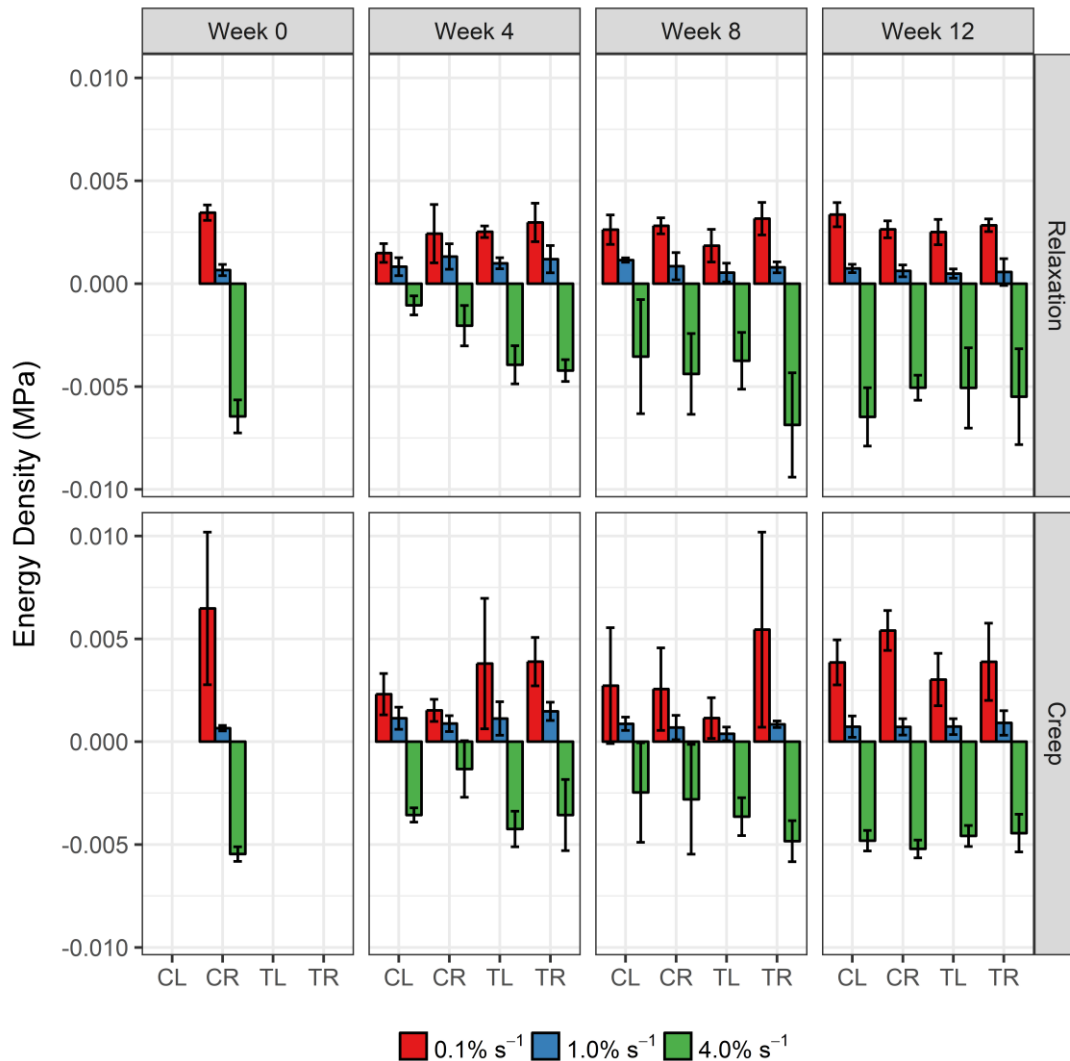
Figure 10-11: Summary (mean ± SD) of the energy density measurements (MPa) for the rabbit Achilles tendon at different strain rates.

Within the bounds of the experiment, that is up to 2% strain, the elastic modulus of each group showed no sensitivity to strain rate (p>0.05 in all samples). Significant differences (p<0.05) were seen between CL8 and TR8 samples during loading at 1% s^{-1}, and unloading at all three strain rates. There were no differences between loading and unloading, suggesting elastic nonlinear behaviour.

Interestingly, the curve of the fastest strain rate (4% s^{-1}) showed slightly higher stresses during unloading than loading. Since hysteresis is the difference between energy stored and energy returned, this would suggest more energy was returned. This net positive energy return (seen as a negative hysteresis)

was observed in all groups at the highest strain rate (Figure 10-11). It is likely that this was an artefact caused by inertia of the Instron 5566 cross-head and is discussed further in subsection 10.7. A net energy loss was measured at 0.1% s^{-1} and a near neutral energy difference was measure at 1% s^{-1}.

Strains and stresses were maintained at physiological levels in agreement with previous studies (West *et al.*, 2004). Behaviour did not extend outside the linear region and, in some cases, may not have left the toe region.

Force-displacement response

Forces were below 40N up to 2% strain, in agreement with findings by West *et al.* (2004). Figure 10-12 and Figure 10-13 show similar behaviour to the stress-strain response of the tendon. This is expected from the similarities in CSA between groups.

Stiffness was not significantly different between groups, strain rates or between load and unload curves. Values (56 ± 22 N/mm) were similar to those reported by Chen *et al.* (2011b), Trudel *et al.* (2007), and Awad *et al.* (1999), and lower than Wang *et al.* (2015), suggesting 2% is near the transition into the linear region.
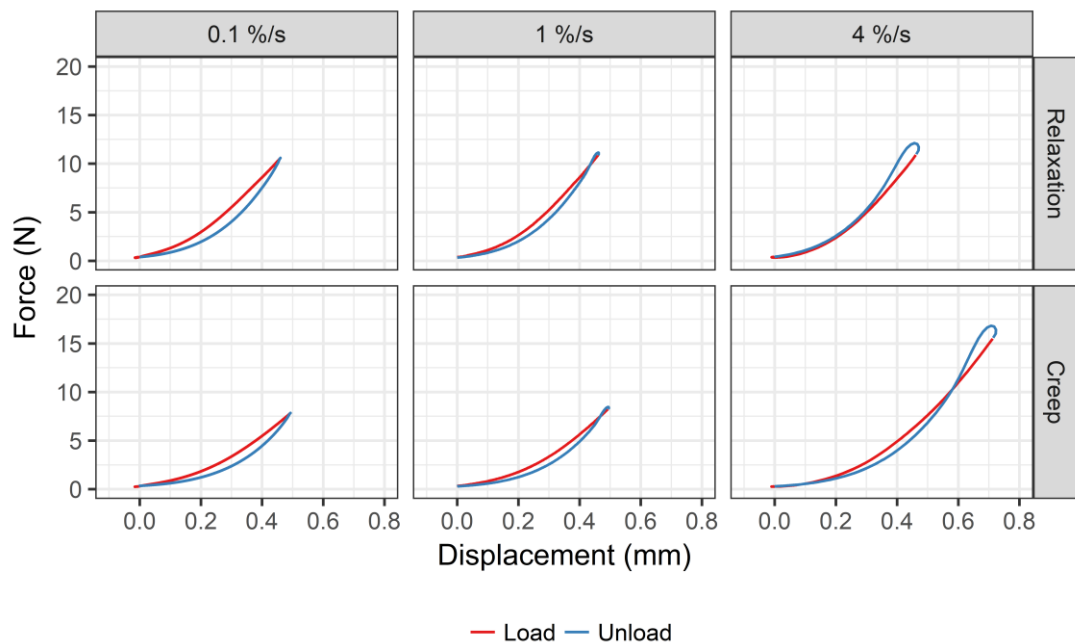
Figure 10-12: Representative force-displacement response of the rabbit Achilles tendon at different strain rates.

Hysteresis measured between 1.3 and -1.5mJ, or 23% and -52% energy loss. In all groups at each week, the highest strain rate was calculated as having a net energy gain. Load-unload curves showed an average difference of $1.3 \pm 0.7N$, $0.6 \pm 0.2N$, and $-1.3 \pm 0.8N$ between the load and unload curve at 0.1% s^{-1}, 1% s^{-1}, and 4% s^{-1}, respectively. The magnitude of this difference
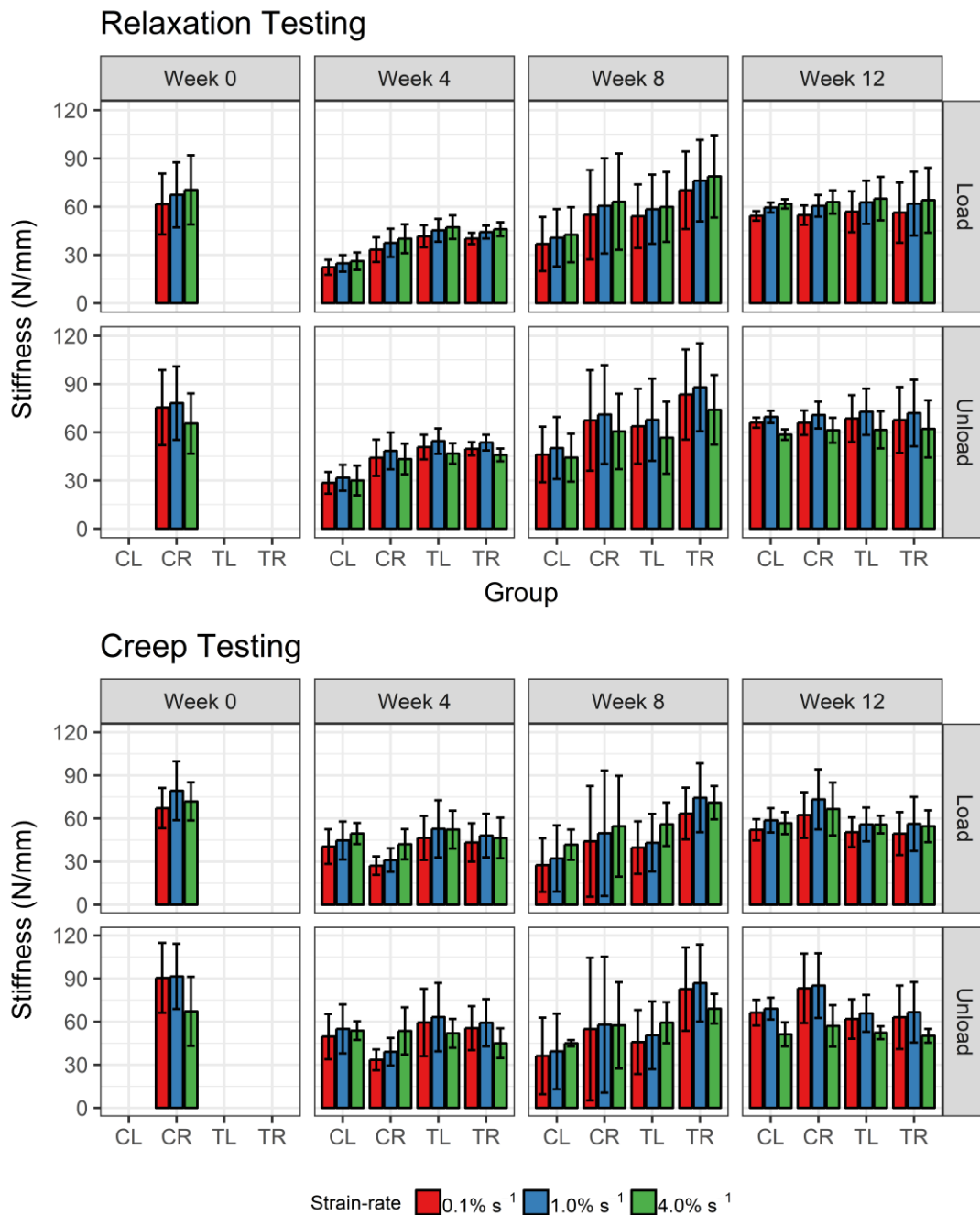
Figure 10-13: Summary (mean ± SD) of the stiffness (N/mm) for the rabbit Achilles tendon in relaxation (top) and creep (bottom) at different strain rates.

supports the notion that inertia of the cross-head may have created measurement error.

10.4.3.   Dynamic response

The change in stiffness, hysteresis, storage modulus, loss modulus and loss tangent were calculated from the dynamic segment at the start of each stage. Rate of relaxation and creep, and percentage change, were calculated from the peak values in each dynamic set for comparison with the static response.

Change in stiffness and modulus
Stiffness and modulus increased over the first 5–10 cycles until reaching a steady state (Figure 10-14 & Figure 10-15). There was no significant
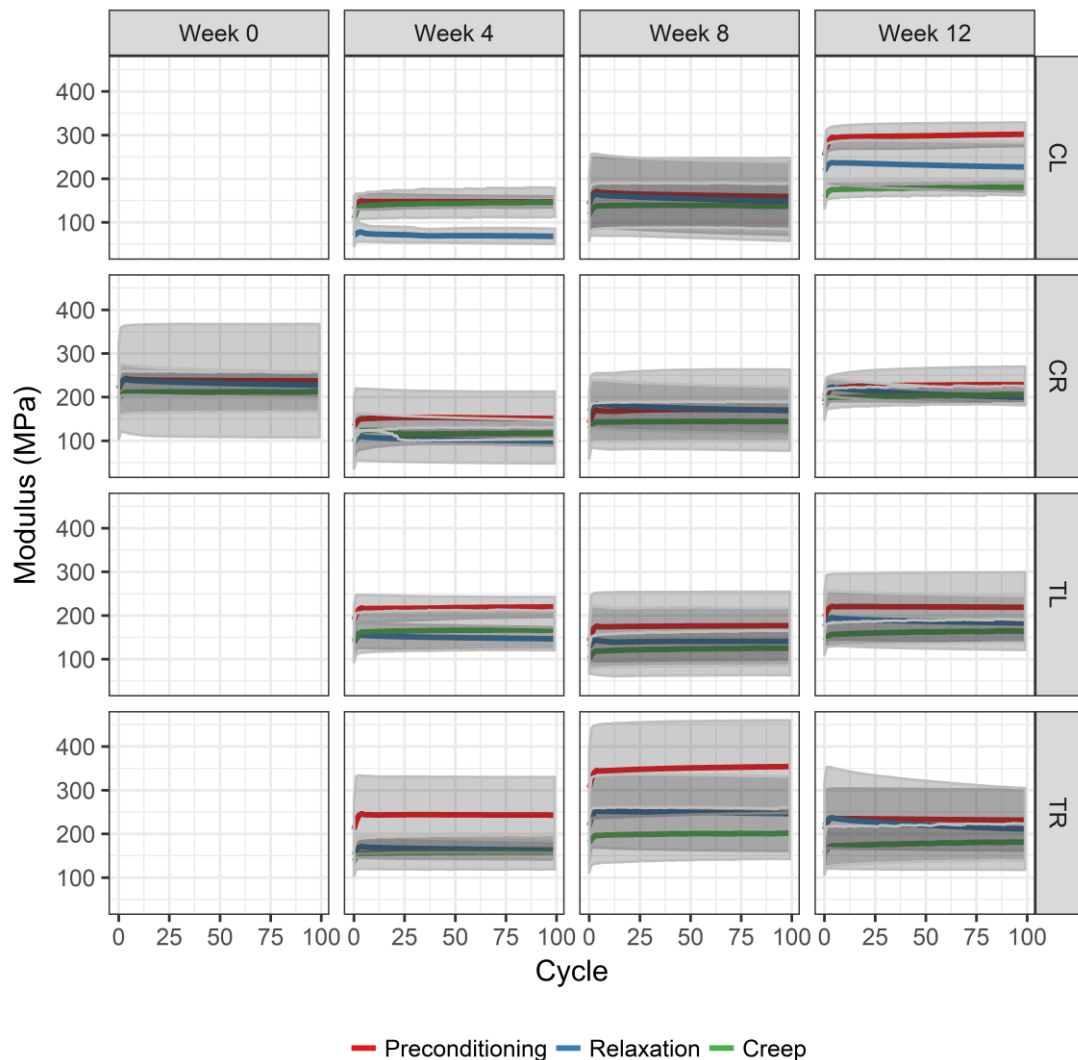
Figure 10-14: Elastic modulus (MPa) of the loading segment in the rabbit Achilles tendon increased for 5-10 cycles before reaching a plateau.

difference between cycles, type, or group suggesting that the toe region was unaffected by tendinopathy.
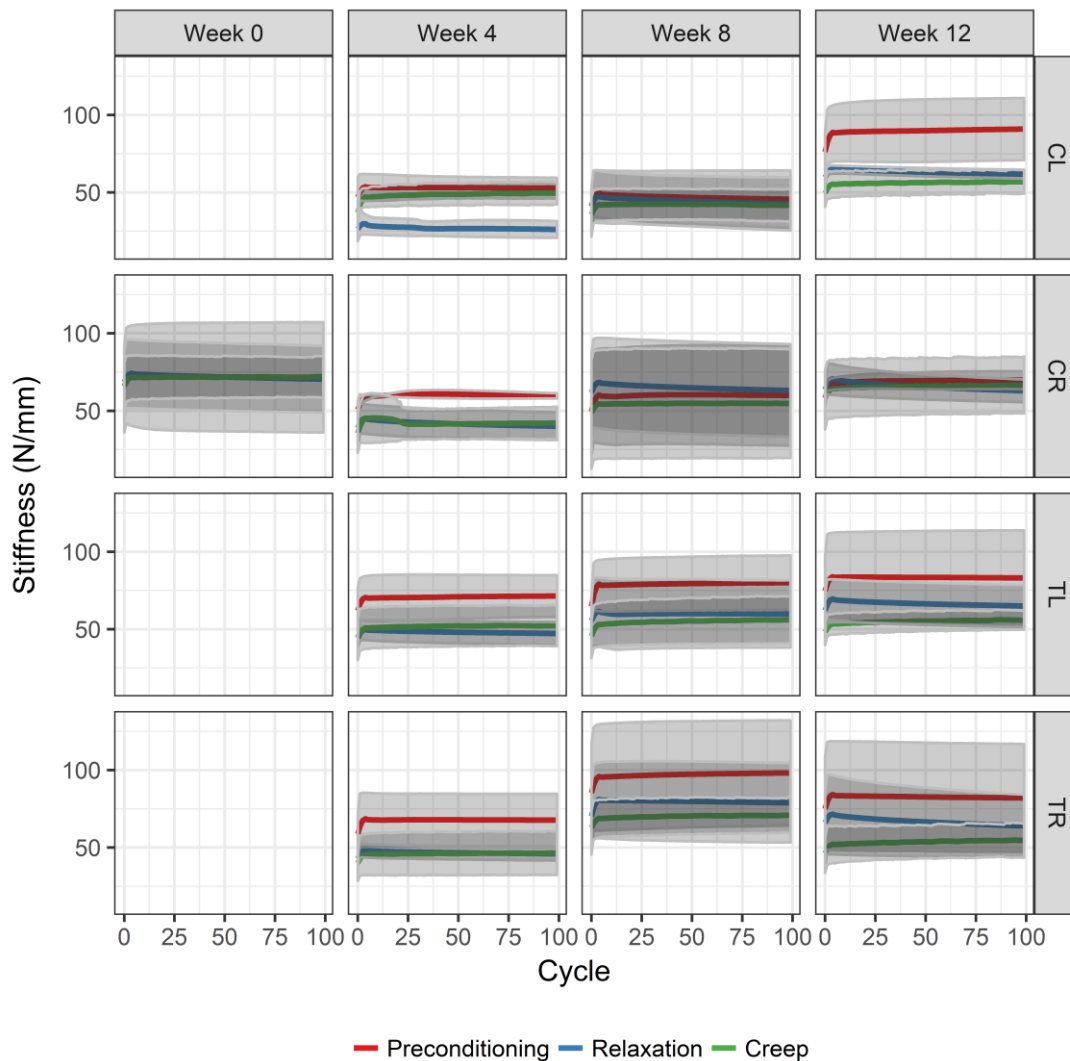
Figure 10-15: Stiffness (N/mm) of the loading segment in the rabbit Achilles tendon increased for 5-10 cycles before reaching a plateau.

Hysteresis

Hysteresis, calculated using a trapezium approximation of area under the curve, reached a steady-state after 5–10 cycles (Figure 10-16). As with the isochronal hysteresis measurements, high strain rates led to measurement errors and a positive net energy gain (Figure 10-17). In this case, preconditioning (8% s^{-1}) was more pronounced than the creep and relaxation cycling (4% s^{-1}).

Since positive net energy gain in this system is not possible, no statistical test was performed. This is discussed further in subsection 10.7.
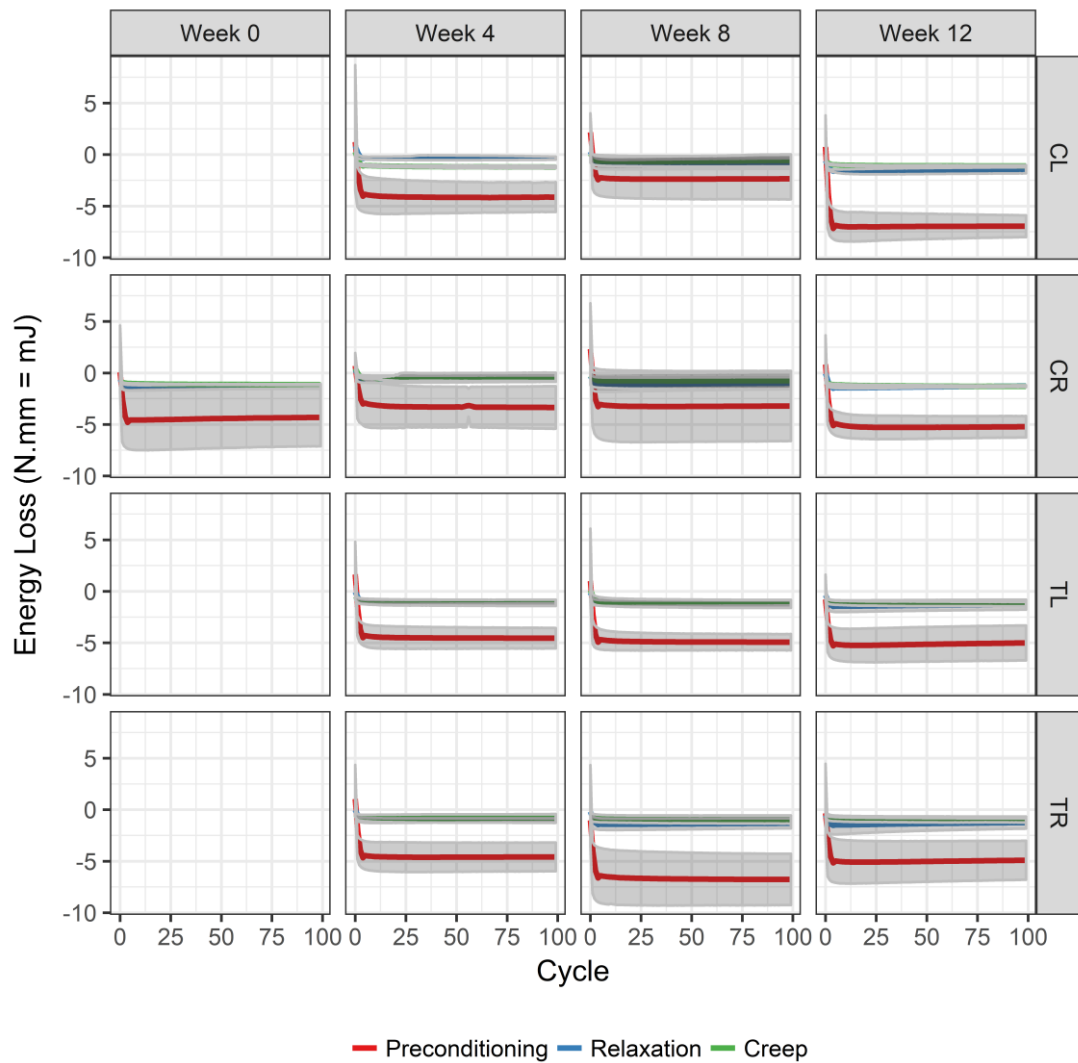
Figure 10-16: Hysteresis (mJ) of the loading segment in the rabbit Achilles tendon decreased for 5-10 cycles before reaching a plateau.
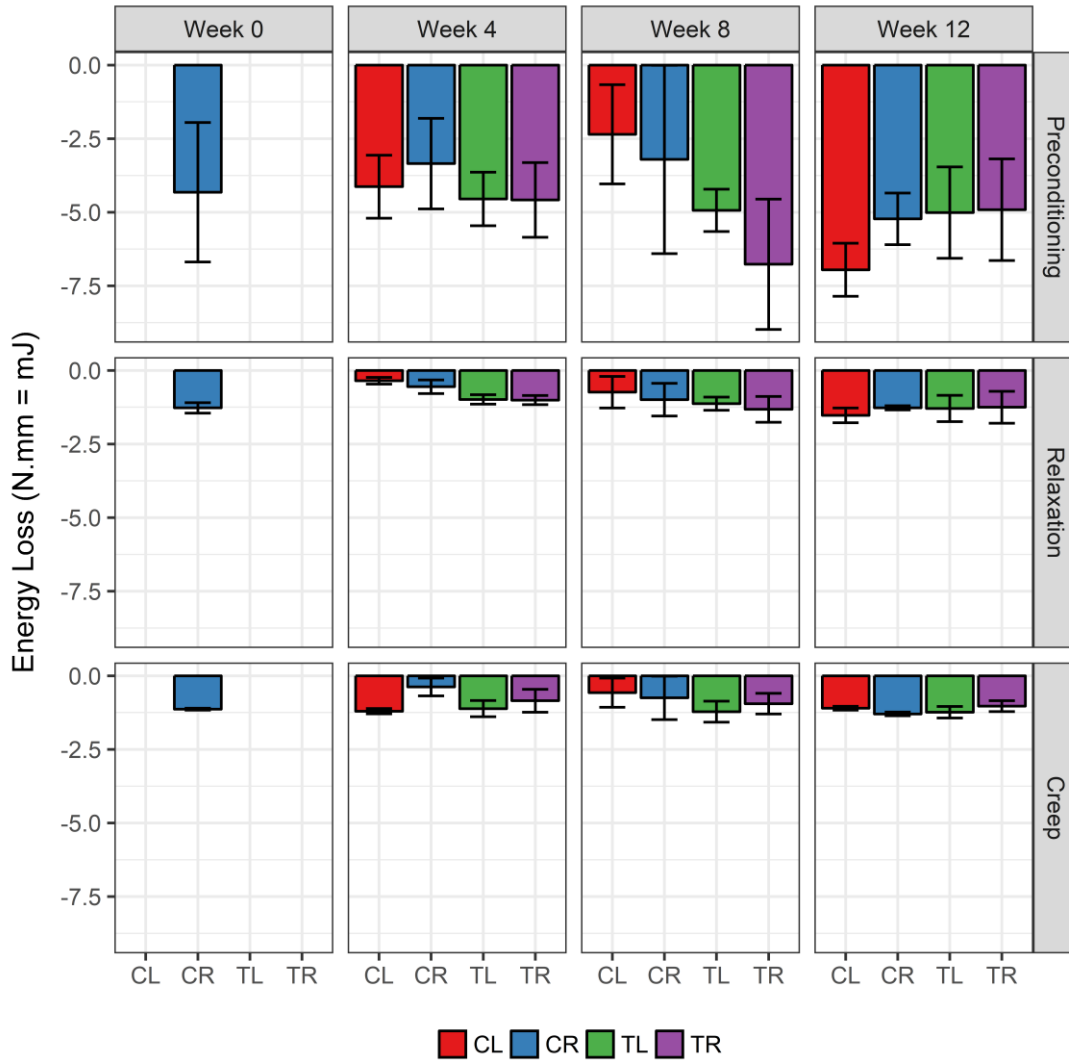
Figure 10-17: Summary (mean ± SD) of the hysteresis (mJ), averaged across the last five cycles, during dynamic testing of the rabbit Achilles tendon.

Storage and loss modulus, and tan(δ)

Strain versus time and stress versus time curves for each sample and cycle were fitted via maximum likelihood estimates (MLE) using the triangle waveform equation:

$$f(t) = \frac{A}{\pi} \sin^{-1}\left(\sin\left(\frac{2\pi t}{p} - \delta\right)\right) + \frac{A}{2}$$

Equation 10-1: Function to describe triangle waveform.

Storage Modulus

Loss Modulus

Ratio between the loss and storage modulus
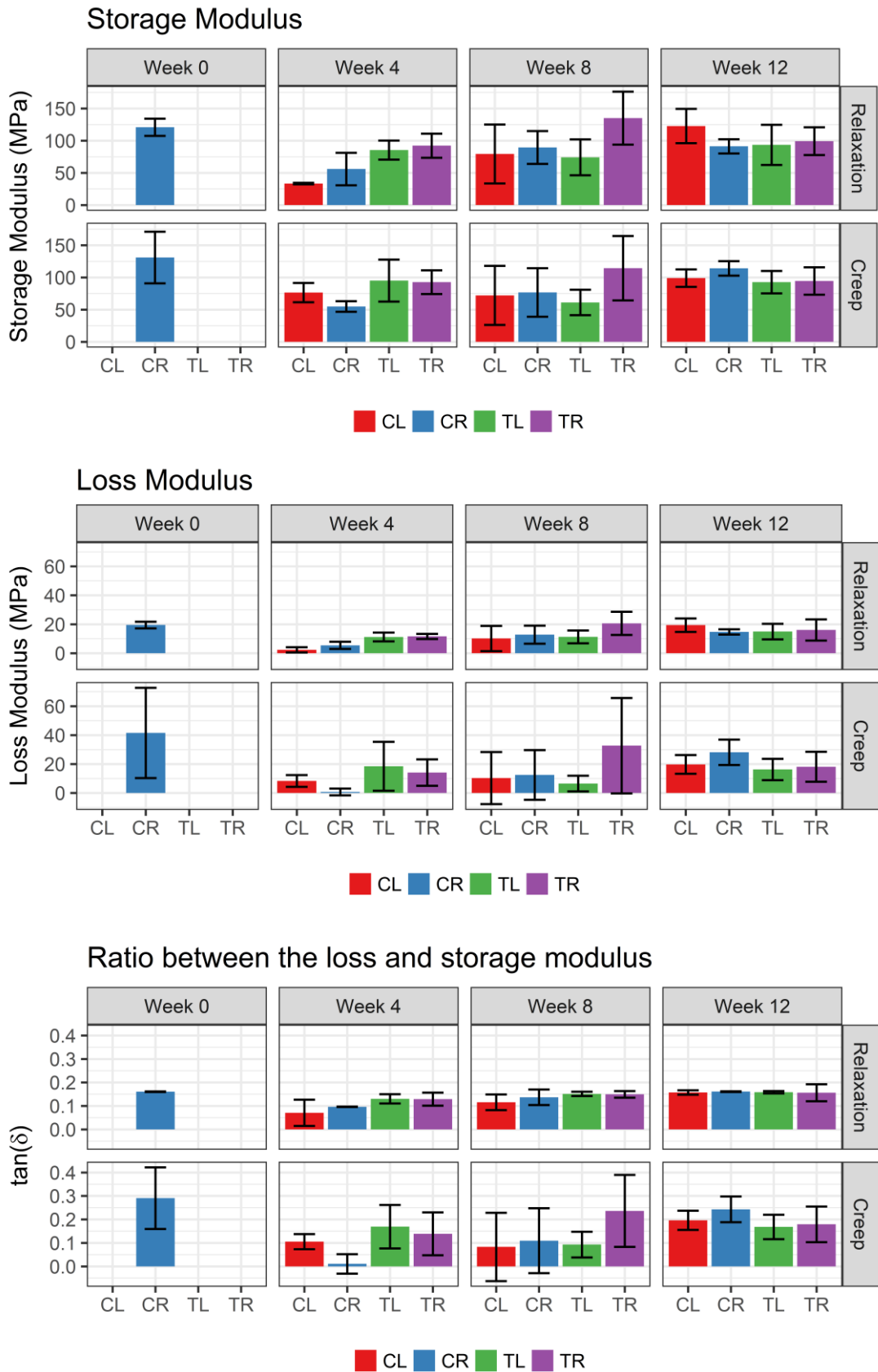
Figure 10-18: Summary (mean ± SD) of the (top) Storage modulus (MPa), (middle) Loss modulus (MPa), and (bottom) tangent delta for the rabbit Achilles tendon, average across the last five cycles of the dynamic segment of testing.

191

Amplitude and phase angle (δ) estimates were used to calculate the storage(E') and loss (E'') moduli and *tan(δ)* using the equations:

$$E' = \frac{\sigma_0}{\varepsilon_0}\cos\delta \text{ and } E'' = \frac{\sigma_0}{\varepsilon_0}\sin\delta$$

Equation 10-2: (L) Storage modulus (E'), and (R) Loss modulus (E'').

A representative curve fit is shown in Figure 10-19, and the average values in Figure 10-18. Control variables were fitted with an R^2 of 0.993±0.002, while response variables were fitted with an R^2 of 0.764±0.069. There was no significant difference between groups in storage, loss, and *tan(δ),* with the exception of *tan(δ)* between CR0 and CR4.

Dynamic Modulus
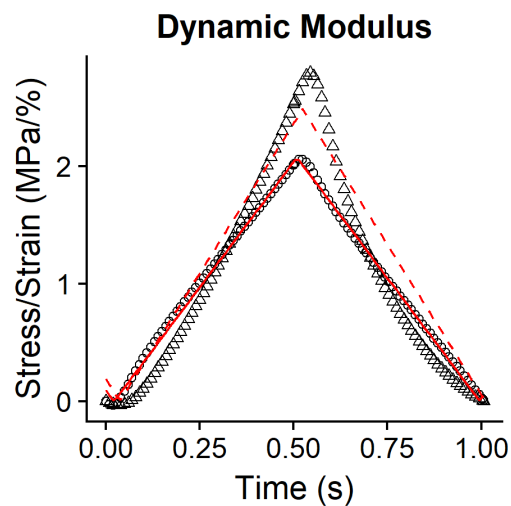
Figure 10-19: Representative cycle from the dynamic testing showing triangle waveform fit (red).

10.4.4.   Static response

Magnitude of change

There was no significant difference in the magnitude of creep within or between groups. Relaxation showed significant differences in the Tendinopathy Right group between step 1 and steps 3, and step 1 and step 4 within each week, and between step 1 and step 2 at week 12.

Percentage change

Tendons showed little sensitivity to percentage change between groups and time points at each step. Significant differences were only seen in the percentage relaxation between TL8 and CL8 at all steps, and between TL8 and CR8 at steps 1 and 2. TR8 was significantly different to CL8 at step 4.

Within groups, CR8, TR8, and TL12 showed a greater creep at 4MPa compared to 2MPa. TR12 showed greater creep at 4MPa compared to 1MPa and 2MPa. Percentage relaxation as a measure showed a greater sensitivity to differences, with significance between 1% strain and at least one other step

in all groups except CR0 and CR4. However, the magnitude of relaxation at 1% strain was small in absolute terms.

Rate of change

Curve fitting was performed as recommended in Chapter 8; that is, using data from time greater than 2.5 t_r to remove noise caused by overshoot from the ramp. Viscoelastic behaviour was measured in terms of rate of change and magnitude of change for each step. From this, the effect of stress and strain magnitude was able to verify or falsify quasilinear models as per Duenwald *et al.* (2009b).

No significant difference was seen in the rate of change within each group, with the exception of rate of relaxation in CR8, which was significantly different between 1% and 3%, and 1% and 4%. Similarly, no significant differences were seen between groups at each step, with the exception of TL8 and CR0 at 3MPa, and TL8 and TR12 at 3MPa. There were significant differences between creep and relaxation in all groups, with the rate of creep larger than the rate of relaxation.

Static versus dynamic response

Creep values for percentage and rate of change were significantly different between the static curves and the dynamic curves (approximated from the peak values from each cycle) in almost all cases. No significant difference was measured in the relaxation curves, or in the magnitude of change for creep. Within the dynamic response, significant differences were seen in the rate of change between TL8 and CR8 in creep, and in the percentage change between CL4 and CL8, and TL8 and CR8.

10.5. Results – Individual

Mean values for the parameters were derived from the population group comprising the control samples independent of time and side. In graphs, control samples are represented as dots and tendinopathy samples as triangles. Individual samples from both groups were compared to the mean values (solid lines), plus or minus one standard deviation (dashed lines), and plus or minus two standard deviations (dotted lines), for each parameter as calculated from the control population. Samples were coloured black if within

one standard deviation, blue if they fell between one and two standard deviations, and red if the values fell outside two standard deviations. Control samples were plotted for consideration of the natural variation.

10.5.1.   Tendon morphology

One contralateral and five tendinopathy samples were identified as having CSAs greater than the population mean, with a further three contralateral samples falling below the mean (Figure 10-20). These elevated CSAs were previously examined in the macroscopic observations and were treated as a measure of degeneration. Four control tendons fell above the range and four fell below the range, suggesting natural variability in the tendons. In this case, further investigation for degeneration in the top four TL tendons would be warranted.

Gauge length was not considered as this was unaffected by tendinopathy.
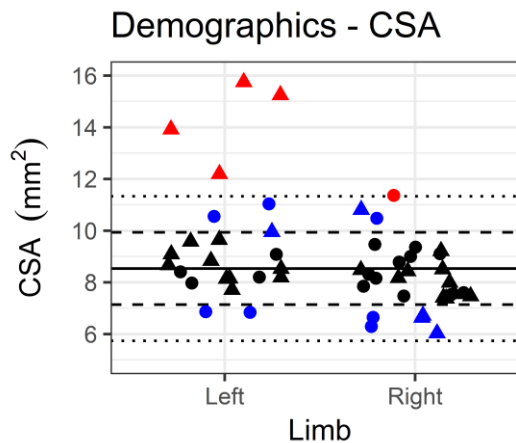
Figure 10-20: CSA (mm²) of individual rabbit Achilles tendons compared to the control population. The solid line represents the population mean, dashed lines represent one standard deviation (SD), and dotted lines represent two SD. Control samples are shown as dots and tendinopathy samples as triangles. Samples within one SD are black, within two SD are blue, and outside of the ranges are red.

10.5.2.   Isochronal response

There appeared to be no discernible difference in the isochronal properties between tendinopathic, contralateral, and control tendons. While several tendons were highlighted as having values outside two standard deviations, this was more prevalent in the contralateral and control tendons, with tendinopathic tendons being within this range in almost all measures of isochronal response. This suggests that either the contralateral tendons were suffering degeneration or, more likely, that tendinopathy does not influence the isochronal properties at the magnitudes used within this protocol.

10.5.3.   Dynamic response

No tendinopathy samples fell outside of the range for stiffness or modulus response during cycling.

Hysteresis was negative in all samples; that is, energy was gained during cycling, an artefact that is discussed further (subsection 10.7). No tendinopathy samples were outside the ranges. Similarly, there were no outliers from the tendinopathy group in any of the measures of dynamic modulus.

10.5.4.   Static response

Of interest is a number of tendinopathy samples exhibiting lower percentages and rates of creep and relaxation. This behaviour contradicts a previous study that showed a small increase (5%) in the percentage relaxation of tendinopathic supraspinatus tendons (Tucker *et al.*, 2016) but suggests that this small change may be real and warrants further investigation.

10.6. Discussion

10.6.1.   Strain rate sensitivity

Strain rate sensitivity was discussed in Chapter 7, with several observations regarding the behaviour of the tendon. The influence of strain rate may have been overstated (Masouros *et al.*, 2009) and dependence may only exist in the toe region (Masouros *et al.*, 2009; Pioletti *et al.*, 1999). Strain rate selection is often a product of machine capabilities and data acquisition rate (Duenwald *et al.*, 2009b).

Within the bounds of the experiment, that is up to 2% strain, this study has indicated that tendons are strain rate insensitive, in terms of both stiffness and elastic modulus. This is true of both control and tendinopathy groups. This is in agreement with the study of control tendons in Chapter 7 and in disagreement with suggestions in the literature reviewed above. However, it should be acknowledged that the range of strain rates was relatively small. It is suggested that the parameters be chosen to include a wider range of strain rates, such as 0.1% s[1], 1% s[1], 10% s[1], 100% s[1] and, if permissible, 1000% s[1] to improve the robustness of the conclusions. If testing through this range of

strain rates cannot elucidate a difference in response, then it is unlikely that a response exists.

Hysteresis measured between 1.3 and -1.5mJ, or 23% and -52% energy loss. Energy density measured between 6.48Pa and -6.8Pa. In all groups, the highest strain rate was calculated as having a net energy gain (see subsection 10.7 for discussion). These values are lower than many reported in literature (Andarawis-Puri *et al.*, 2012; Freedman *et al.*, 2015; Fryhofer *et al.*, 2016; Pardes *et al.*, 2017; Pardes *et al.*, 2016)., but similar to reports of percentage hysteresis (Maganaris and Paul, 2000; Yahia and Drouin, 1990). It has been shown that soft tissues exhibit a decrease in hysteresis following preconditioning (Schatzmann *et al.*, 1998; Yahia and Drouin, 1990). Therefore, it is likely that the low energy and energy-density losses are due to the elasticity of the tendon within the strain region tested, and the effect of preconditioning and cycling prior to performing the load-unload cycles. Despite being well described in literature, few papers report values for the hysteresis.

10.6.2.   Dynamic response

Dynamic modulus has been used to characterise tendons, including human (Schwerdt *et al.*, 1980), rat (Fessel and Snedeker, 2009), and rabbit (Ikoma *et al.*, 2013; Imai *et al.*, 2015; Nagasawa *et al.*, 2008). Figure 10-18 shows values for storage and loss moduli ranging from 33–135MPa and 0.75–42MPa, respectively, and a *tan(δ)* of 0.01–0.29 for the test groups. In comparison, Schwerdt *et al.* (1980), investigating human flexor digitorum, reported that the dynamic, or complex, modulus was strongly influenced by the strain, but that the strain did not influence phase angle. Complex modulus values at 1 Hz were 508MPa at 0.5% strain, 1361MPa at 2% strain, to 3731MPa at 5% strain. Nagasawa *et al.* (2008), reported *tan(δ)* of approximately 0.135 in rabbit Achilles tendon at 1Hz. This increased to 0.173 in regenerating tendon at three weeks after injury, returning to 0.135 by week six. It was concluded that the dynamic mechanical properties recovered faster than the static properties, but with no correlation to histological findings. It was proposed that cross-linking of the collagen may be involved in the dynamic response. Imai *et al.* (2015) reported a *tan(δ)* of approximately 0.1, noting no difference between treated and untreated samples in a collagenase model. Fessel and Snedeker (2009)

provided evidence against the involvement of proteoglycans (PG) in mechanical properties, including dynamic properties. Storage and loss modulus for control samples at 2% excursion were approximately 1400MPa and 60MPa, with an estimated *tan(δ)* of 0.04. Ikoma *et al.* (2013) reported storage moduli of 76GPa for control samples and 56GPa for stress shielded samples, and 10GPa and 7GPa for loss moduli, for an estimated *tan(δ)* of 0.131 and 0.125, respectively. Schechtman and Bader (2002) reported storage and loss moduli of 885–1405Ma and 36–49MPa, respectively, at a stress of 5MPa.

Despite finding improvements in the histological markers and CSA associated with treatment, Imai *et al.* (2015) did not find a significant difference in storage modulus or *tan(δ)* at 1Hz. Loss modulus exhibited a slight increase in untreated samples. Together, these null results may indicate that tendinopathy has limited effect on the dynamic modulus of tendons, but requires further analysis.

10.6.3.   Static response

Tendons did not exhibit significant nonlinear viscoelastic behaviour as hypothesised, with only subtle and not significant differences in the rate of tendon at each step in both creep and relaxation. Percentage relaxation and creep more clearly demonstrate the nonlinear viscoelastic behaviour described in literature (Abramowitch *et al.*, 2010; Davis and De Vita, 2012; Duenwald *et al.*, 2008; Duenwald *et al.*, 2010; Kahn *et al.*, 2010; LaCroix *et al.*, 2013a; Pradas and Calleja, 1990). The results, however, demonstrate a decrease in the creep and relaxation with increasing magnitude, a behaviour more commonly associated with ligament (Duenwald *et al.*, 2010). This finding may highlight functional differences in the tendons used in the studies, as previous studies reporting this behaviour used digital flexor tendons (Duenwald *et al.*, 2008; Duenwald *et al.*, 2009a; Sverdlik and Lanir, 2002).

Static creep and relaxation values were significantly different to the dynamic values obtained from the cyclic portion of each phase of testing. Visually, behaviour between groups was similar between the static and dynamic groups. This should be considered when designing experiments, as the difference in static and dynamic behaviours may offer insight into the influence of different

constituents and structures on tendon behaviour. However, care should be exercised for longer or high amplitude testing protocols, as cyclic testing has been shown to reduce the modulus, strength, and time to rupture (Thornton and Bailey, 2012; Thornton *et al.*, 2007).

Age and PG-deficient mice tendons demonstrated relaxation of an estimated 25–32% over 600s, with younger tendons showing greater relaxation in control and decorin-null tendons (Connizzo *et al.*, 2013). Similar findings were seen as mice developed, with relaxation percentage decreasing from 50% to 40% as the mice aged from four days to four weeks (Ansorge *et al.*, 2011). PG deficiency did not appear to influence the relaxation behaviour (Connizzo *et al.*, 2013). Relaxation rate (0.056–0.095) and percentage relaxation (30–49%) after 100s decreased with age in rat tail tendon (LaCroix *et al.*, 2013a). Despite presenting a multi-step stress relaxation protocol, LaCroix *et al.* (2013a) did not discuss in detail the effect of the strain magnitude on the relaxation behaviour of the test groups. Shepherd *et al.* (2014) reported stress relaxation of 30–48% after 300 cycles in various tendon types, while Screen *et al.* (2013) reported relaxation of 40–65% for incremental stress relaxation. Legerlotz *et al.* (2013b) noted that cyclic stress relaxation resulted in a greater percentage relaxation than statically loaded tendon fascicles, and in the order of 30–40% (estimated) after 100s, with greater relaxation in glycosaminoglycan-deficient samples possibly due to a reduced water content. Screen (2008) reported between 25% and 107% relaxation in fascicles at increments of 2–8% strain for 200s. Human patella tendon showed a relatively constant percentage relaxation as a function of strain magnitude of approximately 40% relaxation after 100s (Pioletti and Rakotomanana, 2000b). Rabbit patellar tendon fascicles showed relaxation of only 20–25% in controls, and 35–40% in stress shielded tendons (Yamamoto *et al.*, 1999). Rat Achilles tendon relaxed 40% after 300s at 2.5% strain (Ng *et al.*, 2011). Tucker *et al.* (2016) found a significant difference in percentage relaxation between healthy and overuse tendons in a supraspinatus rat model, showing relaxations of approximately 35% and 30%, respectively. Perry *et al.* (2009) reported relaxations of 25–38% in rat shoulder tendons, including some significant decreases in relaxation following rotator cuff injury, while exercise immediately

after immobilisation saw a decrease in percentage relaxation compared to cage activity (Peltz *et al.*, 2010). The absence of interleukin-6 (IL-6) resulted in less relaxation (30%) compared to control (~38%) in a mouse patellar tendon model (Lin *et al.*, 2005). Detached rat supraspinatus tendons exhibited lower percentage relaxation (25%) compared to control tendons (35%) following injury (Dourte *et al.*, 2010).

Rate of relaxation and rate of creep in rat medial collateral ligaments (MCL) has been shown to vary from 0.005–0.17 and 0.005–0.06, respectively, in a nonlinear manner under various strain and stress levels (Provenzano *et al.*, 2001). Similar behaviour was noted in rabbit MCLs, with more variance and higher rates of relaxation at low strain magnitudes (0.1–0.4 at 1%) compared to higher magnitudes (0.05–0.1 at 3–5%) and in creep (0.05–0.25 at 1MPa and 0.01–0.05 at 45MPa) (Hingorani *et al.*, 2004). Hingorani *et al.* (2004) highlighted that the creep behaviour is likely related to the fibre recruitment, while the relaxation rate is related to the hydration and non-collagenous content. Duenwald *et al.* (2009a; 2010) found that the rate of relaxation in porcine digital flexor tendon ranged from 0.01–0.15, and increased with increasing strain, unlike ligament which decreased with increasing strain.

In this study, percentage relaxation and percentage creep were 8–41% and 7–17%, respectively, with rate of relaxation and creep ranging from 0.31–0.52 and 0.58–0.83. The values for percentage relaxation are similar to those presented in literature. On the other hand, the rates of relaxation and creep in this chapter are higher than in the few studies presenting this information, including the results of Chapter 8 which reported rate values for relaxation and creep of approximately 0.05 and -0.12, respectively. The author found no published data on the percentage or rate of change in NZW rabbit Achilles tendon for comparison. The difference is likely the result of performing creep and relaxation tests as part of a wider protocol, and not as isolated experiments.

It has been shown in literature that the structural mechanisms of relaxation and creep differ (Miller *et al.*, 2012c) and, therefore, it is of value to compare the behaviour to elucidate the structural components that may be involved in any

degenerative changes in tendon. In this methodology, the benefit of comparing between creep and relaxation at multiple steps and between dynamic and static responses, coupled with the dynamic and isochronal data, outweighs the potential influence of multiple test segments on the rate of change values. This information should be reported to permit comparisons between studies.

10.6.4. Ability to identify tendinopathy

Control data (that is, Control-Left and Control-Right) were pooled to provide a better estimate of population behaviour for each component of testing, independent of time. Individual tendons in the induced (left) and contralateral (right) tendinopathy groups were compared to the pooled control results to evaluate whether any differences were seen, thus providing an indication as to whether tendinopathy exhibits any abnormal behaviours that are not observed in controls. However, as with the grouped data, no practical difference was observed between tendinopathy and control samples in any of the test segments.

10.6.5. Tendinopathy model

With no histology results for the tendons used in this study, it is difficult to adequately assess the collagenase model in terms of inducing tendinopathy. However, macroscopic assessment suggests limited success with induction and no apparent degeneration with time. Using a modified version of the scoring system proposed by Stoll *et al.* (2011), only six out of the 52 tendons assessed showed signs of ill-health (that is, did not receive a perfect score) and, of these, four were tendinopathy tendons (out of 14 inductions). Two of these showed definite signs of tendinopathy (both TL8), with the other two (TL4 and TL12) showing mild signs of ill-health. This correlated with a markedly larger CSA in the case of the TL8 and a moderate increase in size in the case of the TL12 tendon. Two of these rabbits had paired tendons for comparison. The difference between the pairs was ~7.5mm^2 and ~2.4mm^2 for the marked and moderate responses. As mentioned previously, three TL8 tendons were noticeably larger than the average for all samples at 14–15mm^2 (compared to 9.2 ± 0.3mm^2) and could clearly be seen when overlaid on the plot of CSAs (Figure 10-7).

With no reference to the results of testing, it may be inferred that the collagenase-induced tendinopathy model was not reliable. While there are several possible reasons for this, inexperience in induction and a lack of image guidance are likely the key contributors. It is not uncommon for models to be shown to be unsuccessful (Dirks and Warden, 2011; Lake *et al.*, 2008; Lui *et al.*, 2011; Warden, 2007), with at least two studies unable to replicate tendinopathy in the Achilles tendon using validated models (Archambault *et al.*, 2001; Huang *et al.*, 2004).

Within tendinopathy models, examination of the literature also reveals inconsistencies in the findings. Collagenase-induced tendinopathy models, when continued to eight weeks, appear to demonstrate a progressive deterioration comparable to tendinopathy (Chen *et al.*, 2011a; Stone *et al.*, 1999). CSA has been shown to increase in these models (Dowling *et al.*, 2002a, 2002b; Lake *et al.*, 2008; Stone *et al.*, 1999). However, the literature is conflicted as to whether tendinopathy causes an increase or decrease in stiffness and modulus (Chen *et al.*, 2004; Hsu *et al.*, 2004b; Marcos *et al.*, 2014; Marcos *et al.*, 2012; Stone *et al.*, 1999). In addition, maximum failure load has been shown in some studies to decrease, while in others the failure load remained unchanged (Chen *et al.*, 2011a; Chen *et al.*, 2004; Dowling *et al.*, 2002a, 2002b; Hsu *et al.*, 2004a; Hsu *et al.*, 2004b; Lake *et al.*, 2008; Marcos *et al.*, 2014; Marcos *et al.*, 2012; Stone *et al.*, 1999). Structural changes in the tendon were correlated with the ultimate tensile load (Hsu *et al.*, 2004a; Hsu *et al.*, 2004b).

It has been found that the application of strain during collagenase diffusion protected the tendon from degeneration and that no strain, or delayed application of strain, resulted in significantly inferior properties (Bhole *et al.*, 2009; Flynn *et al.*, 2010; Nabeshima *et al.*, 1996). It is, therefore, possible that allowing animals to return to activity immediately following collagenase-induction may prevent the onset of tendinopathy. To achieve a consistent model between animal cohorts it may be necessary to immobilise the tendon for a period of time to permit diffusion of the collagenase into the tendon.

It has been suggested that care should be taken when using the contralateral side as a control, since it is usually compromised in patients with unilateral Achilles tendinopathy and through intervention (Andersson *et al.*, 2011; Docking *et al.*, 2015). This study did not find evidence for this, within the limits of the testing, as the contralateral tendinopathy tendon was not different to the control tendons. However, there may be microstructural changes that are evident on histological examination and this should be explored further.

10.7. Limitations

10.7.1. Tendinopathy model

As discussed in 10.6.5, the tendinopathy model did not appear to be reliable. Furthermore, there was no histopathological information to evaluate the efficacy of inducing tendinopathy using collagenase. This is a significant limitation in the study. Samples used in this study were induced as part of a related study, and therefore, there was limited scope to influence the selection or induction of the tendinopathy. However, the techniques, methodologies, and evaluations presented may still be useful in future complex mechanical testing of soft tissues. Further studies, using a reliable and validated model, are necessary to evaluate these findings.

10.7.2. Strain rate

The Instron 5566 used for this study is limited to a maximum cross-head speed of 500mm/min, thereby restricting the testing to a maximum of approximately 30% s^{-1}, highlighting some of the machine restrictions described in literature (Duenwald *et al.*, 2009b). The results showed that the tendons are strain rate insensitive, in both stiffness and elastic modulus. However, it should be acknowledged that the range of strain rates was relatively small. As such, it is suggested that future testing could be expanded to include strain rates of 0.1% s^{1}, 1% s^{1}, 10% s^{1}, 100% s^{1}, and if permissible, 1000% s^{1} to capture a greater range of data.

10.7.3. Crosshead

Interestingly, the curve of the fastest strain rate (4% s^{-1}) showed slightly higher stresses during unloading than loading. Since hysteresis is the difference between energy stored and energy returned, this would suggest more energy

was returned. This net positive energy return (seen as a negative hysteresis) was observed in all groups at the highest strain rate (Figure 10-11). A net energy loss was measured at 0.1% s^{-1} and a near neutral energy difference was measure at 1% s^{-1}. From these results, it may be inferred that the inertia caused by motion of the cross-head resulted in measurement errors in the load cell for all tests, and that this effect increased with the strain rate. For example, overshoot (seen in this study as rounding of the stress-strain curve at peak stress) is clearly evident at high strain rates, but is subtle at lower strain rates. This also highlights the issues with equipment limitations mentioned in discussions on ramp speed (Duenwald *et al.*, 2009b; Gimbel *et al.*, 2005), as the issues were more pronounced at the faster strain rate.

Load-unload curves showed an average difference of 1.3 ± 0.7N, 0.6 ± 0.2N, and -1.3 ± 0.8N between the load and unload curve at 0.1% s^{1}, 1% s^{1}, and 4% s^{1}, respectively (Figure 10-21).

The magnitude of this difference supports the inference that inertia of the cross-head may have created measurement errors during testing. A 100N load cell was selected for this study to ensure that the sensitivity of the load cell was greater than the potential error. However, unlike the dynamic load cells produced by the manufacturer, the load cell used was a 'static' load cell with no inertial compensation. Therefore, post-testing inertial compensation may be required: for example, a temporal offset between the displacement and load.
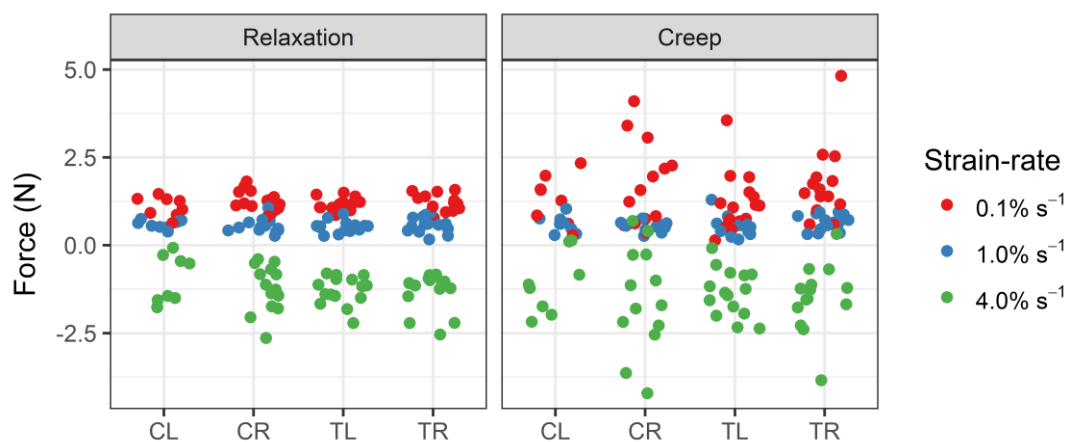
Figure 10-21: Difference in mean force (N) between load and unload curves at different strain rates during testing.

Additionally, the software was limited to a triangle waveform, which requires greater acceleration than a typical sine-waveform, leading to inertial measurement errors.

With appropriate management of the physical limitations of the machine these measurement errors may be reduced. When testing small samples, larger machines may need to be operated at a slower strain rate to avoid error from crosshead inertia that was observed in this study. For larger machines, a dynamic load cell with inertia compensation may also be useful. Preferably, a machine with a smaller cross-head designed for smaller samples should be used. The drive mechanism should also be considered – screw-driven machines may be susceptible to backlash at high strain rates.

10.7.4.   Waveform

Despite preconditioning resulting in stiffer and more repeatable and linear isochronal behaviour, the toe region is still present in the tendon behaviour (Figure 10-19) and, therefore, it is not sufficiently linearly elastic to be represented by a triangle waveform. This is seen in the difference in the coefficient of determination (R^2) between the control and response variables, where R^2 for the control variable was strong while the response variable was only moderate. The lower R^2 suggests that the results calculated from the response variable may not be truly representative of the sample. This was unexpected, as pilot testing had demonstrated a more linear response. The amplitude of the stress component was generally underestimated due to the presence of this toe region, leading to underestimated storage and loss modulus. However, *tan(δ)* is independent of amplitude and provided a reasonable measure of dynamic response.

To the author's knowledge, results of dynamic testing using a triangle waveform have not been reported for tendon. From a mathematical perspective and a machine perspective, using a sine waveform is preferable as it simplifies the calculation of the phase difference (δ) between stress and strain responses and provides a gentler acceleration profile, reducing inertia-related measurement errors. While it is still possible to use a triangle waveform

if necessary, it is recommended that a sine or haversine waveform be used where possible to more accurately account for this nonlinearity.

10.8. Conclusion

This is the first study to describe the isochronal, dynamic, and static viscoelastic responses of individual tendons, and at multiple steps. Tendons exhibited typical nonlinear responses, including a decrease in creep and relaxation response with increasing step magnitude. Tendon was also shown to be strain rate insensitive. The methodology described in Chapter 9 has been presented as a means of describing the mechanical behaviour of soft tissue, validated against the literature, and may offer a standard protocol for future work in comprehensively describing the mechanical behaviour of individual samples.

Within the bounds and limitations of this study, it may be concluded that collagenase-induced tendinopathy does not appear to influence the mechanical behaviour of the Achilles tendon. However, considering the results of previous studies and the analysis of the literature, it may be that tendinopathy influences the failure properties of the tendon, as evidenced by the high proportion of ruptures exhibiting tendinopathic changes. These ruptures are also generally seen in people returning to explosive sports where the tendon may experience near-failure loads. This finding may help to better inform clinical management of tendinopathy.

10.9. Appendix

Table 10-5: Summary (mean ± SD) of the rabbit Achilles tendon CSA measurements (mm^2) for control and tendinopathy groups.

		Weeks			
Group	**Limb**	**0**	**4**	**8**	**12**
Control	Left		10.98 ± 0.27	8.15 ± 0.83	8.35 ± 0.52
	Right	7.78 ± 1.00	10.33 ± 1.33	8.84 ± 2.07	8.80 ± 0.82
Tendinopathy	Left		9.25 ± 1.41	12.40 ± 3.08	9.67 ± 1.64
	Right		7.84 ± 0.65	7.70 ± 0.75	8.51 ± 1.09
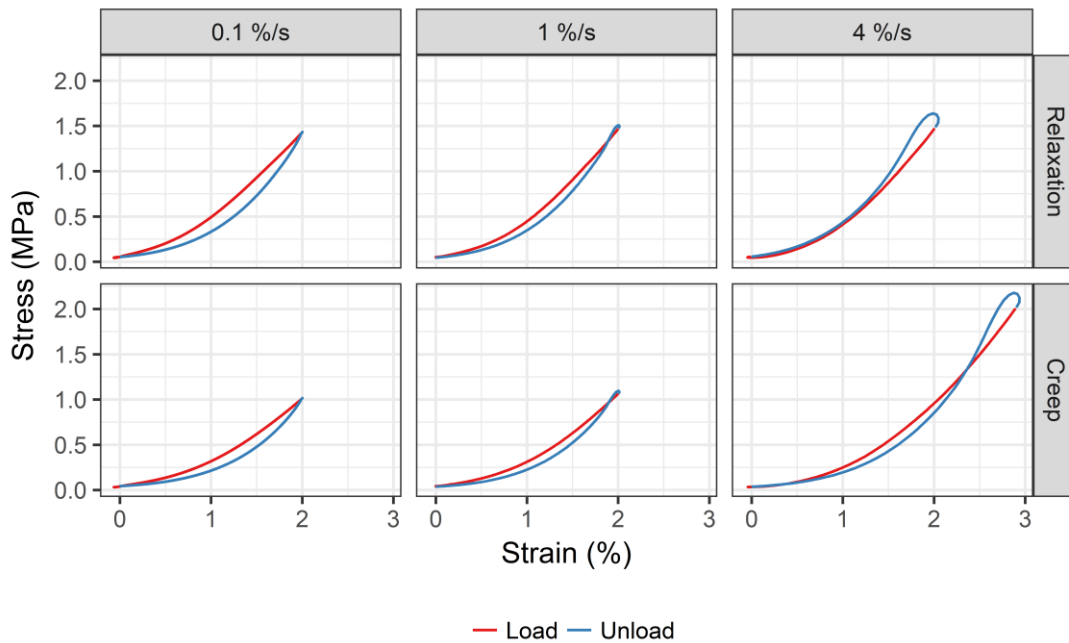
Figure 10-22: Representative stress-strain response of the rabbit Achilles tendon at different strain rates.
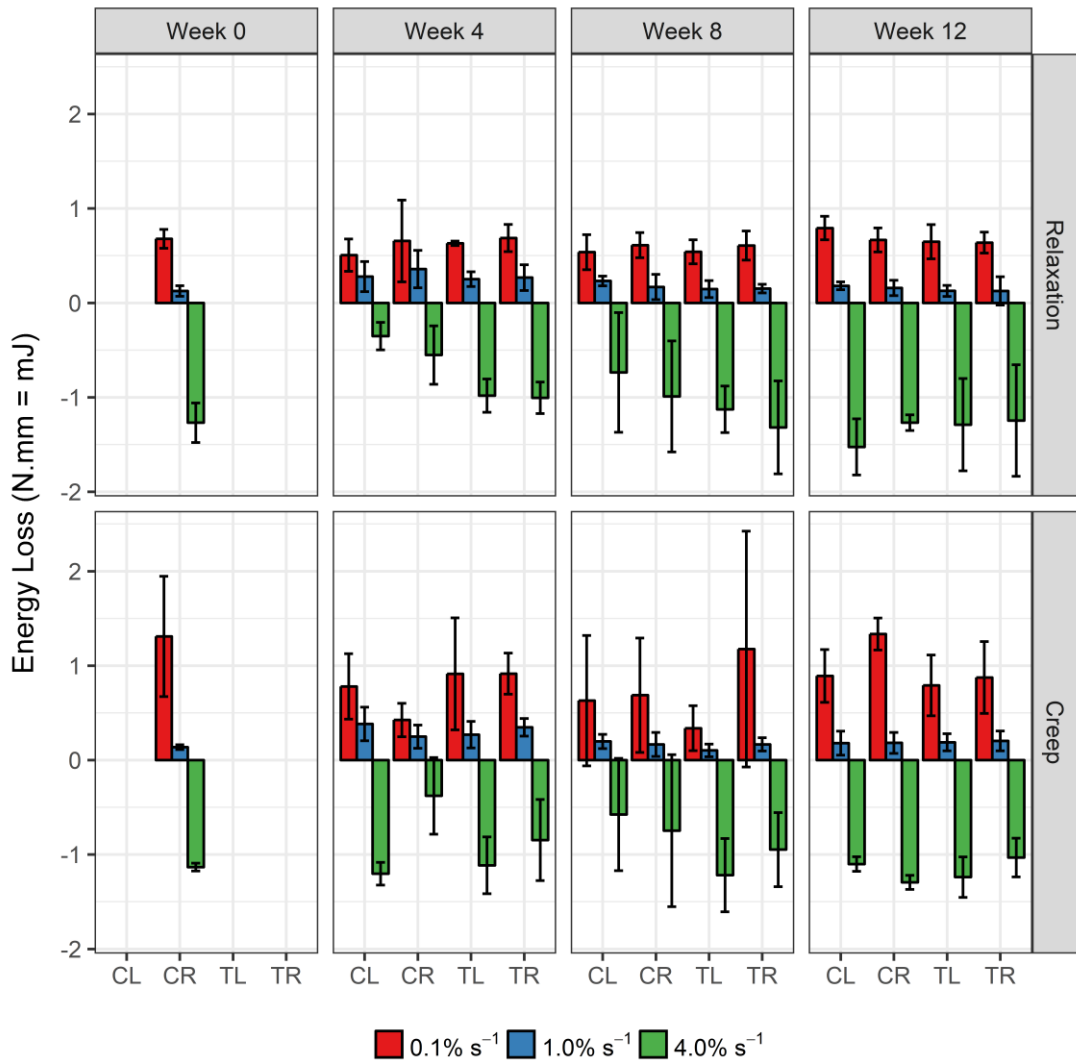
Figure 10-23: Summary (mean ± SD) of the hysteresis (mJ) for the rabbit Achilles tendon at different strain rates.
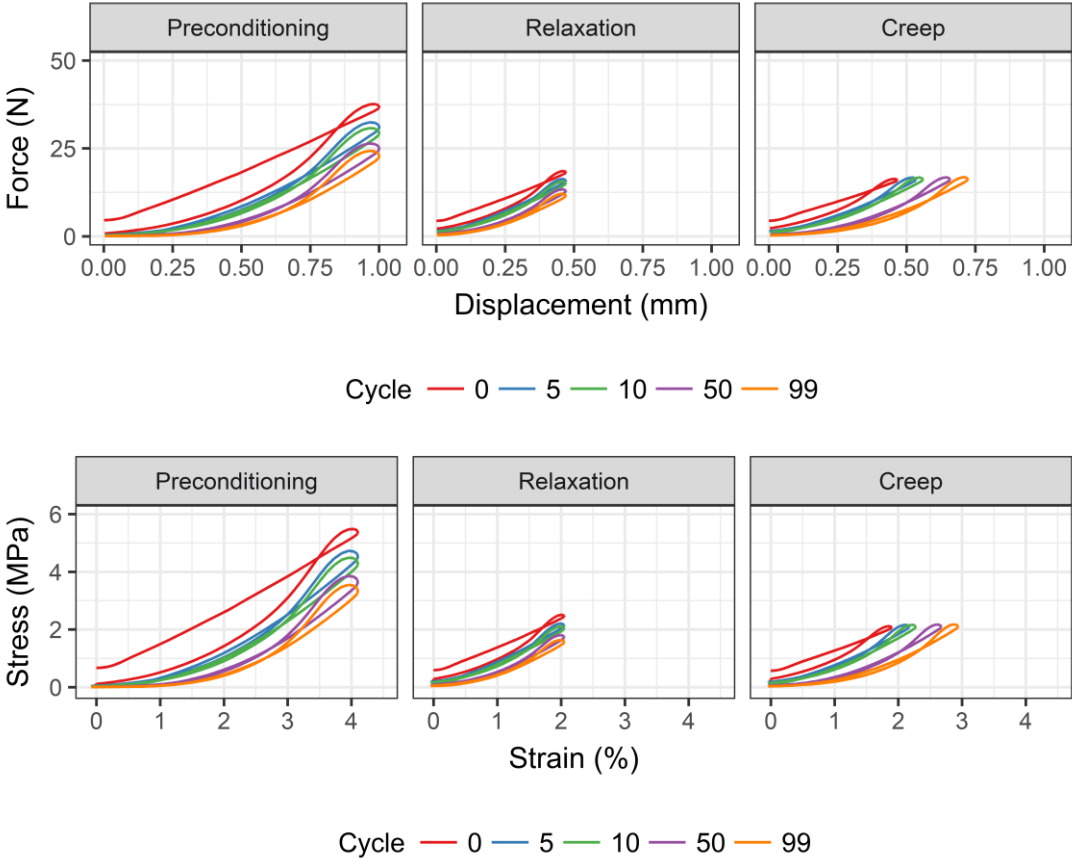
Figure 10-24: Representative force-displacement (top) and stress-strain (bottom) behaviour of the rabbit Achilles tendon during cycling.

Modulus - Loading
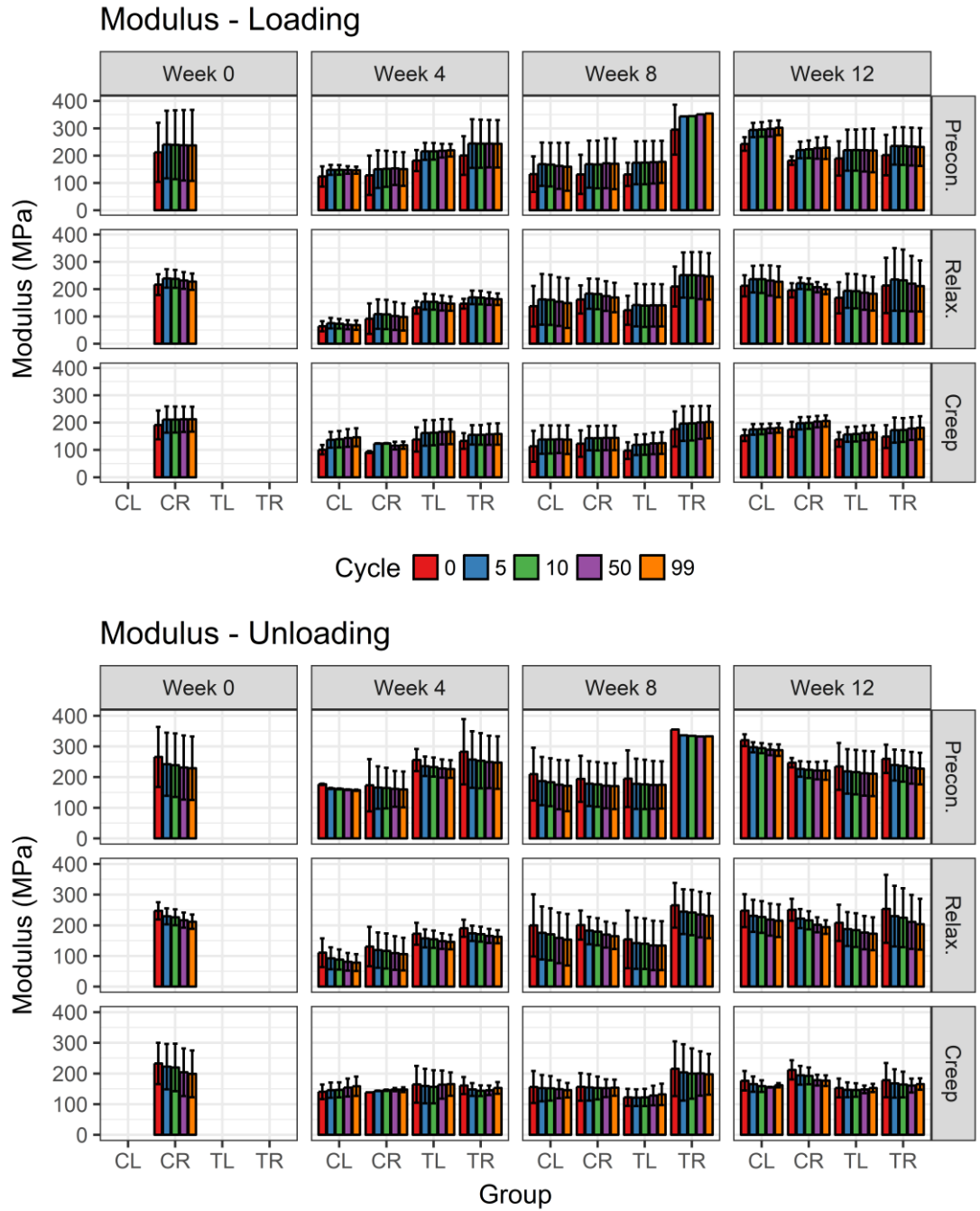
Modulus - Unloading

Figure 10-25: Summary (mean ± SD) of the elastic modulus (MPa) in loading (top) and unloading (bottom) at various cycles during dynamic testing of the rabbit Achilles tendon.
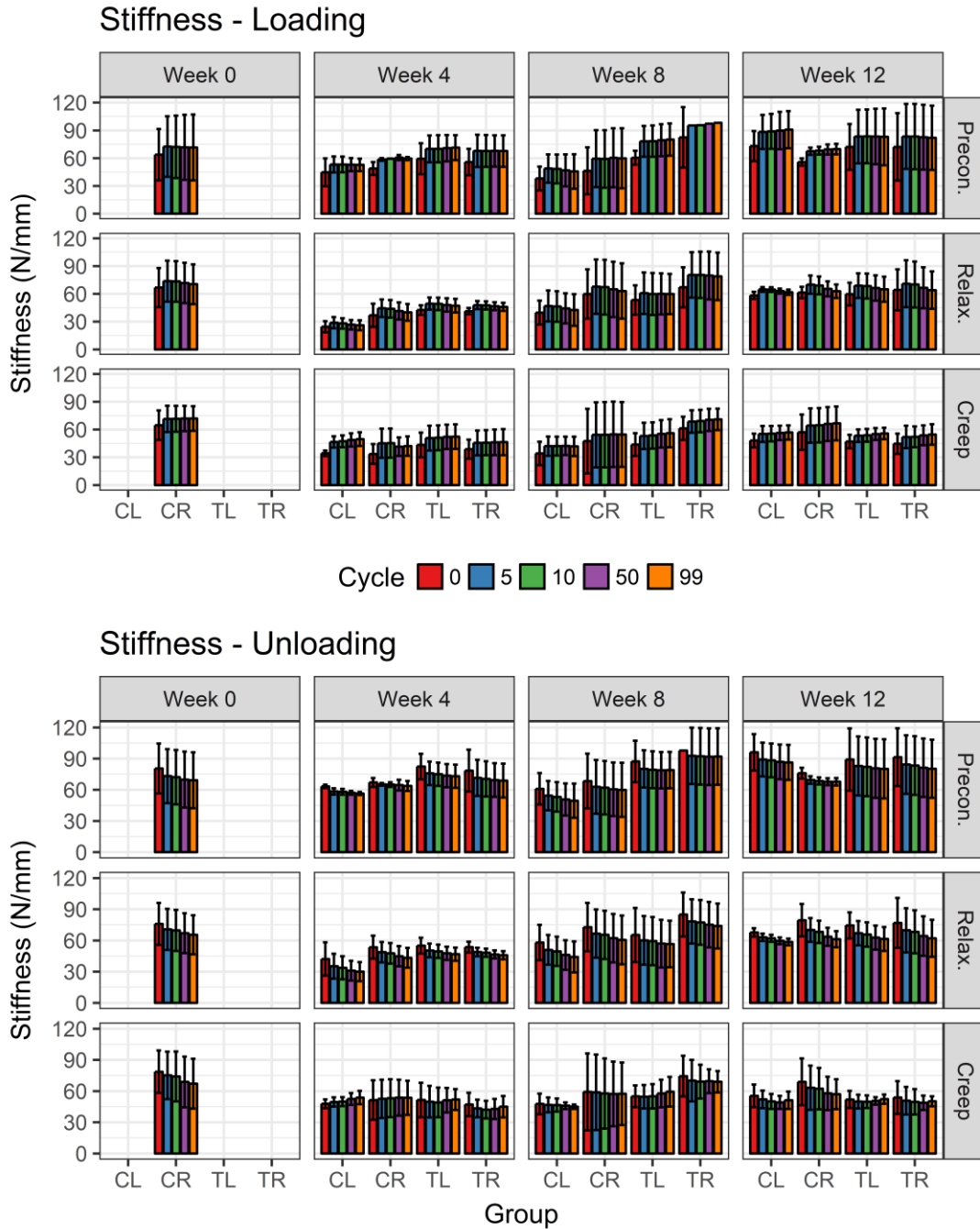
Figure 10-26: Summary (mean ± SD) of the stiffness (N/mm) in loading (top) and unloading (bottom) at various cycles during dynamic testing of the rabbit Achilles tendon.
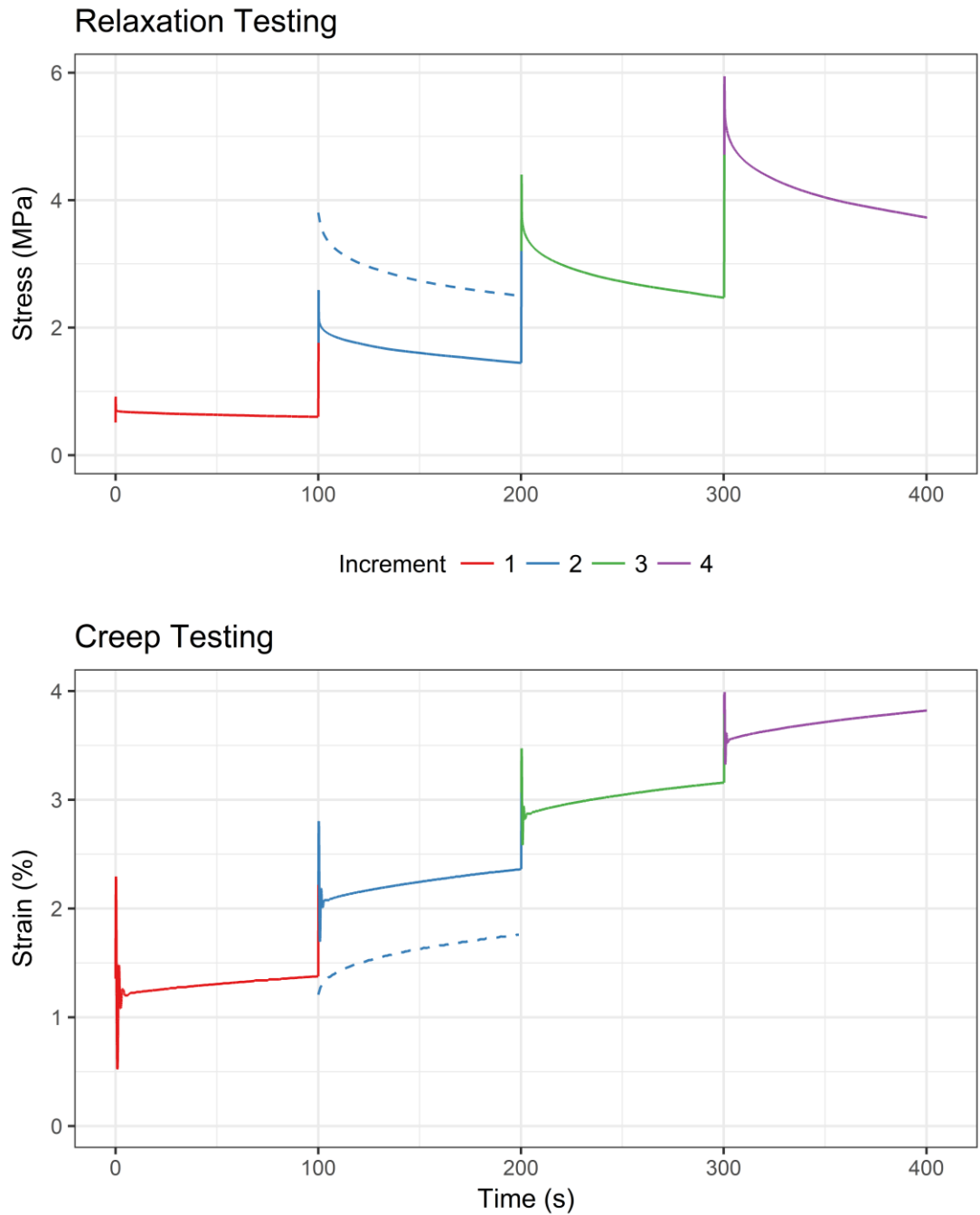
Figure 10-27: Representative example of stress relaxation (top) and creep (bottom) response of the rabbit Achilles tendon during the static viscoelastic portion of the testing protocol. The dynamic response is shown as a dashed line.
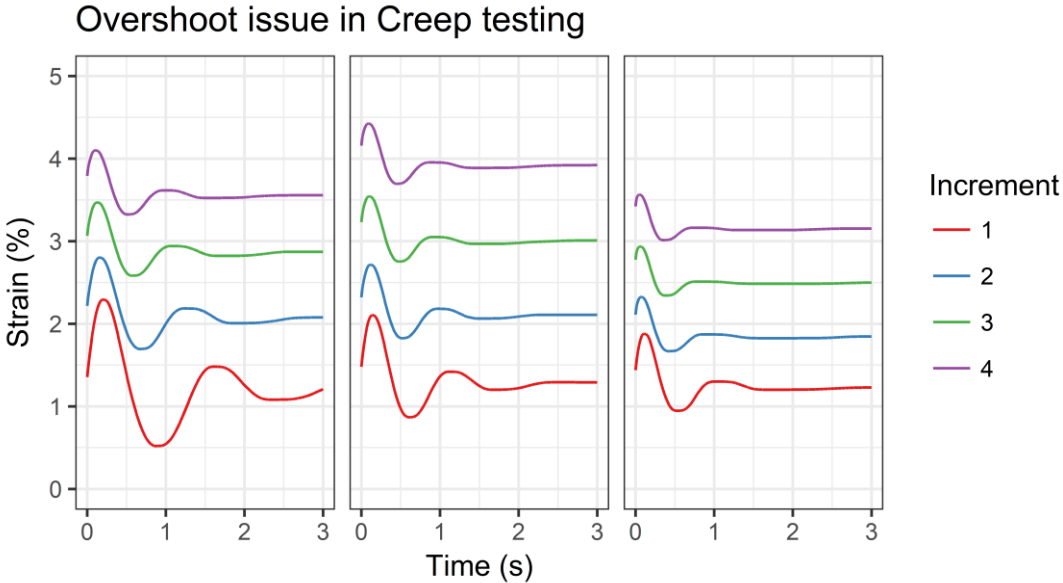
Figure 10-28: Representative overshoot in a rabbit Achilles tendon undergoing static creep testing at different increments.

Relaxation Testing
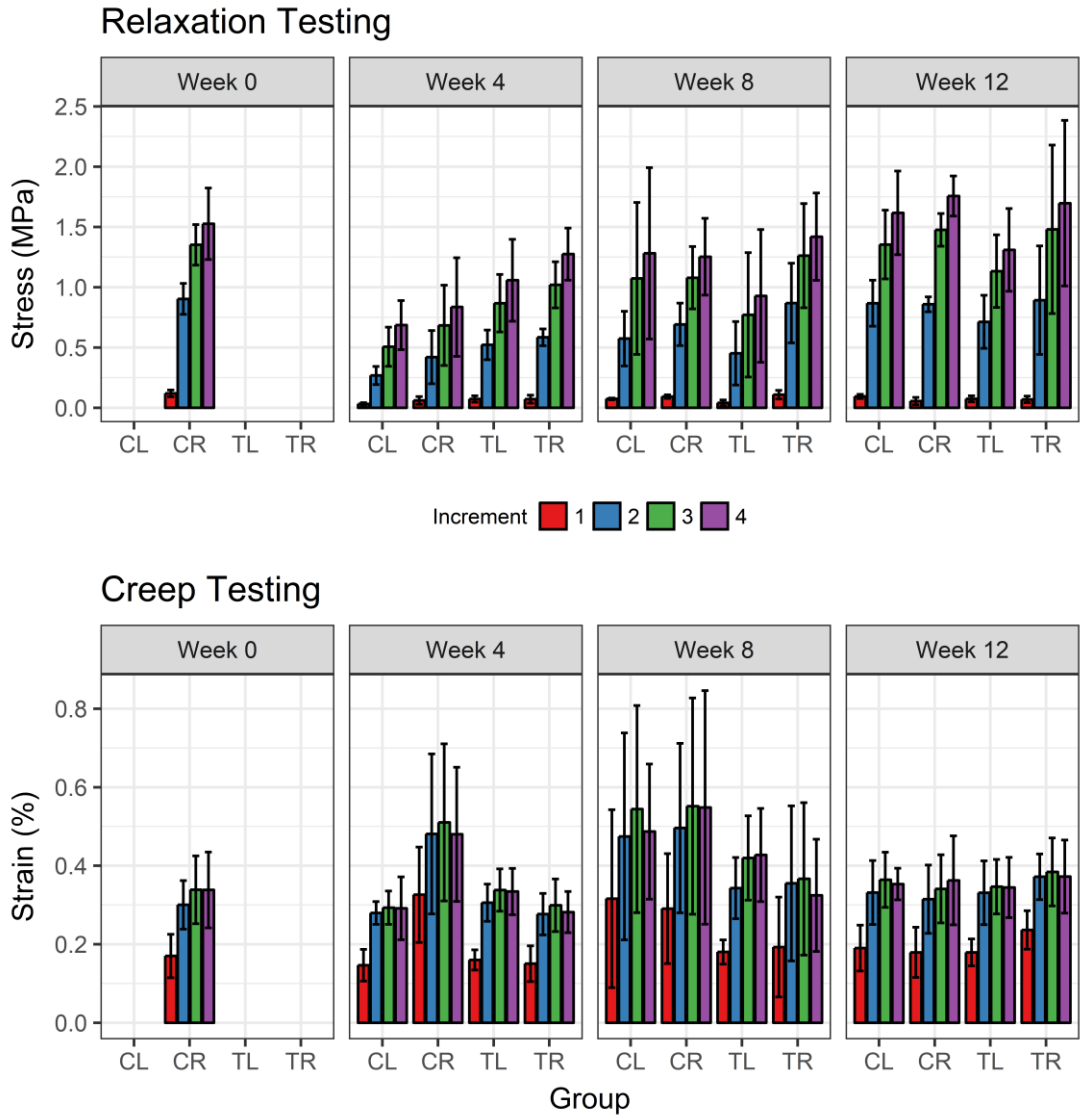
Creep Testing

Figure 10-29: Summary (mean ± SD) of the magnitude of change in the static relaxation (top) and creep (bottom) testing at different increments in the rabbit Achilles tendon.
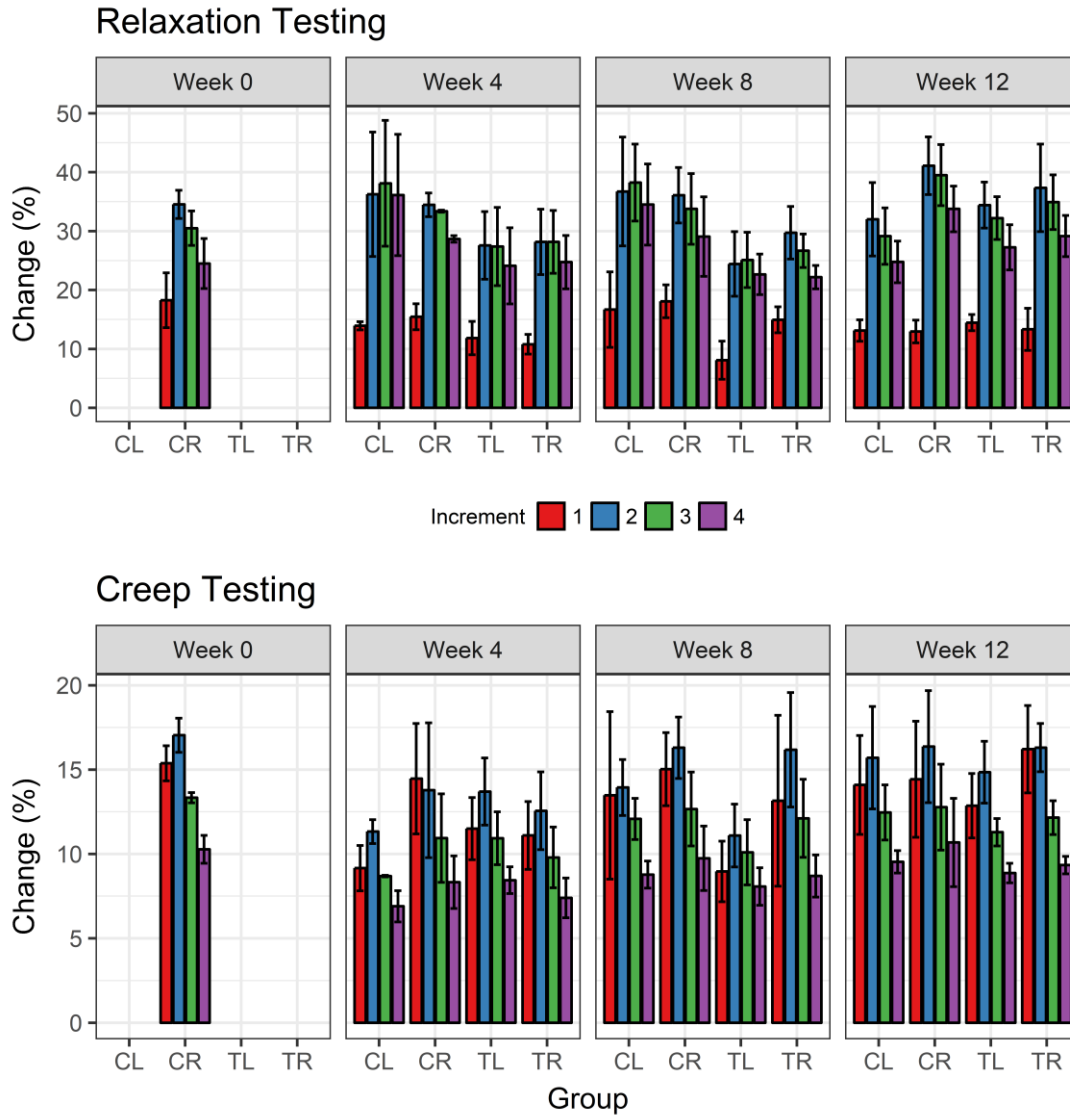
Figure 10-30: Summary (mean ± SD) of the percentage change in the static relaxation (top) and creep (bottom) testing at different increments in the rabbit Achilles tendon.

Relaxation Testing
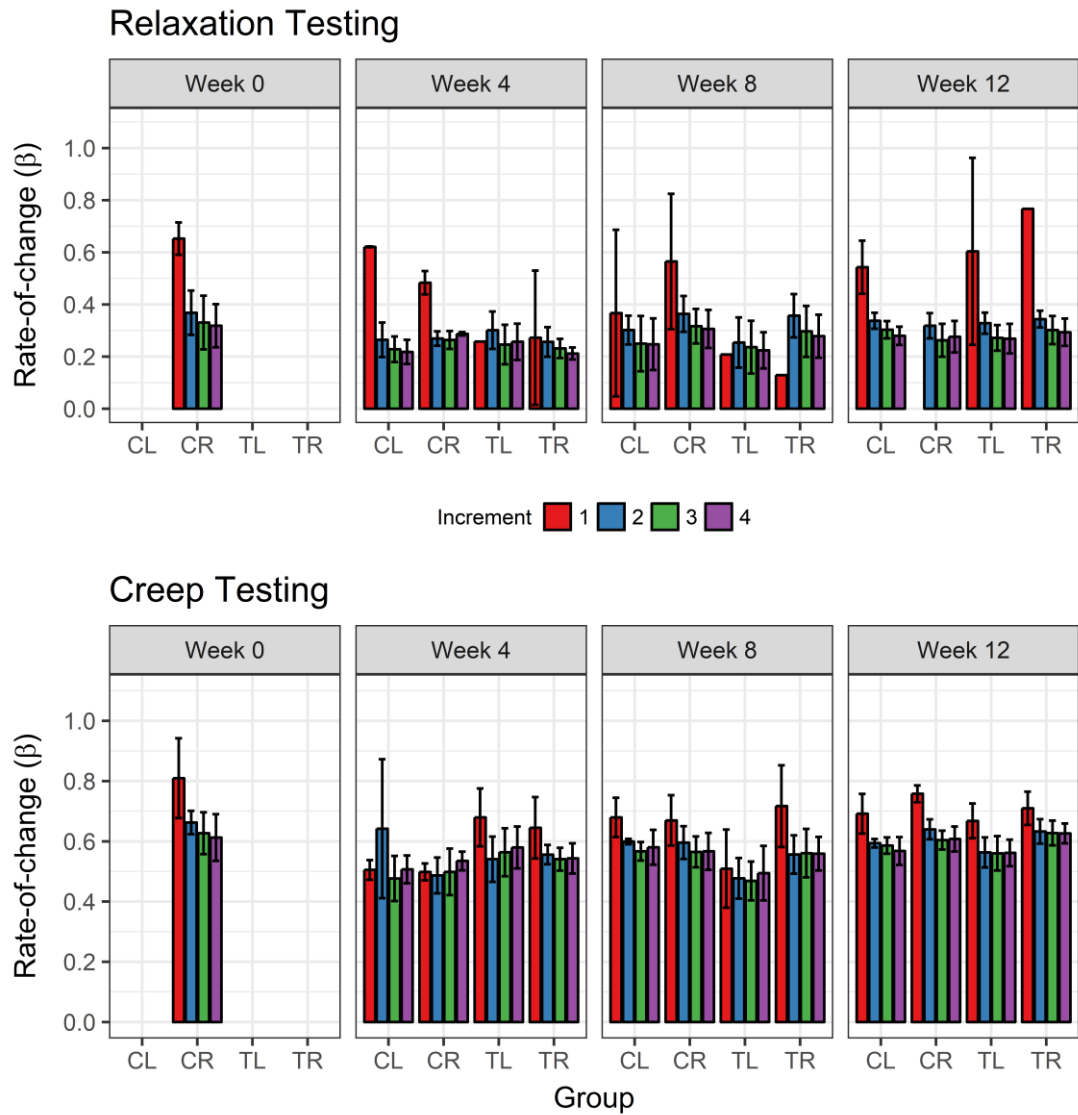
Creep Testing

Figure 10-31: Summary (mean ± SD) of the rate of change (β) in the static relaxation (top) and creep (bottom) testing at different increments in the rabbit Achilles tendon.

Relaxation Testing
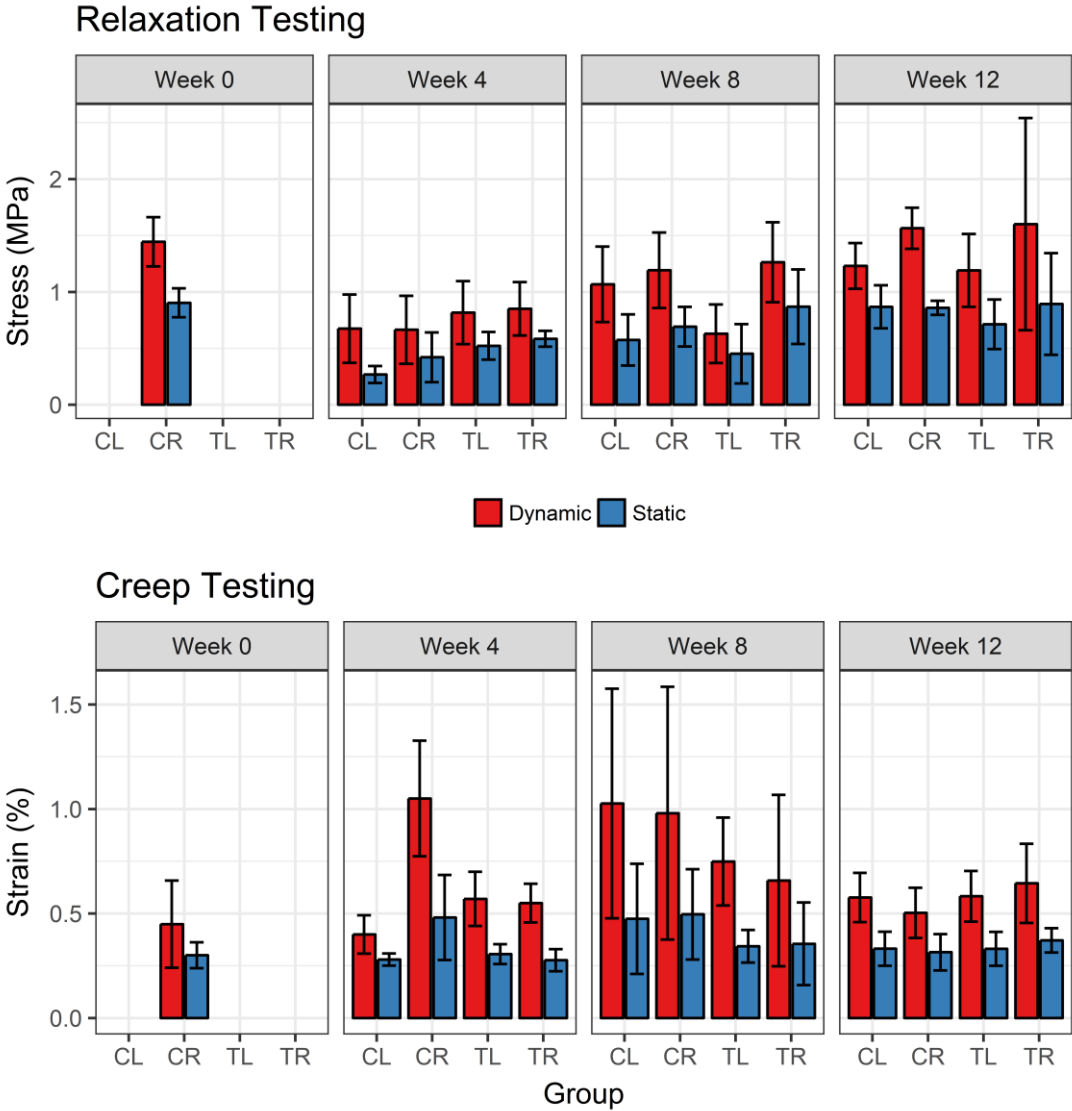
Creep Testing

Figure 10-32: Summary (mean ± SD) of the magnitude of change in the static and dynamic relaxation (top) and creep (bottom) testing at different increments in the rabbit Achilles tendon.

Relaxation Testing
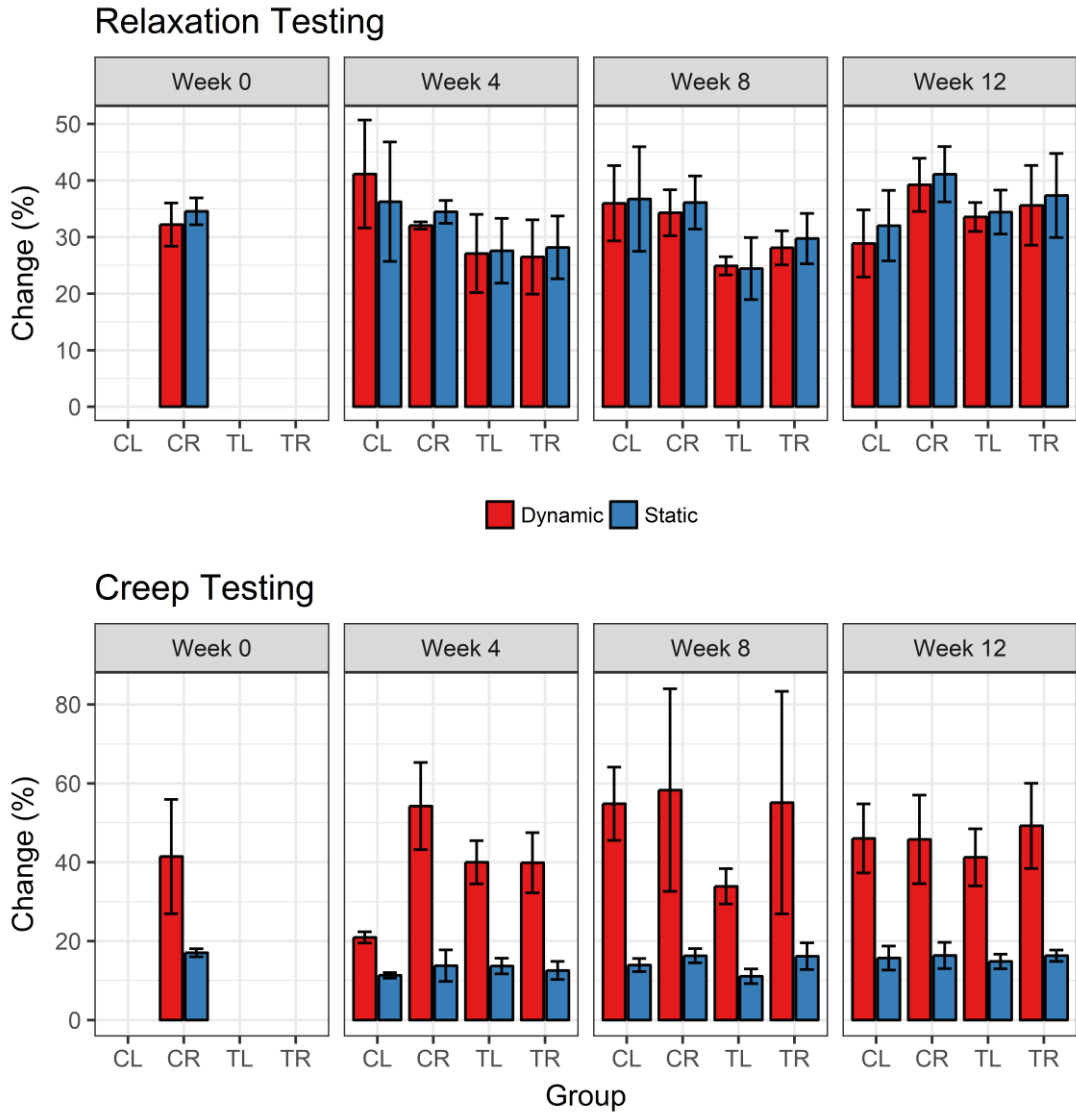
Creep Testing

Figure 10-33: Summary (mean ± SD) of the percentage change in the static and dynamic relaxation (top) and creep (bottom) testing at different increments in the rabbit Achilles tendon.
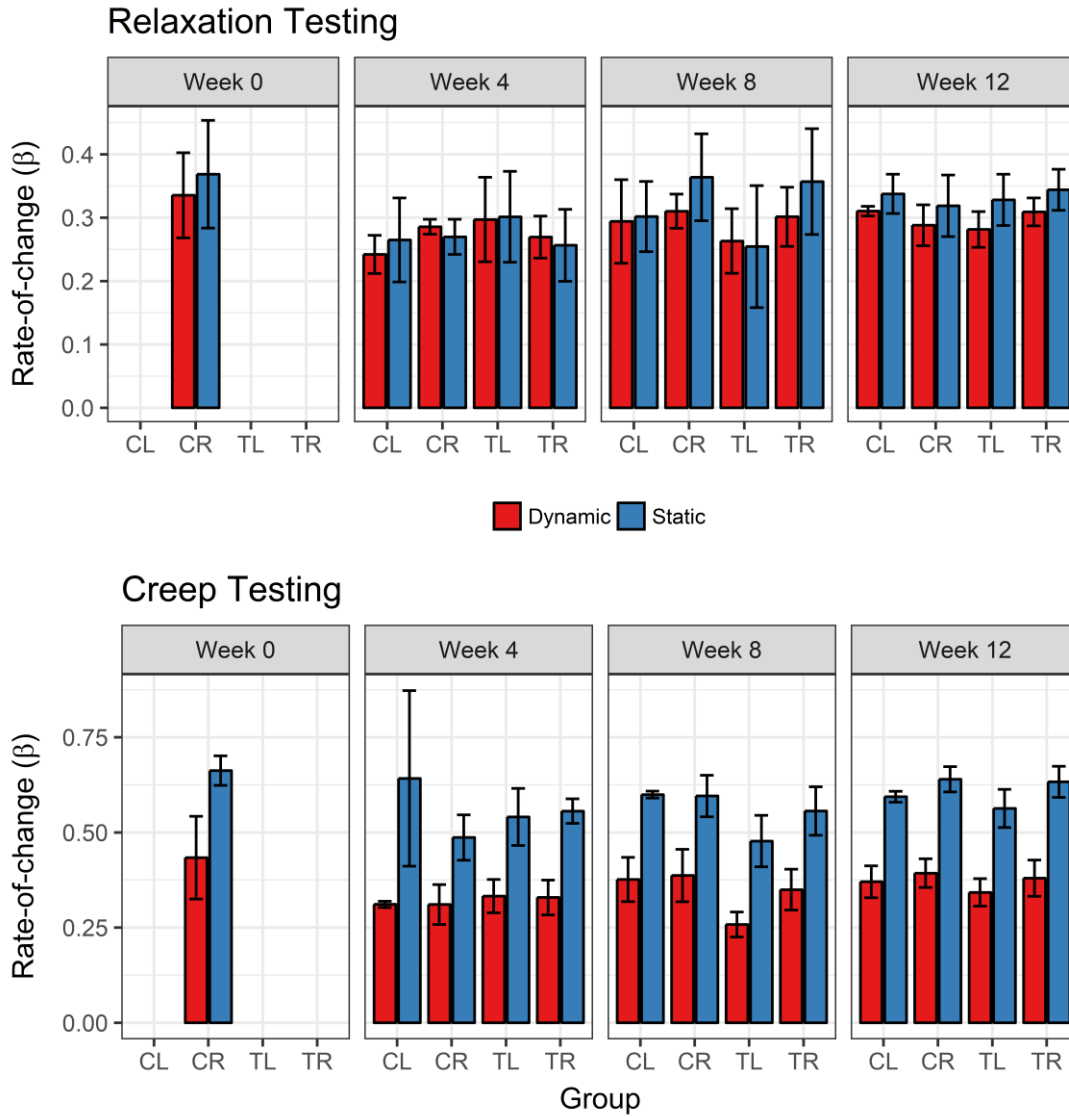
Figure 10-34: Summary (mean ± SD) of the rate of change (β) in the static and dynamic relaxation (top) and creep (bottom) testing at different increments in the rabbit Achilles tendon.

Strain-Rate Sensitivity - Stiffness

Strain-Rate Sensitivity - Modulus
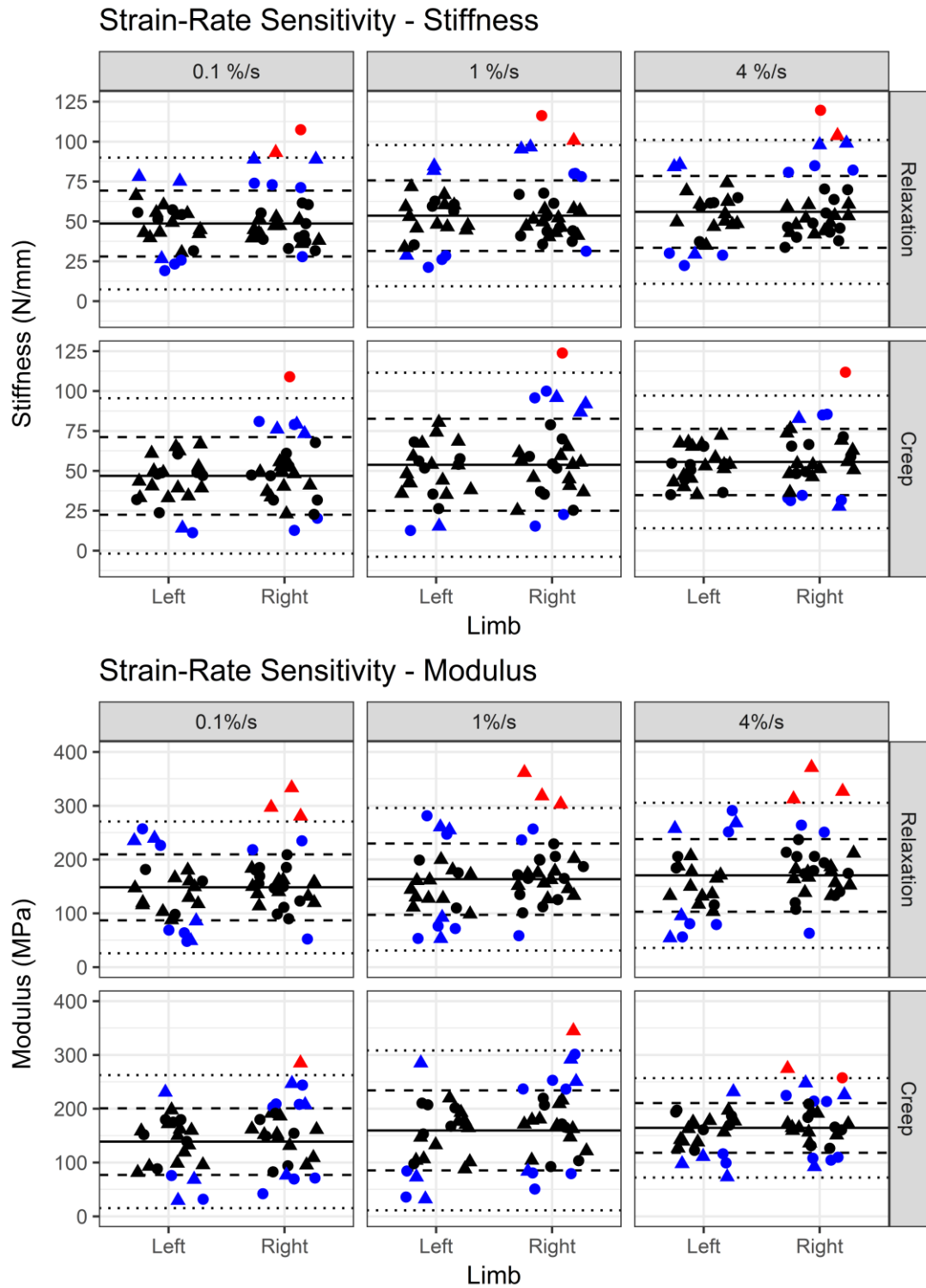
Figure 10-35: (Top) Stiffness (N/mm) and (bottom) elastic modulus (MPa) of individual rabbit Achilles tendons compared to the control population. The solid line represents the population mean, dashed lines represent one standard deviation (SD), and dotted lines represent two SD. Control samples are shown as dots and tendinopathy samples as triangles. Samples within one SD are black, within two SD are blue, and outside of the ranges are red.
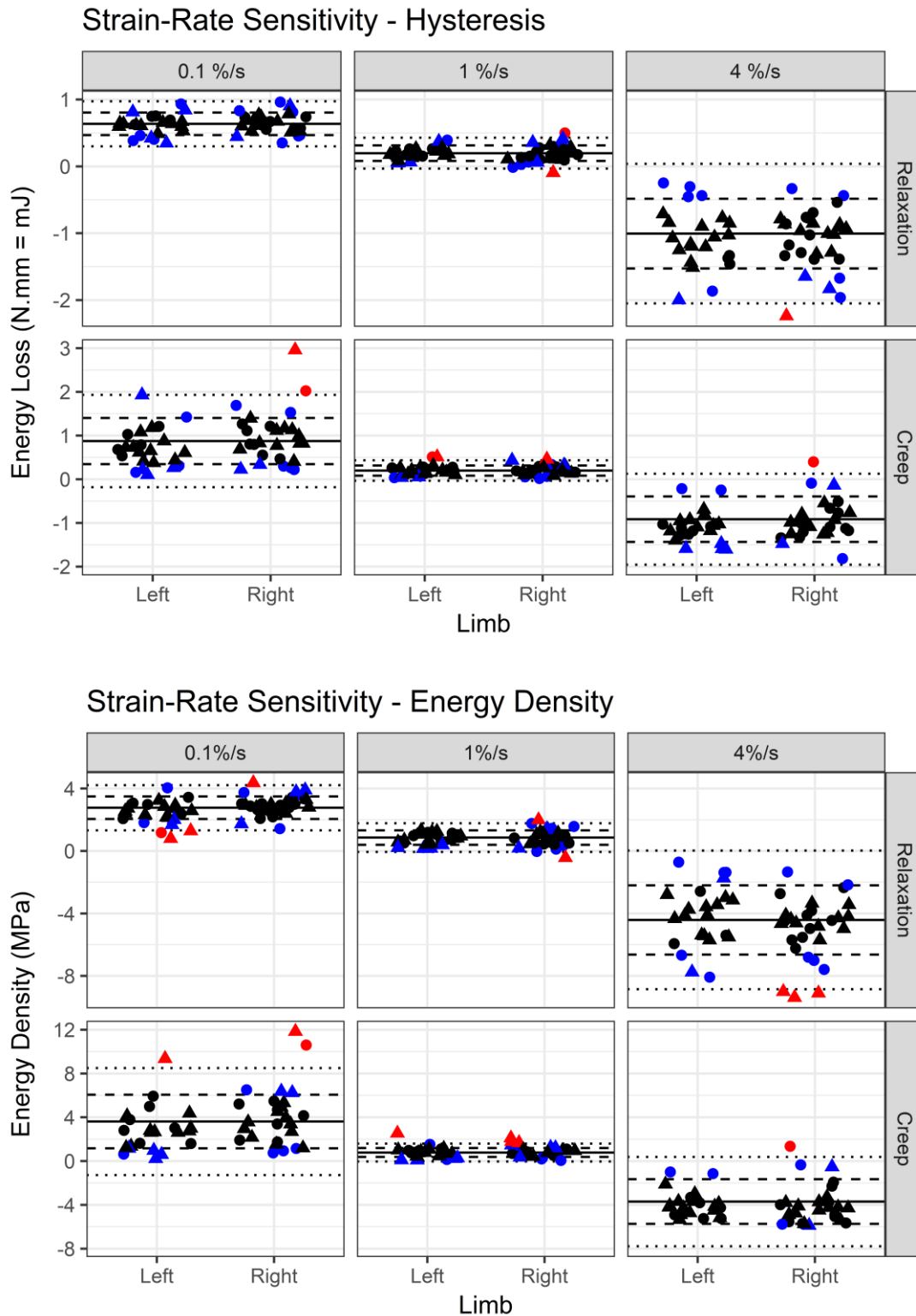
Figure 10-36: (Top) Hysteresis (mJ) and (bottom) energy density (MPa) of the individual rabbit Achilles tendons, calculated from the isochronal portion of the testing, compared to control population. The solid line represents the population mean, dashed lines represent one standard deviation (SD), and dotted lines represent two SD. Control samples are shown as dots and tendinopathy samples as triangles. Samples within one SD are black, within two SD are blue, and outside of the ranges are red.

Dynamic Modulus - Storage

Dynamic Modulus - Loss

Dynamic Modulus - Tangent Delta
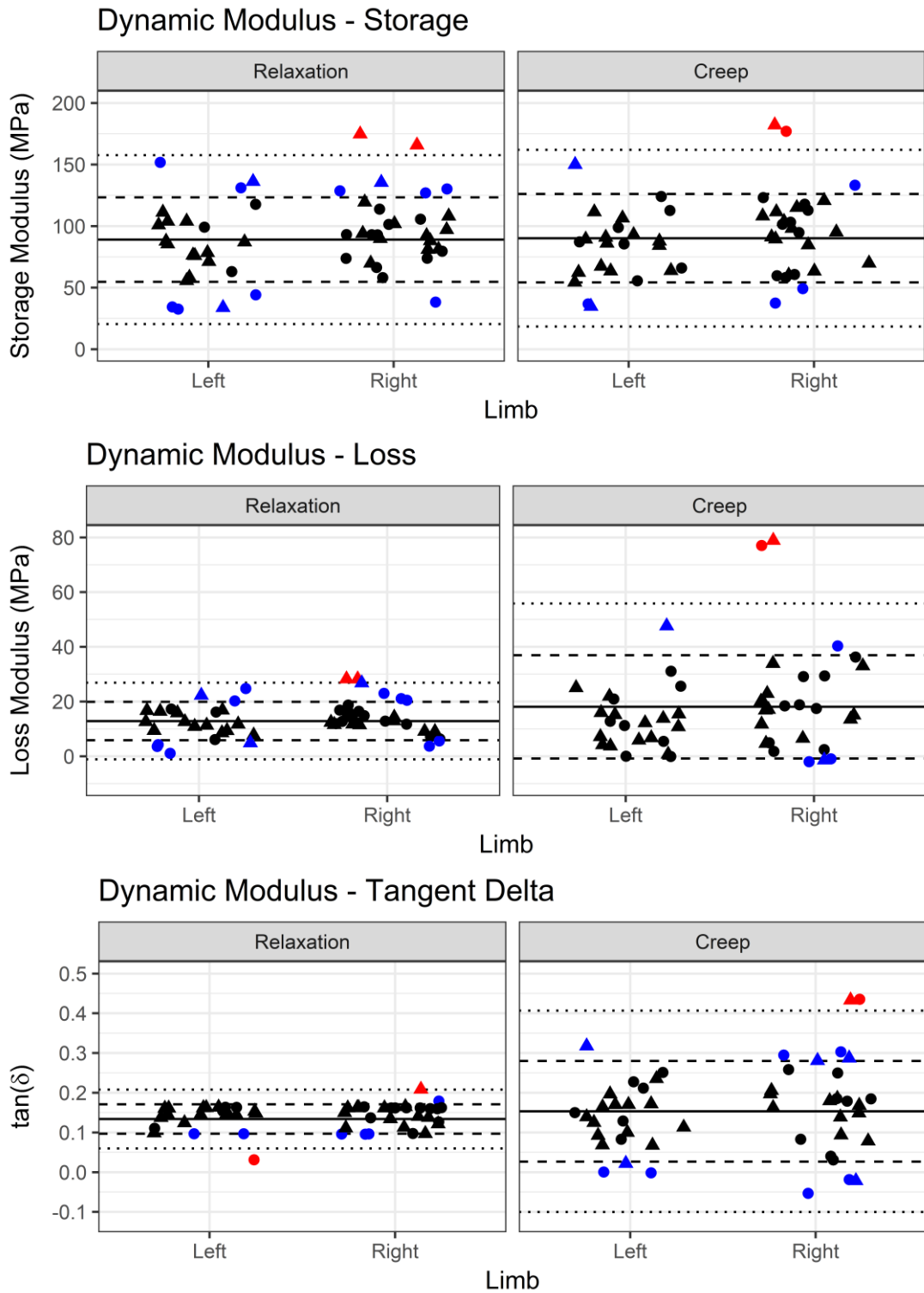
Figure 10-37: (Top) Storage modulus (MPa), (middle) Loss modulus, and (bottom) tangent delta of the individual rabbit Achilles tendons, averaged from the last five cycles of the dynamic portion of the testing, compared to control population. The solid line represents the population mean, dashed lines represent one standard deviation (SD), and dotted lines represent two SD. Control samples are shown as dots and tendinopathy samples as triangles. Samples within one SD are black, within two SD are blue, and outside of the ranges are red.

Dynamic - Stiffness
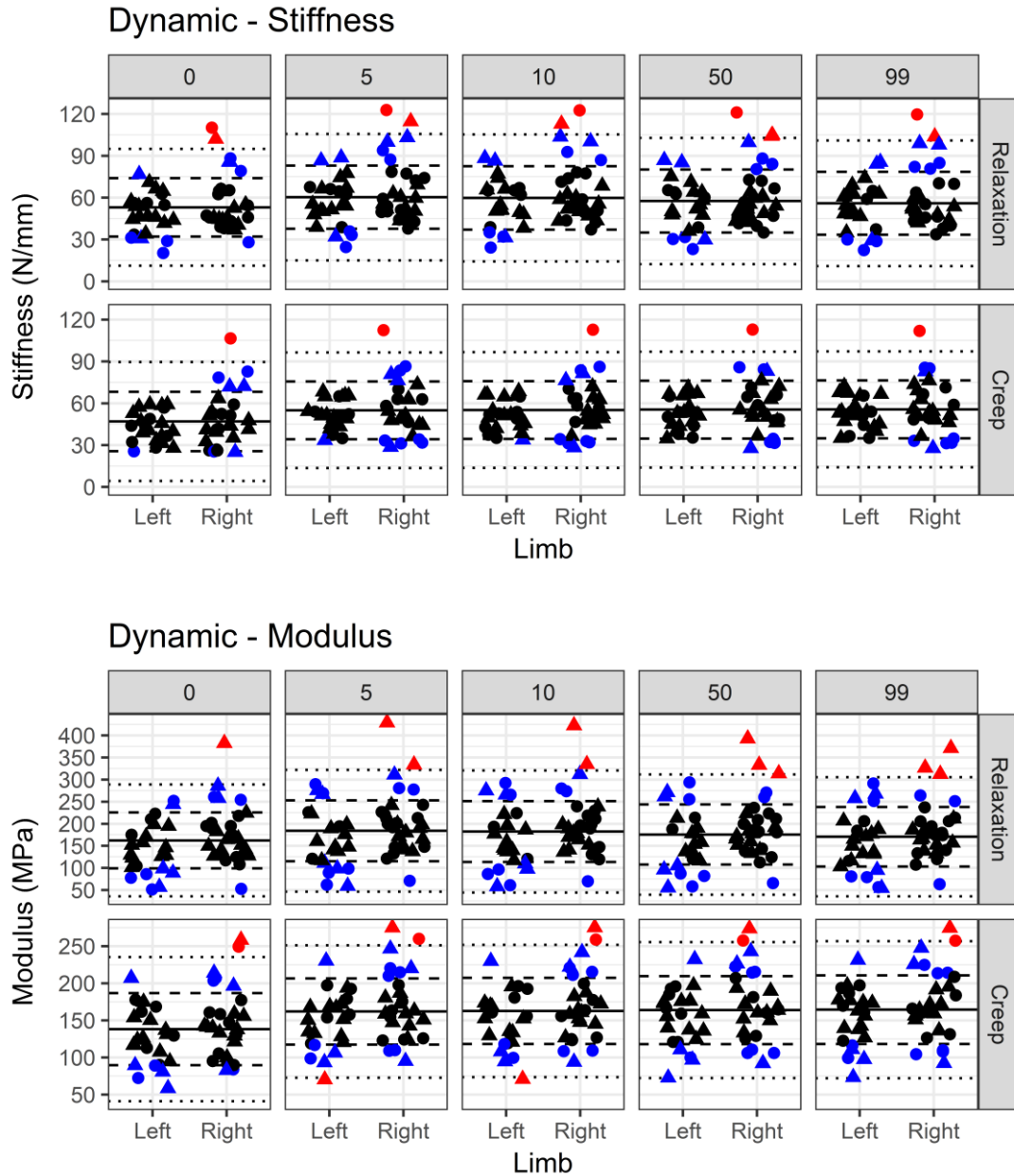
Dynamic - Modulus

Figure 10-38: (Top) Stiffness (N/mm) and (bottom) elastic modulus (MPa) of the individual rabbit Achilles tendons, averaged from the last five cycles of the dynamic portion of the testing, compared to control population. The solid line represents the population mean, dashed lines represent one standard deviation (SD), and dotted lines represent two SD. Control samples are shown as dots and tendinopathy samples as triangles. Samples within one SD are black, within two SD are blue, and outside of the ranges are red.
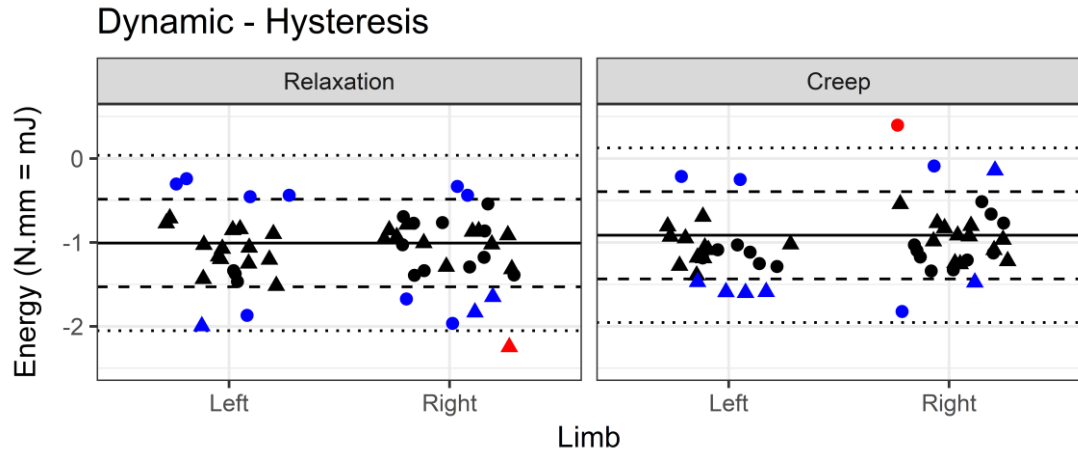
Figure 10-39: Hysteresis (mJ) of the individual rabbit Achilles tendons, averaged from the last five cycles of the dynamic portion of the testing, compared to control population. The solid line represents the population mean, dashed lines represent one standard deviation (SD), and dotted lines represent two SD. Control samples are shown as dots and tendinopathy samples as triangles. Samples within one SD are black, within two SD are blue, and outside of the ranges are red.
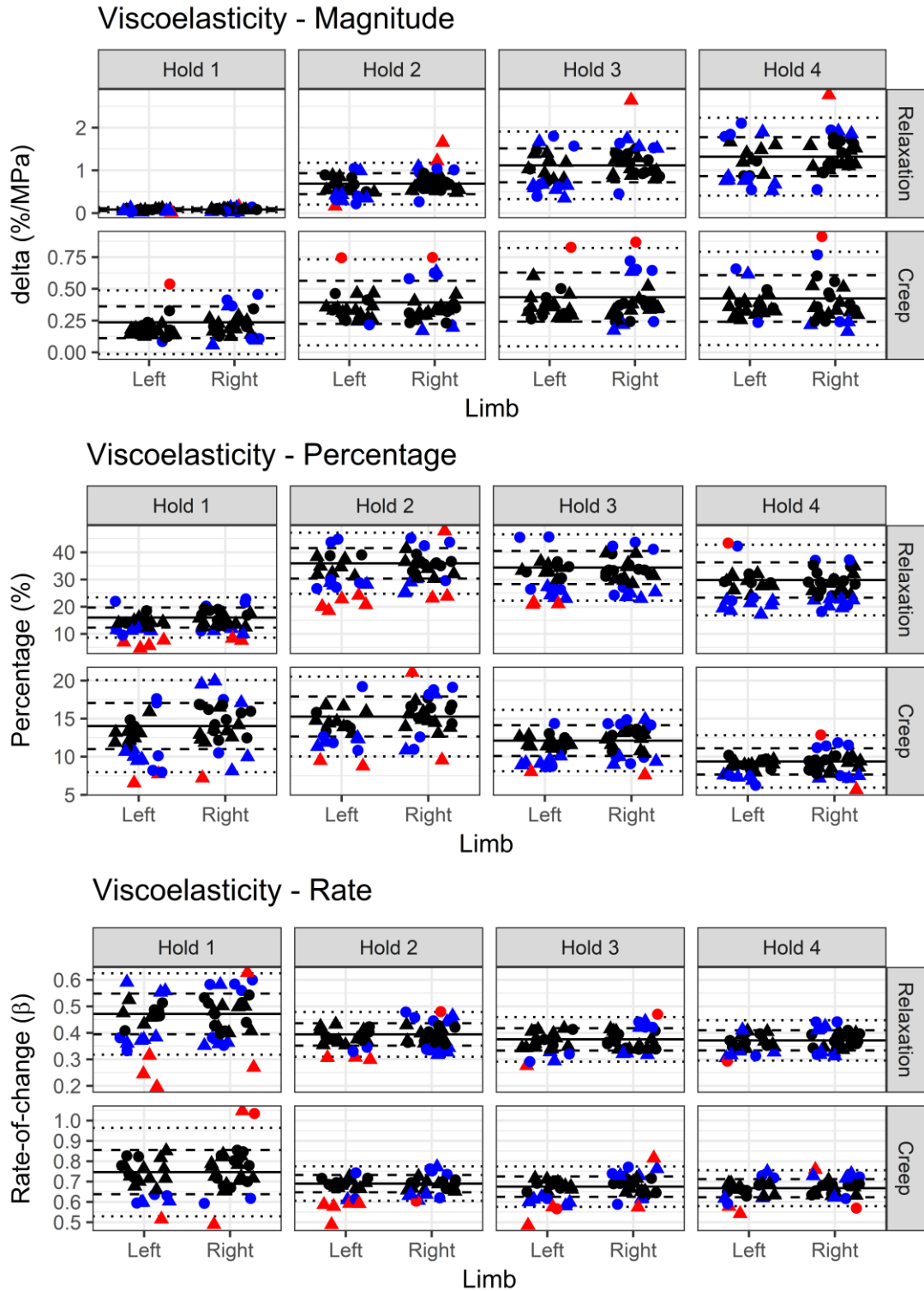
Figure 10-40: (Top) Magnitude of change (MPa/%), (middle) Percentage change (%), and (bottom) rate of change (β) in static relaxation and creep of the individual rabbit Achilles tendons at each increment, compared to control population. The solid line represents the population mean, dashed lines represent one standard deviation (SD), and dotted lines represent two SD. Control samples are shown as dots and tendinopathy samples as triangles. Samples within one SD are black, within two SD are blue, and outside of the ranges are red.

CHAPTER 11.   EPILOGUE

11.1. Summary of chapters

The Australian Research Council (ARC) Linkage project, LP110100581, titled *Bioengineered Bioscaffolds for Achilles Tendinopathy Treatment*, aimed to improve the outcomes of surgical treatment of Achilles tendinopathy via research based on a New Zealand White (NZW) rabbit (*Oryctolagus cuniculus*) tendinopathy model. This dissertation aimed to evaluate the tendinopathy model from an engineering perspective, by developing a methodology to evaluate the mechanical behaviour of tendons within the tendinopathy model. This information was intended to aid in the understanding of how degeneration affects the behaviour of tendons, as well as to assist in the development of computational models of tendon degeneration and healing. The thesis, stated at the beginning of this dissertation, was that tendinopathy adversely affects the mechanical behaviour of tendon, via disruption of the collagen matrix, resulting in a decrease in strength, stiffness, and resilience.

11.1.1.   Structured light scanning of tendon (Chapters 4 and 5)

Cross-sectional area (CSA) is often used as an indication of injury, as enlarged area may suggest swelling and inflammation. CSA is also an important measurement in mechanical testing, as it allows for the force measurement to be normalised and presented as 'stress'. The literature described few techniques capable of capturing the total volume of the tendon from a single scan, which is necessary to adequately describe the complete morphology for finite element analysis (FEA). Ideally, a method would be applicable to materials testing systems (MTS) as a way of measuring deformation of the tendon under load and for use in calculating true stress, as well as to inform finite element models (FEM). Using structured light scanning (SLS), a method was developed and validated in Chapter 4 to measure CSA along the entire length of tissue with high accuracy and repeatability (Hayes *et al.*, 2016). This method was subsequently used to measure CSA of tendons in all other test methods.

It was hypothesised in Chapter 5 that rabbit Achilles tendon would show a decrease in CSA proportional to an applied load. Using the technique

described in Chapter 4, CSA of rabbit Achilles tendon was found to decrease approximately 0.6%/MPa to stresses up to 8MPa. This corresponds to the end of the toe region, suggesting that as well as being of low stiffness, this region exhibits only small changes in morphology. It was found that, for testing at or near the toe region, engineering stress is sufficient to approximate true stress. It is anticipated that greater differences will be evident as the tendon enters the linear region and transverse strains increase. The SLS technique was able to rapidly capture the entire three-dimensional (3D) morphology of the tendon as loads were manually applied. The advantages of this technique were well demonstrated for use in an MTS and should be considered as an alternative to laser-based measurement tools for 3D measurements.

11.1.2. Tensile testing protocol (Chapter 7)

A rigorous analysis of the literature showed that there is no consistent mechanical testing protocol to measure the tensile properties of soft tissue (for example, elastic modulus, ultimate tensile force, ultimate tensile strain), making it difficult to directly compare between studies. To ensure the application of an appropriate methodology, tensile testing parameters were studied in detail to develop a recommended experimental protocol for measuring the tensile properties of tendons and other suitable soft tissues. Despite many studies utilising similar test setups, few have detailed the selection of testing parameters, despite many reviews indicating the importance of factors such as strain rate on the behaviour of samples.

This dissertation presents what may be considered a current best-practice methodology for uniaxial tensile testing of soft tissue. This methodology was developed from recommendations in literature and subsequently validated against published results. It was found that samples should be tested as bone-tendon-muscle constructs at high strain rates to ensure failure of the tendon body rather than the bony interface. Additionally, strain appears to determine the point of failure of the tendon, with all groups failing at approximately the same strain, regardless of strain rate and gripping method.

11.1.3. Required duration of viscoelastic testing (Chapter 8)

One of the key parameters in viscoelastic testing is the duration of testing required to adequately define the time-dependent properties. Analysis of literature showed little consensus in the duration of testing used in studies, with few authors offering any justification for their selected value. Despite its importance, only a single study investigated the effect of duration on the ability to measure static viscoelastic properties, such as rate of change. Manley Jr *et al.* (2003) tested ligament in both creep and stress relaxation, finding that 100 seconds was sufficient to adequately predict the behaviour of tissue up to 10,000 seconds. Shorter testing durations allow for more tests on the same samples, with less risk of damage or dehydration, as well as being more practical for researchers (Duenwald *et al.*, 2009b).

While tendons and ligaments are often considered interchangeably, they have been shown to exhibit different viscoelastic properties, and so it was necessary to investigate if the findings of Manley Jr *et al.* (2003) were applicable to tendon. Following a modified protocol, including exploring alternative curve fitting methods, it was confirmed that 100 seconds is sufficient to predict the behaviour of tissue to 3600 seconds with minimal loss of accuracy. This study also recommended a preferred method of curve fitting for individual and grouped samples. By confirming the work of Manley Jr *et al.* (2003) in tendon, it was possible in this dissertation to develop a more comprehensive methodology of the viscoelastic behaviours of tendon in subsequent testing.

To the author's knowledge, this work also provides the first reported values for rate of change in relaxation and creep for rabbit Achilles tendon. These values may serve as a baseline against which to measure changes in tendon behaviour.

11.1.4. Viscoelastic testing (Chapters 9 & 10)

Disease of the tendon, known as tendinopathy, is characterised by pain and reduced mobility and functionality. The pathology is complex, with markers including disordered healing causing fibre disruption and disorientation, generally with an absence of inflammatory cells. Degenerated tendons exhibit decreased mechanical properties, such as stiffness and ultimate tensile stress

(UTS) (Hansen *et al.*, 2013; Helland *et al.*, 2013), and are generally observed to be disordered with a larger CSA, a lower stiffness, and a lower elastic modulus (Arya and Kulig, 2010; Helland *et al.*, 2013). Tendinopathy models in the literature have not fully explored the mechanical behaviours of tendons under physiological loading conditions. Most tests used simple uniaxial traction tests to measure failure properties of the tendons. This offers an insight into why tendons may fail during high-intensity exercises; however, it does not provide information on changes that may affect the performance of the tendon during daily activities.

Despite calls in the literature to perform complex testing protocols to help identify underlying behaviours, such as nonlinearity, relatively few studies have measured the behaviour of soft tissue at multiple strain or stress levels and fewer have measured the static and dynamic properties of tissue in the same test. Based on rigorous analysis of the available literature, a methodology was proposed to incorporate all practical aspects of mechanical behaviour in a single protocol that could be applied to each tendon to provide a comprehensive assessment of the tissue. This methodology is designed to prevent damage while maximising the amount of data available for analysis. This is the first methodology to assess the isochronal, dynamic, and static properties of creep and stress relaxation at multiple steps in a single protocol to be applied to individual samples. The methodology may be used as a standard protocol for defining the behaviour of soft tissues.

The methodology was subsequently applied to the rabbit cohort used in the collagenase-induced tendinopathy model for the ARC Linkage project. To the author's knowledge, this is the first study to perform complex testing protocols on a tendinopathic model and the first to report results on the viscoelastic behaviour of rabbit Achilles tendon in a tendinopathy model. The study described mechanical properties including elastic modulus, energy density, dynamic modulus, and rate of creep and relaxation in both control, contralateral, and tendinopathic tendons. Using two techniques for analysing the tendons – grouped and individual – it was demonstrated that, within the bounds and limitations of the study, tendinopathy does not influence the properties of the tendon under the physiological conditions used in the study.

Due to planned post-testing analysis of the tendon for further studies under the ARC Linkage Project, no failure testing was performed. However, the findings, coupled with the failure properties from the literature, offer a significant insight into the influence of tendinopathy and have implications for evidence-based management of the disease.

11.2. Implications

11.2.1.   Methodologies

A comprehensive review of the literature revealed that the selection of parameters in many simple protocols, such as tensile and static viscoelastic testing of tissue, was not well justified, despite these being reported as having significant influence on the properties. Therefore, in this thesis consideration was given to many parameters and factors with a view to improving the justification for choices during testing. The methodologies developed in this thesis represent best-practice as determined via rigorous analysis of the literature and validation against published results. Adoption as standard practice would contribute to reduction of intra- and inter-laboratory differences and improve the comparability of results between studies.

11.2.2.   Mechanical behaviour of tendinopathy

The work presented in this dissertation demonstrates that, within the limitations of the study, tendinopathy may not influence the behaviour of tendon across the range of strains and loads experienced during daily activities. Findings suggest that tendinopathy does not influence the behaviour of tendon toward the toe region of the stress-strain curve, in isochronal or viscoelastic testing protocols. Since the tendons in this study were not tested to failure, no conclusion can be drawn regarding the failure behaviour of this tendinopathy model; however, adding this to the protocol in future studies would enhance the value of these studies and provide a more complete suite of results.

Achilles tendon rupture is often seen in older athletes returning to sports involving explosive actions, such as jumping. Tendinopathic degeneration is more commonly seen in ruptured tendons than symptomatic tendons, suggesting tendinopathy has a greater influence in their failure. This is supported by previous studies of tendinopathy that reported a reduction in

failure properties. Despite histological and other analyses in literature describing clear structural changes, the primary indication for tendinopathy is pain.

The findings of this dissertation may help to guide evidence-based management of tendinopathy. Clinical focus on pain management would permit the patient to return to daily activities unencumbered. The use of eccentric exercise has been identified as showing positive signs in the management of tendinopathy. Explanations of the potential mechanism for its efficacy have been proposed in relation to the mechanical underuse theory, that is, eccentric exercises are able to apply greater loads to the tendon which in turn elicits a mechanotransducive response from cells that were 'disconnected' from the tendon via micro-failures of the fibrils. It is the author's opinion that, as well as stimulating these cells to promote healing, eccentric exercises may be acting to improve the mechanical strength of the tendon, thereby returning the tendon properties to functionally normal levels. Since eccentric exercises are generally not explosive, it is plausible that sufficiently large loads could be applied without exceeding the failure strength of the tendon. Thus, clinical management of the tendon would involve pain relief, coupled with tendon strengthening exercises. It is noted that this may not truly deal with the aetiology of the disease and may not restore the tendon to a pre-disease state as defined in literature; however, it may return the tendon to a clinically functional state, which may be of more practical significance.

11.3. Future work

Dynamic measurement of soft tissue morphology during mechanical testing was not achieved in this dissertation. SLS was demonstrated to be a reliable technique; however, the available scanner and MTSs were found to be incompatible for the purposes of this study. Digital image correlation (DIC), or speckle imaging, has also demonstrated promise, but was not utilised due to difficulty in applying a speckle pattern to the tendon. Both techniques offer the ability to measure true stress and instantaneous morphology, which would aid in the development of more accurate computational models of tissue behaviour. Additionally, DIC offers the ability to measure surface strains, providing additional data for comparison. Since these techniques have

potential applications outside of biological materials testing, they warrant further investigation for implementation in materials testing protocols.

Testing protocols for metals, polymers, and other engineered materials, are often dictated by a set of testing standards, such as International Organization for Standardization (ISO), American Society for Testing and Materials (ASTM), and Australia Standards (AS). This allows for comparison within and between batches and laboratories, to ensure consistent measurement and reporting. In a similar way, there a need to perform standardised testing, where possible, in the field of biological systems to achieve intra- and inter-laboratory consistency. Several chapters in this dissertation were dedicated to developing a standardised methodology for each aspect of testing. More work is required and is recommended as a collaborative project to ensure that the most suitable and robust protocols are developed. This includes all the parameters discussed in Chapters 7–9.

There is a clear need to describe the progression of tendinopathy, from acute to subacute injury and on to chronic tendinopathy, and the associated mechanisms of pain in order to understand the aetiology and help guide clinical management. One of the possible management pathways includes use of tissue-engineered constructs to assist the natural healing response of the body. This is a long-term focus of the ARC Linkage Project.

Tendinopathy models are not mechanically well validated, which could have negative implications when comparing the outcomes of models against clinical outcomes. Ultimately, the mechanical behaviour of tendinopathy models must be validated against human tendinopathy. Models, such as collagenase-induction, have been criticised as not truly representing the appearance of clinical tendinopathy in many cases. This assumes that appearance and function are interrelated, which itself requires further investigation. Future mechanical assessment of tendinopathy models should include both the sub-failure properties, including viscoelastic and dynamic, and failure properties of tendinopathic tendons for each sample to assess the validity of the conclusions presented. This should be performed in conjunction with biochemical and histological assessments to validate both the model and conclusions.

11.4. Conclusions

Tendinopathy is a debilitating disease affecting millions of people worldwide. The aetiology of this disease is not well understood, and treatment remains difficult due to a lack of evidence-based management. This dissertation presents a series of methodologies for assessing the mechanical behaviour of tendons to determine differences caused by degeneration and disease. These methodologies, derived from rigorous analysis of the literature and validated through testing, may be considered best-practice for measurement CSA, uniaxial mechanical testing, and static viscoelastic testing of tendon. A comprehensive protocol for evaluating changes in tendon behaviour was proposed and validated against a collagenase-induced tendinopathy model. These methodologies offer researchers standardised means of assessing mechanical properties of soft tissues, in particular elucidating abnormal behaviours with a view to isolating and identifying contributory factors to the aetiology and true effect of the disease.

The following conclusions may be drawn from the results of this dissertation:

1. SLS is an effective tool for measuring the morphology of soft tissue;
2. Tendon demonstrates a measurable change in CSA with stress;
3. Engineering stress may be used as an approximation of true stress when testing is performed in or near the toe region;
4. Rabbit Achilles tendons should be tested as bone-tendon-muscle constructs to preserve the anatomy of the tendon;
5. Rabbit Achilles tendon is strain rate insensitive;
6. Strain is the limiting factor in determining failure properties;
7. The minimum required duration of testing required to assess the viscoelastic properties of tendon is 100 seconds;
8. Tendinopathy does not result in significant differences compared with control values, within the bounds of the testing protocol; and,
9. Management of the tendon should involve pain relief, coupled with tendon strengthening exercises.

This dissertation represents the first study to investigate the rate of change for creep and relaxation in a rabbit model, to report viscoelastic properties in rabbit

tendinopathy model, and to provide a detailed mechanical analysis of tendinopathic tendons. While the findings did not support the thesis that tendinopathy adversely affects the mechanical behaviour of tendon, via disruption of the collagen matrix, resulting in a decrease in strength, stiffness, and resilience, the outcomes offer significant insights that may contribute toward the development of better clinical management of tendinopathy.

REFERENCES

ABATE, M., SILBERNAGEL, K. G., SILJEHOLM, C., DI IORIO, A., DE AMICIS, D., SALINI, V., WERNER, S. & PAGANELLI, R. 2009. Pathogenesis of Tendinopathies: Inflammation or Degeneration? *Arthritis Res Ther,* 11**,** 235.

ABDEL-WAHAB, A. A., ALAM, K. & SILBERSCHMIDT, V. V. 2011. Analysis of Anisotropic Viscoelastoplastic Properties of Cortical Bone Tissues. *Journal of the Mechanical Behavior of Biomedical Materials,* 4**,** 807-820.

ABRAHAMS, M. 1967. Mechanical Behaviour of Tendon in Vitro. A Preliminary Report. *Medical & Biological Engineering & Computing,* 5**,** 433-43.

ABRAMOWITCH, S. D., WOO, S. L.-Y., CLINEFF, T. D. & DEBSKI, R. E. 2004. An Evaluation of the Quasi-Linear Viscoelastic Properties of the Healing Medial Collateral Ligament in a Goat Model. *Annals of Biomedical Engineering,* 32**,** 329-335.

ABRAMOWITCH, S. D. & WOO, S. L. Y. 2004. An Improved Method to Analyze the Stress Relaxation of Ligaments Following a Finite Ramp Time Based on the Quasi-Linear Viscoelastic Theory. *Journal of Biomechanical Engineering,* 126**,** 92-97.

ABRAMOWITCH, S. D., ZHANG, X., CURRAN, M. & KILGER, R. 2010. A Comparison of the Quasi-Static Mechanical and Non-Linear Viscoelastic Properties of the Human Semitendinosus and Gracilis Tendons. *Clinical Biomechanics,* 25**,** 325-331.

AHMADZADEH, H., FREEDMAN, B. R., CONNIZZO, B. K., SOSLOWSKY, L. J. & SHENOY, V. B. 2015. Micromechanical Poroelastic Finite Element and Shear-Lag Models of Tendon Predict Large Strain Dependent Poisson's Ratios and Fluid Expulsion under Tensile Loading. *Acta Biomaterialia,* 22**,** 83-91.

AHMED, A. F., ELGAYED, S. S. A. & IBRAHIM, I. M. 2012. Polarity Effect of Microcurrent Electrical Stimulation on Tendon Healing: Biomechanical and Histopathological Studies. *Journal of Advanced Research,* 3**,** 109-117.

AHN, H.-W., CHANG, Y.-J., KIM, K.-A., JOO, S.-H., PARK, Y.-G. & PARK, K.-H. 2014. Measurement of Three-Dimensional Perioral Soft Tissue Changes in Dentoalveolar Protrusion Patients after Orthodontic Treatment Using a Structured Light Scanner. *The Angle Orthodontist,* 84**,** 795-802.

AKIZUKI, K. H., GARTMAN, E. J., NISONSON, B., BEN-AVI, S. & ET AL. 2001. The Relative Stress on the Achilles Tendon During Ambulation in an Ankle Immobiliser: Implications for Rehabilitation after Achilles Tendon Repair / Commentary. *British Journal of Sports Medicine,* 35**,** 329.

AL-ABBAD, H. & SIMON, J. V. 2013. The Effectiveness of Extracorporeal Shock Wave Therapy on Chronic Achilles Tendinopathy: A Systematic Review. *Foot & Ankle International,* 34**,** 33-41.

ALBERS, I. S., ZWERVER, J., DIERCKS, R. L., DEKKER, J. H. & VAN DEN AKKER-SCHEEK, I. 2016. Incidence and Prevalence of Lower Extremity Tendinopathy in a Dutch General Practice Population: A Cross Sectional Study. *BMC Musculoskeletal Disorders,* 17**,** 16.

ALLARD, P., THIRY, P. S., BOURGAULT, A. & DROUIN, G. 1979. Pressure Dependence of 'the Area Micrometer' Method in Evaluation of Cruciate Ligament Cross-Section. *Journal of Biomedical Engineering,* 1**,** 265-267.

ALMEKINDERS, L. C. 1998. Etiology, Diagnosis, and Treatment of Tendonitis: An Analysis of the Literature. *Med Sci Sports Exerc,* 30**,** 1183-90.

ALMEKINDERS, L. C., WEINHOLD, P. S. & MAFFULLI, N. 2003. Compression Etiology in Tendinopathy. *Clin Sports Med,* 22**,** 703-10.

ALRASHIDI, Y., ALRABAI, H. M., ALSAYED, H. & VALDERRABANO, V. 2015. Achilles Tendon in Sport. *Sports Orthopaedics and Traumatology Sport-Orthopädie - Sport-Traumatologie,* 31**,** 282-292.

AMIS, A. & SCAMMELL, B. 1993. Biomechanics of Intra-Articular and Extra-Articular Reconstruction of the Anterior Cruciate Ligament. *The Journal of bone and joint surgery. British volume,* 75-B**,** 812-817.

ANDARAWIS-PURI, N., FLATOW, E. L. & SOSLOWSKY, L. J. 2015. Tendon Basic Science: Development, Repair, Regeneration, and Healing. *Journal of orthopaedic research : official publication of the Orthopaedic Research Society,* 33**,** 780-784.

ANDARAWIS-PURI, N., SEREYSKY, J. B., JEPSEN, K. J. & FLATOW, E. L. 2012. The Relationships between Cyclic Fatigue Loading, Changes in Initial Mechanical

Properties, and the in Vivo Temporal Mechanical Response of the Rat Patellar Tendon. *Journal of Biomechanics,* 45**,** 59-65.

ANDERSSON, G., FORSGREN, S., SCOTT, A., GAIDA, J. E., STJERNFELDT, J. E., LORENTZON, R., ALFREDSON, H., BACKMAN, C. & DANIELSON, P. 2011. Tenocyte Hypercellularity and Vascular Proliferation in a Rabbit Model of Tendinopathy: Contralateral Effects Suggest the Involvement of Central Neuronal Mechanisms. *British Journal of Sports Medicine,* 45**,** 399-406.

ANSORGE, H. L., ADAMS, S., BIRK, D. E. & SOSLOWSKY, L. J. 2011. Mechanical, Compositional, and Structural Properties of the Post-Natal Mouse Achilles Tendon. *Annals of Biomedical Engineering,* 39**,** 1904-1913.

ANSSARI-BENAM, A., BADER, D. L. & SCREEN, H. R. C. 2011. Anisotropic Time-Dependant Behaviour of the Aortic Valve. *Journal of the Mechanical Behavior of Biomedical Materials,* 4**,** 1603-1610.

ANSSARI-BENAM, A., GUPTA, H. S. & SCREEN, H. R. C. 2012a. Strain Transfer through the Aortic Valve. *Journal of Biomechanical Engineering,* 134.

ANSSARI-BENAM, A., LEGERLOTZ, K., BADER, D. L. & SCREEN, H. R. C. 2012b. On the Specimen Length Dependency of Tensile Mechanical Properties in Soft Tissues: Gripping Effects and the Characteristic Decay Length. *Journal of Biomechanics,* 45**,** 2481-2482.

ANSSARI-BENAM, A., LEGERLOTZ, K., BADER, D. L. & SCREEN, H. R. C. 2013. Response to Letter to the Editor: "End Effects in Mechanical Testing of Biomaterials". *Journal of Biomechanics,* 46**,** 1042.

ARAMPATZIS, A., KARAMANIDIS, K., MOREY-KLAPSING, G., DE MONTE, G. & STAFILIDIS, S. 2007. Mechanical Properties of the Triceps Surae Tendon and Aponeurosis in Relation to Intensity of Sport Activity. *Journal of Biomechanics,* 40**,** 1946-1952.

ARAMPATZIS, A., PEPER, A., BIERBAUM, S. & ALBRACHT, K. 2010. Plasticity of Human Achilles Tendon Mechanical and Morphological Properties in Response to Cyclic Strain. *Journal of Biomechanics,* 43**,** 3073-3079.

ARAMPATZIS, A., STAFILIDIS, S., DEMONTE, G., KARAMANIDIS, K., MOREY-KLAPSING, G. & BRÜGGEMANN, G. P. 2005. Strain and Elongation of the Human Gastrocnemius Tendon and Aponeurosis During Maximal Plantarflexion Effort. *Journal of Biomechanics,* 38**,** 833-841.

ARCHAMBAULT, J. M., HART, D. A. & HERZOG, W. 2001. Response of Rabbit Achilles Tendon to Chronic Repetitive Loading. *Connective Tissue Research,* 42**,** 13-23.

ARCHAMBAULT, J. M., JELINSKY, S. A., LAKE, S. P., HILL, A. A., GLASER, D. L. & SOSLOWSKY, L. J. 2007. Rat Supraspinatus Tendon Expresses Cartilage Markers with Overuse. *Journal of Orthopaedic Research,* 25**,** 617-624.

ARNDT, A. N., KOMI, P. V., BRÜGGEMANN, G. P. & LUKKARINIEMI, J. 1998. Individual Muscle Contributions to the in Vivo Achilles Tendon Force. *Clinical Biomechanics,* 13**,** 532-541.

ARNOCZKY, S. P., LAVAGNINO, M. & EGERBACHER, M. 2007. The Mechanobiological Aetiopathogenesis of Tendinopathy: Is It the over-Stimulation or the under-Stimulation of Tendon Cells? *International Journal of Experimental Pathology,* 88**,** 217-226.

ARNOCZKY, S. P., LAVAGNINO, M., WHALLON, J. H. & HOONJAN, A. 2002a. In Situ Cell Nucleus Deformation in Tendons under Tensile Load; a Morphological Analysis Using Confocal Laser Microscopy. *Journal of Orthopaedic Research,* 20**,** 29-35.

ARNOCZKY, S. P., TIAN, T., LAVAGNINO, M. & GARDNER, K. 2004. Ex Vivo Static Tensile Loading Inhibits Mmp-1 Expression in Rat Tail Tendon Cells through a Cytoskeletally Based Mechanotransduction Mechanism. *Journal of Orthopaedic Research,* 22**,** 328-333.

ARNOCZKY, S. P., TIAN, T., LAVAGNINO, M., GARDNER, K., SCHULER, P. & MORSE, P. 2002b. Activation of Stress-Activated Protein Kinases (Sapk) in Tendon Cells Following Cyclic Strain: The Effects of Strain Frequency, Strain Magnitude, and Cytosolic Calcium. *Journal of Orthopaedic Research,* 20**,** 947-952.

ARYA, S. & KULIG, K. 2010. Tendinopathy Alters Mechanical and Material Properties of the Achilles Tendon. *Journal of Applied Physiology,* 108**,** 670-675.

ATKINSON, T. S., EWERS, B. J. & HAUT, R. C. 1999. The Tensile and Stress Relaxation Responses of Human Patellar Tendon Varies with Specimen Cross-Sectional Area. *Journal of Biomechanics,* 32**,** 907-914.

AUSTRALIAN INSTITUTE OF HEALTH AND WELFARE 2010. Australia's Health 2010. *Australia's health.* 12 ed. Canberra: AIHW.

AUSTRALIAN INSTITUTE OF HEALTH AND WELFARE 2017. The Burden of Musculoskeletal Conditions in Australia: A Detailed Analysis of the Australian Burden of Disease Study 2011. *Australian Burden of Disease Study.* 18 ed. Canberra: AIHW.

AWAD, H. A., BUTLER, D. L., BOIVIN, G. P., SMITH, F. N. L., MALAVIYA, P., HUIBREGTSE, B. & CAPLAN, A. I. 1999. Autologous Mesenchymal Stem Cell-Mediated Repair of Tendon. *Tissue Engineering,* 5**,** 267-277.

BACKMAN, C., BOQUIST, L., FRIDÉN, J., LORENTZON, R. & TOOLANEN, G. 1990. Chronic Achilles Paratenonitis with Tendinosis: An Experimental Model in the Rabbit. *Journal of Orthopaedic Research,* 8**,** 541-547.

BANES, A. J., HORESOVSKY, G., LARSON, C., TSUZAKI, M., JUDEX, S., ARCHAMBAULT, J., ZERNICKE, R., HERZOG, W., KELLEY, S. & MILLER, L. 1999. Mechanical Load Stimulates Expression of Novel Genesin Vivoandin Vitroin Avian Flexor Tendon Cells. *Osteoarthritis and Cartilage,* 7**,** 141-153.

BARATTA, R. & SOLOMONOW, M. 1991. The Effect of Tendon Viscoelastic Stiffness on the Dynamic Performance of Isometric Muscle. *Journal of Biomechanics,* 24**,** 109-116.

BARIA, K. E., BADER, D. L., SCREEN, H. R. C. & LEE, D. A. 2005. The Effect of Substrate and Medium Composition on the Response of Human Dermal Fibroblasts to Cyclic Tensile Strain in Vitro. *International Journal of Experimental Pathology,* 86**,** A32-A33.

BATES, D., MÄCHLER, M., BOLKER, B. & WALKER, S. 2015. Fitting Linear Mixed-Effects Models Using Lme4. *2015,* 67**,** 48.

BATTERY, L. & MAFFULLI, N. 2011. Inflammation in Overuse Tendon Injuries. *Sports Med Arthrosc,* 19**,** 213-217.

BAYMURAT, A. C., OZTURK, A. M., YETKIN, H., ERGUN, M. A., HELVACIOGLU, F., OZKIZILCIK, A., TUZLAKOGLU, K., SENER, E. E. & ERDOGAN, D. 2015. Bio-Engineered Synovial Membrane to Prevent Tendon Adhesions in Rabbit Flexor Tendon Model. *Journal of Biomedical Materials Research Part A,* 103**,** 84-90.

BELL, R., LI, J., GORSKI, D. J., BARTELS, A. K., SHEWMAN, E. F., WYSOCKI, R. W., COLE, B. J., BACH, J. B. R., MIKECZ, K., SANDY, J. D., PLAAS, A. H. & WANG, V. M. 2013. Controlled Treadmill Exercise Eliminates Chondroid Deposits and Restores Tensile Properties in a New Murine Tendinopathy Model. *Journal of Biomechanics,* 46**,** 498-505.

BENEDICT, J. V., WALKER, L. B. & HARRIS, E. H. 1968. Stress-Strain Characteristics and Tensile Strength of Unembalmed Human Tendon. *Journal of Biomechanics,* 1**,** 53-63.

BENJAMIN, M., KAISER, E. & MILZ, S. 2008. Structure-Function Relationships in Tendons: A Review. *J Anat,* 212**,** 211-228.

BENJAMIN, M. & RALPHS, J. R. 1996. Tendons in Health and Disease. *Manual Therapy,* 1**,** 186-191.

BENJAMIN, M. & RALPHS, J. R. 2004. Biology of Fibrocartilage Cells. *In:* KWANG, W. J. (ed.) *International Review of Cytology.* Academic Press.

BENJAMIN, M., TOUMI, H., RALPHS, J. R., BYDDER, G., BEST, T. M. & MILZ, S. 2006. Where Tendons and Ligaments Meet Bone: Attachment Sites ('Entheses') in Relation to Exercise and/or Mechanical Load. *J Anat,* 208**,** 471-490.

BERGOMI, M., ANSELM WISKOTT, H. W., BOTSIS, J., SHIBATA, T. & BELSER, U. C. 2009. Mechanical Response of Periodontal Ligament: Effects of Specimen Geometry, Preconditioning Cycles and Time Lapse. *Journal of Biomechanics,* 42**,** 2410-2414.

BHOLE, A. P., FLYNN, B. P., LILES, M., SAEIDI, N., DIMARZIO, C. A. & RUBERTI, J. W. 2009. Mechanical Strain Enhances Survivability of Collagen Micronetworks in the Presence of Collagenase: Implications for Load-Bearing Matrix Growth and Stability. *Philosophical Transactions of the Royal Society A: Mathematical, Physical and Engineering Sciences,* 367**,** 3339-3362.

BIRCH, H. L., BAILEY, J. V. B., BAILEY, A. J. & GOODSHIP, A. E. 1999. Age-Related Changes to the Molecular and Cellular Components of Equine Flexor Tendons. *Equine Veterinary Journal,* 31**,** 391-396.

BIRCH, H. L., THORPE, C. T. & RUMIAN, A. P. 2013. Specialisation of Extracellular Matrix for Function in Tendons and Ligaments. *Muscles Ligaments Tendons J,* 3**,** 12-22.

BLANTON, P. L. & BIGGS, N. L. 1970. Ultimate Tensile Strength of Fetal and Adult Human Tendons. *Journal of Biomechanics,* 3**,** 181-189.

BOGAERTS, S., DESMET, H., SLAGMOLEN, P. & PEERS, K. 2016. Strain Mapping in the Achilles Tendon - a Systematic Review. *Journal of Biomechanics,* 49**,** 1411-1419.

BOHM, S., MERSMANN, F. & ARAMPATZIS, A. 2015. Human Tendon Adaptation in Response to Mechanical Loading: A Systematic Review and Meta-Analysis of Exercise Intervention Studies on Healthy Adults. *Sports Medicine - Open,* 1**,** 7.

BOHM, S., MERSMANN, F., TETTKE, M., KRAFT, M. & ARAMPATZIS, A. 2014. Human Achilles Tendon Plasticity in Response to Cyclic Strain: Effect of Rate and Duration. *The Journal of Experimental Biology,* 217**,** 4010-4017.

BOKHARI, A. R. & MURRELL, G. A. C. 2012. The Role of Nitric Oxide in Tendon Healing. *Journal of Shoulder and Elbow Surgery,* 21**,** 238-244.

BOLKER, B. & R DEVELOPMENT CORE TEAM 2017. Bbmle: Tools for General Maximum Likelihood Estimation. 1.0.19 ed.

BONNER, T. J., NEWELL, N., KARUNARATNE, A., PULLEN, A. D., AMIS, A. A., M.J. BULL, A. & MASOUROS, S. D. 2015. Strain-Rate Sensitivity of the Lateral Collateral Ligament of the Knee. *Journal of the Mechanical Behavior of Biomedical Materials,* 41**,** 261-270.

BOWMAN, S. M., KEAVENY, T. M., GIBSON, L. J., HAYES, W. C. & MCMAHON, T. A. 1994. Compressive Creep Behavior of Bovine Trabecular Bone. *Journal of Biomechanics,* 27**,** 301-310.

BUTLER, D. L., GROOD, E. S., NOYES, F. R. & ZERNICKE, R. F. 1978. Biomechanics of Tendons and Ligaments. *Exercise and Sport Sciences Reviews,* 6.

BUTLER, D. L., GROOD, E. S., NOYES, F. R., ZERNICKE, R. F. & BRACKETT, K. 1984. Effects of Structure and Strain Measurement Technique on the Material Properties of Young Human Tendons and Fascia. *Journal of Biomechanics,* 17**,** 579-596.

BUTLER, D. L., GUAN, Y., KAY, M. D., CUMMINGS, J. F., FEDER, S. M. & LEVY, M. S. 1992. Location-Dependent Variations in the Material Properties of the Anterior Cruciate Ligament. *Journal of Biomechanics,* 25**,** 511-518.

BUTLER, D. L., JUNCOSA-MELVIN, N., BOIVIN, G. P., GALLOWAY, M. T., SHEARN, J. T., GOOCH, C. & AWAD, H. 2008. Functional Tissue Engineering for Tendon Repair: A Multidisciplinary Strategy Using Mesenchymal Stem Cells, Bioscaffolds, and Mechanical Stimulation. *Journal of Orthopaedic Research,* 26**,** 1-9.

BUTLER, D. L., KAY, M. D. & STOUFFER, D. C. 1986. Comparison of Material Properties in Fascicle-Bone Units from Human Patellar Tendon and Knee Ligaments. *Journal of Biomechanics,* 19**,** 425-432.

CACCHIOLI, A., RAVANETTI, F., SOLIANI, L. & BORGHETTI, P. 2012. Preliminary Study on the Mineral Apposition Rate in Distal Femoral Epiphysis of New Zealand White Rabbit at Skeletal Maturity. *Anatomia, Histologia, Embryologia,* 41**,** 163-169.

CALVE, S., DENNIS, R. G., KOSNIK, P. E., BAAR, K., GROSH, K. & ARRUDA, E. M. 2004. Engineering of Functional Tendon. *Tissue Engineering,* 10**,** 755-761.

CANAVESE, F., DIMEGLIO, A., D'AMATO, C., VOLPATTI, D., GRANIER, M., STEBEL, M., CAVALLI, F. & CANAVESE, B. 2010. Dorsal Arthrodesis in Prepubertal New Zealand White Rabbits Followed to Skeletal Maturity: Effect on Thoracic Dimensions, Spine Growth and Neural Elements. *Indian Journal of Orthopaedics,* 44**,** 14-22.

CARMIGNATO, S. 2012. Accuracy of Industrial Computed Tomography Measurements: Experimental Results from an International Comparison. *CIRP Annals - Manufacturing Technology,* 61**,** 491-494.

CARNIEL, E. L., FONTANELLA, C. G., STEFANINI, C. & NATALI, A. N. 2013. A Procedure for the Computational Investigation of Stress-Relaxation Phenomena. *Mechanics of Time-Dependent Materials,* 17**,** 25-38.

CARPENTER, J. E., FLANAGAN, C. L., THOMOPOULOS, S., YIAN, E. H. & SOSLOWSKY, L. J. 1998. The Effects of Overuse Combined with Intrinsic or Extrinsic Alterations in an Animal Model of Rotator Cuff Tendinosis. *Am J Sports Med,* 26**,** 801-807.

CHANDRASHEKAR, N., SLAUTERBECK, J. & HASHEMI, J. 2012. Effects of Cyclic Loading on the Tensile Properties of Human Patellar Tendon. *The Knee,* 19**,** 65-68.

CHATZISTERGOS, P. E., TSITSILONIS, S. I., MITOUSOUDIS, A. S., PERREA, D. N., ZOUBOS, A. B. & KOURKOULIS, S. K. 2010. The Fracture Stress of Rat Achilles Tendons. *Scandinavian Journal of Laboratory Animal Science,* 37**,** 149-156.

CHAUDHURY, S., HOLLAND, C., THOMPSON, M. S., VOLLRATH, F. & CARR, A. J. 2012. Tensile and Shear Mechanical Properties of Rotator Cuff Repair Patches. *Journal of Shoulder and Elbow Surgery,* 21**,** 1168-1176.

CHEN, J., XIA, G., ZHOU, K., XIA, G. & QIN, Y. 2005. Two-Step Digital Image Correlation for Micro-Region Measurement. *Optics and Lasers in Engineering,* 43**,** 836-846.

CHEN, J., YU, Q., WU, B., LIN, Z., PAVLOS, N. J., XU, J., OUYANG, H., WANG, A. & ZHENG, M. H. 2011a. Autologous Tenocyte Therapy for Experimental Achilles Tendinopathy in a Rabbit Model. *Tissue Engineering Part A,* 17**,** 2037-2048.

CHEN, L., WU, Y., YU, J., JIAO, Z., AO, Y., YU, C., WANG, J. & CUI, G. 2011b. Effect of Repeated Freezing–Thawing on the Achilles Tendon of Rabbits. *Knee Surgery, Sports Traumatology, Arthroscopy,* 19**,** 1028-1034.

CHEN, Y.-J., WANG, C.-J., YANG, K. D., KUO, Y.-R., HUANG, H.-C., HUANG, Y.-T., SUN, Y.-C. & WANG, F.-S. 2004. Extracorporeal Shock Waves Promote Healing of Collagenase-Induced Achilles Tendinitis and Increase Tgf-B1 and Igf-I Expression. *Journal of Orthopaedic Research,* 22**,** 854-861.

CHENG, S., CLARKE, E. C. & BILSTON, L. E. 2009. The Effects of Preconditioning Strain on Measured Tissue Properties. *Journal of Biomechanics,* 42**,** 1360-1362.

CHENG, T. & GAN, R. Z. 2008. Experimental Measurement and Modeling Analysis on Mechanical Properties of Tensor Tympani Tendon. *Medical Engineering & Physics,* 30**,** 358-366.

CHENG, V. W. T. & SCREEN, H. R. C. 2007. The Micro-Structural Strain Response of Tendon. *Journal of Materials Science,* 42**,** 8957-8965.

CHEUNG, J. T.-M. & ZHANG, M. 2006. A Serrated Jaw Clamp for Tendon Gripping. *Medical Engineering & Physics,* 28**,** 379-382.

CIARLETTA, P., DARIO, P. & MICERA, S. 2008. Pseudo-Hyperelastic Model of Tendon Hysteresis from Adaptive Recruitment of Collagen Type I Fibrils. *Biomaterials,* 29**,** 764-770.

CIARLETTA, P., MICERA, S., ACCOTO, D. & DARIO, P. 2006. A Novel Microstructural Approach in Tendon Viscoelastic Modelling at the Fibrillar Level. *Journal of Biomechanics,* 39**,** 2034-2042.

CLAUSET, A., SHALIZI, C. R. & NEWMAN, M. E. 2009. Power-Law Distributions in Empirical Data. *SIAM review,* 51**,** 661-703.

CLAVERT, P., CLAVERT, J. F., KEMPF, F., BONNOMET, P., BOUTEMY, L., MARCELIN, J. L. & KAHN 2001. Effects of Freezing/Thawing on the Biomechanical Properties of Human Tendons. *Surgical and radiologic anatomy,* 23**,** 259-262.

CLEMMER, J., LIAO, J., DAVIS, D., HORSTEMEYER, M. F. & WILLIAMS, L. N. 2010. A Mechanistic Study for Strain Rate Sensitivity of Rabbit Patellar Tendon. *Journal of Biomechanics,* 43**,** 2785-2791.

COHEN, R. E., HOOLEY, C. J. & MCCRUM, N. G. 1976. Viscoelastic Creep of Collagenous Tissue. *Journal of Biomechanics,* 9**,** 175-184.

CONNELLY, J. T., VANDERPLOEG, E. J., MOUW, J. K., WILSON, C. G. & LEVENSTON, M. E. 2010. Tensile Loading Modulates Bone Marrow Stromal Cell Differentiation and the Development of Engineered Fibrocartilage Constructs. *Tissue Engineering Part A,* 16**,** 1913-1923.

CONNIZZO, B. K., SARVER, J. J., HAN, L. & SOSLOWSKY, L. J. 2014. In Situ Fibril Stretch and Sliding Is Location-Dependent in Mouse Supraspinatus Tendons. *Journal of Biomechanics,* 47**,** 3794-3798.

CONNIZZO, B. K., SARVER, J. J., IOZZO, R. V., BIRK, D. E. & SOSLOWSKY, L. J. 2013. Effect of Age and Proteoglycan Deficiency on Collagen Fiber Re-Alignment and Mechanical Properties in Mouse Supraspinatus Tendon. *Journal of Biomechanical Engineering,* 135**,** 021019-021019-8.

COUPPE, C., HANSEN, P., KONGSGAARD, M., KOVANEN, V., SUETTA, C., AAGAARD, P., KJAER, M. & MAGNUSSON, S. P. 2009. Mechanical Properties and Collagen Cross-Linking of the Patellar Tendon in Old and Young Men. *Journal of Applied Physiology,* 107**,** 880-6.

CRAMMOND, G., BOYD, S. W. & DULIEU-BARTON, J. M. 2013. Speckle Pattern Quality Assessment for Digital Image Correlation. *Optics and Lasers in Engineering,* 51**,** 1368-1378.

CRISCO, J. J., MOORE, D. C. & MCGOVERN, R. D. 2002. Strain-Rate Sensitivity of the Rabbit Mcl Diminishes at Traumatic Loading Rates. *Journal of Biomechanics,* 35**,** 1379-1385.

CRONKITE, A. E. 1936. The Tensile Strength of Human Tendons. *The Anatomical Record,* 64**,** 173-186.

D'ADDONA, A., MAFFULLI, N., FORMISANO, S. & ROSA, D. 2017. Inflammation in Tendinopathy. *Surgeon,* 15**,** 297-302.

DAVIS, F. M. & DE VITA, R. 2012. A Nonlinear Constitutive Model for Stress Relaxation in Ligaments and Tendons. *Annals of Biomedical Engineering,* 40**,** 2541-2550.

DE CHIFFRE, L., CARMIGNATO, S., KRUTH, J.-P., SCHMITT, R. & WECKENMANN, A. 2014. Industrial Applications of Computed Tomography. *CIRP Annals - Manufacturing Technology,* 63**,** 655-677.

DE JONGE, S., VAN DEN BERG, C., DE VOS, R. J., VAN DER HEIDE, H. J., WEIR, A., VERHAAR, J. A., BIERMA-ZEINSTRA, S. M. & TOL, J. L. 2011. Incidence of Midportion Achilles Tendinopathy in the General Population. *British Journal of Sports Medicine,* 45**,** 1026-1028.

DEFRATE, L. E., VAN DER VEN, A., GILL, T. J. & LI, G. 2004. The Effect of Length on the Structural Properties of an Achilles Tendon Graft as Used in Posterior Cruciate Ligament Reconstruction. *Am J Sports Med,* 32**,** 993-997.

DEL BUONO, A., CHAN, O. & MAFFULLI, N. 2013. Achilles Tendon: Functional Anatomy and Novel Emerging Models of Imaging Classification. *International Orthopaedics,* 37**,** 715-21.

DELIGIANNI, D. D., MARIS, A. & MISSIRLIS, Y. F. 1994. Stress Relaxation Behaviour of Trabecular Bone Specimens. *Journal of Biomechanics,* 27**,** 1469-1476.

DEVKOTA, A. C. & WEINHOLD, P. S. 2003. Mechanical Response of Tendon Subsequent to Ramp Loading to Varying Strain Limits. *Clinical Biomechanics,* 18**,** 969-974.

DIRKS, R. C. & WARDEN, S. J. 2011. Models for the Study of Tendinopathy. *J Musculoskelet Neuronal Interact,* 11**,** 141-9.

DOCKING, S. I., ROSENGARTEN, S. D., DAFFY, J. & COOK, J. 2015. Structural Integrity Is Decreased in Both Achilles Tendons in People with Unilateral Achilles Tendinopathy. *Journal of Science and Medicine in Sport,* 18**,** 383-387.

DOHERTY, G. P., KOIKE, Y., UHTHOFF, H. K., LECOMPTE, M. & TRUDEL, G. 2006. Comparative Anatomy of Rabbit and Human Achilles Tendons with Magnetic Resonance and Ultrasound Imaging. *Comp Med,* 56**,** 68-74.

DORAL, M. N., ALAM, M., BOZKURT, M., TURHAN, E., ATAY, O. A., DÖNMEZ, G. & MAFFULLI, N. 2010. Functional Anatomy of the Achilles Tendon. *Knee Surgery, Sports Traumatology, Arthroscopy,* 18**,** 638-43.

DOURTE, L. M., PERRY, S. M., GETZ, C. L. & SOSLOWSKY, L. J. 2010. Tendon Properties Remain Altered in a Chronic Rat Rotator Cuff Model. *Clin Orthop Relat Res,* 468**,** 1485-1492.

DOWLING, B. A., DART, A. J., HODGSON, D. R., ROSE, R. J. & WALSH, W. R. 2002a. The Effect of Recombinant Equine Growth Hormone on the Biomechanical Properties of Healing Superficial Digital Flexor Tendons in Horses. *Veterinary Surgery,* 31**,** 320-324.

DOWLING, B. A., DART, A. J., HODGSON, D. R., ROSE, R. J. & WALSH, W. R. 2002b. Recombinant Equine Growth Hormone Does Not Affect the in Vitro Biomechanical Properties of Equine Superficial Digital Flexor Tendon. *Veterinary Surgery,* 31**,** 325-330.

DRESSLER, M. R., BUTLER, D. L. & BOIVIN, G. P. 2006. Age-Related Changes in the Biomechanics of Healing Patellar Tendon. *Journal of Biomechanics,* 39**,** 2205-2212.

DU, Y.-C., CHEN, Y.-F., LI, C.-M., LIN, C.-H., YANG, C.-E., WU, J.-X. & CHEN, T. 2013. Quantitative Ultrasound Method for Assessing Stress–Strain Properties and the Cross-Sectional Area of Achilles Tendon. *Measurement Science and Technology,* 24**,** 125702.

DUENWALD-KUEHL, S., KOBAYASHI, H., LAKES, R. & VANDERBY, J. R. 2012a. Time-Dependent Ultrasound Echo Changes Occur in Tendon During Viscoelastic Testing. *Journal of Biomechanical Engineering,* 134**,** 111006-111006.

DUENWALD-KUEHL, S., KONDRATKO, J., LAKES, R. S. & VANDERBY JR, R. 2012b. Damage Mechanics of Porcine Flexor Tendon: Mechanical Evaluation and Modeling. *Annals of Biomedical Engineering,* 40**,** 1692-1707.

DUENWALD, S., KOBAYASHI, H., FRISCH, K., LAKES, R. & VANDERBY JR, R. 2011. Ultrasound Echo Is Related to Stress and Strain in Tendon. *Journal of Biomechanics,* 44**,** 424-429.

DUENWALD, S., VANDERBY, R., JR. & LAKES, R. 2009a. Viscoelastic Relaxation and Recovery of Tendon. *Annals of Biomedical Engineering,* 37**,** 1131-1140.

DUENWALD, S., VANDERBY, R. & LAKES, R. Nonlinear Viscoelastic Relaxation and Recovery of Porcine Flexor Tendon. 45th meeting, Society of Engineering Science, University of Illinois, 2008.

DUENWALD, S. E., VANDERBY, R., JR. & LAKES, R. S. 2009b. Constitutive Equations for Ligament and Other Soft Tissue: Evaluation by Experiment. *Acta Mechanica,* 205**,** 23-33.

DUENWALD, S. E., VANDERBY, R. & LAKES, R. S. 2010. Stress Relaxation and Recovery in Tendon and Ligament: Experiment and Modeling. *Biorheology,* 47**,** 1-14.

DURRINGTON, P. N., ADAMS, J. E. & BEASTALL, M. D. 1982. The Assessment of Achilles Tendon Size in Primary Hypercholesterolaemia by Computed Tomography. *Atherosclerosis,* 45**,** 345-358.

EJERHED, L., KARTUS, J., KÖHLER, K., SERNERT, N., BRANDSSON, S. & KARLSSON, J. 2001. Preconditioning Patellar Tendon Autografts in Arthroscopic Anterior Cruciate Ligament Reconstruction: A Prospective Randomized Study. *Knee Surgery, Sports Traumatology, Arthroscopy,* 9**,** 6-11.

ELDEN, H. R. 1964. Hydration of Connective Tissue and Tendon Elasticity. *Biochimica et Biophysica Acta (BBA) - Specialized Section on Biophysical Subjects,* 79**,** 592-599.

ELLIOTT, D. M., ROBINSON, P. S., GIMBEL, J. A., SARVER, J. J., ABBOUD, J. A., IOZZO, R. V. & SOSLOWSKY, L. J. 2003. Effect of Altered Matrix Proteins on Quasilinear Viscoelastic Properties in Transgenic Mouse Tail Tendons. *Annals of Biomedical Engineering,* 31**,** 599-605.

ELLIS, D. G. 1969. Cross-Sectional Area Measurements for Tendon Specimens: A Comparison of Several Methods. *Journal of Biomechanics,* 2**,** 175-186.

ELZHOV, T. V., MULLEN, K. M., SPIESS, A.-N. & BOLKER, B. 2016. Minpack.Lm: R Interface to the Levenberg-Marquardt Nonlinear Least-Squares Algorithm Found in Minpack, Plus Support for Bounds. 1.2.1 ed.

ERDEMIR, A., HAMEL, A. J., PIAZZA, S. J. & SHARKEY, N. A. 2003. Fiberoptic Measurement of Tendon Forces Is Influenced by Skin Movement Artifact. *Journal of Biomechanics,* 36**,** 449-455.

EVANS, J. H. & BARBENEL, J. C. 1975. Structural and Mechanical Properties of Tendon Related to Function. *Equine Veterinary Journal,* 7**,** 1-8.

EVANS, S. L., HOLT, C. A., OZTURK, H., SAIDI, K. & SHRIVE, N. G. 2007. Measuring Soft Tissue Properties Using Digital Image Correlation and Finite Element Modelling. *In:* GDOUTOS, E. E. (ed.) *Experimental Analysis of Nano and Engineering Materials and Structures.* Springer Netherlands.

FAN, G. 3d Anatomical Investigation of Achilles Tendon Using a Freehand Ultrasound Imaging System. Bioinformatics and Biomedical Engineering (iCBBE), 2010 4th International Conference on, 18-20 June 2010 2010 Chengdu. 1-3.

FANG, F. & LAKE, S. P. 2015. Multiscale Strain Analysis of Tendon Subjected to Shear and Compression Demonstrates Strain Attenuation, Fiber Sliding, and Reorganization. *Journal of Orthopaedic Research,* 33**,** 1704-1712.

FANG, F. & LAKE, S. P. 2016. Modelling Approaches for Evaluating Multiscale Tendon Mechanics. *Interface Focus,* 6**,** 20150044.

FARAJ, K. A., CUIJPERS, V. M. J. I., WISMANS, R. G., WALBOOMERS, X. F., JANSEN, J. A., VAN KUPPEVELT, T. H. & DAAMEN, W. F. 2009. Micro-Computed Tomographical Imaging of Soft Biological Materials Using Contrast Techniques. *Tissue Engineering Part C: Methods,* 15**,** 493-499.

FARRIS, D. J., TREWARTHA, G., MCGUIGAN, M. P. & LICHTWARK, G. A. 2013. Differential Strain Patterns of the Human Achilles Tendon Determined in Vivo with Freehand Three-Dimensional Ultrasound Imaging. *Journal of Experimental Biology,* 216**,** 594-600.

FESSEL, G. & SNEDEKER, J. G. 2009. Evidence against Proteoglycan Mediated Collagen Fibril Load Transmission and Dynamic Viscoelasticity in Tendon. *Matrix Biology,* 28**,** 503-510.

FINK, B., SCHWINGER, G., SINGER, J., SCHMIELAU, G. & RÜTHER, W. 1999. Biomechanical Properties of Tendons During Lower-Leg Lengthening in Dogs Using the Ilizarov Method. *Journal of Biomechanics,* 32**,** 763-768.

FINNI, T., KOMI, P. V. & LUKKARINIEMI, J. 1998. Achilles Tendon Loading During Walking: Application of a Novel Optic Fiber Technique. *European Journal of Applied Physiology and Occupational Physiology,* 77**,** 289-291.

FLOOD, L. & HARRISON, J. E. 2009. Epidemiology of Basketball and Netball Injuries That Resulted in Hospital Admission in Australia, 2000-2004. *The Medical journal of Australia,* 190**,** 87.

FLYNN, B. P., BHOLE, A. P., SAEIDI, N., LILES, M., DIMARZIO, C. A. & RUBERTI, J. W. 2010. Mechanical Strain Stabilizes Reconstituted Collagen Fibrils against Enzymatic Degradation by Mammalian Collagenase Matrix Metalloproteinase 8 (Mmp-8). *PLoS One,* 5**,** e12337.

FORNELLS, P., GARCIA-AZNAR, J. & DOBLARE, M. 2007. A Finite Element Dual Porosity Approach to Model Deformation-Induced Fluid Flow in Cortical Bone. *Annals of Biomedical Engineering,* 35**,** 1687.

FOURE, A., CORNU, C. & NORDEZ, A. 2012. Is Tendon Stiffness Correlated to the Dissipation Coefficient? *Physiological Measurement,* 33**,** N1-9.

FRANCESCA, R., EDOARDO, S., VITTORIO, F., MARCO, Z., CARLO, G., PAOLO, B. & ANTONIO, C. 2015. The Effect of Age, Anatomical Site and Bone Structure on Osteogenesis in New Zealand White Rabbit. *Journal of Biological Research,* 88.

FRANCHI, M., QUARANTA, M., DE PASQUALE, V., MACCIOCCA, M., ORSINI, E., TRIRE, A., OTTANI, V. & RUGGERI, A. 2007a. Tendon Crimps and Peritendinous Tissues Responding to Tensional Forces. *European Journal Of Histochemistry,* 51**,** 9-14.

FRANCHI, M., TRIRÈ, A., QUARANTA, M., ORSINI, E. & OTTANI, V. 2007b. Collagen Structure of Tendon Relates to Function. *The Scientific World Journal,* 7**,** 404-20.

FREEDMAN, B. R., GORDON, J. A., BHATT, P. R., PARDES, A. M., THOMAS, S. J., SARVER, J. J., RIGGIN, C. N., TUCKER, J. J., WILLIAMS, A. W., ZANES, R. C., HAST, M. W., FARBER, D. C., SILBERNAGEL, K. G. & SOSLOWSKY, L. J. 2016. Nonsurgical Treatment and Early Return to Activity Leads to Improved Achilles Tendon Fatigue Mechanics and Functional Outcomes During Early Healing in an Animal Model. *Journal of Orthopaedic Research,* 34**,** 2172-2180.

FREEDMAN, B. R., GORDON, J. A. & SOSLOWSKY, L. J. 2014a. The Achilles Tendon: Fundamental Properties and Mechanisms Governing Healing. *Muscles Ligaments Tendons J,* 4**,** 245-255.

FREEDMAN, B. R., SARVER, J. J., BUCKLEY, M. R., VOLETI, P. B. & SOSLOWSKY, L. J. 2014b. Biomechanical and Structural Response of Healing Achilles Tendon to Fatigue Loading Following Acute Injury. *Journal of Biomechanics,* 47**,** 2028-2034.

FREEDMAN, B. R., ZUSKOV, A., SARVER, J. J., BUCKLEY, M. R. & SOSLOWSKY, L. J. 2015. Evaluating Changes in Tendon Crimp with Fatigue Loading as an Ex Vivo Structural Assessment of Tendon Damage. *Journal of orthopaedic research : official publication of the Orthopaedic Research Society,* 33**,** 904-910.

FRYHOFER, G. W., FREEDMAN, B. R., HILLIN, C. D., SALKA, N. S., PARDES, A. M., WEISS, S. N., FARBER, D. C. & SOSLOWSKY, L. J. 2016. Postinjury Biomechanics of Achilles Tendon Vary by Sex and Hormone Status. *Journal of Applied Physiology,* 121**,** 1106-1114.

FU, S.-C., ROLF, C., CHEUK, Y.-C., LUI, P. P. Y. & CHAN, K.-M. 2010. Deciphering the Pathogenesis of Tendinopathy: A Three-Stages Process. *Sports Medicine, Arthroscopy, Rehabilitation, Therapy and Technology : SMARTT,* 2**,** 30.

FUJIE, H., YAMAMOTO, N., MURAKAMI, T. & HAYASHI, K. 2000. Effects of Growth on the Response of the Rabbit Patellar Tendon to Stress Shielding: A Biomechanical Study. *Clinical Biomechanics,* 15**,** 370-378.

FUKUTA, S., OYAMA, M., KAVALKOVICH, K., FU, F. H. & NIYIBIZI, C. 1998. Identification of Types Ii, Ix and X Collagens at the Insertion Site of the Bovine Achilles Tendon. *Matrix Biology,* 17**,** 65-73.

FUNK, J. R., HALL, G. W., CRANDALL, J. R. & PILKEY, W. D. 1999. Linear and Quasi-Linear Viscoelastic Characterization of Ankle Ligaments. *Journal of Biomechanical Engineering,* 122**,** 15-22.

GALESKI, A., KASTELIC, J., BAER, E. & KOHN, R. R. 1977. Mechanical and Structural Changes in Rat Tail Tendon Induced by Alloxan Diabetes and Aging. *Journal of Biomechanics,* 10**,** 775-782.

GAO, Z. & DESAI, J. P. 2010. Estimating Zero-Strain States of Very Soft Tissue under Gravity Loading Using Digital Image Correlation. *Medical Image Analysis,* 14**,** 126-137.

GAUT, L. & DUPREZ, D. 2016. Tendon Development and Diseases. *Wiley Interdisciplinary Reviews: Developmental Biology,* 5**,** 5-23.

GAUTIERI, A., VESENTINI, S., REDAELLI, A. & BALLARINI, R. 2013. Modeling and Measuring Visco-Elastic Properties: From Collagen Molecules to Collagen Fibrils. *International Journal of Non-Linear Mechanics,* 56**,** 25-33.

GENOVESE, K., LEE, Y. U. & HUMPHREY, J. D. 2011. Novel Optical System for in Vitro Quantification of Full Surface Strain Fields in Small Arteries: Ii. Correction for Refraction and Illustrative Results. *Computer Methods in Biomechanics and Biomedical Engineering,* 14**,** 227-237.

GENOVESE, K., LEE, Y. U., LEE, A. Y. & HUMPHREY, J. D. 2013. An Improved Panoramic Digital Image Correlation Method for Vascular Strain Analysis and Material Characterization. *Journal of the Mechanical Behavior of Biomedical Materials,* 27**,** 132-142.

GEREMIA, J. M., BOBBERT, M. F., CASA NOVA, M., OTT, R. D., LEMOS FDE, A., LUPION RDE, O., FRASSON, V. B. & VAZ, M. A. 2015. The Structural and Mechanical Properties of the Achilles Tendon 2 Years after Surgical Repair. *Clinical Biomechanics,* 30**,** 485-92.

GIANNINI, S., BUDA, R., CAPRIO, F., AGATI, P., BIGI, A., PASQUALE, V. & RUGGERI, A. 2008. Effects of Freezing on the Biomechanical and Structural Properties of Human Posterior Tibial Tendons. *International Orthopaedics,* 32**,** 145-151.

GIESINGER, K., EBNETER, L., DAY, R. E., STOFFEL, K. K., YATES, P. J. & KUSTER, M. S. 2014. Can Plate Osteosynthesis of Periprosthethic Femoral Fractures Cause Cement Mantle Failure around a Stable Hip Stem? A Biomechanical Analysis. *The Journal of Arthroplasty,* 29**,** 1308-12.

GILBERT, J. A., WEINHOLD, P. S., BANES, A. J., LINK, G. W. & JONES, G. L. 1994. Strain Profiles for Circular Cell Culture Plates Containing Flexible Surfaces Employed to Mechanically Deform Cells in Vitro. *Journal of Biomechanics,* 27**,** 1169-1177.

GILES, J. M., BLACK, A. E. & BISCHOFF, J. E. 2007. Anomalous Rate Dependence of the Preconditioned Response of Soft Tissue During Load Controlled Deformation. *Journal of Biomechanics,* 40**,** 777-785.

GIMBEL, J. A., SARVER, J. J. & SOSLOWSKY, L. J. 2005. The Effect of Overshooting the Target Strain on Estimating Viscoelastic Properties from Stress Relaxation Experiments. *Journal of Biomechanical Engineering,* 126**,** 844-848.

GLAZEBROOK, M. A., WRIGHT, J. R., LANGMAN, M., STANISH, W. D. & LEE, J. M. 2008. Histological Analysis of Achilles Tendons in an Overuse Rat Model. *Journal of Orthopaedic Research,* 26**,** 840-846.

GLOS, D. L., BUTLER, D. L., GROOD, E. S. & LEVY, M. S. 1993. In Vitro Evaluation of an Implantable Force Transducer (Ift) in a Patellar Tendon Model. *Journal of Biomechanical Engineering,* 115**,** 335-43.

GOH, J. C.-H., OUYANG, H.-W., TEOH, S.-H., CHAN, C. K. C. & LEE, E.-H. 2003. Tissue-Engineering Approach to the Repair and Regeneration of Tendons and Ligaments. *Tissue Engineering,* 9**,** 31-44.

GOODSHIP, A. E. & BIRCH, H. L. 2005. Cross Sectional Area Measurement of Tendon and Ligament in Vitro: A Simple, Rapid, Non-Destructive Technique. *Journal of Biomechanics,* 38**,** 605-608.

GUILAK, F. & MOW, V. C. 2000. The Mechanical Environment of the Chondrocyte: A Biphasic Finite Element Model of Cell-Matrix Interactions in Articular Cartilage. *Journal of Biomechanics,* 33**,** 1663-1673.

GUILAK, F., RATCLIFFE, A., LANE, N., ROSENWASSER, M. P. & MOW, V. C. 1994. Mechanical and Biochemical Changes in the Superficial Zone of Articular Cartilage in Canine Experimental Osteoarthritis. *Journal of Orthopaedic Research,* 12**,** 474-484.

GUPTA, H. S., SETO, J., KRAUSS, S., BOESECKE, P. & SCREEN, H. R. C. 2010. In Situ Multi-Level Analysis of Viscoelastic Deformation Mechanisms in Tendon Collagen. *Journal of Structural Biology,* 169**,** 183-191.

HAN, W. M., HEO, S. J., DRISCOLL, T. P., SMITH, L. J., MAUCK, R. L. & ELLIOTT, D. M. 2013. Macro- to Microscale Strain Transfer in Fibrous Tissues Is Heterogeneous and Tissue-Specific. *Biophysical Journal,* 105**,** 807-817.

HANDSFIELD, G. G., INOUYE, J. M., SLANE, L. C., THELEN, D. G., MILLER, G. W. & BLEMKER, S. S. 2017. A 3d Model of the Achilles Tendon to Determine the Mechanisms Underlying Nonuniform Tendon Displacements. *Journal of Biomechanics,* 51**,** 17-25.

HANSEN, P., BOJSEN-MOLLER, J., AAGAARD, P., KJAER, M. & MAGNUSSON, S. P. 2006. Mechanical Properties of the Human Patellar Tendon, in Vivo. *Clinical Biomechanics,* 21**,** 54-58.

HANSEN, P., KOVANEN, V., HÖLMICH, P., KROGSGAARD, M., HANSSON, P., DAHL, M., HALD, M., AAGAARD, P., KJAER, M. & MAGNUSSON, S. P. 2013. Micromechanical Properties and Collagen Composition of Ruptured Human Achilles Tendon. *Am J Sports Med,* 41**,** 437-443.

HANSEN, W., SHIM, V. B., OBST, S., LLOYD, D. G., NEWSHAM-WEST, R. & BARRETT, R. S. 2017. Achilles Tendon Stress Is More Sensitive to Subject-Specific Geometry Than Subject-Specific Material Properties: A Finite Element Analysis. *Journal of Biomechanics,* 56**,** 26-31.

HARALDSSON, B. T., AAGAARD, P., KROGSGAARD, M., ALKJAER, T., KJAER, M. & MAGNUSSON, S. P. 2005. Region-Specific Mechanical Properties of the Human Patella Tendon. *Journal of Applied Physiology,* 98**,** 1006-1012.

HARVEY, A. K., THOMPSON, M. S., COCHLIN, L. E., RAJU, P. A., CUI, Z., CORNELL, H. R., HULLEY, P. A. & BRADY, S. M. 2009. Functional Imaging of Tendon. *Annals of the BMVA,* 8**,** 1-11.

HASHEMI, J., CHANDRASHEKAR, N., COWDEN, C. & SLAUTERBECK, J. 2005a. An Alternative Method of Anthropometry of Anterior Cruciate Ligament through 3-D Digital Image Reconstruction. *Journal of Biomechanics,* 38**,** 551-555.

HASHEMI, J., CHANDRASHEKAR, N. & SLAUTERBECK, J. 2005b. The Mechanical Properties of the Human Patellar Tendon Are Correlated to Its Mass Density and Are Independent of Sex. *Clinical Biomechanics,* 20**,** 645-652.

HAUT, T. L. & HAUT, R. C. 1997. The State of Tissue Hydration Determines the Strain-Rate-Sensitive Stiffness of Human Patellar Tendon. *Journal of Biomechanics,* 30**,** 79-81.

HAWKINS, D., LUM, C., GAYDOS, D. & DUNNING, R. 2009. Dynamic Creep and Pre-Conditioning of the Achilles Tendon in-Vivo. *Journal of Biomechanics,* 42**,** 2813-2817.

HAYES, A., EASTON, K., DEVANABOYINA, P. T., WU, J.-P., KIRK, T. B. & LLOYD, D. 2016. Structured White Light Scanning of Rabbit Achilles Tendon. *Journal of Biomechanics,* 49**,** 3753-3758.

HELLAND, C., BOJSEN-MØLLER, J., RAASTAD, T., SEYNNES, O. R., MOLTUBAKK, M. M., JAKOBSEN, V., VISNES, H. & BAHR, R. 2013. Mechanical Properties of the Patellar Tendon in Elite Volleyball Players with and without Patellar Tendinopathy. *British Journal of Sports Medicine,* 47**,** 862-868.

HELMER, K. G., WELLEN, J., GRIGG, P. & SOTAK, C. H. 2004. Measurement of the Spatial Redistribution of Water in Rabbit Achilles Tendon in Response to Static Tensile Loading. *Journal of Biomechanical Engineering,* 126**,** 651-656.

HENNINGER, H. B., UNDERWOOD, C. J., ATESHIAN, G. A. & WEISS, J. A. 2010. Effect of Sulfated Glycosaminoglycan Digestion on the Transverse Permeability of Medial Collateral Ligament. *Journal of Biomechanics,* 43**,** 2567-2573.

HEUER, F., WOLFRAM, U., SCHMIDT, H. & WILKE, H.-J. 2008. A Method to Obtain Surface Strains of Soft Tissues Using a Laser Scanning Device. *Journal of Biomechanics,* 41**,** 2402-2410.

HINGORANI, R. V., PROVENZANO, P. P., LAKES, R. S., ESCARCEGA, A. & VANDERBY, R. 2004. Nonlinear Viscoelasticity in Rabbit Medial Collateral Ligament. *Annals of Biomedical Engineering,* 32**,** 306-312.

HOOLEY, C. J. & COHEN, R. E. 1979. A Model for the Creep Behaviour of Tendon. *International Journal of Biological Macromolecules,* 1**,** 123-132.

HOOLEY, C. J., MCCRUM, N. G. & COHEN, R. E. 1980. The Viscoelastic Deformation of Tendon. *Journal of Biomechanics,* 13**,** 521-528.

HORGAN, C. O. 2013. End Effects in Mechanical Testing of Biomaterials. *Journal of Biomechanics,* 46**,** 1040-1041.

HSU, R. W.-W., HSU, W.-H., TAI, C.-L. & LEE, K.-F. 2004a. Effect of Shock-Wave Therapy on Patellar Tendinopathy in a Rabbit Model. *Journal of Orthopaedic Research,* 22**,** 221-227.

HSU, R. W., HSU, W. H., TAI, C. L. & LEE, K. F. 2004b. Effect of Hyperbaric Oxygen Therapy on Patellar Tendinopathy in a Rabbit Model. *The Journal of Trauma Injury Infection and Critical Care,* 57**,** 1060-4.

HUANG, C.-Y., WANG, V. M., FLATOW, E. L. & MOW, V. C. 2009. Temperature-Dependent Viscoelastic Properties of the Human Supraspinatus Tendon. *Journal of Biomechanics,* 42**,** 546-549.

HUANG, H., ZHANG, J., SUN, K., ZHANG, X. & TIAN, S. 2011. Effects of Repetitive Multiple Freeze–Thaw Cycles on the Biomechanical Properties of Human Flexor Digitorum Superficialis and Flexor Pollicis Longus Tendons. *Clinical Biomechanics,* 26**,** 419-423.

HUANG, T.-F., PERRY, S. M. & SOSLOWSKY, L. J. 2004. The Effect of Overuse Activity on Achilles Tendon in an Animal Model: A Biomechanical Study. *Annals of Biomedical Engineering,* 32**,** 336-341.

HUGATE, R., PENNYPACKER, J., SAUNDERS, M. & JULIANO, P. 2004. The Effects of Intratendinous and Retrocalcaneal Intrabursal Injections of Corticosteroid on the Biomechanical Properties of Rabbit Achilles Tendons. *Journal of Bone and Joint Surgery. American Volume,* 86-A**,** 794-801.

HUTTUNEN, T. T., KANNUS, P., ROLF, C., FELLANDER-TSAI, L. & MATTILA, V. M. 2014. Acute Achilles Tendon Ruptures: Incidence of Injury and Surgery in Sweden between 2001 and 2012. *Am J Sports Med,* 42**,** 2419-23.

IACONIS, F., STEINDLER, R. & MARINOZZI, G. 1987. Measurements of Cross-Sectional Area of Collagen Structures (Knee Ligaments) by Means of an Optical Method. *Journal of Biomechanics,* 20**,** 1003-1010.

IKOMA, K., KIDO, M., NAGAE, M., IKEDA, T., SHIRAI, T., UESHIMA, K., ARAI, Y., ODA, R., FUJIWARA, H. & KUBO, T. 2013. Effects of Stress-Shielding on the Dynamic Viscoelasticity and Ordering of the Collagen Fibers in Rabbit Achilles Tendon. *Journal of Orthopaedic Research,* 31**,** 1708-1712.

IMAI, K., IKOMA, K., CHEN, Q., ZHAO, C., AN, K.-N. & GAY, R. E. 2015. Biomechanical and Histological Effects of Augmented Soft Tissue Mobilization Therapy on Achilles Tendinopathy in a Rabbit Model. *Journal of Manipulative & Physiological Therapeutics,* 38**,** 112-118.

INGBER, D. E. 1997. Tensegrity: The Architectural Basis of Cellular Mechanotransduction. *Annual Review of Physiology,* 59**,** 575-599.

INGBER, D. E. 2006. Cellular Mechanotransduction: Putting All the Pieces Together Again. *The FASEB Journal,* 20**,** 811-827.

INGBER, D. E. 2008. Tensegrity and Mechanotransduction. *Journal of Bodywork and Movement Therapies,* 12**,** 198-200.

IRIUCHISHIMA, T., YORIFUJI, H., AIZAWA, S., TAJIKA, Y., MURAKAMI, T. & FU, F. H. 2014. Evaluation of Acl Mid-Substance Cross-Sectional Area for Reconstructed Autograft Selection. *Knee Surgery, Sports Traumatology, Arthroscopy,* 22**,** 207-213.

IYO, T., MAKI, Y., SASAKI, N. & NAKATA, M. 2004. Anisotropic Viscoelastic Properties of Cortical Bone. *Journal of Biomechanics,* 37**,** 1433-1437.

JAFARI, L., VACHON, P., BEAUDRY, F. & LANGELIER, E. 2015. Histopathological, Biomechanical, and Behavioral Pain Findings of Achilles Tendinopathy Using an Animal Model of Overuse Injury. *Physiological Reports,* 3**,** e12265-n/a.

JAGLOWSKI, J. R., WILLIAMS, B. T., TURNBULL, T. L., LAPRADE, R. F. & WIJDICKS, C. A. 2016. High-Load Preconditioning of Soft Tissue Grafts: An in Vitro Biomechanical Bovine Tendon Model. *Knee Surgery, Sports Traumatology, Arthroscopy,* 24**,** 895-902.

JAMES, R., KESTURU, G., BALIAN, G. & CHHABRA, A. B. 2008. Tendon: Biology, Biomechanics, Repair, Growth Factors, and Evolving Treatment Options. *Journal of Hand Surgery-American Volume,* 33A**,** 102-112.

JANUÁRIO, A. L., BARRIVIERA, M. & DUARTE, W. R. 2008. Soft Tissue Cone-Beam Computed Tomography: A Novel Method for the Measurement of Gingival Tissue and the Dimensions of the Dentogingival Unit. *Journal of Esthetic and Restorative Dentistry,* 20**,** 366-373.

JENSEN, K., DWYER, K., LAKES, R. & VANDERBY, R. 2004. Rate of Viscoelastic Recovery Is Faster Than the Rate of Creep. *50th Annual Meeting of the Orthopaedic Research Society.* San Francisco, CA: Orthopaedic Research Society.

JIMENEZ, M. L., BROWN, T. D. & BRAND, R. A. 1989. The Effects of Grip Proximity on Perceived Local in Vitro Tendon Strain. *Journal of Biomechanics,* 22**,** 949-955.

JISA, K. A., WILLIAMS, B. T., JAGLOWSKI, J. R., TURNBULL, T. L., LAPRADE, R. F. & WIJDICKS, C. A. 2016. Lack of Consensus Regarding Pretensioning and

Preconditioning Protocols for Soft Tissue Graft Reconstruction of the Anterior Cruciate Ligament. *Knee Surgery, Sports Traumatology, Arthroscopy,* 24**,** 2884-2891.

JOHNSON, G. A., LIVESAY, G. A., WOO, S. L. Y. & RAJAGOPAL, K. R. 1996. A Single Integral Finite Strain Viscoelastic Model of Ligaments and Tendons. *Journal of Biomechanical Engineering,* 118**,** 221-226.

JOHNSON, G. A., TRAMAGLINI, D. M., LEVINE, R. E., OHNO, K., CHOI, N.-Y. & L-Y. WOO, S. 1994. Tensile and Viscoelastic Properties of Human Patellar Tendon. *Journal of Orthopaedic Research,* 12**,** 796-803.

JUNCOSA, N., WEST, J. R., GALLOWAY, M. T., BOIVIN, G. P. & BUTLER, D. L. 2003. In Vivo Forces Used to Develop Design Parameters for Tissue Engineered Implants for Rabbit Patellar Tendon Repair. *Journal of Biomechanics,* 36**,** 483-488.

JUNG, H.-J., FISHER, M. & WOO, S. 2009. Role of Biomechanics in the Understanding of Normal, Injured, and Healing Ligaments and Tendons. *Sports Medicine, Arthroscopy, Rehabilitation, Therapy & Technology,* 1**,** 9.

JUNG, H.-J., VANGIPURAM, G., FISHER, M. B., YANG, G., HSU, S., BIANCHI, J., RONHOLDT, C. & WOO, S. L. Y. 2011. The Effects of Multiple Freeze–Thaw Cycles on the Biomechanical Properties of the Human Bone-Patellar Tendon-Bone Allograft. *Journal of Orthopaedic Research,* 29**,** 1193-1198.

KADER, D., MAFFULLI, N., LEADBETTER, W. B. & RENSTRÖM, P. 2005. Achilles Tendinopathy. *In:* MAFFULLI, N., RENSTRÖM, P. & LEADBETTER, W. B. (eds.) *Tendon Injuries: Basic Science and Clinical Medicine.* London: Springer London.

KADER, D., SAXENA, A., MOVIN, T. & MAFFULLI, N. 2002. Achilles Tendinopathy: Some Aspects of Basic Science and Clinical Management. *British Journal of Sports Medicine,* 36**,** 239-249.

KAHN, C. J. F., DUMAS, D., ARAB-TEHRANY, E., MARIE, V., TRAN, N., WANG, X. & CLEYMAND, F. 2013. Structural and Mechanical Multi-Scale Characterization of White New-Zealand Rabbit Achilles Tendon. *Journal of the Mechanical Behavior of Biomedical Materials,* 26**,** 81-89.

KAHN, C. J. F., WANG, X. & RAHOUADJ, R. 2010. Nonlinear Model for Viscoelastic Behavior of Achilles Tendon. *Journal of Biomechanical Engineering,* 132**,** 111002-111002.

KAINBERGER, F., MITTERMAIER, F., SEIDL, G., PARTH, E. & WEINSTABL, R. 1997. Imaging of Tendons—Adaptation, Degeneration, Rupture. *European Journal of Radiology,* 25**,** 209-222.

KALSON, N. S., HOLMES, D. F., KAPACEE, Z., OTERMIN, I., LU, Y., ENNOS, R. A., CANTY-LAIRD, E. G. & KADLER, K. E. 2010. An Experimental Model for Studying the Biomechanics of Embryonic Tendon: Evidence That the Development of Mechanical Properties Depends on the Actinomyosin Machinery. *Matrix Biology,* 29**,** 678-689.

KAMINENI, S., BUTTERFIELD, T. & SINAI, A. 2015. Percutaneous Ultrasonic Debridement of Tendinopathy—a Pilot Achilles Rabbit Model. *Journal of Orthopaedic Surgery and Research,* 10**,** 70.

KAMIŃSKI, A., GUT, G., MAROWSKA, J., ŁADA-KOZŁOWSKA, M., BIWEJNIS, W. & ZASACKA, M. 2009. Mechanical Properties of Radiation-Sterilised Human Bone-Tendon-Bone Grafts Preserved by Different Methods. *Cell and Tissue Banking,* 10**,** 215-219.

KANNUS, P. 2000. Structure of the Tendon Connective Tissue. *Scandinavian Journal of Medicine & Science in Sports,* 10**,** 312-320.

KANNUS, P. & JÓZSA, L. 1991. Histopathological Changes Preceding Spontaneous Rupture of a Tendon. A Controlled Study of 891 Patients. *The Journal of Bone and Joint Surgery,* 73**,** 1507-1525.

KASTELIC, J., GALESKI, A. & BAER, E. 1978. The Multicomposite Structure of Tendon. *Connective Tissue Research,* 6**,** 11-23.

KER, R. F. 1981. Dynamic Tensile Properties of the Plantaris Tendon of Sheep (Ovis Aries). *Journal of Experimental Biology,* 93**,** 283-302.

KHAN, M. H., LI, Z. & WANG, J. H.-C. 2005. Repeated Exposure of Tendon to Prostaglandin-E2 Leads to Localized Tendon Degeneration. *Clin J Sport Med,* 15**,** 27-33.

KHODABAKHSHI, G. Three Dimensional Strain Measurement by Image Registration Technique. Biomedical Engineering (ICBME), 2011 18th Iranian Conference of, 14-16 Dec. 2011 2011. 268-273.

KHODABAKHSHI, G., WALKER, D., SCUTT, A., WAY, L., COWIE, R. M. & HOSE, D. R. 2013. Measuring Three-Dimensional Strain Distribution in Tendon. *Journal of Microscopy,* 249**,** 195-205.

KIM, B. S., JOO, Y. C., CHOI, B. H., KIM, K. H., KANG, J. S. & PARK, S. R. 2015. The Effect of Dry Needling and Treadmill Running on Inducing Pathological Changes in Rat Achilles Tendon. *Connective Tissue Research,* 56**,** 452-460.

KIM, K. E., HSU, S.-L. & WOO, S. L. Y. 2014. Tensile Properties of the Medial Patellofemoral Ligament: The Effect of Specimen Orientation. *Journal of Biomechanics,* 47**,** 592-595.

KISS, M.-O., HAGEMEISTER, N., LEVASSEUR, A., FERNANDES, J., LUSSIER, B. & PETIT, Y. 2009. A Low-Cost Thermoelectrically Cooled Tissue Clamp for in Vitro Cyclic Loading and Load-to-Failure Testing of Muscles and Tendons. *Medical Engineering & Physics,* 31**,** 1182-1186.

KJÆR, M., LANGBERG, H., HEINEMEIER, K., BAYER, M. L., HANSEN, M., HOLM, L., DOESSING, S., KONGSGAARD, M., KROGSGAARD, M. R. & MAGNUSSON, S. P. 2009. From Mechanical Loading to Collagen Synthesis, Structural Changes and Function in Human Tendon. *Scandinavian Journal of Medicine & Science in Sports,* 19**,** 500-510.

KOFRON, M. D. & LAURENCIN, C. T. 2005. Orthopaedic Applications of Gene Therapy. *Current Gene Therapy,* 5**,** 37-61.

KOMATSU, K., SANCTUARY, C., SHIBATA, T., SHIMADA, A. & BOTSIS, J. 2007. Stress–Relaxation and Microscopic Dynamics of Rabbit Periodontal Ligament. *Journal of Biomechanics,* 40**,** 634-644.

KOMI, P. V. 1990. Relevance of in Vivo Force Measurements to Human Biomechanics. *Journal of Biomechanics,* 23**,** 23-34.

KOMI, P. V., FUKASHIRO, S. & JÄRVINEN, M. 1992. Biomechanical Loading of Achilles Tendon During Normal Locomotion. *Clin Sports Med,* 11**,** 521.

KONGSGAARD, M., AAGAARD, P., KJAER, M. & MAGNUSSON, S. P. 2005. Structural Achilles Tendon Properties in Athletes Subjected to Different Exercise Modes and in Achilles Tendon Rupture Patients. *Journal of Applied Physiology,* 99**,** 1965-1971.

KONGSGAARD, M., NIELSEN, C. H., HEGNSVAD, S., AAGAARD, P. & MAGNUSSON, S. P. 2011. Mechanical Properties of the Human Achilles Tendon, in Vivo. *Clinical Biomechanics,* 26**,** 772-777.

KORVICK, D. L., CUMMINGS, J. F., GROOD, E. S., HOLDEN, J. P., FEDER, S. M. & BUTLER, D. L. 1996. The Use of an Implantable Force Transducer to Measure Patellar Tendon Forces in Goats. *Journal of Biomechanics,* 29**,** 557-561.

KRUTH, J. P., BARTSCHER, M., CARMIGNATO, S., SCHMITT, R., DE CHIFFRE, L. & WECKENMANN, A. 2011. Computed Tomography for Dimensional Metrology. *CIRP Annals - Manufacturing Technology,* 60**,** 821-842.

KUO, C. K. & TUAN, R. S. 2010. Mechanoactive Tenogenic Differentiation of Human Mesenchymal Stem Cells. *Advances in Tissue Engineering: Volume 2.*

KUO, P.-L., LI, P.-C., SHUN, C.-T. & LAI, J.-S. 1999. Strain Measurements of Rabbit Achilles Tendons by Ultrasound. *Ultrasound in Medicine & Biology,* 25**,** 1241-1250.

LACROIX, A. S., DUENWALD-KUEHL, S. E., BRICKSON, S., AKINS, T. L., DIFFEE, G., AIKEN, J., VANDERBY, R., JR. & LAKES, R. S. 2013a. Effect of Age and Exercise on the Viscoelastic Properties of Rat Tail Tendon. *Annals of Biomedical Engineering,* 41**,** 1120-8.

LACROIX, A. S., DUENWALD-KUEHL, S. E., LAKES, R. S. & VANDERBY, R. 2013b. Relationship between Tendon Stiffness and Failure: A Metaanalysis. *Journal of Applied Physiology,* 115**,** 43-51.

LAKE, S. P., ANSORGE, H. L. & SOSLOWSKY, L. J. 2008. Animal Models of Tendinopathy. *Disabil Rehabil,* 30**,** 1530-1541.

LAKE, S. P., MILLER, K. S., ELLIOTT, D. M. & SOSLOWSKY, L. J. 2009. Effect of Fiber Distribution and Realignment on the Nonlinear and Inhomogeneous Mechanical Properties of Human Supraspinatus Tendon under Longitudinal Tensile Loading. *Journal of orthopaedic research : official publication of the Orthopaedic Research Society,* 27**,** 1596.

LAKE, S. P., MILLER, K. S., ELLIOTT, D. M. & SOSLOWSKY, L. J. 2010. Tensile Properties and Fiber Alignment of Human Supraspinatus Tendon in the Transverse Direction Demonstrate Inhomogeneity, Nonlinearity and Regional Isotropy. *Journal of Biomechanics,* 43**,** 727-732.

LAKES, R. S. & VANDERBY, R. 1999. Interrelation of Creep and Relaxation: A Modeling Approach for Ligaments. *Journal of Biomechanical Engineering,* 121**,** 612-5.

LAM, T. C., FRANK, C. B. & SHRIVE, N. G. 1992. Calibration Characteristics of a Video Dimension Analyser (Vda) System. *Journal of Biomechanics,* 25**,** 1227-1231.

LANGELIER, E., DUPUIS, D., GUILLOT, M., GOULET, F. & RANCOURT, D. 2004. Cross-Sectional Profiles and Volume Reconstructions of Soft Tissues Using Laser Beam Measurement. *Journal of Biomechanical Engineering,* 126**,** 796-802.

LANIR, Y. 1976. Biaxial Stress-Relaxation in Skin. *Annals of Biomedical Engineering,* 4**,** 250-270.

LANIR, Y. 2010. Physical Mechanisms of Soft Tissues Rheological Properties. *In:* CHIEN, S., CHEN, P. C. Y., SCHMID-SCHÖNBEIN, G. W., TONG, P. & WOO, S. L. Y. (eds.) *Tributes to Yuan-Cheng Fung on His 90th Birthday: Biomechanics: From Molecules to Man.* Singapore: World Scientific Publishing Co. Pte. Ltd.

LANTTO, I., HEIKKINEN, J., FLINKKILA, T., OHTONEN, P. & LEPPILAHTI, J. 2015. Epidemiology of Achilles Tendon Ruptures: Increasing Incidence over a 33-Year Period. *Scandinavian Journal of Medicine & Science in Sports,* 25**,** e133-8.

LAVAGNINO, M. & ARNOCZKY, S. P. 2005. In Vitro Alterations in Cytoskeletal Tensional Homeostasis Control Gene Expression in Tendon Cells. *Journal of Orthopaedic Research,* 23**,** 1211-1218.

LAVAGNINO, M., ARNOCZKY, S. P., EGERBACHER, M., GARDNER, K. L. & BURNS, M. E. 2006. Isolated Fibrillar Damage in Tendons Stimulates Local Collagenase Mrna Expression and Protein Synthesis. *Journal of Biomechanics,* 39**,** 2355-2362.

LAVAGNINO, M., ARNOCZKY, S. P., FRANK, K. & TIAN, T. 2005. Collagen Fibril Diameter Distribution Does Not Reflect Changes in the Mechanical Properties of in Vitro Stress-Deprived Tendons. *Journal of Biomechanics,* 38**,** 69-75.

LAVAGNINO, M., ARNOCZKY, S. P., KEPICH, E., CABALLERO, O. & HAUT, R. C. 2008. A Finite Element Model Predicts the Mechanotransduction Response of Tendon Cells to Cyclic Tensile Loading. *Biomechanics and Modeling in Mechanobiology,* 7**,** 405-16.

LAVAGNINO, M., BEDI, A., WALSH, C. P., SIBILSKY ENSELMAN, E. R., SHEIBANI-RAD, S. & ARNOCZKY, S. P. 2014. Tendon Contraction after Cyclic Elongation Is an Age-Dependent Phenomenon. *Am J Sports Med,* 42**,** 1471-1477.

LEE, T. Q. & WOO, S. L.-Y. 1988. A New Method for Determining Cross-Sectional Shape and Area of Soft Tissues. *Journal of Biomechanical Engineering,* 110**,** 110-114.

LEGERLOTZ, K., JONES, G. C., SCREEN, H. R. C. & RILEY, G. P. 2013a. Cyclic Loading of Tendon Fascicles Using a Novel Fatigue Loading System Increases Interleukin-6 Expression by Tenocytes. *Scandinavian Journal of Medicine & Science in Sports,* 23**,** 31-37.

LEGERLOTZ, K., RILEY, G. P. & SCREEN, H. R. C. 2010. Specimen Dimensions Influence the Measurement of Material Properties in Tendon Fascicles. *Journal of Biomechanics,* 43**,** 2274-2280.

LEGERLOTZ, K., RILEY, G. P. & SCREEN, H. R. C. 2013b. Gag Depletion Increases the Stress-Relaxation Response of Tendon Fascicles, but Does Not Influence Recovery. *Acta Biomaterialia,* 9**,** 6860-6866.

LEGRAND, A., KAUFMAN, Y., LONG, C. & FOX, P. M. 2017. Molecular Biology of Flexor Tendon Healing in Relation to Reduction of Tendon Adhesions. *Journal of Hand Surgery (American Volume),* 42**,** 722-726.

LEPETIT, J., FAVIER, R., GRAJALES, A. & SKJERVOLD, P. O. 2004. A Simple Cryogenic Holder for Tensile Testing of Soft Biological Tissues. *Journal of Biomechanics,* 37**,** 557-562.

LERSCH, C., GROTSCH, A., SEGESSER, B., KOEBKE, J., BRUGGEMANN, G. P. & POTTHAST, W. 2012. Influence of Calcaneus Angle and Muscle Forces on Strain Distribution in the Human Achilles Tendon. *Clinical Biomechanics,* 27**,** 955-61.

LEWIS, G. & SHAW, K. M. 1997. Tensile Properties of Human Tendo Achillis: Effect of Donor Age and Strain Rate. *The Journal of Foot and Ankle Surgery,* 36**,** 435-445.

LIANOGLOU, M. D. T. S. S. & ANTONYAN, A. S. W. C. F. R. S. A. E. 2014. Data.Table: Extension of Data.Frame. R package version 1.9.4. ed.: data.table: Extension of data.frame.

LICHTWARK, G. A. & WILSON, A. M. 2005. In Vivo Mechanical Properties of the Human Achilles Tendon During One-Legged Hopping. *Journal of Experimental Biology,* 208**,** 4715-25.

LIN, T. W., CARDENAS, L. & SOSLOWSKY, L. J. 2005. Tendon Properties in Interleukin-4 and Interleukin-6 Knockout Mice. *Journal of Biomechanics,* 38**,** 99-105.

LIONELLO, G., SIRIEIX, C. & BALEANI, M. 2014. An Effective Procedure to Create a Speckle Pattern on Biological Soft Tissue for Digital Image Correlation Measurements. *Journal of the Mechanical Behavior of Biomedical Materials,* 39**,** 1-8.

LIU, J., CHOU, S. M. & GOH, K. L. 2009. Age Effects on the Tensile and Stress Relaxation Properties of Mouse Tail Tendons. *In:* LIM, C. T. & GOH, J. C. H. (eds.) *13th International Conference on Biomedical Engineering: Icbme 2008 3–6 December 2008 Singapore.* Berlin, Heidelberg: Springer Berlin Heidelberg.

LIU, M. J. J., CHOU, S. M., GOH, K. L. & TAN, S. H. 2008. Cross-Sectional Area Measurement of Soft Tissues in Vitro: A Non-Contact Laser Scan Method. *Journal of Mechanics in Medicine and Biology,* 8**,** 353-361.

LIU, Z. & YEUNG, K. On Preconditioning and Stress Relaxation Behaviour of Fresh Swine Skin in Different Fibre Direction. 2006 International Conference on Biomedical and Pharmaceutical Engineering, 11-14 Dec. 2006 2006. 221-226.

LIU, Z. & YEUNG, K. 2008. The Preconditioning and Stress Relaxation of Skin Tissue. *Journal of Biomedical & Pharmaceutical Engineering,* 2**,** 22-28.

LOCKWOOD, W. C., MARCHETTI, D. C., DAHL, K. D., MIKULA, J. D., WILLIAMS, B. T., KHEIR, M. M., TURNBULL, T. L. & LAPRADE, R. F. 2016. High-Load Preconditioning of Human Soft Tissue Hamstring Grafts: An in Vitro Biomechanical Analysis. *Knee Surgery, Sports Traumatology, Arthroscopy,* 25**,** 1-6.

LONGO, U. G., RONGA, M. & MAFFULLI, N. 2009. Achilles Tendinopathy. *Sports Med Arthrosc,* 17**,** 112-26.

LU, H. H. & THOMOPOULOS, S. 2013. Functional Attachment of Soft Tissues to Bone: Development, Healing, and Tissue Engineering. *Annual Review of Biomedical Engineering,* 15**,** 201-226.

LUI, P. P.-Y., FU, S.-C., CHAN, L.-S., HUNG, L.-K. & CHAN, K.-M. 2009. Chondrocyte Phenotype and Ectopic Ossification in Collagenase-Induced Tendon Degeneration. *J Histochem Cytochem,* 57**,** 91-100.

LUI, P. P. Y., MAFFULLI, N., ROLF, C. & SMITH, R. K. W. 2011. What Are the Validated Animal Models for Tendinopathy? *Scandinavian Journal of Medicine & Science in Sports,* 21**,** 3-17.

LYNCH, H. A., JOHANNESSEN, W., WU, J. P., JAWA, A. & ELLIOTT, D. M. 2003. Effect of Fiber Orientation and Strain Rate on the Nonlinear Uniaxial Tensile Material Properties of Tendon. *Journal of Biomechanical Engineering,* 125**,** 726-731.

MACHIRAJU, C., PHAN, A. V., PEARSALL, A. W. & MADANAGOPAL, S. 2006. Viscoelastic Studies of Human Subscapularis Tendon: Relaxation Test and a Wiechert Model. *Computer Methods and Programs in Biomedicine,* 83**,** 29-33.

MAEDA, E., FLEISCHMANN, C., MEIN, C. A., SHELTON, J. C., BADER, D. L. & LEE, D. A. 2010. Functional Analysis of Tenocytes Gene Expression in Tendon Fascicles Subjected to Cyclic Tensile Strain. *Connective Tissue Research,* 51**,** 434-444.

MAFFULLI, N. 1998. Overuse Tendon Conditions: Time to Change a Confusing Terminology. *Arthroscopy: The Journal of Arthroscopic & Related Surgery,* 14**,** 840-843.

MAFFULLI, N., LONGO, U. G. & DENARO, V. 2010. Novel Approaches for the Management of Tendinopathy. *The Journal of Bone & Joint Surgery,* 92**,** 2604-2613.

MAFFULLI, N., SHARMA, P. & LUSCOMBE, K. L. 2004. Achilles Tendinopathy: Aetiology and Management. *J R Soc Med,* 97**,** 472-476.

MAFFULLI, N., VIA, A. G. & OLIVA, F. 2015. Chronic Achilles Tendon Disorders: Tendinopathy and Chronic Rupture. *Clin Sports Med,* 34**,** 607-24.

MAGANARIS, C. N. & NARICI, M. V. 2005. Mechanical Properties of Tendons. *In:* MAFFULLI, N., RENSTRÖM, P. & LEADBETTER, W. B. (eds.) *Tendon Injuries: Basic Science and Clinical Medicine.* London: Springer London.

MAGANARIS, C. N. & PAUL, J. P. 2000. Hysteresis Measurements in Intact Human Tendon. *Journal of Biomechanics,* 33**,** 1723-1727.

MAGANARIS, C. N. & PAUL, J. P. 2002. Tensile Properties of the in Vivo Human Gastrocnemius Tendon. *Journal of Biomechanics,* 35**,** 1639-1646.

MAGNAN, B., BONDI, M., PIERANTONI, S. & SAMAILA, E. 2014. The Pathogenesis of Achilles Tendinopathy: A Systematic Review. *Foot and Ankle Surgery,* 20**,** 154-9.

MAJIMA, T., YASUDA, K., FUJII, T., YAMAMOTO, N., HAYASHI, K. & KANEDA, K. 1996. Biomechanical Effects of Stress Shielding of the Rabbit Patellar Tendon Depend on the Degree of Stress Reduction. *Journal of Orthopaedic Research,* 14**,** 377-383.

MÄKELÄ, J. T. A. & KORHONEN, R. K. 2016. Highly Nonlinear Stress-Relaxation Response of Articular Cartilage in Indentation: Importance of Collagen Nonlinearity. *Journal of Biomechanics,* 49**,** 1734-1741.

MALAVIYA, P., BUTLER, D. L., KORVICK, D. L. & PROCH, F. S. 1998. In Vivo Tendon Forces Correlate with Activity Level and Remain Bounded: Evidence in a Rabbit Flexor Tendon Model. *Journal of Biomechanics,* 31**,** 1043-1049.

MANLEY JR, E., PROVENZANO, P. P., HEISEY, D., LAKES, R. & VANDERBY JR, R. 2003. Required Test Duration for Group Comparisons in Ligament Viscoelasticity: A Statistical Approach. *Biorheology,* 40**,** 441-450.

MARCOS, R. L., ARNOLD, G., MAGNENET, V., RAHOUADJ, R., MAGDALOU, J. & LOPES-MARTINS, R. Á. B. 2014. Biomechanical and Biochemical Protective Effect of Low-Level Laser Therapy for Achilles Tendinitis. *Journal of the Mechanical Behavior of Biomedical Materials,* 29**,** 272-285.

MARCOS, R. L., LEAL-JUNIOR, E. C. P., ARNOLD, G., MAGNENET, V., RAHOUADJ, R., WANG, X., DEMEURIE, F., MAGDALOU, J., DE CARVALHO, M. H. C. & LOPES-MARTINS, R. Á. B. 2012. Low-Level Laser Therapy in Collagenase-Induced Achilles Tendinitis in Rats: Analyses of Biochemical and Biomechanical Aspects. *Journal of Orthopaedic Research,* 30**,** 1945-1951.

MASOUROS, S. D., PARKER, K. H., HILL, A. M., AMIS, A. A. & BULL, A. M. J. 2009. Testing and Modelling of Soft Connective Tissues of Joints: A Review. *The Journal of Strain Analysis for Engineering Design,* 44**,** 305-318.

MATTHEWS, L. S. & ELLIS, D. 1968. Viscoelastic Properties of Cat Tendon: Effects of Time after Death and Preservation by Freezing. *Journal of Biomechanics,* 1**,** 65-71.

MATTUCCI, S. F. E., MOULTON, J. A., CHANDRASHEKAR, N. & CRONIN, D. S. 2013. Strain Rate Dependent Properties of Human Cranioverterbral Ligaments. *Journal of the Mechanical Behavior of Biomedical Materials,* 23**,** 71-79.

MEYER, D. C., JACOB, H. A. C., NYFFELER, R. W. & GERBER, C. 2004. In Vivo Tendon Force Measurement of 2-Week Duration in Sheep. *Journal of Biomechanics,* 37**,** 135-140.

MICHEL, M. C., ZYSSET, P. K. & ANGST, M. P. 1994. Creep Behaviour of Bovine Trabecular Bone. *Journal of Biomechanics,* 27**,** 840.

MIKOS, A. G., HERRING, S. W., OCHAREON, P., ELISSEEFF, J., LU, H. H., KANDEL, R., SCHOEN, F. J., TONER, M., MOONEY, D., ATALA, A., VAN DYKE, M. E., KAPLAN, D. & VUNJAK-NOVAKOVIC, G. 2006. Engineering Complex Tissues. *Tissue Engineering,* 12**,** 3307-3339.

MILLER, K. S., CONNIZZO, B. K., FEENEY, E. & SOSLOWSKY, L. J. 2012a. Characterizing Local Collagen Fiber Re-Alignment and Crimp Behavior Throughout Mechanical Testing in a Mature Mouse Supraspinatus Tendon Model. *Journal of Biomechanics,* 45**,** 2061-2065.

MILLER, K. S., CONNIZZO, B. K., FEENEY, E., TUCKER, J. J. & SOSLOWSKY, L. J. 2012b. Examining Differences in Local Collagen Fiber Crimp Frequency Throughout Mechanical Testing in a Developmental Mouse Supraspinatus Tendon Model. *Journal of Biomechanical Engineering,* 134**,** 41004-NaN.

MILLER, K. S., EDELSTEIN, L., CONNIZZO, B. K. & SOSLOWSKY, L. J. 2012c. Effect of Preconditioning and Stress Relaxation on Local Collagen Fiber Re-Alignment: Inhomogeneous Properties of Rat Supraspinatus Tendon. *Journal of Biomechanical Engineering,* 134**,** 31007-NaN.

MOON, D. K., ABRAMOWITCH, S. D. & WOO, S. L.-Y. 2006a. The Development and Validation of a Charge-Coupled Device Laser Reflectance System to Measure the Complex Cross-Sectional Shape and Area of Soft Tissues. *Journal of Biomechanics,* 39**,** 3071-3075.

MOON, D. K., WOO, S. L. Y., TAKAKURA, Y., GABRIEL, M. T. & ABRAMOWITCH, S. D. 2006b. The Effects of Refreezing on the Viscoelastic and Tensile Properties of Ligaments. *Journal of Biomechanics,* 39**,** 1153-1157.

MORELLI, F., FERRETTI, A., CONTEDUCA, F., NANNI, F., MONTELEONE, L. & VALENTE, M. 2002. A Modified Cryo-Jaw for in Vitro Biomechanical Testing of Tendons. *Journal of Applied Biomechanics,* 18**,** 384-389.

MORRISON, S. M., DICK, T. J. & WAKELING, J. M. 2015. Structural and Mechanical Properties of the Human Achilles Tendon: Sex and Strength Effects. *Journal of Biomechanics,* 48**,** 3530-3.

MURRELL, G. A. C. 2007. Oxygen Free Radicals and Tendon Healing. *Journal of Shoulder and Elbow Surgery,* 16**,** S208-S214.

MYERS, B. S., MCELHANEY, J. H. & DOHERTY, B. J. 1991. The Viscoelastic Responses of the Human Cervical Spine in Torsion: Experimental Limitations of Quasi-Linear Theory, and a Method for Reducing These Effects. *Journal of Biomechanics,* 24**,** 811-817.

NABESHIMA, Y., GROOD, E. S., SAKURAI, A. & HERMAN, J. H. 1996. Uniaxial Tension Inhibits Tendon Collagen Degradation by Collagenase in Vitro. *Journal of Orthopaedic Research,* 14**,** 123-130.

NAGASAWA, K., NOGUCHI, M., IKOMA, K. & KUBO, T. 2008. Static and Dynamic Biomechanical Properties of the Regenerating Rabbit Achilles Tendon. *Clinical Biomechanics,* 23**,** 832-838.

NAITO, K., YANG, J.-M., TANAKA, Y. & KAGAWA, Y. 2011. The Effect of Gauge Length on Tensile Strength and Weibull Modulus of Polyacrylonitrile (Pan)- and Pitch-Based Carbon Fibers. *Journal of Materials Science,* 47**,** 632-642.

NAKAGAWA, Y., HAYASHI, K., YAMAMOTO, N. & NAGASHIMA, K. 1996. Age-Related Changes in Biomechanical Properties of the Achilles Tendon in Rabbits. *European Journal of Applied Physiology and Occupational Physiology,* 73**,** 7-10.

NEBEL, J.-C. 2001. Soft Tissue Modeling from 3d Scanned Data. *Proceedings of the IFIP TC5/WG5.10 DEFORM'2000 Workshop and AVATARS'2000 Workshop on Deformable Avatars.* Kluwer, B.V.

NEKOUZADEH, A., PRYSE, K. M., ELSON, E. L. & GENIN, G. M. 2007. A Simplified Approach to Quasi-Linear Viscoelastic Modeling. *Journal of Biomechanics,* 40**,** 3070-3078.

NEVIASER, A., ANDARAWIS-PURI, N. & FLATOW, E. 2012. Basic Mechanisms of Tendon Fatigue Damage. *Journal of shoulder and elbow surgery / American Shoulder and Elbow Surgeons ... [et al.],* 21**,** 158-163.

NG, G. Y.-F., CHUNG, P. Y.-M., WANG, J. S. & CHEUNG, R. T.-H. 2011. Enforced Bipedal Downhill Running Induces Achilles Tendinosis in Rats. *Connective Tissue Research,* 52**,** 466-471.

NICKISCH, F. 2009. Anatomy of the Achilles Tendon. *The Achilles Tendon: Treatment and Rehabilitation,* 3-16.

NIRMALANANDHAN, V. S., RAO, M., SACKS, M. S., HARIDAS, B. & BUTLER, D. L. 2007. Effect of Length of the Engineered Tendon Construct on Its Structure-Function Relationships in Culture. *Journal of Biomechanics,* 40**,** 2523-2529.

NOGUCHI, M., KITAURA, T., IKOMA, K. & KUSAKA, Y. 2002. A Method of in-Vitro Measurement of the Cross-Sectional Area of Soft Tissues, Using Ultrasonography. *Journal of Orthopaedic Science,* 7**,** 247-251.

NOYES, F. R., DELUCAS, J. L. & TORVIK, P. J. 1974. Biomechanics of Anterior Cruciate Ligament Failure: An Analysis of Strain-Rate Sensitivity and Mechanisms of Failure in Primates. *Journal of Bone and Joint Surgery,* 56**,** 236-53.

O'BRIEN, M. 2005. Anatomy of Tendons. *In:* MAFFULLI, N., RENSTRÖM, P. & LEADBETTER, W. B. (eds.) *Tendon Injuries: Basic Science and Clinical Medicine.* London: Springer London.

O'CONNELL, G. D., JACOBS, N. T., SEN, S., VRESILOVIC, E. J. & ELLIOTT, D. M. 2011. Axial Creep Loading and Unloaded Recovery of the Human Intervertebral Disc and the Effect of Degeneration. *Journal of the Mechanical Behavior of Biomedical Materials,* 4**,** 933-942.

OBST, S. J., BARRETT, R. S. & NEWSHAM-WEST, R. 2013. Immediate Effect of Exercise on Achilles Tendon Properties: Systematic Review. *Medicine & Science in Sports & Exercise,* 45**,** 1534-44.

OBST, S. J., NEWSHAM-WEST, R. & BARRETT, R. S. 2014a. In vivo Measurement of Human Achilles Tendon Morphology Using Freehand 3-D Ultrasound. *Ultrasound in Medicine & Biology,* 40**,** 62-70.

OBST, S. J., RENAULT, J.-B., NEWSHAM-WEST, R. & BARRETT, R. S. 2014b. Three-Dimensional Deformation and Transverse Rotation of the Human Free Achilles Tendon in Vivo During Isometric Plantarflexion Contraction. *Journal of Applied Physiology,* 116**,** 376-384.

OHNO, K., YASUDA, K., YAMAMOTO, N., KANEDA, K. & HAYASHI, K. 1993. Effects of Complete Stress-Shielding on the Mechanical Properties and Histology of in Situ Frozen Patellar Tendon. *Journal of Orthopaedic Research,* 11**,** 592-602.

OKOTIE, G., KOBAYASHI, H., WU, M.-J., VANDERBY, R. & DUENWALD-KUEHL, S. 2012. Tendon Strain Measurements with Dynamic Ultrasound Images: Evaluation of Digital Image Correlation. *Journal of Biomechanical Engineering,* 134**,** 024504-024504.

OLIVEIRA, L. F., PEIXINHO, C. C., SILVA, G. A. & MENEGALDO, L. L. 2016. In Vivo Passive Mechanical Properties Estimation of Achilles Tendon Using Ultrasound. *Journal of Biomechanics,* 49**,** 507-13.

OZA, A., VANDERBY JR, R. & LAKES, R. S. 2006a. Generalized Solution for Predicting Relaxation from Creep in Soft Tissue: Application to Ligament. *International Journal of Mechanical Sciences,* 48**,** 662-673.

OZA, A., VANDERBY, R., JR. & LAKES, R. 2003. Interrelation of Creep and Relaxation for Nonlinearly Viscoelastic Materials: Application to Ligament and Metal. *Rheologica Acta,* 42**,** 557-568.

OZA, A. L., VANDERBY, R. & LAKES, R. S. 2006b. Creep and Relaxation in Ligament: Theory, Methods and Experiment. *Mechanics of Biological Tissue.*

PAAVOLA, M., KANNUS, P., JÄRVINEN, T. A. H., KHAN, K., JÓZSA, L. & JÄRVINEN, M. 2002. Achilles Tendinopathy. *The Journal of Bone & Joint Surgery,* 84-A**,** 2062-2076.

PAAVOLA, M., KANNUS, P., PAAKKALA, T., PASANEN, M. & JÄRVINEN, M. 2000. Long-Term Prognosis of Patients with Achilles Tendinopathy. *Am J Sports Med,* 28**,** 634-642.

PAILLER-MATTEI, C., LAQUIÈZE, L., DEBRET, R., TUPIN, S., AIMOND, G., SOMMER, P. & ZAHOUANI, H. 2014. Rheological Behaviour of Reconstructed Skin. *Journal of the Mechanical Behavior of Biomedical Materials,* 37**,** 251-263.

PAJALA, A., MELKKO, J., LEPPILAHTI, J., OHTONEN, P., SOINI, Y. & RISTELI, J. 2009. Tenascin-C and Type I and Iii Collagen Expression in Total Achilles Tendon Rupture. An Immunohistochemical Study. *Histology and histopathology,* 24**,** 1207 - 1211.

PANG, X., WU, J. P., ALLISON, G. T., XU, J., RUBENSON, J., ZHENG, M.-H., LLOYD, D. G., GARDINER, B., WANG, A. & KIRK, T. B. 2016. The Three Dimensional Microstructural Network of Elastin, Collagen and Cells in Achilles Tendons. *Journal of Orthopaedic Research,* 35**,** n/a-n/a.

PARDES, A. M., BEACH, Z. M., RAJA, H., RODRIGUEZ, A. B., FREEDMAN, B. R. & SOSLOWSKY, L. J. 2017. Aging Leads to Inferior Achilles Tendon Mechanics and Altered Ankle Function in Rodents. *Journal of Biomechanics,* 60**,** 30-38.

PARDES, A. M., FREEDMAN, B. R., FRYHOFER, G. W., SALKA, N. S., BHATT, P. R. & SOSLOWSKY, L. J. 2016. Males Have Inferior Achilles Tendon Material Properties Compared to Females in a Rodent Model. *Annals of Biomedical Engineering,* 44**,** 2901-2910.

PATTERSON-KANE, J. C., BECKER, D. L. & RICH, T. 2012. The Pathogenesis of Tendon Microdamage in Athletes: The Horse as a Natural Model for Basic Cellular Research. *Journal of Comparative Pathology,* 147**,** 227-247.

PAVAN, P. G., PACHERA, P., STECCO, C. & NATALI, A. N. 2014. Constitutive Modeling of Time-Dependent Response of Human Plantar Aponeurosis. *Computational and Mathematical Methods in Medicine,* 2014**,** 8.

PEARSON, S. J., BURGESS, K. & ONAMBELE, G. N. L. 2007. Creep and the in Vivo Assessment of Human Patellar Tendon Mechanical Properties. *Clinical Biomechanics,* 22**,** 712-717.

PEARSON, S. J. & HUSSAIN, S. R. 2014. Region-Specific Tendon Properties and Patellar Tendinopathy: A Wider Understanding. *Sports medicine,* 44**,** 1101-1112.

PEEK, A. C., MALAGELADA, F. & CLARK, C. I. M. 2016. The Achilles Tendon. *Orthopaedics and Trauma,* 30**,** 1-7.

PELTONEN, J., CRONIN, N. J., STENROTH, L., FINNI, T. & AVELA, J. 2013. Viscoelastic Properties of the Achilles Tendon in Vivo. *Springerplus,* 2**,** 1-8.

PELTZ, C. D., SARVER, J. J., DOURTE, L. M., WÜERGLER-HAURI, C. C., WILLIAMS, G. R. & SOSLOWSKY, L. J. 2010. Exercise Following a Short Immobilization Period Is Detrimental to Tendon Properties and Joint Mechanics in a Rat Rotator Cuff Injury Model. *Journal of orthopaedic research : official publication of the Orthopaedic Research Society,* 28**,** 841-845.

PEÑA, E., CALVO, B., MARTÍNEZ, M. A. & DOBLARÉ, M. 2007. An Anisotropic Visco-Hyperelastic Model for Ligaments at Finite Strains. Formulation and Computational Aspects. *International Journal of Solids and Structures,* 44**,** 760-778.

PERRY, S. M., GETZ, C. L. & SOSLOWSKY, L. J. 2009. Following Rotator Cuff Tears, the Remaining (Intact) Tendons Are Mechanically Altered. *Journal of shoulder and elbow surgery / American Shoulder and Elbow Surgeons ... [et al.],* 18**,** 52-57.

PERUCCA ORFEI, C., LOVATI, A. B., VIGANÒ, M., STANCO, D., BOTTAGISIO, M., DI GIANCAMILLO, A., SETTI, S. & DE GIROLAMO, L. 2016. Dose-Related and Time-Dependent Development of Collagenase-Induced Tendinopathy in Rats. *PLoS One,* 11**,** e0161590.

PETERS, J. A., ZWERVER, J., DIERCKS, R. L., ELFERINK-GEMSER, M. T. & VAN DEN AKKER-SCHEEK, I. 2016. Preventive Interventions for Tendinopathy: A Systematic Review. *Journal of Science and Medicine in Sport,* 19**,** 205-211.

PETERSEN, W., VAROGA, D., ZANTOP, T., HASSENPFLUG, J., MENTLEIN, R. & PUFE, T. 2004. Cyclic Strain Influences the Expression of the Vascular Endothelial Growth Factor (Vegf) and the Hypoxia Inducible Factor 1 Alpha (Hif-1[Alpha]) in Tendon Fibroblasts. *Journal of Orthopaedic Research,* 22**,** 847-853.

PIERLOT, C. M., MOELLER, A. D., LEE, J. M. & WELLS, S. M. 2015. Biaxial Creep Resistance and Structural Remodeling of the Aortic and Mitral Valves in Pregnancy. *Annals of Biomedical Engineering,* 43**,** 1772-1785.

PIOLETTI, D. P. & RAKOTOMANANA, L. R. 2000a. Non-Linear Viscoelastic Laws for Soft Biological Tissues. *European Journal of Mechanics - A/Solids,* 19**,** 749-759.

PIOLETTI, D. P. & RAKOTOMANANA, L. R. 2000b. On the Independence of Time and Strain Effects in the Stress Relaxation of Ligaments and Tendons. *Journal of Biomechanics,* 33**,** 1729-1732.

PIOLETTI, D. P., RAKOTOMANANA, L. R., BENVENUTI, J. F. & LEYVRAZ, P. F. 1998. Viscoelastic Constitutive Law in Large Deformations: Application to Human Knee Ligaments and Tendons. *Journal of Biomechanics,* 31**,** 753-757.

PIOLETTI, D. P., RAKOTOMANANA, L. R. & LEYVRAZ, P. F. 1999. Strain Rate Effect on the Mechanical Behavior of the Anterior Cruciate Ligament–Bone Complex. *Medical Engineering & Physics,* 21**,** 95-100.

POKHAI, G. G., OLIVER, M. L. & GORDON, K. D. 2009. A New Laser Reflectance System Capable of Measuring Changing Cross-Sectional Area of Soft Tissues During Tensile Testing. *Journal of Biomechanical Engineering,* 131**,** 094504-1 - 094504-5.

PRADAS, M. M. & CALLEJA, R. D. 1990. Nonlinear Viscoelastic Behaviour of the Flexor Tendon of the Human Hand. *Journal of Biomechanics,* 23**,** 773-781.

PROVENZANO, P., LAKES, R., KEENAN, T. & VANDERBY, R. 2001. Nonlinear Ligament Viscoelasticity. *Annals of Biomedical Engineering,* 29**,** 908-914.

PROVENZANO, P. P., ALEJANDRO-OSORIO, A. L., VALHMU, W. B., JENSEN, K. T. & VANDERBY, J. R. 2005. Intrinsic Fibroblast-Mediated Remodeling of Damaged Collagenous Matrices in Vivo. *Matrix Biology,* 23**,** 543-555.

PROVENZANO, P. P., HAYASHI, K., KUNZ, D. N., MARKEL, M. D. & VANDERBY, R. 2002a. Healing of Subfailure Ligament Injury: Comparison between Immature and Mature Ligaments in a Rat Model. *Journal of Orthopaedic Research,* 20**,** 975-983.

PROVENZANO, P. P., HEISEY, D., HAYASHI, K., LAKES, R. & VANDERBY, R. 2002b. Subfailure Damage in Ligament: A Structural and Cellular Evaluation. *Journal of Applied Physiology,* 92**,** 362-371.

PROVENZANO, P. P., LAKES, R. S., CORR, D. T. & VANDERBY, R., JR. 2002c. Application of Nonlinear Viscoelastic Models to Describe Ligament Behavior. *Biomechanics and Modeling in Mechanobiology,* 1**,** 45-57.

PROVENZANO, P. P. & VANDERBY, J. R. 2006. Collagen Fibril Morphology and Organization: Implications for Force Transmission in Ligament and Tendon. *Matrix Biology,* 25**,** 71-84.

PYNE, J. D., GENOVESE, K., CASALETTO, L. & VANDE GEEST, J. P. 2014. Sequential-Digital Image Correlation for Mapping Human Posterior Sclera and Optic Nerve Head Deformation. *Journal of Biomechanical Engineering,* 136**,** 021002-021002.

QUAGLINI, V., RUSSA, V. L. & CORNEO, S. 2009. Nonlinear Stress Relaxation of Trabecular Bone. *Mechanics Research Communications,* 36**,** 275-283.

QUINN, K. P. & WINKELSTEIN, B. A. 2011. Preconditioning Is Correlated with Altered Collagen Fiber Alignment in Ligament. *Journal of Biomechanical Engineering,* 133**,** 064506-064506.

R CORE TEAM 2014. R: A Language and Environment for Statistical Computing. Version 3.0.3 ed. Vienna, Austria: R Foundation for Statistical Computing.

R CORE TEAM 2015. R: A Language and Environment for Statistical Computing. Version 3.2.3 ed. Vienna, Austria: R Foundation for Statistical Computing.

RACE, A. & AMIS, A. A. 1996. Cross-Sectional Area Measurement of Soft Tissue. A New Casting Method. *Journal of Biomechanics,* 29**,** 1207-1212.

RATCHADA, S. 2013. A New Viscoelastic Model for Preconditioning in Ligaments and Tendons. *Lecture Notes in Engineering and Computer Science,* 2206**,** 1717-1722.

REES, J. D., MAFFULLI, N. & COOK, J. 2009. Management of Tendinopathy. *Am J Sports Med,* 37**,** 1855-1867.

REESE, S. P. & WEISS, J. A. 2013. Tendon Fascicles Exhibit a Linear Correlation between Poisson's Ratio and Force During Uniaxial Stress Relaxation. *Journal of Biomechanical Engineering,* 135**,** 034501-034501.

REIHSNER, R. & MENZEL, E. J. 1998. Two-Dimensional Stress-Relaxation Behavior of Human Skin as Influenced by Non-Enzymatic Glycation and the Inhibitory Agent Aminoguanidine. *Journal of Biomechanics,* 31**,** 985-993.

REN, D., SUN, K., TIAN, S., YANG, X., ZHANG, C., WANG, W., HUANG, H., ZHANG, J. & DENG, Y. 2012. Effects of Gamma Irradiation and Repetitive Freeze–Thaw Cycles on the Biomechanical Properties of Human Flexor Digitorum Superficialis Tendons. *Journal of Biomechanics,* 45**,** 252-256.

RENSTROM, P. 1991. Sports Traumatology Today - a Review of Common Current Sports Injury Problems. *Annales chirurgiae et gynaecologiae,* 80**,** 81-93.

RIEMERSA, D. J. & SCHAMHARDT, H. C. 1982. The Cryo-Jaw, a Clamp Designed for in Vitro Rheology Studies of Horse Digital Flexor Tendons. *Journal of Biomechanics,* 15**,** 619-620.

RIGBY, B. J., HIRAI, N., SPIKES, J. D. & EYRING, H. 1959. The Mechanical Properties of Rat Tail Tendon. *J Gen Physiol,* 43**,** 265-83.

RIGOZZI, S., MÜLLER, R. & SNEDEKER, J. G. 2009. Local Strain Measurement Reveals a Varied Regional Dependence of Tensile Tendon Mechanics on Glycosaminoglycan Content. *Journal of Biomechanics,* 42**,** 1547-1552.

RIGOZZI, S., MÜLLER, R., STEMMER, A. & SNEDEKER, J. G. 2013. Tendon Glycosaminoglycan Proteoglycan Sidechains Promote Collagen Fibril Sliding—Afm Observations at the Nanoscale. *Journal of Biomechanics,* 46**,** 813-818.

RINCÓN, L., SCHATZMANN, L., BRUNNER, P., STÄUBLI, H. U., FERGUSON, S. J., OXLAND, T. R. & NOLTE, L. P. 2001. Design and Evaluation of a Cryogenic Soft Tissue Fixation Device — Load Tolerances and Thermal Aspects. *Journal of Biomechanics,* 34**,** 393-397.

ROBINSON, P. S., LIN, T. W., REYNOLDS, P. R., DERWIN, K. A., IOZZO, R. V. & SOSLOWSKY, L. J. 2004. Strain-Rate Sensitive Mechanical Properties of Tendon Fascicles from Mice with Genetically Engineered Alterations in Collagen and Decorin. *Journal of Biomechanical Engineering,* 126**,** 252-257.

ROCHE, A. J. & CALDER, J. D. F. 2013. Achilles Tendinopathy: A Review of the Current Concepts of Treatment. *Bone & Joint Journal,* 95-B**,** 1299-1307.

RODENBERG, R. E., BOWMAN, E. & RAVINDRAN, R. 2013. Overuse Injuries. *Primary Care: Clinics in Office Practice,* 40**,** 453-473.

ROWE, V., HEMMINGS, S., BARTON, C., MALLIARAS, P., MAFFULLI, N. & MORRISSEY, D. 2012. Conservative Management of Midportion Achilles Tendinopathy: A Mixed Methods Study, Integrating Systematic Review and Clinical Reasoning. *Sports medicine,* 42**,** 941-967.

RSTUDIO 2013. Rstudio: Integrated Development Environment for R. Version 0.98.501 ed. Boston, MA.

RSTUDIO 2016. Rstudio: Integrated Development Environment for R. Version 0.99.892 ed. Boston, MA.

SABER, S., ZHANG, A. Y., KI, S. H., LINDSEY, D. P., SMITH, R. L., RIBOH, J., PHAM, H. & CHANG, J. 2010. Flexor Tendon Tissue Engineering: Bioreactor Cyclic Strain Increases Construct Strength. *Tissue Engineering Part A,* 16**,** 2085-2090.

SAFE WORK AUSTRALIA 2016. Australian Workers' Compensation Statistics, 2014–15.

SAHOO, S., TOH, S. L. & GOH, J. C. H. 2010. A Bfgf-Releasing Silk/Plga-Based Biohybrid Scaffold for Ligament/Tendon Tissue Engineering Using Mesenchymal Progenitor Cells. *Biomaterials,* 31**,** 2990-2998.

SALADIN, K. S. 2003. *Anatomy & Physiology: The Unity of Form and Function,* Boston, McGraw-Hill Higher Education.

SALISBURY, S. T. S., BUCKLEY, C. P. & ZAVATSKY, A. B. 2008. Image-Based Non-Contact Method to Measure Cross-Sectional Areas and Shapes of Tendons and Ligaments. *Measurement Science and Technology,* 19**,** 045705+09.

SARVER, J. J., ROBINSON, P. S. & ELLIOTT, D. M. 2003. Methods for Quasi-Linear Viscoelastic Modeling of Soft Tissue: Application to Incremental Stress-Relaxation Experiments. *Journal of Biomechanical Engineering,* 125**,** 754-758.

SASAKI, N. & ENYO, A. 1995. Viscoelastic Properties of Bone as a Function of Water Content. *Journal of Biomechanics,* 28**,** 809-815.

SAYEGH, E. T., SANDY, J. D., VIRK, M. S., ROMEO, A. A., WYSOCKI, R. W., GALANTE, J. O., TRELLA, K. J., PLAAS, A. & WANG, V. M. 2015. Recent Scientific Advances Towards the Development of Tendon Healing Strategies. *Current tissue engineering,* 4**,** 128-143.

SCHATZMANN, L., BRUNNER, P. & STÄUBLI, H. U. 1998. Effect of Cyclic Preconditioning on the Tensile Properties of Human Quadriceps Tendons and Patellar Ligaments. *Knee Surgery, Sports Traumatology, Arthroscopy,* 6**,** S56-S61.

SCHECHTMAN, H. & BADER, D. L. 1994. Dynamic Characterization of Human Tendons. *Proceedings of the Institution of Mechanical Engineers, Part H: Journal of Engineering in Medicine,* 208**,** 241-248.

SCHECHTMAN, H. & BADER, D. L. 1997. In Vitro Fatigue of Human Tendons. *Journal of Biomechanics,* 30**,** 829-835.

SCHECHTMAN, H. & BADER, D. L. 2002. Fatigue Damage of Human Tendons. *Journal of Biomechanics,* 35**,** 347-353.

SCHMIDT, K. H. & LEDOUX, W. R. 2010. Quantifying Ligament Cross-Sectional Area Via Molding and Casting. *Journal of Biomechanical Engineering,* 132**,** 091012-1 - 091012-6.

SCHNEIDER, C. A., RASBAND, W. S. & ELICEIRI, K. W. 2012. Nih Image to Imagej: 25 Years of Image Analysis. *Nature Methods,* 9**,** 671-675.

SCHWARTZ, A., WATSON, J. N. & HUTCHINSON, M. R. 2015. Patellar Tendinopathy. *Sports Health,* 7**,** 415-420.

SCHWERDT, H., CONSTANTINESCO, A. & CHAMBRON, J. 1980. Dynamic Viscoelastic Behaviour of the Human Tendon in Vitro. *Journal of Biomechanics,* 13**,** 913-922.

SCOTT, A. R. P. T. P., HUISMAN, E. M. & KHAN, K. M. D. P. 2011. Conservative Treatment of Chronic Achilles Tendinopathy. *Canadian Medical Association. Journal,* 183**,** 1159-65.

SCREEN, H. R. C. 2008. Investigating Load Relaxation Mechanics in Tendon. *Journal of the Mechanical Behavior of Biomedical Materials,* 1**,** 51-58.

SCREEN, H. R. C. 2009. Hierarchical Approaches to Understanding Tendon Mechanics. *Journal of Biomechanical Science and Engineering,* 4**,** 481-499.

SCREEN, H. R. C., BADER, D. L., LEE, D. A. & SHELTON, J. C. 2004a. Local Strain Measurement within Tendon. *Strain,* 40**,** 157-163.

SCREEN, H. R. C., BADER, D. L., SHELTON, J. C. & LEE, D. A. 2002a. Non-Collagenous Matrix Components Influence the Micro-Mechanical Environment of Tenocytes within Tendon Fascicles Subjected to Tensile Strain. *European Cells and Materials,* 4**,** 41-42.

SCREEN, H. R. C., CHHAYA, V. H., GREENWALD, S. E., BADER, D. L., LEE, D. A. & SHELTON, J. C. 2006. The Influence of Swelling and Matrix Degradation on the Microstructural Integrity of Tendon. *Acta Biomaterialia,* 2**,** 505-513.

SCREEN, H. R. C. & EVANS, S. L. 2009. Measuring Strain Distributions in the Tendon Using Confocal Microscopy and Finite Elements. *The Journal of Strain Analysis for Engineering Design,* 44**,** 327-335.

SCREEN, H. R. C., LEE, D. A., BADER, D. L. & SHELTON, J. C. 2002b. Development of a Technique to Determine Strains in Tendons Using the Cell Nuclei. *Biorheology,* 40**,** 361-368.

SCREEN, H. R. C., LEE, D. A., BADER, D. L. & SHELTON, J. C. 2004b. An Investigation into the Effects of the Hierarchical Structure of Tendon Fascicles on Micromechanical

Properties. *Proceedings of the Institution of Mechanical Engineers, Part H: Journal of Engineering in Medicine,* 218**,** 109-119.

SCREEN, H. R. C., SETO, J., KRAUSS, S., BOESECKE, P. & GUPTA, H. S. 2011. Extrafibrillar Diffusion and Intrafibrillar Swelling at the Nanoscale Are Associated with Stress Relaxation in the Soft Collagenous Matrix Tissue of Tendons. *Soft Matter, 7***,** 11243-11251.

SCREEN, H. R. C., SHELTON, J. C., BADER, D. L. & LEE, D. A. 2005a. Cyclic Tensile Strain Upregulates Collagen Production in Isolated Tendon Fascicles. *International Journal of Experimental Pathology,* 86**,** A8-A9.

SCREEN, H. R. C., SHELTON, J. C., BADER, D. L. & LEE, D. A. 2005b. Cyclic Tensile Strain Upregulates Collagen Synthesis in Isolated Tendon Fascicles. *Biochemical and Biophysical Research Communications,* 336**,** 424-429.

SCREEN, H. R. C., SHELTON, J. C., CHHAYA, V. H., KAYSER, M. V., BADER, D. L. & LEE, D. A. 2005c. The Influence of Noncollagenous Matrix Components on the Micromechanical Environment of Tendon Fascicles. *Annals of Biomedical Engineering,* 33**,** 1090-1099.

SCREEN, H. R. C., TOORANI, S. & SHELTON, J. C. 2013. Microstructural Stress Relaxation Mechanics in Functionally Different Tendons. *Medical Engineering & Physics,* 35**,** 96-102.

SEITZ, A. M., WOLFRAM, U., WIEDENMANN, C., IGNATIUS, A. & DÜRSELEN, L. 2012. Impact of Measurement Errors on the Determination of the Linear Modulus of Human Meniscal Attachments. *Journal of the Mechanical Behavior of Biomedical Materials,* 10**,** 120-127.

SHADWICK, R. E. 1990. Elastic Energy Storage in Tendons: Mechanical Differences Related to Function and Age. *Journal of Applied Physiology,* 68**,** 1033-1040.

SHARKEY, N. A., SMITH, T. S. & LUNDMARK, D. C. 1995. Freeze Clamping Musculo-Tendinous Junctions for in Vitro Simulation of Joint Mechanics. *Journal of Biomechanics,* 28**,** 631-635.

SHARMA, P. & MAFFULLI, N. 2005a. Basic Biology of Tendon Injury and Healing. *The Surgeon,* 3**,** 309-316.

SHARMA, P. & MAFFULLI, N. 2008. Tendinopathy and Tendon Injury: The Future. *Disabil Rehabil,* 30**,** 1733-1745.

SHARMA, P. P. & MAFFULLI, N. N. 2005b. Tendon Injury and Tendinopathy: Healing and Repair. *The Journal of bone and joint surgery. American volume,* 87**,** 187-202.

SHEARN, J. T., JUNCOSA-MELVIN, N., BOIVIN, G. P., GALLOWAY, M. T., GOODWIN, W., GOOCH, C., DUNN, M. G. & BUTLER, D. L. 2007. Mechanical Stimulation of Tendon Tissue Engineered Constructs: Effects on Construct Stiffness, Repair Biomechanics, and Their Correlation. *Journal of Biomechanical Engineering,* 129**,** 848-854.

SHEN, ZHILEI L., KAHN, H., BALLARINI, R. & EPPELL, STEVEN J. 2011. Viscoelastic Properties of Isolated Collagen Fibrils. *Biophysical Journal,* 100**,** 3008-3015.

SHEPHERD, J. H., LEGERLOTZ, K., DEMIRCI, T., KLEMT, C., RILEY, G. P. & SCREEN, H. R. C. 2014. Functionally Distinct Tendon Fascicles Exhibit Different Creep and Stress Relaxation Behaviour. *Proceedings of the Institution of Mechanical Engineers, Part H: Journal of Engineering in Medicine,* 228**,** 49-59.

SHETYE, S. S., TROYER, K. L., STREIJGER, F., LEE, J. H. T., KWON, B. K., CRIPTON, P. A. & PUTTLITZ, C. M. 2014. Nonlinear Viscoelastic Characterization of the Porcine Spinal Cord. *Acta Biomaterialia,* 10**,** 792-797.

SHI, D., WANG, D., WANG, C. & LIU, A. 2012. A Novel, Inexpensive and Easy to Use Tendon Clamp for in Vitro Biomechanical Testing. *Medical Engineering & Physics,* 34**,** 516-520.

SHIM, V., FERNANDEZ, J., GARDINER, B., SMITH, D., LLOYD, D. & BESIER, T. F. 2015. The Biomechanical Role of Fibre Twist in the Achilles Tendon. *Orthopaedic Research Society 2015 Annual Meeting.* Las Vegas, Nevada: Orthopaedic Research Society.

SHIM, V. B., FERNANDEZ, J. W., GAMAGE, P. B., REGNERY, C., SMITH, D. W., GARDINER, B. S., LLOYD, D. G. & BESIER, T. F. 2014. Subject-Specific Finite Element Analysis to Characterize the Influence of Geometry and Material Properties in Achilles Tendon Rupture. *Journal of Biomechanics,* 47**,** 3598-3604.

SHOEMAKER, P. A., SCHNEIDER, D., LEE, M. C. & FUNG, Y. C. 1986. A Constitutive Model for Two-Dimensional Soft Tissues and Its Application to Experimental Data. *Journal of Biomechanics,* 19**,** 695-702.

SMITH, C. W., YOUNG, I. S. & KEARNEY, J. N. 1996. Mechanical Properties of Tendons: Changes with Sterilization and Preservation. *Journal of Biomechanical Engineering,* 118**,** 56-61.

SMUTZ, W. P., DREXLER, M., BERGLUND, L. J., GROWNEY, E. & AN, K. N. 1996. Accuracy of a Video Strain Measurement System. *Journal of Biomechanics,* 29**,** 813-817.

SMUTZ, W. P., FRANCE, E. P. & BLOSWICK, D. S. 1995. Measurement of Creep Strain of Flexor Tendons During Low-Force High-Frequency Activities Such as Computer Keyboard Use. *Clinical Biomechanics,* 10**,** 67-72.

SORVARI, J., MALINEN, M. & HÄMÄLÄINEN, J. 2006. Finite Ramp Time Correction Method for Non-Linear Viscoelastic Material Model. *International Journal of Non-Linear Mechanics,* 41**,** 1050-1056.

SOSLOWSKY, L. J., CARPENTER, J. E., DEBANO, C. M., BANERJI, I. & MOALLI, M. R. 1996. Development and Use of an Animal Model for Investigations on Rotator Cuff Disease. *Journal of Shoulder and Elbow Surgery,* 5**,** 383-392.

SOSLOWSKY, L. J., THOMOPOULOS, S., ESMAIL, A., FLANAGAN, C. L., IANNOTTI, J. P., WILLIAMSON, J. D., III & CARPENTER, J. E. 2002. Rotator Cuff Tendinosis in an Animal Model: Role of Extrinsic and Overuse Factors. *Annals of Biomedical Engineering,* 30**,** 1057-63.

SOSLOWSKY, L. J., THOMOPOULOS, S., TUN, S., FLANAGAN, C. L., KEEFER, C. C., MASTAW, J. & CARPENTER, J. E. 2000. Neer Award 1999: Overuse Activity Injures the Supraspinatus Tendon in an Animal Model: A Histologic and Biomechanical Study. *Journal of Shoulder and Elbow Surgery,* 9**,** 79-84.

SPERA, D., GENOVESE, K. & VOLOSHIN, A. 2011. Application of Stereo-Digital Image Correlation to Full-Field 3-D Deformation Measurement of Intervertebral Disc. *Strain,* 47**,** e572-e587.

STELLA, J. A., LIAO, J., HONG, Y., DAVID MERRYMAN, W., WAGNER, W. R. & SACKS, M. S. 2008. Tissue-to-Cellular Level Deformation Coupling in Cell Micro-Integrated Elastomeric Scaffolds. *Biomaterials,* 29**,** 3228-3236.

STENROTH, L., CRONIN, N. J., PELTONEN, J., KORHONEN, M. T., SIPILÄ, S. & FINNI, T. 2016. Triceps Surae Muscle-Tendon Properties in Older Endurance- and Sprint-Trained Athletes. *Journal of Applied Physiology,* 120**,** 63-69.

STOLL, C., JOHN, T., CONRAD, C., LOHAN, A., HONDKE, S., ERTEL, W., KAPS, C., ENDRES, M., SITTINGER, M., RINGE, J. & SCHULZE-TANZIL, G. 2011. Healing Parameters in a Rabbit Partial Tendon Defect Following Tenocyte/Biomaterial Implantation. *Biomaterials,* 32**,** 4806-4815.

STONE, D., GREEN, C., RAO, U., AIZAWA, H., YAMAJI, T., NIYIBIZI, C., CARLIN, G. & WOO, S. L. Y. 1999. Cytokine-Induced Tendinitis: A Preliminary Study in Rabbits. *Journal of Orthopaedic Research,* 17**,** 168-177.

SU, W.-R., CHEN, H.-H. & LUO, Z.-P. 2008. Effect of Cyclic Stretching on the Tensile Properties of Patellar Tendon and Medial Collateral Ligament in Rat. *Clinical Biomechanics,* 23**,** 911-917.

SULLIVAN, J. C. & BEST, T. M. 2005. Injury of the Musculotendinous Junction. *In:* MAFFULLI, N., RENSTRÖM, P. & LEADBETTER, W. B. (eds.) *Tendon Injuries: Basic Science and Clinical Medicine.* London: Springer London.

SULLO, A., MAFFULLI, N., CAPASSO, G. & TEST, V. 2001. The Effects of Prolonged Peritendinous Administration of Pge1 to the Rat Achilles Tendon: A Possible Animal Model of Chronic Achilles Tendinopathy. *J Orthop Sci,* 6**,** 349-57.

SUN, H. B., SCHANIEL, C., LEONG, D. J. & WANG, J. H. C. 2015. Biology and Mechano-Response of Tendon Cells: Progress Overview and Perspectives. *Journal of Orthopaedic Research,* 33**,** 785-792.

SUSSMILCH-LEITCH, S. P., COLLINS, N. J., BIALOCERKOWSKI, A. E., WARDEN, S. J. & CROSSLEY, K. M. 2012. Physical Therapies for Achilles Tendinopathy: Systematic Review and Meta-Analysis. *Journal of foot and ankle research,* 5**,** 15.

SVENSSON, R. B., HANSEN, P., HASSENKAM, T., HARALDSSON, B. T., AAGAARD, P., KOVANEN, V., KROGSGAARD, M., KJAER, M. & MAGNUSSON, S. P. 2012. Mechanical Properties of Human Patellar Tendon at the Hierarchical Levels of Tendon and Fibril. *J Appl Physiol (1985),* 112**,** 419-26.

SVENSSON, R. B., HASSENKAM, T., HANSEN, P. & PETER MAGNUSSON, S. 2010. Viscoelastic Behavior of Discrete Human Collagen Fibrils. *Journal of the Mechanical Behavior of Biomedical Materials,* 3**,** 112-115.

SVENSSON, R. B., HERCHENHAN, A., STARBORG, T., LARSEN, M., KADLER, K. E., QVORTRUP, K. & MAGNUSSON, S. P. 2017. Evidence of Structurally Continuous Collagen Fibrils in Tendons. *Acta Biomaterialia,* 50**,** 293-301.

SVERDLIK, A. & LANIR, Y. 2002. Time-Dependent Mechanical Behavior of Sheep Digital Tendons, Including the Effects of Preconditioning. *Journal of Biomechanical Engineering,* 124**,** 78-84.

SZCZESNY, S. E., PELOQUIN, J. M., CORTES, D. H., KADLOWEC, J. A., SOSLOWSKY, L. J. & ELLIOTT, D. M. 2012. Biaxial Tensile Testing and Constitutive Modeling of Human Supraspinatus Tendon. *Journal of Biomechanical Engineering,* 134**,** 021004.

TAKAI, S., WOO, S. L. Y., HORIBE, S., TUNG, D. K. L. & GELBERMAN, R. H. 1991. The Effects of Frequency and Duration of Controlled Passive Mobilization on Tendon Healing. *Journal of Orthopaedic Research,* 9**,** 705-713.

TALLON, C., MAFFULLI, N. & EWEN, S. W. B. 2001. Ruptured Achilles Tendons Are Significantly More Degenerated Than Tendinopathic Tendons. *Medicine & Science in Sports & Exercise,* 33**,** 1983-1990.

TAMIWA, M., SCREEN, H. C. R., SHELTON, J. C. & BADER, D. L. 2006. Tendon Micromechanics and Its Implications in Mechanotransduction. *Journal of Biomechanics,* 39**,** S58-S58.

TERAMOTO, A. & LUO, Z.-P. 2008. Temporary Tendon Strengthening by Preconditioning. *Clinical Biomechanics,* 23**,** 619-622.

THANIKAIVELAN, P., SHELLY, D. C. & RAMKUMAR, S. S. 2006. Gauge Length Effect on the Tensile Properties of Leather. *Journal of Applied Polymer Science,* 101**,** 1202-1209.

THEIS, N., MOHAGHEGHI, A. A. & KORFF, T. 2012. Method and Strain Rate Dependence of Achilles Tendon Stiffness. *Journal of Electromyography and Kinesiology,* 22**,** 947-953.

THORNTON, G. M. & BAILEY, S. J. 2012. Repetitive Loading Damages Healing Ligaments More Than Sustained Loading Demonstrated by Reduction in Modulus and Residual Strength. *Journal of Biomechanics,* 45**,** 2589-2594.

THORNTON, G. M., OLIYNYK, A., FRANK, C. B. & SHRIVE, N. G. 1997. Ligament Creep Cannot Be Predicted from Stress Relaxation at Low Stress: A Biomechanical Study of the Rabbit Medial Collateral Ligament. *Journal of Orthopaedic Research,* 15**,** 652-656.

THORNTON, G. M., SCHWAB, T. D. & OXLAND, T. R. 2007. Cyclic Loading Causes Faster Rupture and Strain Rate Than Static Loading in Medial Collateral Ligament at High Stress. *Clinical Biomechanics,* 22**,** 932-940.

THORNTON, G. M., SHRIVE, N. G. & FRANK, C. B. 2001. Altering Ligament Water Content Affects Ligament Pre-Stress and Creep Behavior. *Journal of Orthopaedic Research,* 19**,** 845-851.

THORPE, C. T., BIRCH, H. L., CLEGG, P. D. & SCREEN, H. R. 2012a. The Micro-Structural Response of Tendon Fascicles to Applied Strain Is Altered with Ageing. *Osteoarthritis and Cartilage,* 20, Supplement 1**,** S246-S247.

THORPE, C. T., BIRCH, H. L., CLEGG, P. D. & SCREEN, H. R. C. 2013a. The Role of the Non-Collagenous Matrix in Tendon Function. *International Journal of Experimental Pathology,* 94**,** 248-259.

THORPE, C. T. & SCREEN, H. R. C. 2016. Tendon Structure and Composition. *In:* ACKERMANN, P. W. & HART, D. A. (eds.) *Metabolic Influences on Risk for Tendon Disorders.* Cham: Springer International Publishing.

THORPE, C. T., UDEZE, C. P., BIRCH, H. L., CLEGG, P. D. & SCREEN, H. R. C. 2012b. Specialization of Tendon Mechanical Properties Results from Interfascicular Differences. *Journal of The Royal Society Interface,* 9**,** 3108-3117.

THORPE, C. T., UDEZE, C. P., BIRCH, H. L., CLEGG, P. D. & SCREEN, H. R. C. 2013b. Capacity for Sliding between Tendon Fascicles Decreases with Ageing in Injury Prone Equine Tendons: A Possible Mechanism for Age-Related Tendinopathy? *European Cells and Materials,* 25**,** 48-60.

TOHYAMA, H., OHNO, K., YAMAMOTO, N., HAYASHI, K., YASUDA, K. & KANEDA, K. 1992. Stress-Strain Characteristics of in Situ Frozen and Stress-Shielded Rabbit Patellar Tendon. *Clinical Biomechanics,* 7**,** 226-230.

TOMS, S. R., DAKIN, G. J., LEMONS, J. E. & EBERHARDT, A. W. 2002. Quasi-Linear Viscoelastic Behavior of the Human Periodontal Ligament. *Journal of Biomechanics,* 35**,** 1411-1415.

TROTTER, J. A. 2002. Structure-Function Considerations of Muscle-Tendon Junctions. *Comparative Biochemistry and Physiology - Part A: Molecular & Integrative Physiology,* 133**,** 1127-1133.

TROYER, K. L., ESTEP, D. J. & PUTTLITZ, C. M. 2012a. Viscoelastic Effects During Loading Play an Integral Role in Soft Tissue Mechanics. *Acta Biomaterialia,* 8**,** 234-243.

TROYER, K. L. & PUTTLITZ, C. M. 2012. Nonlinear Viscoelasticty Plays an Essential Role in the Functional Behavior of Spinal Ligaments. *Journal of Biomechanics,* 45**,** 684-691.

TROYER, K. L., SHETYE, S. S. & PUTTLITZ, C. M. 2012b. Experimental Characterization and Finite Element Implementation of Soft Tissue Nonlinear Viscoelasticity. *Journal of Biomechanical Engineering,* 134**,** 114501-114501.

TRUDEL, G., KOIKE, Y., RAMACHANDRAN, N., DOHERTY, G., DINH, L., LECOMPTE, M. & UHTHOFF, H. K. 2007. Mechanical Alterations of Rabbit Achilles' Tendon after Immobilization Correlate with Bone Mineral Density but Not with Magnetic Resonance or Ultrasound Imaging. *Archives of Physical Medicine and Rehabilitation,* 88**,** 1720-1726.

TUCKER, J. J., RIGGIN, C. N., CONNIZZO, B. K., MAUCK, R. L., STEINBERG, D. R., KUNTZ, A. F., SOSLOWSKY, L. J. & BERNSTEIN, J. 2016. Effect of Overuse-Induced Tendinopathy on Tendon Healing in a Rat Supraspinatus Repair Model. *Journal of orthopaedic research : official publication of the Orthopaedic Research Society,* 34**,** 161-166.

TUNG, S.-H., SHIH, M.-H. & KUO, J.-C. 2010. Application of Digital Image Correlation for Anisotropic Plastic Deformation During Tension Testing. *Optics and Lasers in Engineering,* 48**,** 636-641.

UPTON, M. L., GILCHRIST, C. L., GUILAK, F. & SETTON, L. A. 2008. Transfer of Macroscale Tissue Strain to Microscale Cell Regions in the Deformed Meniscus. *Biophysical Journal,* 95**,** 2116-2124.

VAN BAVEL, H., DROST, M. R., WIELDERS, J. D. L., HUYGHE, J. M., HUSON, A. & JANSSEN, J. D. 1996. Strain Distribution on Rat Medial Gastrocnemius (Mg) During Passive Stretch. *Journal of Biomechanics,* 29**,** 1069-1074.

VAN DER VEEN, A. J., BISSCHOP, A., MULLENDER, M. G. & VAN DIEËN, J. H. 2013. Modelling Creep Behaviour of the Human Intervertebral Disc. *Journal of Biomechanics,* 46**,** 2101-2103.

VAN GRIENSVEN, M., ZEICHEN, J., SKUTEK, M., BARKHAUSEN, T., KRETTEK, C. & BOSCH, U. 2003. Cyclic Mechanical Strain Induces No Production in Human Patellar Tendon Fibroblasts - a Possible Role for Remodelling and Pathological Transformation. *Experimental and Toxicologic Pathology,* 54**,** 335-338.

VERGARI, C., POURCELOT, P., HOLDEN, L., RAVARY-PLUMIOËN, B., GERARD, G., LAUGIER, P., MITTON, D. & CREVIER-DENOIX, N. 2011. True Stress and Poisson's Ratio of Tendons During Loading. *Journal of Biomechanics,* 44**,** 719-724.

VERGARI, C., POURCELOT, P., HOLDEN, L., RAVARY-PLUMIOËN, B., LAUGIER, P., MITTON, D. & CREVIER-DENOIX, N. 2010. A Linear Laser Scanner to Measure Cross-Sectional Shape and Area of Biological Specimens During Mechanical Testing. *Journal of Biomechanical Engineering,* 132**,** 105001-1 - 105001-7.

VOLETI, P. B., BUCKLEY, M. R. & SOSLOWSKY, L. J. 2012. Tendon Healing: Repair and Regeneration. *Annual Review of Biomedical Engineering,* 14**,** 47-71.

WAGGETT, A. D., BENJAMIN, M. & RALPHS, J. R. 2006. Connexin 32 and 43 Gap Junctions Differentially Modulate Tenocyte Response to Cyclic Mechanical Load. *European Journal of Cell Biology,* 85**,** 1145-1154.

WALCHER, M. G., GIESINGER, K., DU SART, R., DAY, R. E. & KUSTER, M. S. 2016. Plate Positioning in Periprosthetic or Interprosthetic Femur Fractures with Stable Implants-a Biomechanical Study. *The Journal of Arthroplasty,* 31**,** 2894-2899.

WALDEN, G., LIAO, X., DONELL, S., RAXWORTHY, M. J., RILEY, G. P. & SAEED, A. 2016. A Clinical, Biological, and Biomaterials Perspective into Tendon Injuries and Regeneration. *Tissue Engineering Part B: Reviews,* 23**,** 44-58.

WANG, J. H. C. 2006. Mechanobiology of Tendon. *Journal of Biomechanics,* 39**,** 1563-1582.

WANG, J. H. C., IOSIFIDIS, M. I. & FU, F. H. 2006. Biomechanical Basis for Tendinopathy. *Clin Orthop Relat Res,* 443**,** 320-332.

WANG, T., LIN, Z., NI, M., THIEN, C., DAY, R. E., GARDINER, B., RUBENSON, J., KIRK, T. B., SMITH, D. W., WANG, A., LLOYD, D. G., WANG, Y., ZHENG, Q. & ZHENG, M.

H. 2015. Cyclic Mechanical Stimulation Rescues Achilles Tendon from Degeneration in a Bioreactor System. *Journal of Orthopaedic Research,* 33**,** 1888-1896.

WARDEN, S. J. 2007. Animal Models for the Study of Tendinopathy. *British Journal of Sports Medicine,* 41**,** 232-240.

WEST, J. R., JUNCOSA, N., GALLOWAY, M. T., BOIVIN, G. P. & BUTLER, D. L. 2004. Characterization of in Vivo Achilles Tendon Forces in Rabbits During Treadmill Locomotion at Varying Speeds and Inclinations. *Journal of Biomechanics,* 37**,** 1647-1653.

WICKHAM, H. 2009. Ggplot2: Elegant Graphics for Data Analysis. New York: Springer.

WICKHAM, H. 2011. The Split-Apply-Combine Strategy for Data Analysis. *Journal of Statistical Software,* 40**,** 1-29.

WICKHAM, H. 2015. Stringr: Simple, Consistent Wrappers for Common String Operations. R package version 1.0.0. ed.

WIELOCH, P., BUCHMANN, G., ROTH, W. & RICKERT, M. 2004. A Cryo-Jaw Designed for in Vitro Tensile Testing of the Healing Achilles Tendons in Rats. *Journal of Biomechanics,* 37**,** 1719-1722.

WILKES, R., ZHAO, Y., CUNNINGHAM, K., KIESWETTER, K. & HARIDAS, B. 2009. 3d Strain Measurement in Soft Tissue: Demonstration of a Novel Inverse Finite Element Model Algorithm on Microct Images of a Tissue Phantom Exposed to Negative Pressure Wound Therapy. *Journal of the Mechanical Behavior of Biomedical Materials,* 2**,** 272-287.

WOO, S. L.-Y., ALMARZA, A. J., LIANG, R. & FISHER, M. B. 2007. Functional Tissue Engineering of Ligament and Tendon Injuries. *In:* MAO, J. J., MIKOS, A. & VUNJAK-NOVAKOVIC, G. (eds.) *Translational Approaches in Tissue Engineering and Regenerative Medicine.* Artech House Publishers.

WOO, S. L.-Y., DANTO, M. I., OHLAND, K. J., LEE, T. Q. & NEWTON, P. O. 1990. The Use of a Laser Micrometer System to Determine the Cross-Sectional Shape and Area of Ligaments: A Comparative Study with Two Existing Methods. *Journal of Biomechanical Engineering,* 112**,** 426-431.

WOO, S. L. Y., ALMARZA, A. J., KARAOGLU, S., LIANG, R. & FISHER, M. B. 2011. Functional Tissue Engineering of Ligament and Tendon Injuries. *Principles of Regenerative Medicine (Second Edition).* San Diego: Academic Press.

WOO, S. L. Y., DEBSKI, R. E., ZEMINSKI, J., ABRAMOWITCH, S. D., CHAN SAW, S. S. & FENWICK, J. A. 2000. Injury and Repair of Ligaments and Tendons. *Annual Review of Biomedical Engineering,* 2**,** 83-118.

WOO, S. L. Y., LEE, T. Q., GOMEZ, M. A., SATO, S. & FIELD, F. P. 1987. Temperature Dependent Behavior of the Canine Medial Collateral Ligament. *Journal of Biomechanical Engineering,* 109**,** 68-71.

WOO, S. L. Y., NEWTON, P. O., MACKENNA, D. A. & LYON, R. M. 1992. A Comparative Evaluation of the Mechanical Properties of the Rabbit Medial Collateral and Anterior Cruciate Ligaments. *Journal of Biomechanics,* 25**,** 377-386.

WOO, S. L. Y., ORLANDO, C. A., CAMP, J. F. & AKESON, W. H. 1986. Effects of Postmortem Storage by Freezing on Ligament Tensile Behavior. *Journal of Biomechanics,* 19**,** 399-404.

WREN, T. A. L., YERBY, S. A., BEAUPRÉ, G. S. & CARTER, D. R. 2001a. Influence of Bone Mineral Density, Age, and Strain Rate on the Failure Mode of Human Achilles Tendons. *Clinical Biomechanics,* 16**,** 529-534.

WREN, T. A. L., YERBY, S. A., BEAUPRÉ, G. S. & CARTER, D. R. 2001b. Mechanical Properties of the Human Achilles Tendon. *Clinical Biomechanics,* 16**,** 245-251.

WREN, T. L., LINDSEY, D., BEAUPRÉ, G. & CARTER, D. 2003. Effects of Creep and Cyclic Loading on the Mechanical Properties and Failure of Human Achilles Tendons. *Annals of Biomedical Engineering,* 31**,** 710-717.

WU, J. P., SWIFT, B. J., BECKER, T., SQUELCH, A., WANG, A., ZHENG, Y. C., ZHAO, X., XU, J., XUE, W., ZHENG, M., LLOYD, D. & KIRK, T. B. 2017. High-Resolution Study of the 3d Collagen Fibrillary Matrix of Achilles Tendons without Tissue Labelling and Dehydrating. *Journal of Microscopy,* 266**,** 273-287.

YAHIA, L. H. & DROUIN, G. 1990. Study of the Hysteresis Phenomenon in Canine Anterior Cruciate Ligaments. *Journal of Biomedical Engineering,* 12**,** 57-62.

YAMAMOTO, E., HAYASHI, K. & YAMAMOTO, N. 1999. Mechanical Properties of Collagen Fascicles from Stress-Shielded Patellar Tendons in the Rabbit. *Clinical Biomechanics,* 14**,** 418-425.

YAMAMOTO, E., HAYASHI, K. & YAMAMOTO, N. 2000. Effects of Stress Shielding on the Transverse Mechanical Properties of Rabbit Patellar Tendons. *Journal of Biomechanical Engineering,* 122**,** 608-614.

YAN, R., GU, Y., RAN, J., HU, Y., ZHENG, Z., ZENG, M., HENG, B. C., CHEN, X., YIN, Z., CHEN, W., SHEN, W. & OUYANG, H. 2017. Intratendon Delivery of Leukocyte-Poor Platelet-Rich Plasma Improves Healing Compared with Leukocyte-Rich Platelet-Rich Plasma in a Rabbit Achilles Tendinopathy Model. *Am J Sports Med,* X**,** 1-12.

YANG, L., VAN DER WERF, K. O., DIJKSTRA, P. J., FEIJEN, J. & BENNINK, M. L. 2012. Micromechanical Analysis of Native and Cross-Linked Collagen Type I Fibrils Supports the Existence of Microfibrils. *Journal of the Mechanical Behavior of Biomedical Materials,* 6**,** 148-158.

YANG, W., FUNG, T. C., CHIAN, K. S. & CHONG, C. K. 2006. Investigations of the Viscoelasticity of Esophageal Tissue Using Incremental Stress-Relaxation Test and Cyclic Extension Test. *Journal of Mechanics in Medicine and Biology,* 06**,** 261-272.

YASUDA, T., KINOSHITA, M., ABE, M. & SHIBAYAMA, Y. 2000. Unfavorable Effect of Knee Immobilization on Achilles Tendon Healing in Rabbits. *Acta Orthopaedica Scandinavica,* 71**,** 69-73.

YASUI, Y., TONOGAI, I., ROSENBAUM, A. J., SHIMOZONO, Y., KAWANO, H. & KENNEDY, J. G. 2017. The Risk of Achilles Tendon Rupture in the Patients with Achilles Tendinopathy: Healthcare Database Analysis in the United States. *BioMed Research International,* 2017**,** 7021862.

YOO, L., KIM, H., GUPTA, V. & DEMER, J. L. 2009. Quasilinear Viscoelastic Behavior of Bovine Extraocular Muscle Tissue. *Investigative Ophthalmology & Visual Science,* 50**,** 3721-3728.

YOO, S. D., CHOI, S., LEE, G.-J., CHON, J., JEONG, Y. S., PARK, H.-K. & KIM, H.-S. 2012. Effects of Extracorporeal Shockwave Therapy on Nanostructural and Biomechanical Responses in the Collagenase-Induced Achilles Tendinitis Animal Model. *Lasers in Medical Science,* 27**,** 1195-1204.

ZHOU, J., KOIKE, Y., UHTHOFF, H. K. & TRUDEL, G. 2007. Quantitative Histology and Ultrastructure Fail to Explain Weakness of Immobilized Rabbit Achilles' Tendons. *Archives of Physical Medicine and Rehabilitation,* 88**,** 1177-1184.

COPYRIGHT STATEMENT

Alex Hayes

Dear Mr hayes,

Thank you for your email.

I confirm that one of your author retained rights is to include your article in a thesis or dissertation as far as you include a full acknowledgement and, if appropriate, a link to the final published version hosted on Science Direct.

With kind regards,

Sergio Oreni Gordillo

Senior Right Associate - Global Rights Department | ELSEVIER |

The Boulevard| Langford Lane | Kidlington | Oxford OX5 1GB |

Tel: +44 1865 843857 Fax: +44 1865 853333

s.orenigordillo@elsevier.com

*** External email: use caution ***

Good evening

I was wondering if you could assist with my query below?

Regards

Alex Hayes
PhD Candidate | **Department of Mechanical Engineering**
Curtin University of Technology

BEFORE PRINTING THIS E-MAIL
please consider the environment

From: Alex Hayes
Sent: Saturday, 26 August 2017 13:39
To: oxfordcopyrights@elsevier.com
Subject: Use of Publication in PhD dissertation

Good afternoon

I wish to use a publication as a chapter of my PhD dissertation. The publication in question is:
HAYES, A., EASTON, K., DEVANABOYINA, P. T., WU, J.-P., KIRK, T. B. & LLOYD, D. 2016. Structured white light scanning of rabbit Achilles tendon. Journal of Biomechanics, 49, 3753-3758.
https://doi.org/10.1016/j.jbiomech.2016.09.042

I have read the document on Author Rights -
https://www.elsevier.com/__data/assets/pdf_file/0007/55654/AuthorUserRights.pdf - and wish to confirm with you that it is acceptable for me to reformat the publication to include as a chapter, with appropriate recognition.

I look forward to hearing from you.

Regards

Alex Hayes
BE(Mech)
PhD Student | Department of Mechanical Engineering

Curtin University
Mobile | +61 410 733 879
Email | alex.hayes@postgrad.curtin.edu.au
Web | http://mech-eng.curtin.edu.au/

Mr A J Hayes
21 Cinnabar Place
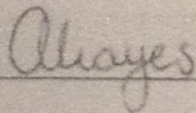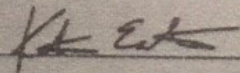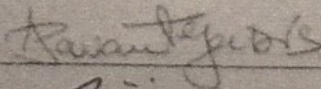CARINE WA 6020

17 March 2018

Thesis Examination Officer
Office of Research and Development
Curtin University of Technology

To whom it may concern

I, Alex John Cullen Hayes, contributed to the conception and design of the experiment, analysis and interpretation of the data, and drafted significant parts of the publication entitled *Structured white light scanning of rabbit Achilles tendon*, the details of which are presented below.

HAYES, A., EASTON, K., DEVANABOYINA, P. T., WU, J.-P., KIRK, T. B. & LLOYD, D. 2016. Structured White Light Scanning of Rabbit Achilles Tendon. *Journal of Biomechanics*, 49, 3753-3758.

Alex Hayes _____*Ahayes*_____ 17 March 2018

I, as a Co-Author, endorse that this level of contribution by the candidate indicated above

is appropriate.

Katrina Easton _____
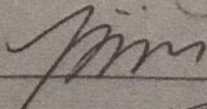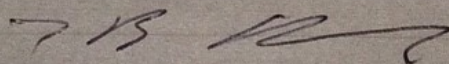
Pavan Devanaboyina _____

Jian-Ping Wu _____

Thomas Brett Kirk _____

David Lloyd _____

Mr A J Hayes
21 Cinnabar Place
CARINE WA 6020

17 March 2018

Thesis Examination Officer
Office of Research and Development
Curtin University of Technology

To whom it may concern

I, Alex John Cullen Hayes, contributed to the conception and design of the experiment, analysis and interpretation of the data, and drafted significant parts of the publication entitled *Structured white light scanning of rabbit Achilles tendon,* the details of which are presented below.

HAYES, A., EASTON, K., DEVANABOYINA, P. T., WU, J.-P., KIRK, T. B. & LLOYD, D. 2016. Structured White Light Scanning of Rabbit Achilles Tendon. *Journal of Biomechanics,* 49**,** 3753-3758.

Alex Hayes   _____   17 March 2018

I, as a Co-Author, endorse that this level of contribution by the candidate indicated above
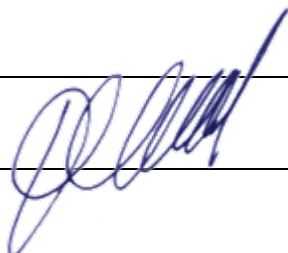
is appropriate.

Katrina Easton   _____

Pavan Devanaboyina   _____

Jian-Ping Wu   _____

Thomas Brett Kirk   _____

David Lloyd   _____

Our Ref: KA/ICTS/P18/1237

30 June 2018

Dear Alex Hayes,

Material requested: Figure 27 from J. Kastelic, A. Galeski & E. Baer (1978) The Multicomposite Structure of Tendon, Connective Tissue Research, 6:1, 11-23,

Thank you for your correspondence requesting permission to reproduce the above mentioned material from our Journal in your printed thesis and to be posted in the university's repository – Curtin University,   http://espace.curtin.edu.au

We will be pleased to grant entirely free permission on the condition that you acknowledge the original source of publication and insert a reference to the Journal's web site: http://www.tandfonline.com

Please note that this licence does not allow you to post our content on any third party websites or repositories.

Thank you for your interest in our Journal.

Yours sincerely

Kendyl

Kendyl Anderson – Permissions Administrator, Journals
Taylor & Francis Group
3 Park Square, Milton Park, Abingdon, Oxon, OX14 4RN, UK.
Tel: +44 (0)20 7017 7617
Fax:+44 (0)20 7017 6336
Web: www.tandfonline.com
e-mail: kendyl.anderson@tandf.co.uk

Taylor & Francis is a trading name of Informa UK Limited,
registered in England under no. 1072954

an informa business